

**Fuzzy Systems in Real-Time Condition
Monitoring and Fault Diagnosis,
with a Diesel Engine Case Study.**

A thesis submitted for the degree of
Doctor of Philosophy
at the University of Leicester

by

John A. Twiddle
Department of Engineering
University of Leicester

August 2001

UMI Number: U149848

All rights reserved

INFORMATION TO ALL USERS

The quality of this reproduction is dependent upon the quality of the copy submitted.

In the unlikely event that the author did not send a complete manuscript and there are missing pages, these will be noted. Also, if material had to be removed, a note will indicate the deletion.



UMI U149848

Published by ProQuest LLC 2013. Copyright in the Dissertation held by the Author.
Microform Edition © ProQuest LLC.

All rights reserved. This work is protected against
unauthorized copying under Title 17, United States Code.



ProQuest LLC
789 East Eisenhower Parkway
P.O. Box 1346
Ann Arbor, MI 48106-1346

ABSTRACT

Diesel engines have become a common source of power, both for vehicles and for static equipment because they are fuel efficient, robust and reliable. It is important that diesel engines run in their correct condition and properly controlled in order to maintain efficiency, low emissions levels and high reliability.

The following thesis aims to assess the application of fuzzy systems in real-time condition monitoring and fault diagnosis. A 65kW diesel powered generator set has been purchased 'off the shelf' as an example of a typical application which may benefit from the development of CMFD techniques. As a test case, the diesel engine is appropriate as its sub-systems are complex, non-linear and subject to noise and uncertainty.

A diagnostic structure comprising fuzzy systems in three distinct roles has been proposed. Fuzzy reference models, incorporating heuristics and approximate non-linear mathematical relationships, are used for the generation of residuals by comparison with signals from a small number of low cost transducers. The residuals are classified and the diagnosis is inferred from the pattern of residual classes using a fuzzy rule-base. The diagnostic results obtained for three diesel engine sub-systems, show this to be a powerful technique for CMFD system design which may generalised, both for other types of plant and other forms of reference model.

This fuzzy model-based approach to fault diagnosis is shown to have benefits over other techniques by way of its transparency, ease of development, performance under variable engine load conditions, high level output and the lack of any requirement for fault data in the development process.

The robustness of the fuzzy reference models to certain fault conditions remains a key issue. The fuzzy models were generally effective at generating residuals where deviations from the normal condition are small. For larger deviations, robustness of models is not guaranteed or expected. A number of techniques were successfully deployed to reduce the number of misclassifications caused by this lack of robustness.

ACKNOWLEDGEMENTS.

There are many people to whom I owe a debt of gratitude for helping to make my work in producing this thesis not only possible, but also most enjoyable. I'd like to express my thanks to the following people;

To mam and dad for their constant support and for not talking me out of resigning my job to attempt a Ph.D. Special thanks for shopping at Tesco, laundry and sea-front fish and chips.

To Barrie, Sarah and Mike for their motivation, encouragement and support. Special thanks to Barrie for his wise supervision and confidence in me throughout the course of this project.

To the industrial collaborators and the EPSRC for both their financial support and motivation. In particular, thanks to Mark Scaife, David Wareing and Peter Ladlow at Perkins Engines Company Ltd., and Peter Scotson at TRW Automotive; many thanks for all the encouragement, ideas and practical support. Special thanks to David Wareing for his active role in specifying and setting up the test bed and instrumentation. Also thanks to Peter Essex and his team of technicians for the use of their facilities to accommodate our initial test program.

To Chinmay, Keng Boon, Yuhua, Aamer, Chen Pang and all the other inhabitants of the fourth floor. Respect and grateful thanks for your friendship, support, and for putting up with me over the last four years. Thanks for making coming to work such a pleasure.

To Pete Barwell, Dipak Raval and Graham Clark, for their invaluable assistance in setting up the test bed in the thermo lab and for keeping it up and running. Thanks also for helping me to filter out some of my dafter ideas. Special thanks to Dipak for his patience and practical expertise.

To everyone in the Department of Engineering, thanks for making the last four years so enjoyable (and giving me the opportunity to play some cricket!).

Finally, thanks to all at KuHAC for giving me the opportunity to get away from it all at the weekends

CONTENTS

Abstract	
Acknowledgements.	... i
Contents.	... ii
Introduction.	... xv
List of publications.	... xvii
Notation.	... xx

SECTION 1: The Literature Review

Chapter 1. Techniques for Condition Monitoring and Fault Diagnosis of Diesel Engine Systems: A Review	... 1
--	--------------

	Page
1.1 Introduction to diesel engine systems	... 3
1.2 The need for condition monitoring and fault diagnosis	... 4
1.3 An overview of condition monitoring	... 5
1.4 Selection of appropriate transducers and measurands for condition monitoring.	... 5
1.5 Cost benefit of on-board CMFD	... 8
1.6 Fault diagnosis techniques	... 9
1.6.1 Definitions	... 10
1.6.2 Spectral analysis techniques in fault diagnosis	... 11
1.6.3 Classification techniques	... 12
1.6.4 Model based techniques for fault diagnosis	... 13
1.6.4.1 Model selection	... 14
1.6.4.2 Identification and parameter estimation	... 14
1.6.4.3 State and output observers	... 16
1.6.4.4 Parity equations	... 16

1.6.5	Fuzzy systems in fault diagnosis	... 17
1.6.6	Expert Systems in fault diagnosis	... 18
1.7	Requirements for a diesel engine CMFD system	... 20
1.7.1	Instrumentation	... 20
1.7.2	Functional specification	... 20
1.7.3	Selection of appropriate diagnostic techniques	... 22
1.8	Conclusions	... 23
<hr/>		
Chapter 2. An introduction to the theory of logic and sets.		... 25
<hr/>		
2.1	Application of logic.	... 26
2.2	Origins of formal logic	... 27
2.3	An algebra for binary logic	... 29
2.4	Classical set theory	... 30
2.4.1	Mappings and functions	... 31
2.5	Fuzzy logic and fuzzy sets	... 32
2.6	Fuzzy membership functions	... 34
2.7	Fuzzy sets and probability	... 35
2.8	Concluding remarks	... 37
<hr/>		
Chapter 3. Introduction to fuzzy systems and mappings		... 38
<hr/>		
3.1.	The generic fuzzy system	... 39
3.2.	The structure and design of fuzzy systems	... 41
3.2.1.	Fuzzification	... 41
3.2.2.	Operators	... 43
3.2.2.1.	Fuzzy complement	... 44
3.2.2.2.	Fuzzy union	... 45
3.2.2.3.	Fuzzy intersection	... 46
3.2.2.4.	Discussion	... 46

3.2.3.	Implication	... 47
3.2.4.	Aggregation	... 49
3.2.5.	Defuzzification	... 50
3.2.5.1.	Output membership functions	... 51
3.2.5.2.	Centre average defuzzifiers	... 52
3.2.5.3.	Centre of gravity defuzzifiers	... 52
3.2.5.4.	Maximum defuzzifiers	... 53
3.2.5.5.	Weighted average defuzzifiers for Takagi-Sugeno fuzzy systems	... 54
3.3.	Summary	... 54
<hr/>		
Chapter 4.	Identification and training of fuzzy systems.	... 56
<hr/>		
4.1	A comparison of non-linear modelling techniques.	... 57
4.2	A review of algorithmic approaches to fuzzy system. identification and training.	... 59
4.2.1	Fuzzy system design from table look-up.	... 62
4.2.2	Takagi and Sugeno's algorithm for fuzzy system identification.	... 63
4.2.3	Least squares algorithms in fuzzy identification.	... 64
4.2.4	Neuro-fuzzy approaches to fuzzy system identification.	... 65
4.2.4.1	The back-propagation technique.	... 65
4.2.4.2	A hybrid system for fuzzy identification – ANFIS	... 66
4.2.4.3	A radial basis function approach with rule generation.	... 67
4.2.5	Fuzzy clustering techniques.	... 68
4.2.5.1	Motivation for use of clustering techniques.	... 68
4.2.5.2	Clustering algorithms.	... 69
4.3	Summary and conclusions.	... 72

SECTION 2: The Case Study

Chapter 5. The Case Study: An Introduction ... 74

5.1	Introduction.	... 75
5.2	A review of section 1	... 76
5.3	The applicability of fuzzy systems to CMFD.	... 77
5.4	The case study: Objectives	... 78
5.5	The case study: A justification	... 79
5.6	Summary	... 81

Chapter 6. Experimental arrangements ... 82

6.1.	Introduction	... 83
6.2.	Diesel generator test-bed description	... 84
6.3.	Sub-division of diesel engine into appropriate sub-systems.	... 84
6.4.	Prioritisation of the case study	... 85
6.5.	Diesel engine sub-System characteristics	... 87
6.5.1	The combustion system.	... 87
6.5.2	The cooling system.	... 89
6.5.3	The aspiration and exhaust systems.	... 91
6.6.	Additional instrumentation: Celesco smoke detector.	... 92
6.7.	Data acquisition and signal processing for fuzzy model identification.	... 93
6.8.	Data acquisition hardware and software.	... 95
6.9.	Models and estimators: Definitions	... 95
6.10.	Concluding remarks.	... 96

Chapter 7. Fuzzy model based condition monitoring and fault diagnosis of a diesel engine cooling system	... 97
7.1 Introduction.	... 98
7.2 Fuzzy model format.	... 98
7.3 Cooling system description.	... 99
7.4. Fuzzy model based CMFD for a diesel engine cooling system: An overview.	... 101
7.5. Development of the fuzzy thermostatic valve model.	... 106
7.6. Estimation of radiator coolant flow rate from temperature measurements.	... 108
7.7. Fuzzy models for coolant temperature differences across engine block and radiator.	... 111
7.8. Estimation of confidence weights.	... 113
7.9. Results.	... 117
7.10. Discussion.	... 118
7.11. Conclusions.	... 121

Chapter 8. A high level technique for engine combustion system condition monitoring and fault diagnosis	... 123
8.1 Introduction.	... 124
8.2 Development of fuzzy systems for estimation of engine load.	... 126
8.2.1 Load estimation from frequency analysis of the speed signal.	... 126
8.2.2 Load estimation from air fuel ratio.	... 129
8.3 Implementation and testing of load estimator under normal and fault conditions.	... 130
8.4 Development of a fuzzy reference model for engine speed fluctuations.	... 133
8.5 Development of a fuzzy reference model	

	for boost pressure fluctuations.	... 134
8.6	Implementation and testing of engine speed and boost pressure reference models under normal and fault conditions.	... 136
8.7	The proposed high-level diagnostic system.	... 138
8.8	Discussion.	... 142
8.9	Conclusions.	... 143

Chapter 9. Fuzzy model-based condition monitoring and fault diagnosis for the aspiration and exhaust systems of a turbocharged diesel engine. ... 145

9.1	Introduction	... 146
9.2	Theoretical review	... 146
	9.2.1 The air filter	... 146
	9.2.2 The turbocharger	... 148
	9.2.3 Exhaust system pipework.	... 149
9.3	Potential faults and symptoms in aspiration and exhaust systems	... 150
9.4	Specification of reference models for fault diagnosis.	... 152
	9.4.1 Air inlet filter model.	... 152
	9.4.2 Turbine mass flow estimator.	... 153
	9.4.3 Exhaust pipe-work differential pressure model.	... 153
9.5	Generation of reference models.	... 154
9.6	Rules for classification and reasoning.	... 158
	9.6.1 Residual classifiers.	... 158
	9.6.2 Development of diagnostic reasoning.	... 159
	9.6.3 Concluding remarks.	... 164
9.7	Aspiration and exhaust system test results.	... 165
9.8	Discussion.	... 169
9.9	Conclusions.	... 174

SECTION 3: Analysis of results from the case study

Chapter 10. Discussion	... 176
10.1. Introduction.	... 177
10.2. Application of fuzzy systems in CMFD.	... 179
10.2.1 An assessment of fuzzy systems as models or state estimators.	... 180
10.2.2 Qualitative comparison with other techniques for modelling and state estimation.	... 183
10.2.3 Robustness issues in fuzzy models for diagnosis.	... 188
10.2.4 Fuzzy systems in classification and reasoning.	... 190
10.3 A discussion of diesel engine CMFD.	... 192
10.3.1 A discussion of diesel engine sub-system CMFD results.	... 192
10.3.2 Applicability of results to variable speed diesel engines.	... 197
10.3.3 Structural issues in diesel engine CMFD.	... 198
10.3.4 Applications: Practical issues.	... 199
10.4 Concluding remarks.	... 201
Chapter 11. Conclusions.	... 203
Chapter 12. Further work.	... 207
12.1 A cost benefit analysis.	... 208
12.2 Development of knowledge sources for additional systems and components.	... 208
12.3 Explore the inter-action between diesel engine controller CMFD	... 209
12.4 A cause and effect analysis.	... 209
12.5 Test the applicability of diesel engine CMFD systems to variable	

speed engines.	... 209
12.6 Explore other techniques for fuzzy set definition in residual classifiers	... 209
12.7 Estimation of mechanical efficiency in generator sets	...210
<hr/>	
References.	... 212
<hr/>	
Appendices.	... 224
<hr/>	
Appendix 1. Details of Diesel Generator Test-bed.	... 224
A1.1 Generator set test-bed photos.	... 225
A1.2 ‘Electropak’ 1004TG diesel engine data sheets.	... 227
A1.3 Generator set data sheet and description.	... 231
A1.4 Crestchic load bank data sheet.	... 233
Appendix 2. Test Bed Instrumentation.	... 234
A2.1 Instrumentation schematics.	... 235
A2.2 Instrumentation calibration report.	... 239
A2.3 Electronic fuel meter calibration.	... 240
A2.4 Electronic air flow meter calibration.	... 248
A2.5 Smoke meter calibration.	... 251
A2.6 Indication of crank angle with respect to four-stroke cycle.	... 253
A2.7 Specification of sample rates for acquisition of temperature data from diesel engine cooling system.	... 256
A2.8 Correction factors for radiator coolant flow calculation.	... 261
Appendix 3. Cooling system non-linear model validation results.	... 272
Appendix 4. Index of data files.	... 327

LIST OF FIGURES AND CAPTIONS

LIST OF FIGURES AND CAPTIONS

CHAPTER 1.	PAGE
Figure 1.1. Generic fault diagnosis scheme.	... 9
Figure 1.2. Model-based fault diagnosis schematic.	... 13
Figure 1.3. Blackboard systems schematic.	... 19
 CHAPTER 2.	
Figure 2.1. Examples of logic gates.	... 30
Figure 2.2. Crisp (non-fuzzy) membership functions.	... 33
Figure 2.3. Fuzzy membership functions.	... 34
 CHAPTER 3.	
Figure 3.1. An overview of a generic fuzzy system.	... 40
Figure 3.2. The action of the minimum implication on two fuzzy rules.	... 49
Figure 3.3. The action of the product implication on two fuzzy rules.	... 49
Figure 3.4. Aggregation: Algebraic sum.	... 50
Figure 3.5. Aggregation: Max.	... 50
Figure 3.6. Aggregation: Sum.	... 50
Figure 3.7. Centre average defuzzification.	... 52
Figure 3.8. Centre of gravity defuzzification.	... 53
Figure 3.9. Maximum defuzzification.	... 53
 CHAPTER 4.	
Figure 4.1. A schematic of a generic fuzzy training algorithm.	... 61
Figure 4.2. A comparison of clustering and grid partitioning.	... 71
 CHAPTER 7.	
Figure 7.1. A schematic showing the components and instrumentation in the diesel engine cooling system.	... 100

LIST OF FIGURES AND CAPTIONS

Figure 7.2.	A schematic showing the structure of the models and the diagnostic system.	... 103
Figure 7.3.	Membership functions for residual classes.	... 104
Figure 7.4a.	Shows a comparison between thermostat valve model and estimator outputs compared with a set of measured set of test data.	... 106
Figure 7.4b.	Shows the model error as a percentage of maximum flow rate.	... 106
Figure 7.5.	Procedure for generation of fuzzy systems for assignment of confidence weights.	... 116
Figure 7.6.	A Schematic for the on-line estimation of confidence weights.	... 116
Figure 7.7.	Diagnosis vector, D , for test data obtained for normal condition A, shown with the confidence weighting and the estimated radiator volume flow rate, \tilde{V}_r (%).	... 118
CHAPTER 8.		
Figure 8.1.	Ensemble averaged speed fluctuations vs. crank angle.	... 127
Figure 8.2.	Plot of relationships between P.S.D. of engine speed and engine load.	... 128
Figure 8.3.	Schematic of load estimation procedure.	... 129
Figure 8.4.	Relationship between measured air-fuel ratio and engine load.	... 130
Figure 8.5.	Comparison of estimated and applied engine load under normal operating conditions.	... 131
Figure 8.6.	Comparison of load estimates with engine operating under combustion fault condition, C1.	... 132
Figure 8.7.	Plot of averaged engine speed fluctuations with respect to crank angle for normal condition and combustion fault, C1, applied to cylinder 3.	... 133
Figure 8.8.	Schematic of fuzzy speed reference model.	... 134
Figure 8.9.	Comparison of predictive speed model outputs and measured speed fluctuations.	... 135
Figure 8.10.	Plot of averaged speed residual vs crank angle for combustion fault C1 applied to cylinder 3.	... 135

LIST OF FIGURES AND CAPTIONS

Figure 8.11.	Plot of averaged speed residual vs crank angle for inlet valve fault C2. applied to cylinder 4.	... 136
Figure 8.12.	Plots of averaged rms. speed residual values vs. applied resistive load.	... 137
Figure 8.13.	Plots of averaged rms. boost pressure residual values vs. applied resistive load.	... 138
Figure 8.14.	Schematic for the proposed diagnostic scheme.	... 139
CHAPTER 9.		
Figure 9.1.	Example of a Compressor map.	... 150
Figure 9.2.	Comparison of estimated mass flow rate \hat{m}_{exh} through turbocharger compared with sum of measured values for fuel and air mass flow rates with engine in fault free condition.	... 155
Figure 9.3.	Comparison of measured and estimated exhaust pressure differential ΔP_{eo} with engine in fault free condition.	... 156
Figure 9.4.	Comparison of measured and estimated filter pressure differentials ΔP_{af} with engine in its fault free condition.	... 156
Figure 9.5.	Plot of fuzzy classifier membership functions for <i>Negative</i> , <i>Normal</i> and <i>Positive</i> residual classes.	... 160
Figure 9.6.	Plot of fuel volume flow rate vs. applied resistive load for six engine conditions.	... 161
Figure 9.7.	Plot of air mass flow rate vs. applied resistive load for six engine conditions.	... 161
Figure 9.8.	Plot of air fuel ratio vs. applied resistive load for six engine conditions.	... 162
Figure 9.9.	Aspiration and exhaust system diagnosis tests: Typical profile of typical applied resistive load.	... 167
Figure 9.10.	Diagnostic processes for intermittent air inlet manifold leak, d11data file d11_f2_0112.	... 169

LIST OF FIGURES AND CAPTIONS

CHAPTER 10.

- Figure 10.1** Comparison of diagnostic results from three knowledge sources for an intermittent low coolant flow fault. ... 184
- Figure 10.2.** Comparison of estimates of applied load obtained via look-up table and fuzzy mapping. ... 187

LIST OF TABLES	PAGE
Table 1.1. Available instrumentation	... 7
Table 2.1. Examples of Boolean logic truth tables	... 30
Table 3.1. Summary of selected fuzzy membership functions	... 43
Table 3.2. Truth table for the classical proposition if p then q 47
Table 6.1. List of diesel engine sub-systems and components.	... 85
Table 7.1. Residual classes for stage 2 diagnostic rules.	... 105
Table 7.2. Results table for conditions A – D.	... 120
Table 8.1. Confusion matrix of diagnostic results.	... 140
Table 8.2. Fuzzy rules for diagnostic reasoning.	... 141
Table 9.1. Aspiration system condition descriptions.	... 151
Table 9.2. Aspiration and exhaust system model test errors.	... 157
Table 9.3. Aspiration and exhaust system diagnostic rules.	... 164
Table 9.4. Aspiration and exhaust system fault data file descriptions.	... 165
Table 9.5. Aspiration and exhaust system test results confusion matrix.	... 168

INTRODUCTION.

Diesel engines have become a common source of power, both for vehicles and for static equipment because they are fuel efficient, robust and reliable. It is important that diesel engines run in their correct condition and properly controlled in order to maintain efficiency, low emissions levels and high reliability. A research project has been instigated to bring together modern techniques in diagnostics and control to provide good control, as well as monitoring for incipient faults in diesel engine systems.

The research project is undertaken by a small group of researchers, supported by the EPSRC and Perkins Engine Company Ltd [Grant Ref. GR/L42018]. Each of the researchers undertake roles pertaining to different aspects of the project, drawing upon results obtained from the use of blackboard systems in biomedical diagnosis, robust non-linear sliding mode control and 'soft computing' techniques. Diesel engine sub-systems are complex, non-linear and subject to noise and uncertainty. Diagnoses of faults in these systems are tackled by the use of adaptive models and classifiers. These models have varying levels of detail ranging from the overall system down to sub-systems, components and parts and are described using fuzzy, neural network and sliding-mode techniques.

A study of appropriate techniques for 'data-fusion' is undertaken with the aims of improving the diagnostic success rates by combination of evidence from a number of separate knowledge sources. Neural networks, voting, Dempster-Shafer theory and blackboard systems are considered as suitable techniques for the development of a data-fusion engine.

Part of the scheme involves the design of a non-linear control system. This involves a software "observer" which produces estimates of the state of the system under observation. This observer also provides a source of knowledge for the diagnostic process.

A 65kW diesel powered electrical generator set has been provided for use as a test bed, funded by a Joint Research Equipment Initiative grant [JREI (GR/M30777)] provided by the EPSRC and Perkins Engine Company Ltd. The generator set has been bought 'off the shelf' as an example of a typical application which may benefit from the development of diagnostic and control techniques. One stated aim of the project is to develop diagnostic techniques which require a minimum of additional instrumentation, and that the instrumentation employed should be robust and 'tried and tested' to allow cost effective condition monitoring.

Potential applications include 'on-board' fault diagnosis and control, and condition monitoring of remote diesel engine installations via the world-wide web.

Matlab™, Simulink™ and dSpace™ are employed to design and implement data acquisition systems on a dedicated controller board. This arrangement also allows the design and development of diagnostic systems and controllers within the Matlab/Simulink environment and their speedy implementation to run interactively in real-time with the diesel engine test-bed.

The aim of this thesis is to assess the application of fuzzy systems in real-time condition monitoring and fault diagnosis. Thus within the context of the black-board system the fuzzy systems developed as part of this thesis represent knowledge sources, and their outputs are intended as evidence to be combined with that from other knowledge sources. It is within this context that the application of fuzzy systems will be assessed.

The thesis is divided into three sections. Section 1 consists of a literature review in four chapters. Chapter 1 reviews the application of a range of techniques in fault diagnosis with a particular emphasis on diagnostic techniques for engine systems. The chapter concludes by identifying fuzzy logic techniques as a possible common methodology for model-based fault diagnosis in diesel engine systems. This provides the motivation for chapter 2, 3 and 4, which review literature concerning the origins of fuzzy logic theory,

the function and structure of fuzzy systems and techniques for design and identification of fuzzy systems respectively.

Section 2, containing chapters 5 to 9 (inclusive), report on the test work carried out during the case study. Chapter 5 presents an introduction and, based on the conclusions drawn from section 1, outlines the motivation, aims and objectives for the case study. Chapter 6 describes the practical arrangement of the diesel engine generator set test-bed and its instrumentation. Chapters 7 to 9 present results from diagnostic techniques developed for the cooling, combustion, aspiration and exhaust systems of the diesel engine. Chapters 7 and 8 have been submitted to the I.Mech.E. Proceedings, Section I, for publication as, '*Fuzzy model-based condition monitoring and fault diagnosis of a diesel engine cooling system*', and '*A high level technique for engine combustion system condition monitoring and fault diagnosis*', respectively, and are currently under review. Chapter 9 is being prepared for submission as, '*Fuzzy model-based condition monitoring and fault diagnosis for the aspiration and exhaust systems of a turbocharged diesel engine.*'

The third section of the thesis is the discussion and analysis of results. Chapter 10 comprises a discussion of the results obtained in chapters 7 – 9. This is done both in terms of the application of fuzzy systems in fault diagnosis, and in terms of a qualitative and quantitative comparison of the diagnostic techniques compared with other approaches for condition monitoring and fault diagnosis of engine systems. Chapter 11, draws a number of concise conclusions from these results and chapter 12 itemises further work which could be undertaken, motivated by, or as a continuation of, this thesis.

LIST OF PUBLICATIONS

A number of papers have been published as a direct result of the work undertaken in this project. These publications are listed as follows;

- 1) Bhatti, A.I., Twiddle, J.A., Spurgeon, S.K. and Jones, N.B., *Engine coolant system fault diagnostics with sliding mode observers and fuzzy analyser*, Proc. IASTED International Conference on Modelling, Identification and Control, Innsbruck, Austria, 15-18 February, 1999.
- 2) Jones N.B., Spurgeon S.K., Pont M.J., Twiddle J.A., Lim C.L., Parikh C.H. & Goh K.B., *Aspects of diagnostic schemes for biomedical and engineering systems*. Proc. IEE. Science, Measurement and Technology, 147, 2000, 357 – 362.
- 3) Jones, N. B., Spurgeon, S. K., Pont, M. J., Twiddle, J. A., Lim, C.L., Parikh, C. R. and Goh, K.B. (2000), *Diagnostic Schemes for Biomedical and Engineering Systems*, International Conference on Advances in Medical Signal and Information Processing (MEDSIP 2000), Bristol, pp. 1-8
- 4) Li, Y.H., Pont, M.J., Jones, N.B., Twiddle, J.A. (2001). *Applying MLP and RBF classifiers in embedded condition monitoring and fault diagnosis systems*. to appear in 'Transactions of the Institute of Measurement and Control'. 2001 Volume 23
- 5) Parikh, C.R., Pont, M.J., Jones, N.B., Twiddle, J.A., Bhatti, A.I., Li, Y.H., Spurgeon, S.K, Scotson, P. and Scaife, M, (1998), *Towards an Application Framework for Condition Monitoring and Fault Diagnosis*, Proceedings of: 'Workshop on Recent Advances in Soft Computing', July, pp. 128-141.
- 6) Parikh, C.R., Pont, M.J., Li, Y.H., Jones, N.B., Twiddle, J.A., (1998) *Towards a Flexible Application Framework for Data Fusion using Real-Time Design Patterns*, 6th European Congress on Intelligent Techniques & Soft Computing (EUFIT'98), Germany, pp.1131-1135.

- 7) Twiddle, J.A., Jones, N.B., (2001), *Fuzzy model-based condition monitoring and fault diagnosis of a diesel engine cooling system*. Proc I. Mech. E., (submitted, 1st May. 2001).
- 8) Twiddle, J.A., Jones, N.B., (2001), *A high level technique for diesel engine combustion system condition monitoring and fault diagnosis* (Proc I. Mech. E., - Submitted. August 23rd 2001).
- 9) Twiddle, J.A., Jones, N.B., (2001), *Fuzzy model-based condition monitoring and fault diagnosis for the aspiration and exhaust systems of a turbocharged diesel engine*. (In preparation).

NOTATION

VARIABLE	DESCRIPTION	UNITS (WHERE APPLICABLE)
a	Acceleration	ms^{-2}
a_i	Cooling system non-linear model coefficients. (i=1 - 3)	
e_T	Training error vector	
f	Frequency	Hz
f_s	Sampling frequency	Hz
g	Gravity	ms^{-2}
h	Heat transfer coefficient	$\text{kWm}^{-2}\text{K}^{-1}$
k	Unit time delay	s
k	Scalar constant	
k	Thermal conductivity	$\text{kWm}^{-1}\text{K}^{-1}$
k_{af}	Air filter parameter	
k_i	Correction factors (i=1, 2)	
m	Mass	kg
\dot{m}	Mass flow-rate	kgs^{-1}
\dot{m}_f	Fuel mass flow-rate	kgs^{-1}
\dot{m}_a	Charge air mass flow-rate	kgs^{-1}
m_r, m_b	Mass of coolant contained in radiator and engine block respectively.	kg
\dot{m}_r, \dot{m}_b	Mass flow-rate through radiator and engine block respectively.	kgs^{-1}
r	Crank radius	m
u	Flow velocity	ms^{-1}

NOTATION

A	Area	m^2
A	Piston area	m^2
A_{min}	Minimum free flow area through radiator	m^2
C	Scalar constant	
C	Confidence weight vector	
C_p	Specific heat capacity	$\text{kJkg}^{-1}\text{K}^{-1}$
D	Diagnostic vector	
D_h	Hydraulic diameter	m
F	Shape factor	
G	Mass velocity	$\text{kg s}^{-1}\text{m}^{-2}$
I	Inertia	kgm^2
L	Flow length of radiator	m
N	Engine speed	r.p.m.
N_T	Turbocharger rotational speed	r.p.m.
P	Pressure	bar
P_c	Cylinder pressure	bar
P_1	Coolant pump outlet pressure.	bar
P_2	Engine block coolant outlet pressure	bar
P_3	Radiator coolant outlet pressure	bar
P_{ri}	Radiator inlet pressure	bar
P_{ci}	Air inlet pressure (after filter)	bar
P_b	Boost pressure (air inlet manifold)	bar
P_{ti}	Turbine inlet pressure	bar
P_{to}	Turbine outlet pressure	bar
P_{amb}	Ambient pressure	bar
Pr	Prandtl's number	-
\dot{Q}_{amb}	Heat transfer to ambient from radiator	kW
Q_{HV}	Upper heating value	kJkg^{-1}

NOTATION

\mathbf{R}	Residual vector	
Re	Reynolds' number	-
R_0	Universal gas constant	$\text{kJkmol}^{-1}\text{K}^{-1}$
St	Stanton's number	-
T	Temperature	K
T_1	Coolant pump outlet temperature.	K
T_2	Engine block coolant outlet temperature	K
T_3	Radiator coolant outlet temperature	K
T_a	Air temperature at inlet to generator-set canopy	K
T_{amb}	Air temperature at radiator (average of four signals)	K
T_b	Engine block surface temperature	K
T_B	Brake torque	Nm
T_f	Friction torque	Nm
T_{ti}	Turbine inlet temperature	K
T_{to}	Turbine outlet temperature	K
T_{ri}	Coolant temperature at radiator inlet	K
$T_{0,in}$	Stagnation temperature at turbine inlet	K
\dot{V}	Volume flow-rate	ls^{-1}
\dot{V}_{rad}	Coolant volume flow-rate at radiator inlet	ls^{-1}
\dot{V}_b	Coolant volume flow-rate through block	ls^{-1}
W	Engine load	kW
W_B	Brake load	kW
W_P	Pumping work	kW
\hat{W}_1	Load estimate (speed-based)	kW
\hat{W}_2	Load estimate (AFR-based)	kW
\dot{V}_r, \tilde{V}_r	Measured and estimated coolant volume flow-rate at radiator inlet	ls^{-1}

NOTATION

\dot{V}_b	Coolant volume flow-rate through engine block.	ls ⁻¹
X, U, \hat{Y}	Input and output vectors for fuzzy models and estimators	
Y	Vector of variables corresponding to model outputs	
Δh	Pressure head loss	bar
ΔP_{af}	Air filter differential pressure	bar
ΔP_{eo}	Exhaust outlet differential pressure	bar
ΔT_0	Differential temperature across turbine	K
ΔW_f	Incremental increase in load due to a fault	kW
α	Normalised volume flow rate to radiator	
β_i	Regression coefficients (i=1 - 4)	
Σ	Relative emissivity	
ε_N	Speed error (measured speed – 1500r.p.m.)	r.p.m.
ε	Model error	
λ	Arbitrary constant for parameter estimation	
ν	Dynamic viscosity	m ² s ⁻¹
ϕ_i	Parameterised temperature variable	
ϕ	Crank angle	Degrees °
σ	Boltzmann's constant	kWm ⁻² K ⁻⁴
σ	Standard deviation	
ρ	Density	kgm ⁻³
ρ_s	Smoke density	m ⁻¹
ρ_c	Coolant density	kg/m ³
η_c	Combustion efficiency	

NOTATION

η_m	Mechanical efficiency	
η_f	Thermal conversion efficiency	
η_T	Turbine efficiency	
$\mu(\cdot)$	Fuzzy membership function	
μ	Coefficient of molecular viscosity	Pa.s
ω	Crank shaft speed	rad/s

SECTION 1. Literature Review

CHAPTER 1.

**Techniques for Condition Monitoring and Fault Diagnosis
of Diesel Engine Systems: A Review**

1. TECHNIQUES FOR CONDITION MONITORING AND FAULT DIAGNOSIS OF DIESEL ENGINE SYSTEMS: A REVIEW

The introduction to this chapter briefly outlines the history of the diesel engine noting the increase in its complexity and its use in a wide range of applications. The commercial, and environmental pressures facing both the manufacturers and operators of diesel engines are noted and the need for effective condition monitoring and fault diagnosis of engine systems is stated.

A review of methodologies for condition monitoring and fault diagnosis is presented in section 1.6. The emphasis of the review is based on the stated objective, that is: To develop techniques suitable for an *on-board* condition monitoring and fault diagnosis (CMFD) system for a diesel engine application. What is meant by *on-board* is that the CMFD system should be capable of being autonomously fitted to, and continuously monitoring the engine under its normal day-to-day working conditions.

The conclusion of the chapter is to outline the general requirements for an on-board diagnostic system in terms of its function and benefit to the engine operator, and propose a suitable structure for this system.

1.1 INTRODUCTION TO DIESEL ENGINE SYSTEMS

The history of the diesel or compression ignition (CI) engine now goes back over one hundred years to the late 19th century. Combustion in the diesel engine is achieved via auto-ignition of a fuel/air mixture due to a temperature rise under compression in the cylinder. Today, although this basic principle remains unchanged, the complexity of diesel engine systems has increased enormously. The diesel engine has been proven to be capable of a vast range of applications and has demonstrated benefits not only in terms of its adaptability, but also in fuel economy, power output, robustness and reliability. Amongst its many applications are as a power-plant for automotive, rail and marine transport, as a prime mover for power generation [Mahon 93] and other stationary plant, and also in many types of agricultural and construction equipment.

Advances in materials and engine design and construction have led to greater reliability and robustness, and also to improvements in combustion efficiency, by allowing the increase of compression ratios and improvements in fuel/air mixing. Application of such techniques as supercharging, turbo-charging, turbo-compounding and charge cooling have increased specific power outputs for the diesel engine.

Combustion cycle strategies have evolved to suit different applications and several variations exist, including the two stroke cycle, sometimes used in marine and stationary applications, the four stroke cycle, used in the majority of applications, direct injection as used in larger engines and indirect injection as used on smaller higher speed units. Analysis of engine systems has led to improvements in lubrication and cooling techniques and ever more stringent emissions legislation has led to developments in areas such as electronic fuel control and exhaust gas recirculation with the aim of reducing the level of pollutants.

The companies that mass-produce modern diesel engines operate in a fiercely competitive commercial environment. Production methods are constantly under review to maintain and improve the quality of the product, reduce design and manufacturing timescales, improve efficiency, and of course, maximise profits. Increased use of

computer technology has helped in this respect, but increased use of computer control in diesel engine applications has resulted in more complex customer requirements and specifications. Turn-around time from receipt of order from the customer, to the first delivery may be as little as three months increasing the pressure on the manufacturer to minimise the time required for product design.

The notion of *availability* refers to the proportion of the time when an engine is capable of doing useful work at full capacity. Consequently the engine's availability is reduced when the engine is broken down or if frequent maintenance is required or when the engine is forced to operate for periods of time with a fault or impairment that reduces its efficiency or performance. The end user of the diesel engine also operates under commercial pressures and demands availability, reliability and maintainability for the purchased engine, as the success, or even existence of the business may depend on it.

1.2 THE NEED FOR CONDITION MONITORING AND FAULT DIAGNOSIS

Physical degradation of any mechanical plant continuously occurs due to everyday wear and tear. Thus, the purpose of condition monitoring is to ensure that any degradation does not impair the safety, efficacy, efficiency or environmental impact of the plant.

There are clear benefits to be obtained from employing some form of fault detection and isolation strategy to either diagnose faults at an early stage, before they have time to propagate, or better still, to predict the fault before it occurs. Successful fault diagnosis allows improved scheduling of maintenance or repair time, thereby maximising the availability of the engine, or it may allow the system to switch to an alternative mode of operation, bypassing the faulty component or sub-system.

Increasingly strict environmental legislation [Eastwood 00], means that tight emissions standards must be adhered to. Suitable fault diagnosis techniques may also be employed to indicate faults that might impair the ability of the engine to meet these standards.

1.3 AN OVERVIEW OF CONDITION MONITORING

Methodologies in use for collecting engine data are generally dependent on the type of plant involved and its operational characteristics. Techniques may range from an operator with a checklist inspecting the engine on a regular basis, to a sophisticated instrumentation and signal processing system.

Data for engine analysis can be obtained from numerous sources, e.g. maintenance history, oil analysis, vibrations and spectrum analysis, logged operating data or inspections. Typically the engine manufacturer will supply documents containing appropriate maintenance schedules and checklists [Perkins 95], but these are also available in a number of texts, [Lilly 84], [Thiessen 82], [Long 96], [Mahon 92].

An inspection checklist is a source of knowledge comprising several different types of information, both qualitative and quantitative. The methods of acquiring the data may involve *on-line* or *off-line* monitoring and analysis. For instance, temperature or pressure data are continuously recorded and may be acquired on-line. However, detailed analysis of lubrication oil by methods such as mass spectroscopy [Fitch 99], to assess wear of internal engine components, is necessarily carried out off-line, i.e. away from the running engine, due to the size and complexity of the apparatus involved. Visual inspections may necessitate shut down of the engine and in major services, a full strip-down to component level to investigate wear or damage. In the case of vehicle engines, for instance, some other tests may be carried out with the engine running but temporarily taken out of service, or put on a test stand. Examples of this type of testing may include monitoring of emissions or noise. In concordance with the stated objectives of this thesis, the emphasis of this chapter will be placed on those on-line methods that may be suited to inclusion in an on-board diagnostic system.

1.4 SELECTION OF APPROPRIATE TRANSDUCERS AND MEASURANDS FOR CONDITION MONITORING.

The diesel engine may be considered as a number of different subsystems, either fluid, mechanical or electrical. Each one of these sub-systems performs some function within

the engine and is characterised by certain parameters. Clearly, the choice of which states or parameters are the most appropriate for measurement or estimation, will be a trade-off for the user between cost and functionality.

The first consideration is; what will the data be used for? The first priority is to monitor variables from the engine that indicate danger to the operator or to the engine itself, i.e. a set of data to initiate alarms. This may include over-speed or over-temperature alarms, for example, based on speed and temperature signals. Beyond that, it is clearly important to provide information such as coolant and lubricant levels to the user to allow regular maintenance to be carried out. Provision of this small number of alarm and condition signals is sufficient to allow a user, for example, the driver of a family car, to operate an engine safely and effectively by combining their knowledge and experience to both to control the engine and schedule maintenance as appropriate.

In other applications a more systematic approach to condition monitoring may be called for to acquire data which may be analysed with a view to scheduling maintenance, improving efficiency, detecting faults, reducing operating costs, checking performance or meeting emissions standards. Once the specific data requirements are known a variety of different sensors and transducers are available to make the measurements (see table 1.1).

The sensors listed in table 1.1, range in price from relatively cheap (relative to the cost of the engine) such as thermocouples, up to the price of a cylinder pressure measurement transducer or a needle lift transducer, which have prices of approximately £2-3,000 pounds each (2001 prices). Torque measurement on board a vehicle is expensive and difficult to arrange in practice, requiring slip-rings or telemetry to transmit the measurement from a strain gauge mounted on the rotating drive shaft [Jewitt 85]. Exhaust gas emissions monitoring equipment is also prohibitively expensive (at approximately £10-20,000) for consideration for an on board system.

Table 1.1 Available Instrumentation

Instrumentation Description	Measurand
Pressure transducer	Pressures
Thermocouple / Platinum resistance thermometers	Temperatures
Calibrated turbine	Mass flow rate (coolant)
Accelerometer	Vibration (External)
Shaft position encoder	Shaft speed
Torque transducer	Torque
LED/ detector	Smoke opacity
O ₂ meter	Oxygen in exhaust
Displacement transducer	Injector needle lift
Hot wire anemometer	Inlet air flow rate
Flow meter	Fuel flow rate
Hall effect transducer	Flywheel/crank-angle datum
Level gauge	Oil/fuel/coolant levels

It may seem that because such a wide range of transducers is available, that the task of fault diagnosis could be minimised by increasing the numbers of transducers so that a comprehensive picture of engine condition may be obtained from transducer signals alone. However, the prices of certain transducers indicate that this will not always be a cost-effective solution (see section 1.5). For instance, to obtain a full picture of cylinder pressure will clearly require a cylinder pressure transducer for each cylinder. For smaller engines, the cost of such provision is likely to be large compared to the price of the engine itself. Similarly, if the life expectancy of the transducer is less than that of the engine, then the cost of the replacement transducer and loss of engine availability whilst the replacement is fitted will also have an impact.

In summary, the selection of transducers should be sufficient to provide sufficient information to a diagnostic system to allow it perform the CMFD task to some specified level of detail. The selected transducers should be low cost with respect to the engine

and where possible, include information obtainable from the standard instrumentation set typically supplied with the engine. Qualities of robustness and practicality are also requirements for the selected transducers.

1.5 COST BENEFIT OF ON-BOARD CMFD

Of primary interest to the engine operator will be financial considerations in terms of costs and profit. Profit may be lost if the engine is unavailable for work through breakdown or other unexpected fault, and additional cost will be incurred if the engine runs inefficiently. This may also have an impact on the engine manufacturer - if the unit is under warranty for instance, or by loss of good reputation. If the CMFD system is proven to be successful then it will certainly be a useful addition to the company's product range.

Beneficial aspects of an effective CMFD system may be to reduce down time or to increase time between scheduled overhauls. One criterion for a viable CMFD system will be to consider the potential savings due to increased availability and more effective targeting of maintenance against potential faults, versus the cost of installation and operation of the CMFD system. Cost criteria for an on board monitoring and diagnostic system are considered by York [York 85]. York suggests that the justification for the cost of fitting such a system to an engine depends on the engine size, operating environment and existing standard of maintenance. Further justifications for the additional cost of on-board CMFD include its use in safety critical applications, e.g. hospital auxiliary power supplies or in remote applications, where costs of transport and fitting of replacement parts may be significant.

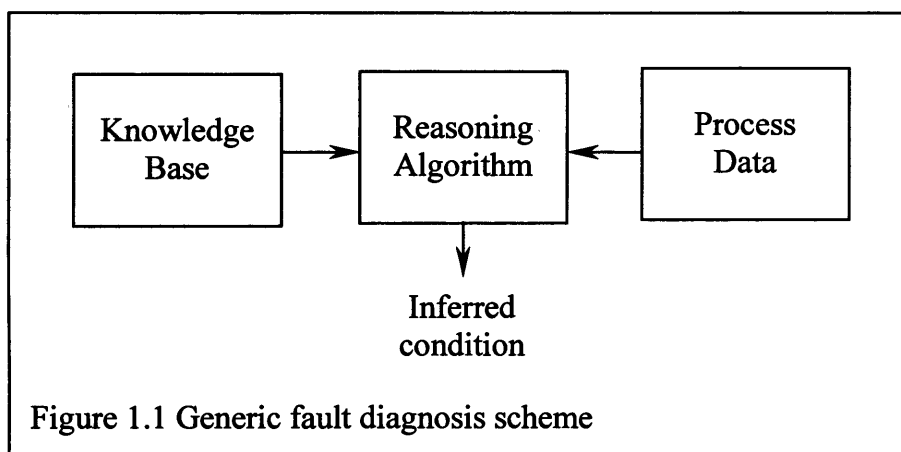
Karpman and Dubuisson [Karpman 85] present an index of complexity for system diagnosability. This approach assumes that the probability of failure for all components in the system is known and that costs of replacement and loss of system availability may be quantified. The index of complexity is based on the number of detectors in the system with an index equal to zero in the situation where each component in the system has an

appropriate detector associated with it. A method is then proposed to optimise the index of complexity with respect to cost benefit of early diagnosis of the system.

1.6 FAULT DIAGNOSIS TECHNIQUES.

The role of a diagnosis system, to infer the fault based on the available symptoms, has already been established. A number of automated schemes have been used to carry out the translation from symptom data to fault diagnosis.

The generic approach to fault diagnosis is to form a knowledge base containing information regarding the subject plant or process, and analyse data acquired with respect to the information contained within the knowledge base using an appropriate reasoning algorithm. The output from the reasoning algorithm is then a statement of the inferred engine condition (see figure 1.1)



This pattern has a number of different realisations, including that of a maintenance engineer who builds up a knowledge base through experience and structured learning from books, manuals, etc., and uses his or her powers of reasoning to deduce faults based on the information obtained via sight, hearing, smell, etc.

Automated CMFD systems vary in the type of structure employed for storage of knowledge, the techniques employed in the reasoning algorithm and the specific data required to obtain the results. Structures for the knowledge base include models, fault trees, data limits or thresholds, design information, signal spectra etc. Techniques for

implementation of reasoning algorithms include fuzzy or Boolean logic rules and heuristics. Whilst some systems may be developed from sampled process data, possible sources of qualitative information to generate the knowledge base include maintenance engineers and operators with experience in recognising fault symptoms, maintenance and repair reports or from other existing information, such as fault trees, maintenance manuals, etc.

Neural networks and fuzzy systems have been employed as classifiers to analyse raw engine data in order to associate the data patterns with certain fault conditions (section 1.6.3). In this approach, training the classifier with suitable data generates a store of information concerning the system which may be regarded as a *knowledge base*. In a primary neural network classifier, that is, one used for analysis of primary or raw data, the knowledge base and reasoning algorithm are contained within the same structure.

CMFD based on analysis of various signal spectra is reviewed in section 1.6.2. A review of model based techniques for state and parameter estimation is presented in section 1.6.4. Expert systems used for fault diagnosis will be reviewed in section 1.6.5. This type of system typically combines inputs from a number of different sub-systems that may include those described in sections 1.6.2 to 1.6.4.

Where only the outputs of the plant are available for analysis, then statistical methods present a potential solution to the problems of fault detection and isolation. Basic approaches include limit checking of monitored variables [York 85] or imposing thresholds on signal variance, for instance, to detect the deviation of the signal from the norm.

1.6.1 DEFINITIONS

Some initial definitions are useful to explain the concept of a condition monitoring and fault diagnosis system. Terminology in some of the subject areas considered here is non-uniform although a very good definition of terms used in CMFD is summarised by

Isermann [Isermann 97]. From Isermann's list of definitions, the following are particularly relevant at this stage;

- *Fault*: An unpermitted deviation of at least one characteristic parameter of the system from the acceptable/usual/standard condition.
- *Fault Diagnosis*: Determination of the kind, size, location and time of detection of a fault.
- *Monitoring*: a continuous real time task of determining the conditions of a physical system, by recording information, recognising and indicating anomalies in behaviour.
- *Residual*: A fault indicator based on a deviation between measurement and model-equation based parameters.
- *Symptom*: A change of an observable quantity from normal behaviour (due to a fault).

1.6.2 SPECTRAL ANALYSIS TECHNIQUES IN FAULT DIAGNOSIS

Analysis of the frequency spectrum of a monitored variable may also reveal useful information for fault identification. A fault condition is a potential cause of a change in the frequency spectrum of a signal.

Signal processing and analysis has been used as the basis for several proposed schemes for fault diagnosis in IC engines. The vibration of a body such as an engine block is a result of dynamic or transient forces acting on the body. Acquisition and analysis of vibration data can be used to derive information about those forces. An example of this technique is cylinder pressure reconstruction from analysis of the engine block vibrations, and has been suggested by a number of authors including Ordubadi [Ordubadi 82], Lyon and DeJong [Lyon 84] and Lynch [Lynch 92]. Ordubadi presents a comparison of the reconstructed pressure waveform from the normally operating engine and a waveform obtained from a cylinder with an injector leak is undertaken, although no classification algorithm is presented.

Faults occurring in the cylinder e.g. misfire or blow-by, cause change in the spectrum of the measured signal. Zhang et al [Zhang 98] use a fuzzy analysis of engine vibration data to detect blow-by in the engine cylinder. Li et al [Li 99] apply spectral and wavelet analysis to an accelerometer data from a six-cylinder SI engine. Results from these two techniques are analysed with a neural network classifier trained to differentiate between normal (fault free) operation and misfire in the engine.

1.6.3 CLASSIFICATION TECHNIQUES

Pattern classification techniques are an alternative approach to fault diagnosis. The classifier, which may be an Artificial Neural Network (ANN) or fuzzy system, for instance, is trained to look for patterns in the measurement vectors that are indicative of certain faults. Parikh *et al* [Parikh 98] use this approach to analyse primary (raw) measurement data other authors use classification techniques to analyse secondary data such as spectral or wavelet data [Li 99]. Meiler and Maas use an ANN system to analyse crankshaft torsional vibration for cylinder fault diagnosis of a marine diesel engine [Meiler 97].

It is necessary to train the ANN with examples of the fault patterns prior to use and because of this the ANN may be thought of as containing the elements of both the model and inference system within the network structure. The output from such a system may be in the form of a ranking vector for a set of possible faults, or other combination of a linguistic fault variable with a likelihood or confidence value.

The fault diagnosis system must be provided with sufficient *a priori* information to diagnose the set of target faults. For a classification technique this may mean a set of training data containing the fault symptom patterns to be recognised. The data may be acquired from actual operation of the system under consideration, or fault simulation via testing. Clearly, acquisition of suitable fault data may be a problem for certain faults where the fault is potentially damaging to the test bed. Parikh et al [Parikh 99] address the problem where only relatively small amounts of fault data are available by use of an 'equal weighting algorithm' or duplication of training data. This research showed that

the best classification results are obtained from classifiers that have been trained with equal amounts of normal and fault data. This is a result of the fact the training algorithms use a training error-based objective function. Where there are unequal amounts of data in certain classes, the minimisation of the objective function is more heavily dependent on the minimisation of the largest class so that the smallest class may not be well represented by the final network.

1.6.4 MODEL BASED TECHNIQUES FOR FAULT DIAGNOSIS

The most common approach to fault detection and diagnosis is to employ an appropriate process model for the generation of residuals. A typical system schematic is shown in figure 1.2. Residuals are then analysed with a decision making or inference system uses some pre-programmed knowledge base, or set of rules derived from quantitative or qualitative knowledge of the system, to infer the system condition.

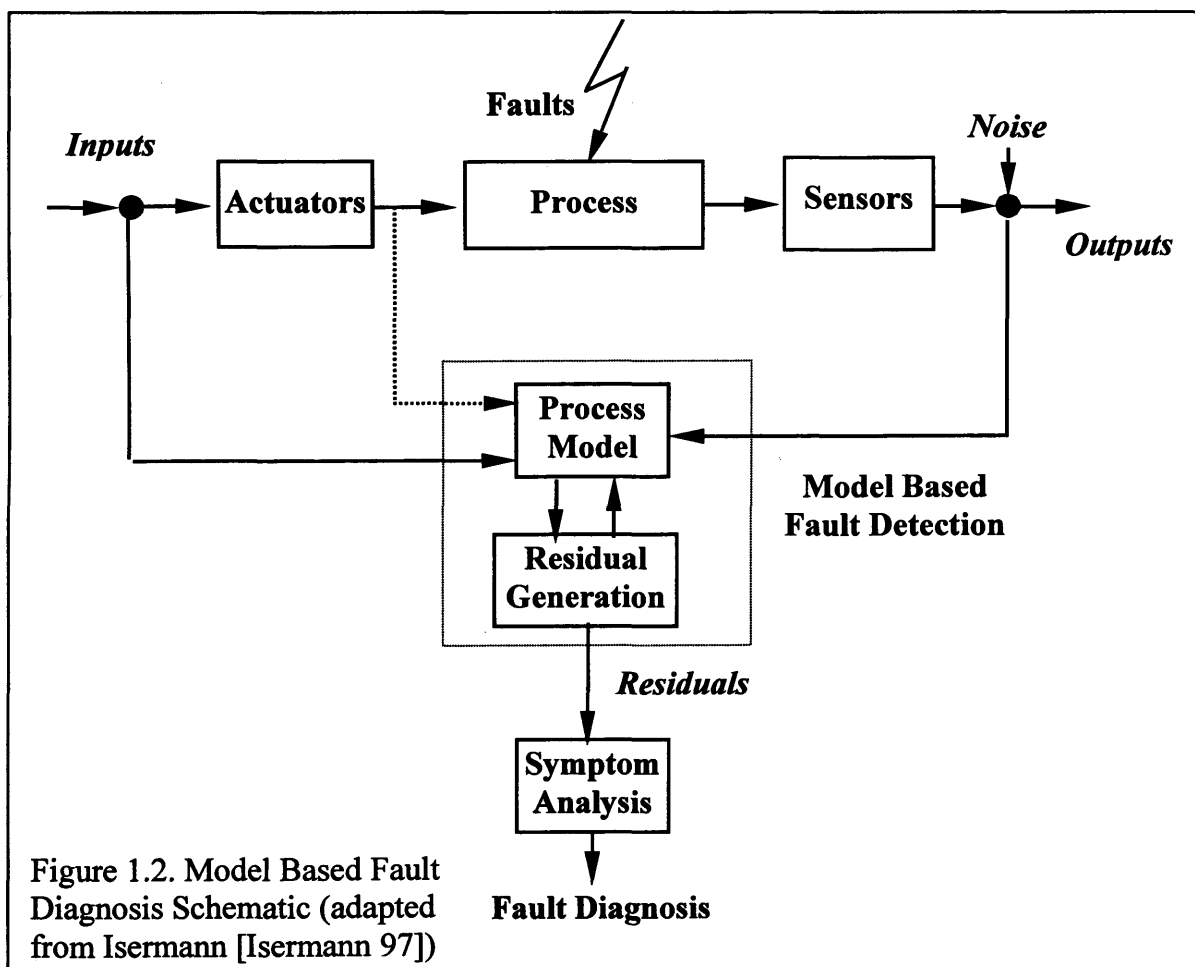


Figure 1.2. Model Based Fault Diagnosis Schematic (adapted from Isermann [Isermann 97])

Residuals to detect sensor faults may be generated by introducing hardware redundancy, i.e. duplication of sensors for a particular measurand and using a majority voting technique for measurement. Chow and Willsky [Chow 84] point out that although hardware or 'direct' redundancy may be useful for detection of sensor failures, it is ineffective for actuator faults.

In the case of hardware redundancy, a residual is generated when one of the sensors sustains a fault. Obviously a further disadvantage of hardware redundancy is increased costs from duplication of sensors. Also, the fact that the duplicate sensors being used will have a similar life expectancy is also a disadvantage. Thus, where hardware redundancy has been used, it is often found that when a sensor fails the duplicate sensors that have been exposed to the same environment often fail at more or less the same time. Chow and Willsky go on to describe the concept of *analytical redundancy*, a technique where a different sensor is employed to measure a second variable, from which the first variable may be analytically inferred, e.g. pressure and temperature. Essentially, this encapsulates the concept of model-based fault diagnosis.

1.6.4.1 MODEL SELECTION

Selection of the appropriate model depends very much on the type of plant to be modelled and the designers' knowledge of the plant processes involved. Prime considerations will be the ability to accurately and robustly estimate the required states over the entire operating range of the plant. However, all models suffer from uncertainty in some way.

1.6.4.2 IDENTIFICATION AND PARAMETER ESTIMATION

If theoretical models are available for the subject system, then the model parameters may be estimated from available data. This technique may be applied even to non-linear systems where the structure is known. However, in a *black box* system, where inputs and outputs are available but the model structure is unknown, a large number of possible candidate structures exist and the task of correctly identifying the system may become insurmountably large.

Least-squares parameter estimation provides a methodology for identification of non-linear systems, and estimated parameters may be used to monitor the condition of the plant. Similarly instrument parameters may also be estimated to give indication of measurement system failures. Luh and Rizzoni [Luh 94] employ a Non-linear Autoregressive Moving-Average Model with Exogenous Outputs (NARMAX), originated by Leontaritis and Billings [Leontaritis 85a and 85b], with an orthogonal, least squares estimator for non-linear systems. This method was used to identify spark ignition (SI) engine models for throttle opening, load torque, speed and a number of other parameters. The models were identified for use in emissions diagnostics as part of the I/M240 emissions test schedule that is designed to test for compliance with emissions standards over a prescribed driving cycle. The least squares estimation technique has also been used to estimate the parameters of harmonic torque fluctuation and total engine inertia to detect fuel delivery faults in a two-stroke diesel engine fault diagnosis scheme [Constantinescu 95]

In his Ph.D. thesis Molteburg [Molteburg 91] develops a set of mathematical models for components of the engine system. A number of parameter estimation techniques of the models are then assessed. A series of faults are simulated experimentally on the test engine. Estimated parameters are compared with those obtained from those obtained from the engine running in the normal state. The thesis concludes that parameter estimation using the Gauss-Newton method is a useful tool for condition monitoring and fault diagnosis, in that certain faults are successfully detected. Problems arise from measurement errors for certain model inputs – particularly from lack of a reliable estimate of engine load and unreliable cylinder pressure measurements. The author recommends using alternative means, such as crank friction parameter or instantaneous engine speed measurements, to test for faults that are otherwise indicated by cylinder pressure. Other limitations are the fact that particular processes in the engine such as blow-by and impulse turbo-charging are not well understood. Also the model employed for flow through a valve port proved to be numerically unstable.

Several authors have used fuzzy logic techniques to identify diagnostic models. Examples of this approach will be considered in section 1.6.5

1.6.4.3 STATE AND OUTPUT OBSERVERS

Certain plant states are known to be non-measurable. Moreover, knowledge of these states may reveal important information regarding the operating condition of the plant. In a linear plant model, or one that may be linearised about an operating point and represented using the state space method, it is possible that plant states may be estimated using a Luenberger observer [Luenberger 71]. In order to confirm that this technique will be suitable, it is necessary to apply the observability criterion to the system. An example of the use of this approach to fault diagnosis of instrumentation systems is presented in Fault Diagnosis in Dynamic Systems [Patton 89]. In this case the state variable is both measured and estimated and the system is arranged to give an error variable as the difference between the two results. In a noise-free system, a fault is detected when the error variable deviates from zero. However, in a real system, subject to noise and uncertainty, a threshold on the error value is defined to give some suitable trade off between sensitivity and false alarm rate. The disadvantages of the linear observer are the stability problems encountered in dealing with non-linearities, which may render this approach totally unsuitable.

Alternatively, in systems that exhibit significant non-linearities, a sliding-mode observer may be employed in a similar role to the one previously described. The sliding mode technique is an inherently non-linear design method and is known to be robust against model uncertainties whilst providing a means of fault reconstruction. Sliding mode techniques provide CMFD of diesel engine coolant system with a fuzzy analyser [Bhatti 99]. Kao and Moskwa use a sliding mode approach for robust estimation of load and equivalence ratio in an IC engine cylinder [Kao 94].

1.6.4.4 PARITY EQUATIONS

Chow and Willsky describe the development of the parity equations technique [Chow 84]. A linear Auto-Regressive Moving Average ARMA model is identified for the

subject system. Based on this model, a 'parity vector' is defined from a set of functions that characterise actuator inputs and sensor outputs in the system. Two approaches to analysing the source of the fault are suggested. The first involves voting, a method which identifies the faulty component by analysis of the parity functions. All the functions containing terms in the variable representing the faulty component will be 'violated' by the error term i.e. caused to deviate from their normal state. Thus the signature of each individual failure may be derived. The second approach to fault identification lies in using knowledge of the development of failure signatures to model the evolution of failures as a function of time. Modelling the failure patterns in such a way allows the individual fault to be recognised. In the example provided by Chow and Willsky, the parity equation approach is used to provide fault detection and isolation for a set of sensors. The robustness of the technique is dependent on the knowledge of dynamics of the system and hence the stability of the identified model.

Parity equation methods for fault diagnosis have been utilised by a number of authors. Krishnaswami et al [Krishnaswami 94] adapt the parity equation approach to be suitable for a Non-linear Auto-Regressive Moving Average model with eXogenous (NARMAX) model. The fault diagnosis system is applied to an automotive test cycle and used to detect two faults, namely speed sensor calibration fault and throttle setting fault, whilst treating the engine load as an unmeasured disturbance.

1.6.5 FUZZY SYSTEMS IN FAULT DIAGNOSIS

Fuzzy systems have been employed in a variety of roles in fault diagnosis systems, as primary or secondary classifiers, as state estimators and in rule-based diagnosis schemes. The theory and properties of fuzzy systems will be discussed in detail in Chapter 3 of this thesis.

Bhatti et al [Bhatti 98] use a fuzzy system as a secondary classifier for diagnosis of faults in a diesel engine cooling system from parameters estimated using a sliding mode observer. Laukonen et al use a fuzzy clustering approach to produce fuzzy systems for state estimation and residual generation. This system is compared with the NARMAX

models used in the automotive test cycle analysis used by Krishnaswami et al [Krishnaswami 94]. Laukonen concluded that although the systems gave similar results the parameters of the fuzzy system were easier to select than those for the NARMAX models. Vachkov [Vachkov 92] uses a fuzzy rule based decision table technique to analyse fault symptoms in a simple process plant. Howlett [Howlett 98] uses fuzzy and ANN techniques to infer cylinder air/fuel ratio from the spark voltage waveform in spark ignition engine.

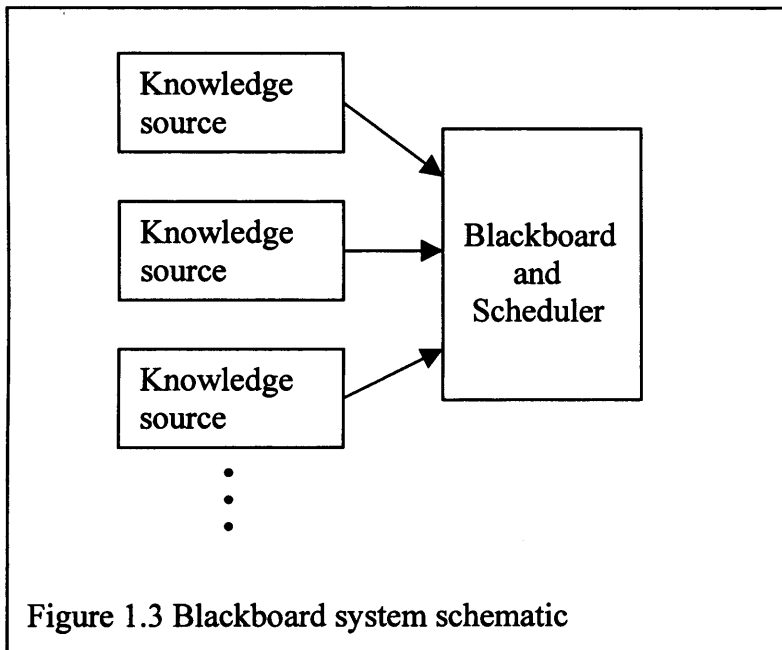
Lu et al [Lu 98] employ a two-stage fault diagnosis system in a fuzzy diagnostic model. The system is rule-based, rather than providing an estimation of state variables, and uses fault data from normal and faulty engines to train a number of fuzzy systems which are used to classify the performance of the engine at component level. The classification data from each individual component is passed to a central agent where the overall diagnosis is made. This system is employed on an end of production-line test facility.

1.6.6 EXPERT SYSTEMS IN FAULT DIAGNOSIS

Heuristic knowledge may be used to create an 'expert' system. An expert system is a computing system designed to encapsulate knowledge-based components of human skill. The system is designed in a form which, when presented with a specific query, will supply an answer based on the system's programmed knowledge. The expert system should also be 'transparent', i.e. it will be able to display and justify its reasoning processes. A number of introductory texts are available on the subject of expert systems [Durkin 94], [Englemore 88] and a number of applications for expert systems in diesel engine diagnosis are reported.

Dabbar and Logan [Dabbar 89] report the use of an expert system to diagnose faults in a marine diesel engine. The system contains model relationships for system parameters that are used to generate residuals and a Boolean rule-base to identify faults. The system offers diagnosis of faults in both system and sensors and advice on required remedial actions. Zhong and Zongying [Zhong 93] propose a similar system using fuzzy logic theory to define the connective rules.

Gelgele and Wang [Gelgele 98] present an expert system for automobile engine diagnosis. The system is designed to assist mechanics and technicians in off-line diagnosis of engine faults and is an implementation of a decision tree structure utilising Boolean reasoning.



One particular realisation of an expert system is a called a *blackboard* system. The blackboard system consists of a set of diagnostic agents or ‘knowledge sources’ the diagnostic output from each of which may be regarded as an *opinion* concerning the state of the system under consideration. The set of these opinions is reported to a central agent, or *blackboard*. A data fusion system may be used to combine the information reported to the blackboard and conclude the most likely true condition.

Blackboard systems have been proposed as medical diagnosis systems [Jones 00]. A blackboard system consisting a number of ANN classifiers [Parikh 98] showed that combination of diagnostic information in this way, gave significantly improved results over the individual knowledge sources taken in isolation.

1.7 REQUIREMENTS FOR A DIESEL ENGINE CMFD SYSTEM

Sections 1.1 – 1.6 have identified a clear need for CMFD systems for diesel engine systems and listed variety of schemes that have been proposed to meet this need.

A summarised version of the requirements and function for an on-board diesel engine CMFD system is now considered in this section.

1.7.1 INSTRUMENTATION

The first part of the CMFD design task is to specify an appropriate instrumentation system. This must be capable of reporting engine parameters at a sampling rate appropriate to the frequency of the system, both in its normal state and also in potential fault states. Sensors should be robust and reliable. The number and sophistication of the sensor set should be carefully considered in terms of sensor cost, probability of system failure, potential cost savings and criticality of the engine application, to ensure the best trade-off between cost and diagnostic system functionality.

Where cost is the limiting factor in sensor set specification, use of reduced sensor set may mean that only a partial diagnosis is possible; however this could be designed to provide a high-level indication of engine performance. Certain measurements are impractical and unlikely to be cost effective for an on-board system (e.g. cylinder pressure measurement, direct indication of engine load torque)

1.7.2 FUNCTIONAL SPECIFICATION

The function of the CMFD system is to perform a mapping from the measured data signals from the engine to a linguistic or numerical variable that describes the engine condition in some meaningful way.

The CMFD systems required for this purpose must be capable of indicating the diesel engine system condition to an appropriate degree of accuracy. This requirement implies that the system must be capable of interpreting dynamic, non-linear, multi-input multi-output processes over the full range of operating conditions and modes of the engine.

The CMFD system must be able to run in parallel with the engine to continuously provide information to the operator, therefore the system must be capable of running in 'real-time'. Deep knowledge of the physical relationships underlying the process will not be required by the operator who will only be concerned with the inputs and outputs of the system and how accurately they represent the condition of the engine. However, the diagnostic system should be structured in a manner that is representative of the engine itself to allow systematic reference to the reasoning process.

The CMFD output should also reflect urgency or magnitude of fault, i.e. from 'immediate shutdown required' alarm to 'change at next service'. The sensitivity of the fault diagnosis system should be defined to provide an appropriate trade-off between early fault detection and false alarm rate, taking into account the combined uncertainties of the sensors, data processing system, and models. A number of authors [Karpman 85], [Vachkov 92] note that the probability of two independent failures occurring at once in the same system may be assumed to be negligible, therefore the diagnostic system need not accommodate the possibility of simultaneous multiple faults.

In design of the diagnostic, other practical considerations need to be taken into account. For instance the level of diagnosis required need only extend down to the smallest replaceable component in the system. For instance, if a pump impeller fails and the maintenance policy in that event is to replace the whole pump, then the diagnostic system need only diagnose the fault as being a pump failure.

In order to produce a commercial on-board CMFD package, the diagnostic system should be capable of being calibrated for use on an individual engine, with a facility for recalibration where appropriate, to compensate for the ageing of the engine for instance. The control and diagnosis system package should have a design life at least equal to that of the engine itself, and the system should exhibit the same qualities of availability, reliability and maintainability.

1.7.3 SELECTION OF APPROPRIATE DIAGNOSTIC TECHNIQUES

Section 1.6 reviewed a number of potential CMFD techniques, the suitability of each technique is summarised here with recommendations for a possible CMFD system structure.

Analysis of signal spectra represents a well-founded and powerful technique which has been shown to be capable of diagnosing a class of combustion faults. However, although the system provides a high level analysis, based on a single robust transducer, the system is generally unsuitable for identifying the exact location of the fault (i.e. the individual cylinders concerned), nor for diagnosis of faults that do not have a characteristic vibration signature. Feature extraction required for symptoms is a complex process and may require fault data for the training secondary classifiers as part of the reasoning algorithm.

The benefits of model-based or parity equation systems are that the diagnosis system presents the symptoms in a direct way as residual vectors, which are generally more straightforward to interpret than the outputs from spectral analysis. The main problems with these techniques are the development of suitable models. For an on-line diesel engine CMFD system the model needs to be able to cope with measurement noise, non-linearity and uncertainty in the physical system. Full knowledge of the physical system is not always available and system identification techniques may provide the answer in some cases. However, the algorithms for system identification are not well suited to unknown non-linear systems due to the large number of possible candidate structures.

The use of primary ANN or classifiers to analyse raw engine data has some advantages over modelling, in that detailed knowledge of the physical system is not required and the classifiers may be generated from suitable data. However, this implies that fault condition data must also be obtained. Since this may not be possible for certain severe conditions, the classifier approach has only limited robustness to those faults. Also ANN's are not 'transparent' in their operation, i.e. the reasoning process contained within the neurons is not available for examination.

Expert systems are another powerful technique for diagnosis of engine faults. Blackboard systems offer great potential for CMFD of diesel engine systems, particularly as increases in the computational power of micro-controllers, will allow more cost effective implementation of more complex data acquisition and analysis systems. The structure of the blackboard system would incorporate some or all of previously discussed CMFD systems as knowledge sources, and combine their individual outputs using a data fusion approach to conclude the most likely system condition. Evaluation of the performance of the individual knowledge sources in different engine operating conditions, combined with knowledge of the limitations of each individual technique will allow a confidence weight to be allocated to each data fusion system input. Thus the diagnostic output will be associated with a confidence weight indicating the degree of belief in the final result.

1.8 CONCLUSIONS

A wide-ranging review of condition monitoring and fault diagnosis has been undertaken in this section. The need for CMFD has been clearly established and the issues involved in specifying a cost-effective solution in-terms of required instrumentation have been considered.

A number of CMFD techniques have been reviewed in the preceding section and their strengths and limitations have been considered. The limitations of the individual techniques have meant that no single automated on-board CMFD system has yet been widely adopted commercially. Based on the limited successes of individual CMFD techniques, and on previous research in the field of medical diagnoses, the conclusion has been reached that combining evidence from different knowledge sources using a suitable data fusion system represents the best potential solution to the problem of CMFD in diesel engines.

This investigation into CMFD systems has provided the motivation for work in a number of different areas:

- a) Systems modelling for parameter and state estimation in dynamic, non-linear systems subject to noise and uncertainty.
- b) Techniques for reasoning and classification.
- c) Development of a suitable knowledge base for a diesel engine CMFD system.

Fuzzy systems are known to represent a possible common methodology for implementing systems in areas a) – c), listed above. Therefore subsequent sections of this thesis will be focussed upon assessment of the function and properties of fuzzy systems (chapters 2, 3, and 4), followed by development of fuzzy systems for use in a CMFD system case study based on a diesel generator set (chapters 5-9). The resulting CMFD systems are intended for use as knowledge sources in a blackboard-type system for diesel engine CMFD.

CHAPTER 2.

An Introduction to the Theory of Logic and Sets.

2. AN INTRODUCTION TO THE THEORY OF LOGIC AND SETS.

Logical methods can allow a conclusion to be inferred in circumstances where that conclusion may not be directly perceived. In human beings logical thinking is an informal, *ad hoc* process, however over the years many scholars have contributed to the documentation and formalisation of the basis and theories of logic.

Chapter 1 of the thesis has highlighted a number of ways in which fault conditions can be logically inferred from available transducer signals. It was concluded that fuzzy logic systems represent a possible common methodology for implementation of fault diagnosis techniques. Hence this chapter will go on to explore the origins and fundamentals of fuzzy logic theory.

Fuzzy logic has its foundations in the fields of classical and Boolean logic and also in classical set theory. This chapter will explore those foundations in both historical and theoretical contexts and describe the motivations for the development of the theory of fuzzy sets and systems.

Fuzzy sets and systems are well documented elsewhere but a brief introduction to the main aspects of the theory is included here, with appropriate references. Finally, a short discussion is included which presents a comparison of the theories of fuzzy logic and probability. Issues concerning the respective properties and applicability of probability and fuzzy systems have been the subjects of many academic debates.

2.1 APPLICATION OF LOGIC.

Human beings subconsciously apply logical techniques in an *ad hoc* manner to everyday situations. Our capacity for memory allows us to store and recall past patterns and events and use them in the logical processes of prediction or deduction. The ability to learn from experience and apply that knowledge in decision-making may be defined as *intelligence*.

Logic allows us to reach a conclusion where that conclusion may not be made by means of direct observation. For example, astronomers may deduce the presence of an unseen planet orbiting a far off star, from knowledge of how a planetary mass and the force of gravity interact, causing measurable deviations in the position or motion of the star. Or a doctor may view the symptoms of a patient in order to diagnose his or her condition.

Logic also allows the prediction of possible future outcomes from patterns or sequences of events. A *causal system* is defined to be one which does not depend for its output on future inputs or future outputs. Clearly, real physical systems are all causal as they exist in time and time goes forward. Therefore, if the inputs (in this case a particular event or sequence of events in time) and outputs of the system can be identified, then the output of the system may be predicted to some degree of accuracy for any given set of inputs. A linguistic framework is used to express the cause and effect of the system in the form of a proposition or rule. For example, meteorologists may use data such as atmospheric pressure and wind direction to predict future weather, e.g. ‘if the atmospheric pressure is falling and the wind is in the west then the weather will be unsettled.’

The preceding paragraphs have presented an illustration of how logic is applied by human beings for the purposes of deduction and prediction. The following sections will document the formalisation of the fundamentals of logical theory, the interactions between logical theory and set theory, which lead to the introduction of fuzzy set theory.

2.2 ORIGINS OF FORMAL LOGIC

The evolutionary success of the human species over hundreds of thousands of years has been based on our capacity for intelligent thought and decision-making. However, the formalisation and documentation of the logical process has been a product of the last 2,500 years. The ancient Greek philosophers were the first to undertake this task, however little original work was carried out between 200BC and the 19th century when a number of mathematicians and philosophers carried out work to modernise the theories and develop a formal logical algebra.

Origins of formal logic lie in the works of the ancient Greek philosophers. From the documents that are preserved from that time, it seems that although earlier philosophers Zeno, Socrates and Plato were intuitively familiar with the ideas of logic, [Bochenski 51] the first person to attempt to describe a formal logic was Aristotle in his work, *Prior Analytics*. This is notable also for his development of a special terminology for the subject, and the first recorded use of variables to express mathematical ideas.

The phrase ‘formalistic logic’ describes the precise language structures required to express mathematical or scientific truths. Lucasiewicz states [Lukasiewicz 51] that;

‘Formalism requires that the same thought should always be presented by exactly the same manner. When a proof is formed according to this principle, we are able to control its validity on the basis of its external form only, without referring to the meaning of the terms used in the proof.’

Aristotle presents his logic in the form of *sylogisms*, a universally valid example of which is:

If all B is A and all C is B, then all C is A

Certain syllogisms are not universally valid and therefore the terms must be explicitly defined.

An alternative expression of a logical statement is the *logic of propositions*. This form of statement is attributed to the Stoic school of thinkers some 50 years after the writing of *Prior Analytics*. The contrast between Aristotelean syllogism and the propositional logic approach may be seen in the following example of a logical identity:

Aristotelean Identity: All A is A
where A represents a term

Propositional Identity: If p then p

Where p represents a proposition of the form ‘the sky is blue’

This propositional logic provides a system of *rules of inference* known as *modus ponens*. If a proposition, ‘If A then B’, may be demonstrated, then if A is true, B must be true. In *Principia Mathematica*, Whitehead and Russell [Whitehead 10] aim to show that all mathematics can be deduced from formal logic, presenting propositional logic under the title, ‘*The Theory of Deduction*’.

2.3 AN ALGEBRA FOR BINARY LOGIC

Aristotle formulates what has become known as the *principle of the excluded middle* that a statement may be true or not true and that there is no in-between or middle ground. Bochenski [Bochenski 51] reports that although Aristotle writes, ‘every affirmation is true or false’, other statements from his texts indicate that he seriously doubts its universal applicability. However, although Aristotle may have had his doubts, the principle of the excluded middle is at the foundation of his logic.

A formalisation of Aristotelean logic was produced by George Boole and now known as *Boolean algebra*. [Boole 1854]. In order to reduce his algebra to that of a binary system, Boole states that his symbols of logic are subject to a special law such that;

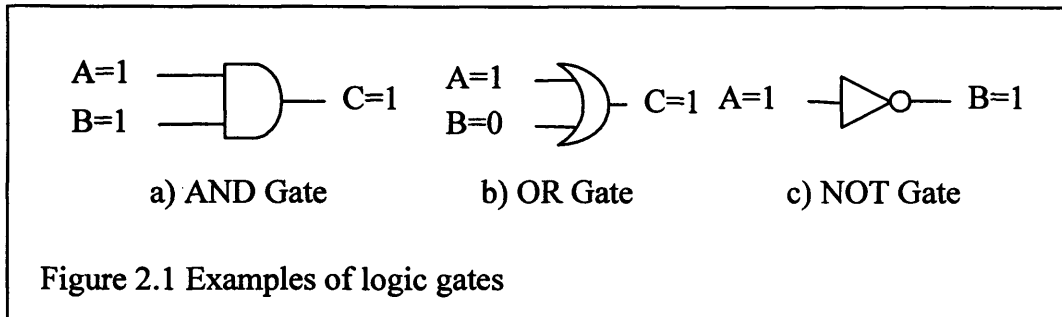
$$x^2 = x$$

The two values that fit this condition are 0 and 1, with the value 1 being assigned to a true statement and the value 0 assigned to a false statement.

Boole could not have foreseen the success of his method in design and analysis of electronic switching circuits where logic gates may be used to represent a proposition diagrammatically, for example three propositions are represented in figure 2.1 a, b and c;

- a. If A is True AND B is True then C is True
- b. If A is True OR B is True then C is True

c. If A is True then B is False



The function of a binary logic proposition with a number of terms in the premise and an appropriate operator may be illustrated in the form of a truth table where the value 1 represents the true and 0 represents false. Some examples are presented in the truth tables below;

'AND'		
Input		Output
A	B	C
0	0	0
0	1	0
1	0	0
1	1	1

'OR'		
Input		Output
A	B	C
0	0	0
0	1	1
1	0	1
1	1	1

'NOT'	
Input	Output
A	B
0	1
1	0

Table 2.1 Examples of Boolean logic truth tables

Detailed explanations of Boolean logic theory, and switching design and their application in computer science, are beyond the scope of this thesis but are available in many references including [Gardner 58].

2.4 CLASSICAL SET THEORY

The subjects of logical propositions may be defined in terms of sets. A *set* is the term used to describe a collection of objects or elements. Each of these elements possesses some property, which is selected to define the membership of the set. Hence, the

membership of a set may be defined by an itemised list of member elements or by some unambiguous rule. As an illustration, a set, A, may be defined synonymously as follows;

$$A = \{x \in A \mid x \text{ is a positive non - zero integer, less than } 10\}$$

$$A = \{x \in A \mid x \in \mathbb{R}^+, 0 < x \leq 10\}$$

$$A = \{1, 2, 3, 4, 5, 6, 7, 8, 9\}$$

Classical set theory has applications including logic, algebra and probability. There are many texts available detailing aspects of set theory, including [Green 88], [Bajpai 74].

2.4.1 MAPPINGS AND FUNCTIONS

A mapping describes a correspondence between two sets. For example, in the case of two sets, A and B, a mapping is a rule or formula which assigns an element, b , of B to each element a of A. If the mapping is denoted, ϕ , the relationship between the two sets may be written;

$$\phi: A \rightarrow B$$

As seen in the previous example, a mapping may describe a relationship between a single element in a set and a single element in another set – a *one to one* relationship. However mappings may also be *one to many*, where a single element maps to more than one element, *many to many* or *many to one*. The concept of mathematical functions may also be explained in terms of mappings, such that a *function* is defined as mapping that exists between two sets, X and Y, such that each element of X is associated with one and only one element of Y. i.e., functions may be *one to one* or *many to one* mappings, but not *one to many* or *many to many*.

2.5 FUZZY LOGIC AND FUZZY SETS

In a multivalent system, instead of the restriction to two truth-values, 1 and 0, to represent true or false, the proposition may take on any value between 1 and 0, i.e. the condition may have a certain *degree of truth*.

Aristotle hints at the need for a multi-valued logic but bases his logical theories on a binary system. Some multivalent schemes have been proposed during the 1920's as a method for dealing with Heisenberg's Uncertainty Principle in quantum mechanics.

Kosko [Kosko 94b] reports that subsequently logicians such as Jan Lucasiewicz, Max Black and Bertrand Russell have expanded the ideas.

Sections 2.1 – 2.3 have provided a brief history of the historical development of a formalised binary logic and noted its success in many applications, however does the traditional approach of bivalent logic always provide the best solutions? Can the state of *any* system be defined as wholly true or wholly false? To take a much-used example: Is the room hot or cold? The usual approach to answering this question is to strictly define the sets, 'hot' and 'cold', measure the temperature, and see to which set the temperature belongs. i.e. to *classify* the temperature. The logical consequence of this definition is that the room changes from being hot to being cold with the addition of an infinitesimally small increment in temperature. One may envisage many similar problems in set definition;

at what height does a short man become a tall man?

at what age does a young man become middle-aged?

Clearly, this situation may arise with any set defined on a continuous variable. A further problem may occur where noise is present in the measurement of the variable that can cause a complete misclassification of the datum.

Kosko [Kosko 94b] concisely defines fuzzy logic as '*reasoning with fuzzy sets*'; What is meant by a fuzzy set is that the *membership value* of an element of the set does not need

to comply with Boole's special law, but may take any value, $0 \leq x \leq 1$. The seminal paper on the subject, and the first one to coin the term 'Fuzzy', was written in 1965 by Lotfi Zadeh entitled 'Fuzzy Sets' [Zadeh 65].

Fuzzy sets provide an approach to solving the classification problems described above. As an illustration, consider the continuous variable room temperature, T . If two non-fuzzy sets are defined in T , 'hot' and 'cold', such that;

$$hot = \{T \in hot | T \geq 20\}$$

$$cold = \{T \in cold | T < 20\}$$

Remembering that binary logic allows two truth-values 1 or 0 to represent the truth of the two statements;

- i) T is a member of the set, *hot*
- ii) T is a member of the set, *cold*

Then the membership of the sets *hot* and *cold* may be plotted on the temperature scale as follows:

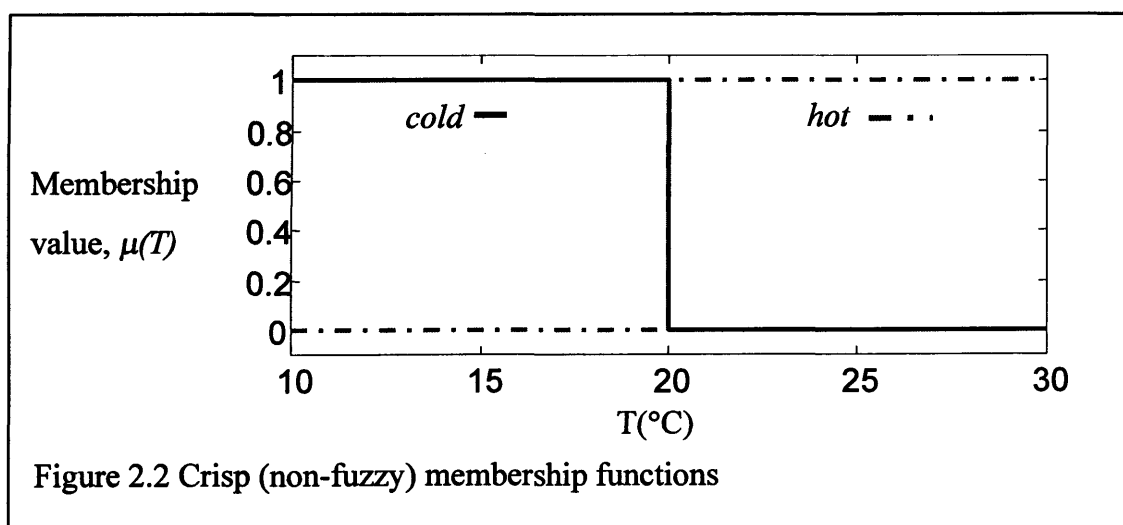


Figure 2.2 Crisp (non-fuzzy) membership functions

2.6 FUZZY MEMBERSHIP FUNCTIONS

The sets, *hot* and *cold*, can (somewhat arbitrarily) be redefined to be fuzzy sets. The membership value of the set, *cold*, is gradually reduced from 1 at 10°C to a value of 0 at 30 °C and *hot*, is gradually increased from 0 to 1 over the same range.

The membership values may be re-plotted as shown below.

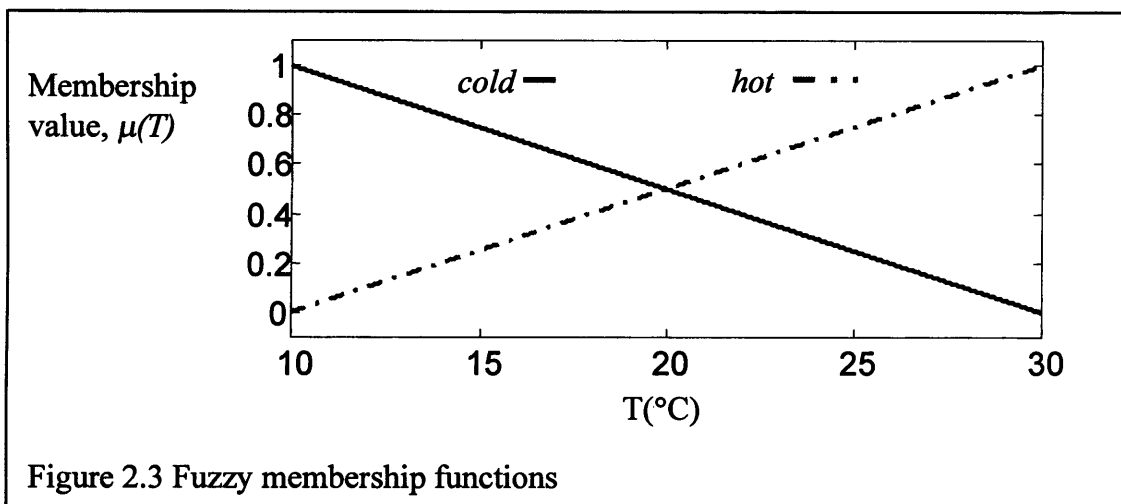


Figure 2.3 Fuzzy membership functions

Intuitively, the reduction in the membership values of *cold* with temperature is a representation of the fact that the room becomes gradually less cold and gradually hotter. This provides an introduction to the concept of the *membership function*.

The membership function is a continuous function used to define the membership value of the set at any point in the universe of discourse, U. Membership functions of a set A, are commonly denoted $\mu_A(x)$ (or $\mu_{Hot}(T)$ in this example) and may be defined using any suitable function, for instance a Gaussian, sigmoidal or generalised bell curve.

Membership functions may also be defined in a piecewise linear manner e.g. triangular or trapezoidal. Thus, the membership functions in the example above could be defined as follows;

$$\mu_{hot}(T) = \left\{ \begin{array}{ll} 0 & T : T \leq 10 \\ 0.05T - 0.5 & T : 10 < T \leq 30 \\ 1 & T : T > 30 \end{array} \right\}$$

$$\mu_{cold}(T) = \left\{ \begin{array}{ll} 1 & T : T \leq 10 \\ -0.05T + 0.5 & T : 10 < T \leq 30 \\ 0 & T : T > 30 \end{array} \right\}$$

Comparing the classification of noisy signals using crisp sets, to classification with fuzzy sets, consider as an example a temperature transducer with an accuracy of $\pm 1^\circ\text{C}$. It may be seen that if datum points between 19°C and 21°C are classified with crisp sets, then the specified measurement noise could result in a complete (100%) misclassification of the datum. However, if the fuzzy sets defined in the example are used to classify the temperature measurement affected by the same transducer error, the result is a misclassification by only 5%. This demonstrates the property of smooth transfer between class memberships, which is made possible through the use of fuzzy sets.

2.7 FUZZY SETS AND PROBABILITY

Since the publication of *Fuzzy Sets* [Zadeh 65], there has been much academic discussion comparing the capabilities and merits of the two branches of theory. Some of this discussion may be due to the name, ‘fuzzy’, which may be seen as somewhat provocative [Kosko 94b].

Consider an event with an uncertain outcome, tossing a coin for instance, probability is a measure of the chance that a specified outcome will occur, in this example there are two equally likely outcomes, heads or tails, so that the probability, p , of either of those outcomes is 0.5. If there are $i=1,2, \dots, N$ possible outcomes to the event then;

$$1 = \sum_{i=1}^N p(i)$$

Therefore any outcome where $p=1$ is a certainty and any outcome where $p=0$ is impossible.

A detailed review of probability theory is beyond the scope of this thesis but may be found elsewhere [Hoyt 67]. However, from the brief introduction above, two similarities with fuzzy theory are already evident, namely the use of probability theory as a methodology for dealing with uncertainty, and the range of membership values, [0,1].

Arguments have been put forward [Bezdek 94] that probability theory may be applied to any of the problems to which fuzzy logic may be applied and give similar results. However this does not detract from the fact that fuzzy systems *have* been applied with functional and commercial success in many applications, thereby demonstrating their practical value.

Given that probability theory and fuzzy theory may be applied to similar problems what is the difference between the two approaches? Probability deals with the expectation of outcomes of particular events. In a probabilistic analysis, the event abides by the principle of the excluded middle, i.e. the event occurs or it does not, the coin in the example is either heads or tails. In order to draw the distinction between the two philosophies, Kosko [Kosko 94b] presents the example of a car driver entering an empty car park of say 100 spaces. If the driver parks at random in one of the spaces (neglecting any probability weighting towards the spaces adjacent to the ticket machine), then there is a probability of 1% that he or she will park in any given space. This assumes that the car is perfectly parked taking up exactly one space. The fuzzy analysis is made once the car is in its parked state and concerns the question of how well the car is parked in the given space. If the car parked perfectly within the markings of a single space, n , then the statement;

‘The car is parked in space n ’

has a truth-value of 1. If the car is parked so that part of the car is outside the markings of that space and is infringing an adjacent space, m , then the truth value of the statement is reduced to some amount, t . The statement;

‘The car is parked in space, m ’

may also now be said to be true with a truth-value of t .

In summary, it seems fair to say that although aspects of both fuzzy logic and probability are similar, probability is most associated with dealing with the expectation of future outcomes, and fuzzy sets are most suited to classification and reasoning with uncertain data and continuous variables.

2.8 CONCLUDING REMARKS

This section has described development and formalisation of logical theory. The formalisation of binary logic as Boolean algebra has been extremely successful in many applications, particularly in switching theory and electronics, however, development of fuzzy logic theory has extended the principles of classical set theory and binary logic and has shown great potential in a number of applications. Fuzzy logic is seen to be of particular benefit in the classification of continuous variables where the measurement of those variables is subject to noise.

The importance of logical inference has been also been described in this section. The following two chapters will build on these ideas to describe the structures of fuzzy inference systems and techniques for generating fuzzy systems and models, suitable for use in fault diagnosis.

CHAPTER 3.

An Introduction to Fuzzy Systems and Mappings

3. AN INTRODUCTION TO FUZZY SYSTEMS AND MAPPINGS

Chapter 1 of this thesis introduced the ideas of a binary logical algebra, the logic of propositions, and classical set theory. The use of fuzzy sets as an appropriate way to represent certain variables was also demonstrated, as was use of membership functions to describe membership values of fuzzy sets across the universe of discourse, U .

A definition of fuzzy logic has also been stated as, 'Fuzzy logic is reasoning with fuzzy sets'. This chapter will go on to review fuzzy systems theory with appropriate examples showing how fuzzy sets are made the subjects of propositions in order to produce a fuzzy mapping or *fuzzy system*. A description of generic fuzzy system will be presented with discussion of a range of techniques for implementation of the premise, consequence and operators. The relative merits of different fuzzy system structures will be considered and recommendations are made where appropriate.

Although this section provides an introduction to the theory of fuzzy systems, a number of texts are available which describe the theory in greater depth [Wang 97], [Zimmerman 91], [Cox 94].

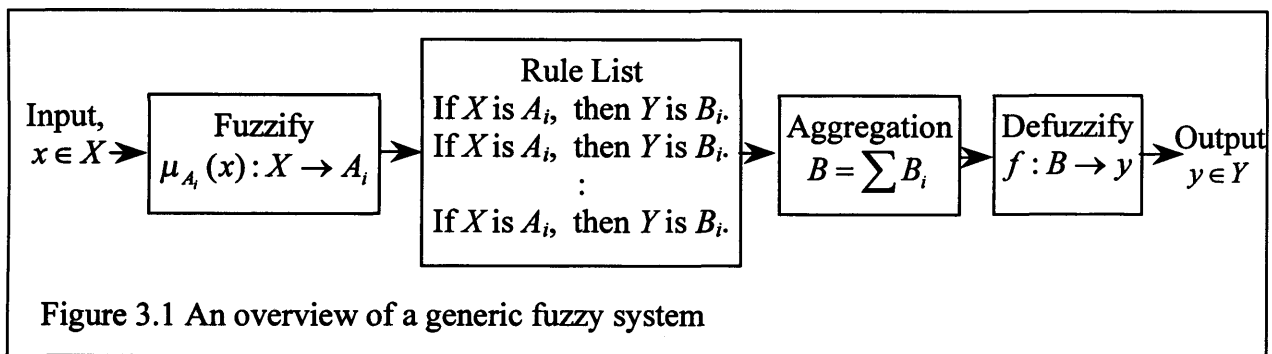
3.1 THE GENERIC FUZZY SYSTEM

A fuzzy system is essentially a mapping between an input space and an output space, via a set of rules. The rules have the linguistic structure of propositional logic as defined in chapter 1, i.e. if p then q , where p and q are propositions. Hence fuzzy systems are sometimes referred to as *fuzzy inference systems* (FIS). This linguistic structure of fuzzy systems facilitates the incorporation of knowledge into the mapping. The knowledge may be expressed in the same form as used by human beings, i.e. as rules of inference or *heuristics*.

Theoretically, a fuzzy system may have any number of inputs and outputs that are connected by as many rules as required. However, in practice, numbers of inputs and outputs are limited by the computational power that is available. This limitation will be discussed in section 4.2.5.

If the desired input to the fuzzy system is, $x \in X$, and the output is, $y \in Y$, then the terms of the proposition may be defined as fuzzy sets in X and Y . Thus, the rules connect sets defined in the input space, with sets defined in the output space. So that if sets A and B are defined in X and Y respectively, then a connective rule takes the form;

If X is A_i , then Y is B_i ... 3.1



Assume that $x \in A_i$ to some degree, as defined by the membership function, $\mu_{A_i}(x)$, for the set A_i . This membership value of x fixes the degree to which the rule is *fired*. What is meant by *firing* a rule is that the degree to which the premise is true, fixes the degree to which the consequent is true, so that if $\mu_{A_i}(x)=0$, then the rule is not fired and conversely if $\mu_{A_i}(x)=1$, then the rule is totally fired. The process of evaluating $\mu_{A_i}(x)$ to establish to what degree x is a member of the fuzzy set, A_i , is known as *fuzzification*. The rule maps the input set onto the defined output set, B_i . Generally, the desired output from the fuzzy system is a discrete, or *crisp*, number. This number is usually obtained as some form of weighted average of the output sets specified by all the fired rules. The method used to combine all the fired output set, B_i , to a single output set, B , is known as *aggregation*. The process for obtaining a crisp number from B is called *defuzzification*. The next section will look at the design and construction of fuzzy systems in more detail.

3.2 THE STRUCTURE AND DESIGN OF FUZZY SYSTEMS

Having briefly described the generic structure of a fuzzy system this section will consider the design options available to the systems engineer. This will include consideration of alternative membership functions for both fuzzification and defuzzification and the implications for the performance of the fuzzy system.

3.2.1 FUZZIFICATION

Fuzzification is the evaluation of an input data point in terms of its membership of a fuzzy set or sets defined in the Universe of discourse, U . Thus, the fuzzification of a system is characterised by the size, shape and number of the fuzzy sets defined in the input space.

The primary aim in the design of the fuzzification process is to define sets that adequately represent the spread of data in the input space, providing a suitable basis for the mapping from input to output. Although there is no optimal approach to designing the fuzzifier, several different approaches are described in the following sections. A number of algorithms have also been developed for identification and training of fuzzy systems, which will be described in chapter 4

If some statistical knowledge of the input data is available then this can be used to define membership of the set. Frequently, fuzzy systems are derived from linguistic rules, which have been accumulated by an expert with experience of the system in question. In such cases the initial approach is to partition the input space with a number of evenly distributed sets, then to modify the initial system by a process of trial and error. Where input data is available, clustering algorithms may be used to define fuzzy sets based on the distribution of data points in the input space. This approach will be described in section 4.2.5.

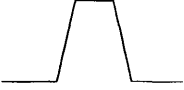
Choosing the number and form of input sets in the fuzzy system is a trade-off between functionality and computational cost. The system's designer should aim to minimise the number of sets whilst maintaining an adequate representation of the system being

modelled. Similarly the evaluation of the membership function (m.f.) requires a greater amount of computational power for more complex curves, such as a Gaussian m.f., than would a triangular m.f. The dimensionality of the input space is a significant factor in this decision because, for a fixed number of m.f.'s, the number of fuzzy rules required increases exponentially with the number of inputs. This issue, '*the curse of dimensionality*' will be further discussed in section 4.2.5.

The approach taken to define fuzzy sets in the input space may have implications for the choices of fuzzy sets that are available. Lu [Lu 98] points out some algorithms used for training or optimisation of fuzzy systems require the membership function to have continuous first order derivatives (see chapter 3). This may be a limitation when choosing membership functions for the premise in that piecewise linear functions (e.g. triangular, trapezoidal) do not meet this criterion.

Fuzzy sets can be shown to have a filtering effect on noise on the input channels [Wang 97]. Fuzzy sets with a larger support can be shown to be more effective in reducing noise. This has implications in choice of both shape and size of the membership functions. Continuously differentiable functions, such as the generalised bell and Gaussian m.f.'s, which have supports which are asymptotic to $\mu_A(x)=0$, show the greatest benefit in noise reduction.

Table 3.1 Summary of selected fuzzy membership functions

Membership Function	Function	Shape
Singleton	$\mu(x) = c$	
First Order Linear	$\mu(x) = p_2x + q_2$	
Triangular	$\mu(x) = \begin{cases} p_1x + q_1 & X : x_1 \leq x < x_2 \\ p_2x + q_2 & X : x_2 \leq x < x_3 \\ 0 & X : x_1 > x \geq x_3 \end{cases}$	
Trapezium	$\mu(x) = \begin{cases} p_1x + q_1 & X : x_1 \leq x < x_2 \\ 1 & X : x_2 \leq x < x_3 \\ p_2x + q_2 & X : x_3 \leq x < x_4 \\ 0 & X : x_1 > x \geq x_4 \end{cases}$	
Generalised Bell	$\mu(x) = \frac{1}{1 + \left(\frac{ x - \bar{x} }{p}\right)^{2q}}$	
Gaussian	$\mu(x) = \exp\left(\frac{-(x - \bar{x})^2}{2\sigma^2}\right)$	

For a given input space and prescribed number of sets, continuously differentiable sets have benefits in terms of noise reduction and also in the fact they may be used in conjunction with certain training or optimisation algorithms. The simplicity of parameter adjustment in piecewise-linear fuzzy sets makes them the choice for many designers for systems designed using trial and error.

3.2.2. OPERATORS

In section 2.3 the use of the operators 'AND', 'OR' and 'NOT' was described using truth-tables to illustrate the function of operators in Boolean logic. In Boolean set algebra the

operator, AND, expresses the *intersection* of two sets. Where A AND B are two sets the intersection is defined as the collection of elements which are simultaneously members of both A AND B , denoted $A \cap B$. The operator, OR, describes the *union* of A AND B , denoted $A \cup B$. The union of A AND B is the collection of elements that belong to either A OR B OR both. The complement of A is denoted, \bar{A} , and is the collection of all the elements which are contained within U , but lie outside the set boundary of A .

The choice of which operator is appropriate for use in the design of a fuzzy system is briefly discussed in the following sections. At issue is the suitability of the operator against the consideration of computational cost and complexity.

A number of researchers have contributed toward a range of functions that extend the principles of operators used in binary logic to operators appropriate for use with fuzzy sets. Dubois and Prade [Dubois 85] and Wang [Wang 97] provide useful summaries of these techniques. Wang uses an axiomatic approach to describe the requirements for fuzzy operators. These are outlined in the following sections:

3.2.2.1 FUZZY COMPLEMENT

A fuzzy membership function of a set, A , is mapped on the membership function of its complement, \bar{A} , with a mapping:

$$c : \mu_A(x) \rightarrow \mu_{\bar{A}}(x)$$

There are two requirements for the mapping, c :

- a) Boundary conditions: $c(0)=1$ and $c(1)=0$.
- b) Non-increasing condition: if $\mu_A(x) < \mu_B(x)$ then $c(\mu_A(x)) \geq c(\mu_B(x))$.

Typically the function used to fulfil these requirements is:

$$c: \mu_A(x) \rightarrow 1 - \mu_A(x) \quad \dots 3.1$$

Although a number of other suitable classes of fuzzy complement with variable parameters (λ and w below) are available including the following;

$$\text{Sugeno class: } c: \mu_A(x) \rightarrow \frac{1 - \mu_A(x)}{1 + \lambda \mu_A(x)} \quad \lambda \in (-1, \infty) \quad \dots 3.2$$

$$\text{Yager class: } c: \mu_A(x) \rightarrow \left(1 - [\mu_A(x)]^w\right)^{1/w} \quad w \in (0, \infty) \quad \dots 3.3$$

It may be seen that the Sugeno and Yager classes reduce to 3.1 when $\lambda=0$ and $w=1$, respectively. Clearly the computational cost of 3.1 is much lower than that of 3.2 or 3.3.

3.2.2.2 FUZZY UNION

The fuzzy union operator is also referred to as the *t-conorm* or *s-norm*. As with the fuzzy complement, there is a range of suitable set relationships, s , which meet the requirements;

- a) Boundary Conditions: $s(1,1)=1$, $s(\mu_A(x),0) = s(0, \mu_A(x)) = \mu_A(x)$
- b) Non-increasing condition: If $\mu_A(x) < \mu_B(x)$ then $s(\mu_A(x)) \geq s(\mu_B(x))$
- c) Commutativity: $s(\mu_A(x), \mu_B(x)) = s(\mu_B(x), \mu_A(x))$
- d) Associativity: $s(s(\mu_A(x), \mu_B(x)), \mu_C(x)) = s(\mu_A(x), s(\mu_B(x), \mu_C(x)))$

The most commonly used relation that meets these conditions is the maximum operator;

$$A \cup B = \max(\mu_A(x), \mu_B(x))$$

However, other suitable relations include the algebraic sum;

$$A \cup B = \mu_A(x) + \mu_B(x) - \mu_A(x) \times \mu_B(x)$$

3.2.2.3 FUZZY INTERSECTION

Also referred to as the *t-norm*, the family of relationships for the fuzzy intersection must meet the following requirements

- a) Boundary Conditions: $t(0,0)=0$, $t(\mu_A(x),1)=t(1,\mu_A(x))=\mu_A(x)$
- b) Non-increasing condition: If $\mu_A(x) < \mu_B(x)$ then $t(\mu_A(x)) \geq t(\mu_B(x))$
- c) Commutativity: $t(\mu_A(x), \mu_B(x)) = t(\mu_B(x), \mu_A(x))$
- a) Associativity: $t(t(\mu_A(x), \mu_B(x)), \mu_C(x)) = t(\mu_A(x), t(\mu_B(x), \mu_C(x)))$

Usually, either the ‘min’ or ‘product’ operator is used. These two are presented below;

- a) Min operator: $A \cap B = \min(\mu_A(x), \mu_B(x))$
- b) Product operator: $A \cap B = \mu_A(x) \times \mu_B(x)$

3.2.2.4 DISCUSSION

The question of which form of a particular operator is most suitable for a given system depends on the system itself, and the required influence of the each set on the result.

Clearly if the union operator is to be used in a rule of the form;

$$\text{If } X_1 \text{ is } A_1 \text{ and } X_2 \text{ is } B_1, \text{ then } Y = C_1$$

then the degree to which the rule is fired is fixed by the operator. Under the *max* operator, the degree to which the rule is fired is only influenced by the membership value of a single input. It may sometimes be more appropriate to incorporate the influence of membership values of all the inputs in the rule, in which case a relationship such as the algebraic sum should be employed. However, the *max* function is computationally less complex and may therefore be an appropriate choice where computational cost is an issue.

As with the fuzzy union the choice of operator is dependent on the system in question. Computational cost for the *min* operator is minimum, however the issue of relative influence of the membership values for each input in firing the rule, is also of concern here. Clearly, the *min* operator is only influenced by membership values of a single input, whereas the product operator and most other operators are affected by membership values of all inputs.

3.2.3 IMPLICATION

If a fuzzy rule of the form, If X is A_i , then Y is B_i is fired to a degree given by $\mu_{A_i}(x)$, then the output set specified in the rule must be scaled or truncated in some way to reflect the truth value of the premise. This process is known as *implication*.

The implication process for fuzzy rules may be derived from that of classical logic theory. Consider a proposition in binary logic, if p then q . The truth-values of the proposition may be presented in a truth table.

Table 3.2 Truth table for the classical proposition if p then q .

Input		Output
p	q	$p \rightarrow q$
0	0	1
0	1	1
1	0	0
1	1	1

Noting that the above truth table is equivalent to the relations, $\bar{p} \vee q$ or alternatively, $(p \wedge q) \vee \bar{p}$, the implications may be constructed using the fuzzy operators described in section 3.2.2. Wang [Wang 97] lists a number of versions by a number of researchers including Dienes-Rescher, Lucasiewicz, Zadeh and Godel.

Wang goes on to draw the distinction between two different classes of implication, namely, *local* and *global*. The propositions listed above are all examples of global implications. From a truth table for binary relationships, one may make global assumptions regarding the proposition; i.e. for a binary proposition if p then q , one may assume that, if \bar{p} then \bar{q} also holds. For fuzzy systems this assumption may not be sound as the rules may only hold in a certain pre-defined space; these are described as *local* rules. Local rules are likely to arise where fuzzy systems are designed from heuristics or identified from data in a non-linear system.

Where the rules may be considered local, the most appropriate techniques for implication are the so-called Mamdani implications. These are the most commonly used implication techniques in fuzzy systems and control, and use either the product or minimum operator as illustrated in figures 3.2 and 3.3 and described as follows:-

a) Product: $\mu_{B'_i}(y) = \mu_{B_i}(y) \times \mu_{A_i}(x)$

b) Minimum: $\mu_{B'_i}(y) = \min(\mu_{B_i}(y), \mu_{A_i}(x))$

This suggests the idea of using the \min operator (see Fig. 3.3) as a suitable technique for the aggregation however Kosko argues [Wang 94] that the most appropriate technique is the composition, as it incorporates the consequent from all the fired rules in their entirety.

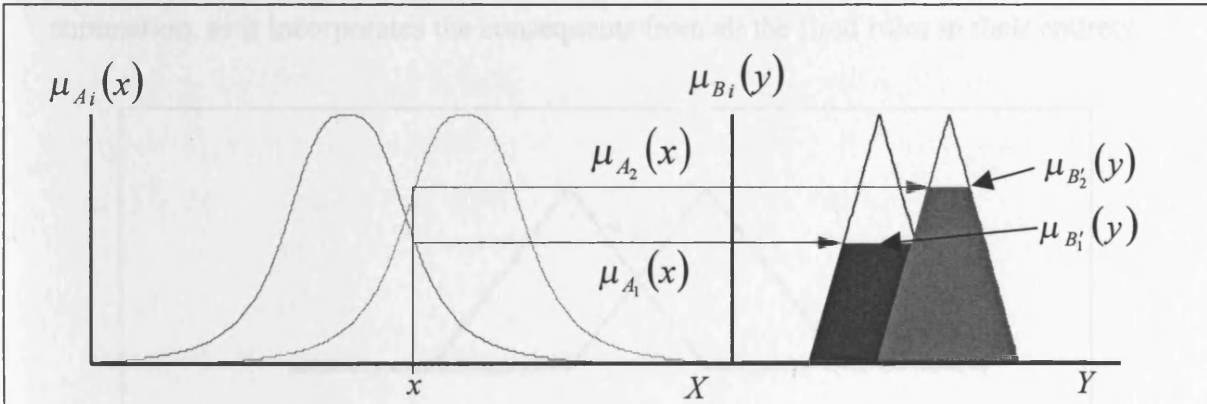


Fig 3.2. The action of the minimum implication on two fuzzy rules.

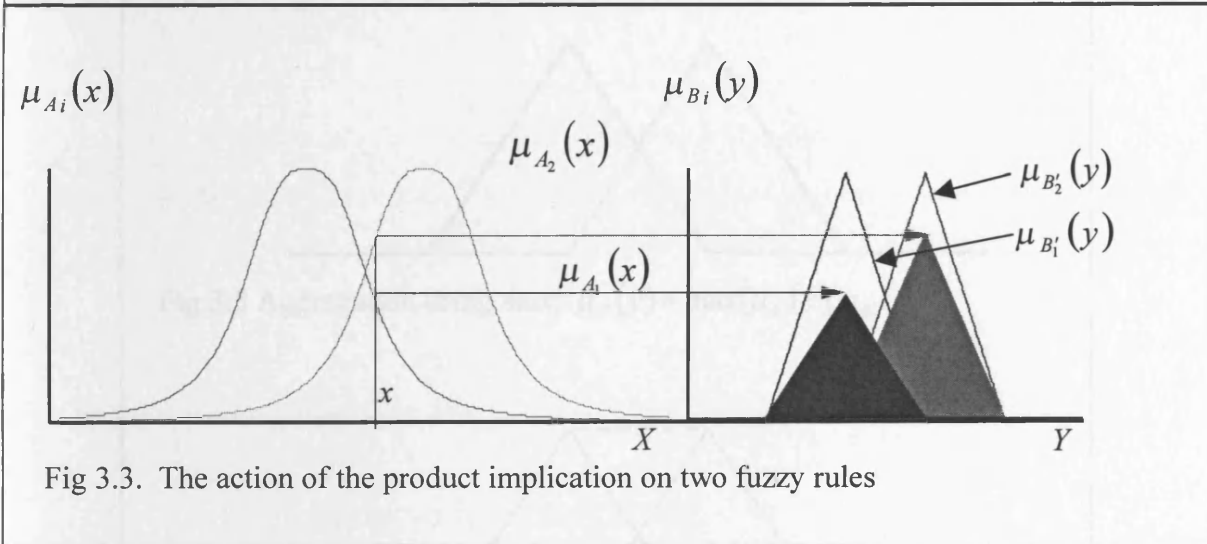


Fig 3.3. The action of the product implication on two fuzzy rules

3.2.4. AGGREGATION

Aggregation is the process for combining the consequent parts of all the fired rules. The process is similar to that of the fuzzy union operation and a number of aggregation techniques are available including the algebraic sum (see figure 3.4). The extension principle [Wang 97] is an identity which leads to the definition of the membership function of the consequent set in a rule as;

$$\mu_B(y) = \max_{x \in f^{-1}(y)} (\mu_{A_i}(x)), y \in Y$$

This suggests the max operator see (see figure 3.5) as a suitable technique for the aggregation however Kosko argues [Kosko 94] that the most appropriate technique is the summation, as it incorporates the consequents from all the fired rules in their entirety.

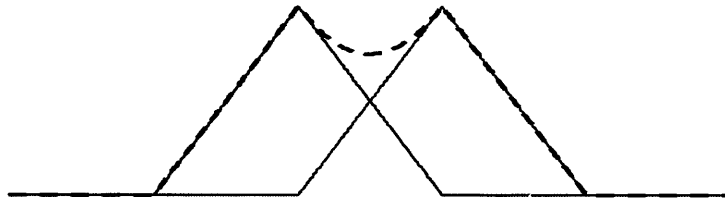


Fig 3.4 Aggregation using the *algebraic sum*;
 $\mu_{B'}(y) = \mu_{B_1}(y) + \mu_{B_2}(y) - \mu_{B_1}(y) \times \mu_{B_2}(y)$

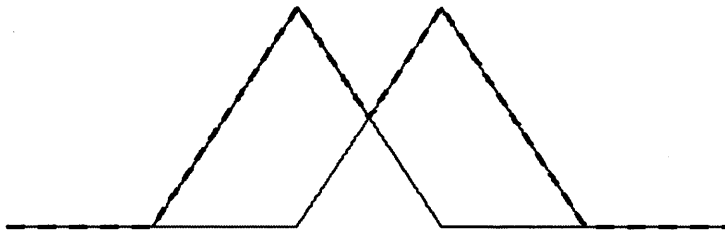


Fig 3.5 Aggregation using *max*; $\mu_{B'}(y) = \max(\mu_{B_1}(y), \mu_{B_2}(y))$

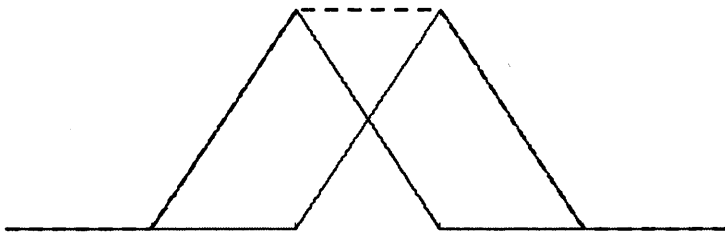


Fig 3.6 Aggregation by *summation*; $\mu_{B'}(y) = \sum_{i=1}^N \mu_{B_i}(y)$

3.2.5 DEFUZZIFICATION

In a fuzzy system a number of fuzzy rules may be fired for each input data point therefore the consequence of each rule will be a fuzzy set. The aim of most fuzzy systems is to

produce a crisp output. The process of obtaining a crisp number from the fuzzy sets in the consequence parts of the fired rules is known as *defuzzification*.

For a rule of the form shown in figure 3.1, the defuzzifier is defined as a mapping from the output fuzzy set, B , to a point $y \in Y$ in the output space. As with fuzzification, the system designer has a number of issues to consider in choosing a suitable form of defuzzification. Wang [Wang 97] states that there are three criteria to be considered in a defuzzification scheme;

- i) **Plausibility:** The technique should give a ‘sensible’ output, i.e. the crisp output from the process should be an intuitively appealing representation of the output sets in the fired rules.
- ii) **Computational Simplicity:** This is a factor of particular importance where the fuzzy system is to be run in real-time as a control algorithm for instance
- iii) **Continuity:** The defuzzification algorithm should provide a smooth output so that a change in the inputs results in a change of corresponding magnitude in the outputs.

The following sections will compare the different techniques for defuzzification

3.2.5.1 OUTPUT MEMBERSHIP FUNCTIONS

The output membership functions of a fuzzy system may be defined in a similar manner to the input membership functions. In addition to the membership function shapes previously discussed, two further types are commonly used in the consequent of fuzzy systems. These are the first order linear functions of the inputs [Takagi 85], so that if the inputs to the fuzzy system are, $X = [x_1, x_2, \dots, x_i]$, then the output membership function is a function of the form:

$$y = g(x) = a_0 + a_1x_1 + a_2x_2 + \dots + a_ix_i$$

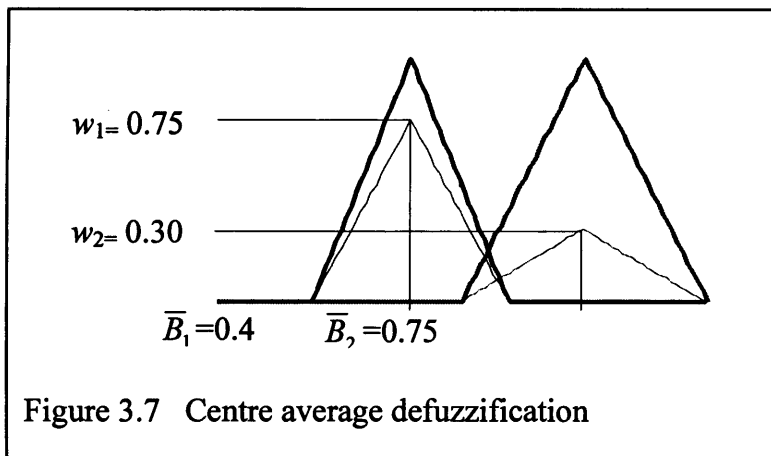
where $a_0, a_1, a_2, \dots, a_i$ are scalars.

Fuzzy systems with this type of output membership function are often known as ‘Takagi-Sugeno’ or ‘type II’ systems. The output membership function may also simply be a constant or *singleton*, a_0 , so that:

$$y = g(x) = a_0$$

3.2.5.2 CENTRE AVERAGE DEFUZZIFIERS

This defuzzification technique calculates a crisp output from a weighted average of the output sets from the fired rules. The weights used w_1 and w_2 in example (figure 3.7) are the truth-values of the premises for the fired rules.

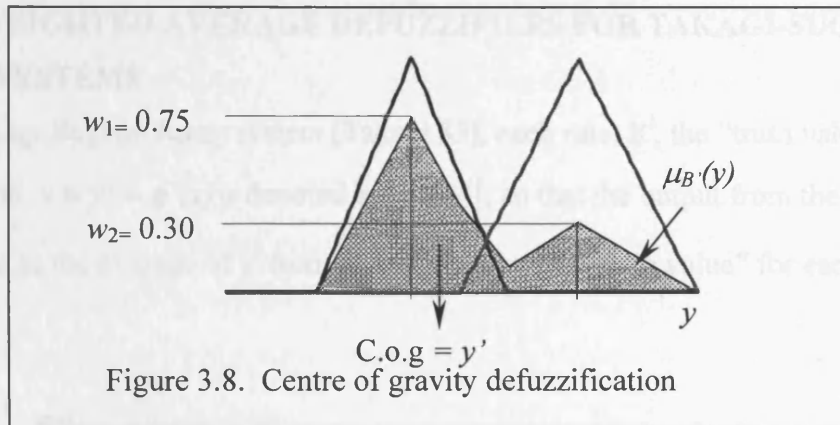


$$y = \frac{w_1 \bar{B}_1 + w_2 \bar{B}_2}{w_1 + w_2}$$

$$y = \frac{0.75 \times 0.4 + 0.30 \times 0.75}{0.75 + 0.30} = 0.5$$

3.2.5.3 CENTRE OF GRAVITY DEFUZZIFIERS

Centre of gravity defuzzifiers (see example figure 3.8) obtain the crisp resultant, y , through calculation of the centroid of the area of the aggregated consequent sets.

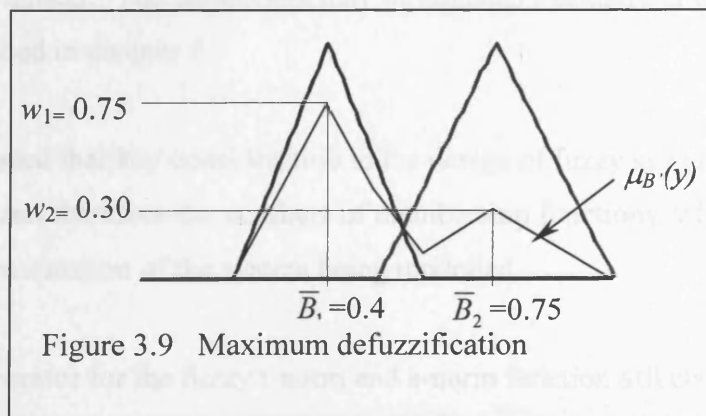


$$y' = \frac{\int y \mu_{B'}(y) dy}{\int \mu_{B'}(y) dy}$$

$$y' = 0.5167$$

3.2.5.4 MAXIMUM DEFUZZIFIERS

A number of defuzzifiers have been proposed where the output y is obtained in some way from the maximum values of the function $\mu_{B'}(y)$. This may simply be the maximum value $\max(\mu_{B'}(y))$, or, where this is not a discrete point, then the average, highest, or lowest value may also be used.



$$y = \max(\mu_{B'}(y))$$

$$y = 0.4.$$

3.2.5.5 WEIGHTED AVERAGE DEFUZZIFIERS FOR TAKAGI-SUGENO FUZZY SYSTEMS

For a Takagi-Sugeno fuzzy system [Takagi 85], each rule, R^i , the “truth value” of the proposition $y = y^i = g^i(x)$ is denoted by $|y = y^i|$, so that the output from the fuzzy system, y , is given as the average of y^i from R^i weighted by the “truth value” for each of the rules so that;

$$y = \frac{\sum |y = y^i| \times y^i}{\sum |y = y^i|}$$

It may be noted that where the output membership function, $g(x) = a_0$ this defuzzification technique is functionally equivalent to the centre average technique whilst the output membership function requires only a single parameter, a_0 , as opposed to the three parameters required by the triangular membership function.

3.3 SUMMARY

It is clear from this chapter, that a multitude of design parameters are available to the fuzzy systems engineer. The parameters may be adjusted manually or using algorithms as will be described in chapter 4.

It may be concluded that key consideration in the design of fuzzy systems is to minimise the complexity, and therefore the numbers of membership functions, whilst maintaining an adequate representation of the system being modelled.

The choice of operator for the fuzzy t-norm and s-norm function affects the smoothness of the mapping. Amongst a wide range of possible functions that may be used, minimum and maximum functions provide the simplest methods for these operators. However these two functions are dominated by the rule with the highest truth-value, whereas use of the algebraic sum for fuzzy union and the product for fuzzy intersection, allows the rules with lower truth-values to influence the result.

It is argued that summation is the most appropriate technique for aggregation of consequents from all the fired rules, as all the fired rules may then influence the outcome.

The most appropriate defuzzification techniques provide a smooth output at low computational cost. The centre of gravity technique provides a smooth, continuous output but has high computational cost, whilst the maximum defuzzifier is not continuous. The centre average defuzzifier provides continuity with low computational cost, however use of singletons as consequents is seen to provide equally good results at a lower computation cost. Linear functions may also be used in the consequent so that the outputs are non-linear mappings of the input variables. Again this is seen to provide a smooth output with a low computational cost compared with a centre of gravity defuzzifier. Although the defuzzification examples give different resultants for the same input values, this does not imply that an error will necessarily exist for that type of defuzzifier. This is due to the nature of fuzzy systems, in that they may be trained to provide the desired outcome thereby minimising the error.

Having studied some of the design parameters which are available for fuzzy systems, a number of algorithms for the identification and training of fuzzy systems from data will be reviewed in chapter 4.

CHAPTER 4.

A Review of Techniques for Identification and Training of Fuzzy Systems.

4. A REVIEW OF TECHNIQUES IDENTIFICATION AND TRAINING OF FUZZY SYSTEMS.

The review of diesel engine CMFD techniques presented in chapter 1 has identified a role for suitable models for use as part of a model based fault diagnosis structure. Although some knowledge of the physical relationships in the system for diagnosis is likely to be available, there is a need for a system identification approach to estimate the model structure and parameters.

Consideration of the requirements for such models has suggested that fuzzy systems are likely to be strong candidates for this role. The fuzzy system properties and structures outlined in chapters 2 and 3 have confirmed this. However, fuzzy systems are just one of several approaches to non-linear systems modelling, therefore section 4.1 assesses the suitability of fuzzy systems for use in modelling by comparison with a number of other techniques. Section 4.2 contains a review of some algorithms which have been produced for the identification and training of fuzzy systems and conclusions are drawn in section 4.3 concerning the relative merits of these systems.

As with any empirical model, fuzzy systems are only valid within the limited range of data on which they are based. Also the validation of the model is an empirical measure of generality, based on evaluation of the model with unseen checking data. Clearly, the quality of the data available for the identification process will also have a strong influence on the resulting model. Identification data requirements for the modelling process will be discussed as part of the case study.

4.1 A COMPARISON OF NON-LINEAR MODELLING TECHNIQUES

Sjoberg [Sjoberg 95a], [Sjoberg 95b] presents an in depth comparison of non-linear modelling techniques. The approach to system identification may be classified according to the amount of *a priori* knowledge of the system available to the designer, as follows;

- *Black box*: The system inputs and outputs are known but nothing is known of the relationship between the two.
- *Grey box*: The system inputs and outputs are known and there is some incomplete knowledge of the relationship between the two.
- *White box*: The system inputs and outputs are known and their relationship is known.

Sjoberg goes on to perform a detailed comparison of different approaches to non-linear modelling, stating a generalised model structure of the form;

$$g(\varphi, \theta) = \sum \alpha_k g_k(\theta) \quad \dots 4.1$$

where, θ , represents the parameter vector, α_k , the co-ordinate parameters, g_k , the basis function, and φ , the regression vector. Included amongst the model structures that conform to the general structure in 4.1, are the family of non-linear auto regressive models, neural network structures, and fuzzy systems. Sjoberg concludes that:

'Fuzzy models are just particular instances of the general model structure (equation 4.1 above) with the advantage of providing the fuzzy rules as a way to describe some previously available prior knowledge'.

Laukonen et al, [Laukonen 95] present results from a fuzzy model based diagnostic scheme for an IC engine drive cycle. He goes on to compare these results with some that were obtained from a NARMAX (Non-Linear Auto-Regressive Moving Average with eXogenous inputs) model. The conclusions from the comparison stated that although the performance of the two structures were similar in terms of model error, the fuzzy system was a more straightforward approach in terms of simplicity of the system identification procedures, and the fuzzy model structures were therefore recommended for future work.

Neural network systems also comply with Sjoberg's generalised model structure and share some common properties with fuzzy systems; e.g. non-linearity, universal

approximation [Kosko 94a]. Certain radial basis function (RBF) structures have been shown to be functionally equivalent to fuzzy systems [Jang 93b]. Therefore neural networks have been used in a number of non-linear modelling applications [Sjoberg 94b], [Schenker 95], [Seng 99]. However, neural networks do not easily facilitate the inclusion of incomplete *a priori* knowledge in the form of heuristics in the initial network structure prior to training the system.

Given the functional equivalence of the different modelling techniques, and similar performance in terms of model error, then it is desirable to employ the most straightforward and transparent of the available techniques to minimise the system development time and to allow clear interpretation of model outputs. Therefore this chapter contains a review of a number of algorithms for fuzzy system identification and training, which build upon the theory reviewed in sections 2 and 3, with the aim of producing suitable models which meet the requirements for model-based fault diagnosis set out in chapter 1.

4.2 A REVIEW OF ALGORITHMIC APPROACHES TO FUZZY SYSTEM IDENTIFICATION AND TRAINING.

The structure of fuzzy systems has been described, but how are the membership functions (m.f.'s) and rules designed to provide the desired mapping from input to output? There are several approaches to identification and training of fuzzy systems. If the dimensionality is low and the relationship between input and output is well understood, it is possible that the fuzzy system may be designed intuitively. The process requires the definition of a number of input variables, the form of the m.f.'s in each variable, then writing in a set of rules and deciding which methods to use for output m.f.'s and defuzzification.

Several researchers have used this approach in fuzzy systems that have been applied to the problem of process control [Abate 90], [Karray 95]. Triangular and trapezoidal m.f.'s are often favoured in a trial and error approach to fuzzy systems' design [Howlett 98], [Huang 00], for their simplicity and the ease with which their parameters may be

adjusted. However, Abate [Abate 90], reports that exponential curves provide improved smoothing capabilities with respect to quantisation effects than triangular m.f.'s.

In a trial and error approach, if relationships between inputs and outputs are unknown or complex, or the system dimension is high, then the task of intuitively defining the systems becomes prohibitively complex. In this situation system identification using algorithms to generate m.f.'s and rules from input/output data pairs becomes desirable.

System identification may be considered in two parts, namely structure identification and parameter identification. Structural identification refers to the process of obtaining the appropriate inputs and form of the fuzzy system, whereas parameter identification commonly referred to as *training* of the fuzzy system refers to the process of optimising the parameters of the system, namely the input and output membership functions and fuzzy rules. The problem of fuzzy systems identification and training is that of generating the initial fuzzy system structure and parameters, evaluating the outputs of the system with the suitable data, then modifying the parameters in some structured way to minimise the model errors with respect to the original data (see figure 4.1).

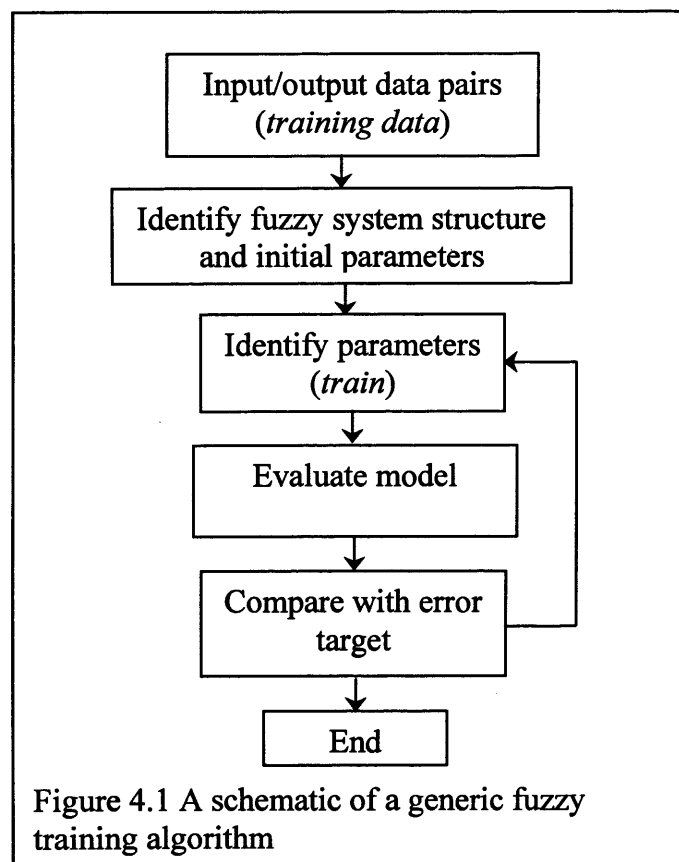
Dimensionality is a key factor in the choice of fuzzy model structure. Two options are available to the system's designer for initialising the fuzzy system structure; firstly a clustering technique (see section 4.2.5) and secondly *grid partitioning* of the input space (See figure 4.2). Grid partitioning means that the input space is subdivided into a number of 'cells' formed by the intersections of the fuzzy sets defined along each input dimension. Each cell in the grid is connected by a fuzzy rule to its associated consequent. The techniques described in sections 4.2.1 – 4.2.3 all result in a grid-partitioned input space. The main issue resulting from this – the so-called *curse of dimensionality* will be discussed in section 4.2.5.

Certain training algorithms are limited to one or two particular classes of fuzzy system and/or types of membership function that may be accommodated in the algorithm. In considering the classes of fuzzy system for which the algorithm is applicable, a

classification system used by a number of authors [Cho 96] [Horikawa 92] and [Jang 93] will be adopted. These authors classify fuzzy systems as types I, II and III. The class definitions are listed below;

- I. Fuzzy membership functions in the premise, constant values in the consequent.
- II. Fuzzy membership functions in the premise, first order linear functions of inputs in the consequent (also known as Sugeno type).
- III. Fuzzy membership functions in the premise, fuzzy membership functions in the consequent.

The following sections will briefly describe with examples, a number of forms of algorithm that have been produced to identify or train systems from sampled input/output data pairs, and assess their applicability in terms of generating fuzzy models and inference systems.



4.2.1 FUZZY SYSTEM DESIGN FROM TABLE LOOK-UP

The table - look up scheme [Wang 97] is a basic technique to connect input/output data pairs using rules. This scheme could be carried out 'manually' to obtain a fuzzy system from appropriate data. The first step is to define a number of fuzzy sets and m.f.'s on the input space. For each data pair, each input and output will be a member to some degree of one or more fuzzy sets defined on the input/output space. The rule is defined by considering each point's membership degree of each set. The set with the maximum membership degree is selected to form the rule. The approach has a number of limitations, contradictory rules may be formed, i.e. rules with the same antecedent but a different consequence, and the number of rules may quickly become very high. Contradictory rules can be formed due to noise in the data, or other uncertainty, and must be eliminated to produce a coherent fuzzy system. Consideration of the reliability of the training data and assigning each rule with a *degree* will eliminate contradictory rules and generally reduce the overall number of rules. The degree of each rule is defined in terms of the product of each data point's membership of the fuzzy sets named in the rule; e.g. for the rule;

$$\text{If } x_{k1} = A_{k1,j1} \text{ AND } x_{k2} = A_{k2,j2} \text{ then } y_k = B_{i,n}$$

and $\mu_{A_{k1,j1}}(x_{k1})$ is the membership degree of x_{k1} in fuzzy set, $A_{k1,j1}$ then in this example the degree of the rule, $D(\text{rule})$, is evaluated from;

$$D(\text{rule}) = \mu_{A_{k1,j1}}(x_{k1}) \times \mu_{A_{k2,j2}}(x_{k2}) \times \mu_{B_{i,n}}(y_k).$$

Thus, for contradictory rules the rule with the highest degree is retained, whilst other rules are eliminated.

A further possibility is that the data points do not cover the whole input/output space, i.e. some combinations of input and output sets are unpopulated. Interpolation or extrapolation from neighbouring rules may be used to generate rules for these empty spaces.

The table-look-up system presents a valid method of fuzzy system production from training data pairs with or without knowledge of the process being modelled. The technique is more formalised than the intuitive method described in 4.2, but the manual approach to system design allows the designer to produce transparent systems and is flexible enough to allow the inclusion of heuristics. However, the algorithm will become increasingly unmanageable with the number of input variables and the number of training data points. The algorithm depends on a set of user defined m.f.'s and for optimisation of the system depends only on the manipulation of the rules, i.e. no indication is given to the user as to the optimum number of fuzzy sets for the system. Using more fuzzy sets will allow better resolution of the mappings at the cost of increased system size.

It is possible to conclude from this description that the look-up table method is most suited to design of fuzzy systems where dimensionality and the number of training data pairs are low. The ability for the designer to strongly influence the generation of rules is beneficial where common sense or intuitive rules will form some part of the system. In terms of CMFD this points to the most likely application of this algorithm as a formalised technique for generation of diagnostic rules from symptom/diagnosis type relationships.

4.2.2 TAKAGI AND SUGENO'S ALGORITHM FOR FUZZY SYSTEM IDENTIFICATION

Takagi and Sugeno [Takagi 85] were some of the earliest researchers to produce an algorithm for a type II fuzzy system design.

Their approach is to grid partition the input space using piecewise linear membership functions, with the initial parameters obtained by observation of the data. The consequents are then obtained using a least squares approach to minimise the model error. The algorithm then uses a non-linear programming method to adapt the input parameters in order to minimise the root mean square (r.m.s.e.) of the modelling errors. An algorithm is employed to subdivide and select the best combinations of the premise parameters to further minimise the modelling error, whilst maintaining the number of

implications in the model within a prescribed bound. The model errors associated with the consequents are minimised after each subsequent iteration of the input parameters.

4.2.3 LEAST SQUARES ALGORITHMS IN FUZZY IDENTIFICATION

Wang and Mendel [Wang 92] and [Wang 97] propose two approaches that adapt the least squares algorithm suitable for fuzzy system identification of type III fuzzy systems.

In the first case a set of fuzzy basis functions (FBF's) are defined with the centre of each fuzzy set defined so that it corresponds to the training data pair. This results in a large number of parameters in the initial system. In the training process the fuzzy system is regarded as a special case of the linear regression model.

$$d(t) = \sum_{j=1}^M p_j(\mathbf{x}(t))\theta_j + e(t) \quad \dots 4.2$$

This is achieved by fixing the input membership function parameters, p , at the start of the training process and modifying only the output parameters, θ , i.e. the centres of the output membership functions. This has the effect of linearising the problem so that it is suitable for solution using the orthogonal least squares algorithm. The algorithm is used to select the FBF's that best fit the training data.

In the second technique the least squares approach is implemented as a recursive algorithm in order to adapt pre-defined fuzzy system parameters to minimise an objective function defined in terms of model error.

The advantages of the least squares techniques compared to the back propagation techniques (section 4.2.4.1) is that the model errors are summed over all the training data set in one iteration, instead of one pair at a time, thus increasing the speed of the system. However the performance of the resulting model system is strongly dependent on the initialisation of the input parameter set, i.e. the definition of the input m.f.'s in terms of their widths and centres, as these are not optimised in the algorithm.

4.2.4 NEURO-FUZZY APPROACHES TO FUZZY SYSTEM IDENTIFICATION

A number of techniques for fuzzy system identification using neural networks have been described. These techniques share the characteristic that the parameters of the fuzzy system are embedded within the nodes of the neural network thereby utilising the well-known adaptive quality of neural networks for training the fuzzy system.

4.2.4.1 THE BACK-PROPAGATION TECHNIQUE

Horikawa et al [Horikawa 92] and Wang [Wang 97] describe the application of the back propagation, (also called the *gradient descent* technique) algorithm to training a fuzzy system.

The back-propagation training algorithm aims to determine three optimised m.f. parameters, namely the centres of the input m.f.'s, the centres of the output m.f.'s and a width parameter for each m.f.. In order to carry out this procedure the parameters are considered as nodes in a three layer feed-forward network. An objective function is defined in terms of the root mean squared error (r.m.s.e.) between the training data output and the fuzzy system output for each point. The task of the training algorithm is therefore to minimise the objective function iteratively by considering the rate of change of the r.m.s.e at each iteration as follows;

$$\hat{y}'(q+1) = \hat{y}'(q) - \alpha \left. \frac{\partial e}{\partial \hat{y}'} \right|_q \quad \dots 4.3$$

$$\hat{x}'(q+1) = \hat{x}'(q) - \alpha \left. \frac{\partial e}{\partial \hat{x}'} \right|_q \quad \dots 4.4$$

$$\sigma'(q+1) = \sigma'(q) - \alpha \left. \frac{\partial e}{\partial \sigma'} \right|_q \quad \dots 4.5$$

σ is the m.f. width parameter

\hat{y} , \hat{x} are centres of output and input m.f.'s for m.f. number, l .

α is a constant stepsize.

e is the rms error

q is the iteration number.

The iterative process is continued until either a pre-defined iteration number or pre-set error criterion has been reached.

The results obtained from using this system depend firstly on the initial choices made for m.f. parameters. If the choice of parameters is close enough to the optimum set, i.e., the parameter set which minimises the objective function, then the system should converge. However, if the parameters are badly defined the system may not converge at all, or may converge to a non-optimal solution or local error minima. The rules obtained from the system are defined in terms of the final fuzzy sets derived from the algorithm and may be seen to have linguistic interpretations that may be useful to the system designer. However, the back propagation method differs from the table look up method in that it is not usual for the designer to be able to influence the outcome of the training process once the initial parameters have been chosen and the iterative process has begun.

This method provides a computational algorithm for creating a fuzzy system based purely on training data. However, there are some drawbacks with the system in that the algorithm tends to be slow as it only updates the m.f.'s for one training pair at a time, and also displays a tendency to become trapped in local minima.

4.2.4.2 A HYBRID SYSTEM FOR FUZZY IDENTIFICATION - ANFIS

Hybrid systems combine characteristics of a number of different approaches. An example of a hybrid system that is of particular interest is Adaptive Neuro-Fuzzy Inference System, ANFIS, developed by Jang [Jang 93a]. This algorithm is available commercially as a learning algorithm, and is part of the Matlab™ Fuzzy Logic Toolbox. [Matlab 97]

ANFIS is used to identify type I or type II fuzzy systems with the proviso that the membership functions in the premise part must be piecewise differentiable. The technique embeds the fuzzy system parameters in a 5 layer feed-forward network. The least squares algorithm is carried out on the forward pass of the network to obtain the consequent parameters, and the gradient descent algorithm is used in the backward pass to modify the premise parameters. The premise parameters for the fuzzy system, i.e. input m.f.'s, are evaluated as the input nodes of the network, the weights are evaluated as the hidden node layers and the consequent parameters, or output m.f.'s, are evaluated as the output nodes.

Apart from the fact that it is commercially available, and therefore no time is required for software implementation, ANFIS, offers an advantage of increased speed of convergence over the other systems considered above. Using results from the identification of a fuzzy model to represent the Mackey-Glass chaotic time series, Jang shows that ANFIS compares favourably in terms of model error with a number of other non-linear mappings including an auto-regressive model and a neural-network.

4.2.4.3 A RADIAL BASIS FUNCTION APPROACH WITH RULE GENERATION

Cho and Wang [Cho 96] propose an adaptive neuro-fuzzy system with the aim of extending the capabilities of the techniques presented in sections 4.2.2 - 4.2.4.2. This technique updates the parameters of the fuzzy system in a similar manner to the ANFIS method described in section 4.2.4.2, in that the parameters are set as the nodes in a hidden layer of a radial basis function network and updated using a back propagation technique. Initially no hidden nodes are assigned to the network, however, as the training data is presented to the network, the algorithm tests to see whether the data pair falls within the hyper-sphere described by the radial basis function at one of the hidden nodes. If not then an additional node is added to the network, thereby increasing the number of rules in the resulting fuzzy system. A further capability of the neuro-fuzzy algorithm is to accommodate the use of fuzzy membership functions in the consequent, i.e. facilitate the identification of type I, II and III fuzzy systems.

Although two ‘benchmark’ examples, namely the chaotic Mackey-Glass time series and a non-linear plant model are identified using this technique, no direct comparison is made between the modelling errors obtained and those obtained when identifying the benchmark system using ANFIS. Comparing results for these benchmark models, using different structures in the consequent, showed that for similar magnitude of model errors the model with type III fuzzy systems seemed to require a lower number of rules. However, no firm conclusions are drawn in explanation of this.

4.2.5 FUZZY CLUSTERING TECHNIQUES

4.2.5.1 MOTIVATION FOR USE OF CLUSTERING TECHNIQUES

Clustering techniques offer a method of sorting data points into spatially related groups. Methods of data clustering are used in a number of applications in pattern recognition. However, the clustering techniques also offer benefits in the field of fuzzy system design based on input/output data pairs.

The methods of fuzzy identification noted in sections 4.2.1 to 4.2.4, sub-divide the input space using *grid partitioning*. This approach results in an exponential increase in the number of rules for the system with respect to the number of input variables and input m.f.’s in the form;

$$\text{Number of rules, } N_r = \prod_{i=1}^n N_m^i \quad \dots 4.6$$

where N_m is the number of membership functions in each input i and n is the total number of inputs. This problem is known as ‘*the curse of dimensionality*’. This may also lead to inefficiency within the system, as certain cells are connected by rules that may never, or rarely be fired as a result of the natural distributions of the input/output data. Similarly sufficient training data may not be available to adequately identify particular rules, resulting in a poorly defined mapping for certain regions of the input space. This may be clearly seen in figure 4.2 (d). Thus, defining the number of rules using grid partitioning may result in an over-complex or computationally inefficient system. Conversely a fuzzy system designed with too few rules, may not achieve the target performance in terms of model errors.

4.2.5.2 CLUSTERING ALGORITHMS

Several clustering algorithms have been developed, notably 'nearest neighbourhood clustering' [Wang 97] and fuzzy c-means algorithm [Bezdek 81]. An extension to the c-means clustering algorithm, 'subtractive clustering', is offered in the Matlab Fuzzy Logic Toolbox [Chiu 94], [Matlab 97].

The clustering algorithms require initial centres to be defined for each cluster and then each data point is associated with each cluster centre, by use of a membership value in the range [0,1]. Each data point is defined as a member of each cluster to some degree, specified by a membership value and dependent on the distance from the data point to the centre of the cluster. An objective function is defined in terms of the least squares distance of any given data point to a cluster centre, weighted by the membership grade of that point. The algorithm proceeds by attempting to minimise the objective function at each step, iteratively updating the cluster centres and membership values.

Additionally, the subtractive clustering algorithm is capable of deriving the number of clusters in a given data set if supplied with a parameter to set the 'sphere of influence' of the data points on each other. The technique works by considering each data point to be a possible cluster centre and calculates its 'potential' by evaluating the density of the data points in the surrounding space bounded by the 'sphere of influence' parameter. The data point with the highest potential is selected as the cluster centre and the potentials of the surrounding data points are recalculated to be inversely proportional to the distance from that cluster centre. The data point with the next highest potential is chosen as the second possible cluster centre. The surrounding data points' potentials are then also recalculated. This process is then repeated iteratively until the potentials of all data points fall below a certain limit. At this point a number of cluster centres have been defined dependent on the specified sphere of influence.

Having used the subtractive clustering method to obtain an optimal fuzzy system structure with fuzzy clusters connected by rules, the system r.m.s.e. may be minimised by use of the ANFIS algorithm (see section 4.2.4.2).

Figures comparing results from system identification of a multi-dimensional function is presented as figure 4.2. Two type II fuzzy systems have been identified to represent the function shown in figure 4.2 (a), using ANFIS (grid partitioning) and subtractive fuzzy clustering respectively. The benefits of the fuzzy clustering algorithm for the representation of such a line-function in multi-dimensional space may be clearly seen. The training r.m.s.e. obtained for the two systems are similar (grid partitioning; r.m.s.e = 0.0070, fuzzy clustering; r.m.s.e = 0.0067) the grid partitioned system requires nine rules whilst the clustered system uses only four.

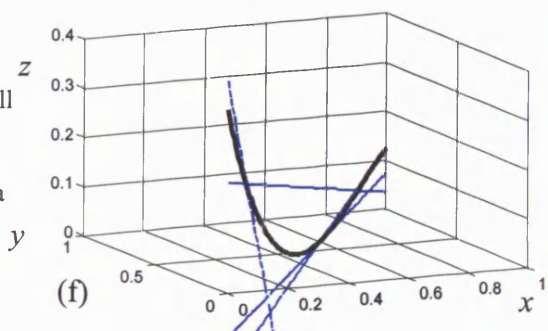
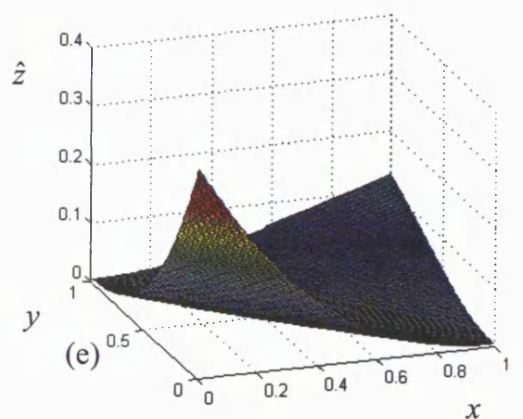
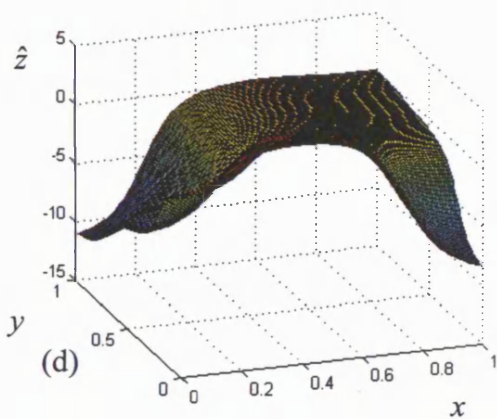
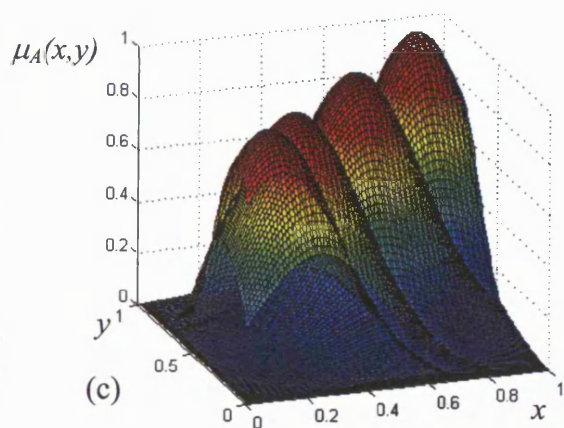
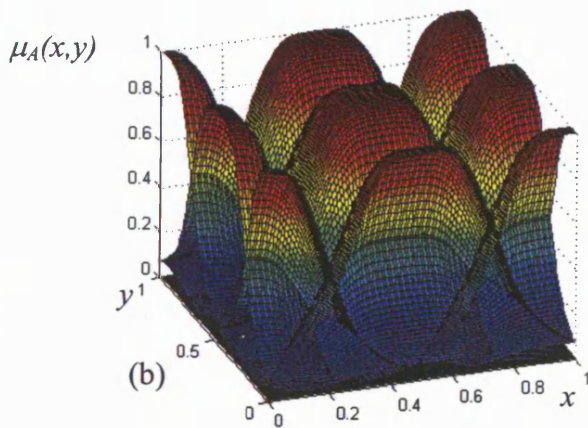
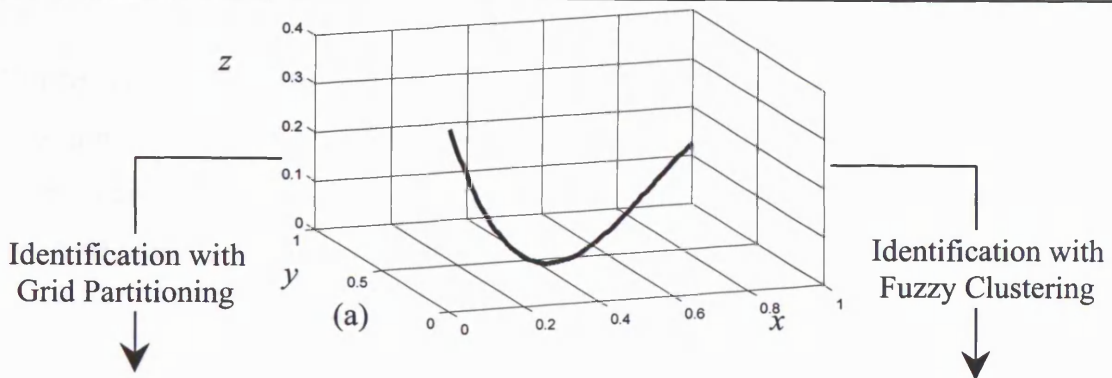


Fig. 4.2 A comparison of clustering and grid Partitioning
 (a) Target function defined as a line $z=f(x,y)$
 (b) Grid partitioning of input space $x \times y$ with generalised bell MF's.
 (c) Partitioning of $x \times y$ with Gaussian m.f.'s obtained from a fuzzy clustering algorithm
 (d) Output surface plot from grid partitioned system.
 (e) Output surface plot from clustered system.
 (f) Type II output m.f.'s for clustered system plotted with original target function

4.3 SUMMARY AND CONCLUSIONS

This section has described a number of techniques for fuzzy systems' identification and training, highlighting a number of characteristics which will influence the design choices to be made in the process of developing fuzzy systems for use in a diagnostic system

Fuzzy systems have been demonstrated to be structurally and functionally equivalent to other techniques commonly used in non-linear modelling. In terms of modelling error, no single one of the available non-linear model structures offer great benefit, with the magnitude of the errors depending on how well the identification algorithm is applied, rather than the structure itself. However, fuzzy systems are seen to offer some benefit over auto-regressive-type models because of the availability of a number of effective identification algorithms, which are straightforward to implement and require less mathematical knowledge. The fuzzy systems obtained from the identification process offer benefit over artificial neural networks, which share many of the same properties, in their transparency or ease of interpretation. Finally, it is argued that the main area where fuzzy systems are of benefit is in grey box modelling, where employing a fuzzy-rule-based structure facilitates the incorporation of partial, or incomplete, knowledge of the system in the initial parameter set defined for the fuzzy system.

A number of identification algorithms have been reviewed and each one is seen to have its particular advantages and disadvantages. The look-up table technique as a 'manual' approach allows the systems designer to influence each stage of the process but is time consuming and increasingly difficult to apply to higher dimension systems. The least squares approach is an inherently faster technique than both table look-up or back propagation, however no optimisation of the premise parameters is carried out in the algorithm so that the result depends very much on the initial parameters. The back-propagation algorithm again requires good initialisation of parameters, but has a tendency to become trapped in local minima in the objective function. The ANFIS technique incorporates the back-propagation algorithm but combines it with a least squares approach to updating the output parameters. This helps to increase its convergence rate

and also to overcome the problem with local minima. In addition to optimising input and output parameters, the radial basis function technique of Cho et al. [Cho 96] also derives the fuzzy system rules from the data. If no *a priori* knowledge of the system is available this may prove to be an advantage however in many cases the systems designer will wish to have some influence on the initial system parameters and rules. Definition of initial parameters using fuzzy clustering has been shown to offer benefit in systems where the dimensionality of the input means that a high computational burden would be imposed by grid partitioning of the inputs.

In general, although the ANFIS technique is limited to type I and II fuzzy systems, its good all-round performance in terms of convergence rate and flexibility, and not least, the fact that it is a well-developed, commercially available system, mean that ANFIS is the appropriate choice for the diesel engine systems identification, reported in the case study (section 2) of this thesis.

SECTION 2.

The Case Study: The development of fuzzy CMFD techniques for diesel engine systems

CHAPTER 5.

The Case Study: An introduction

5.1 INTRODUCTION

The review of condition monitoring and fault diagnosis (CMFD) techniques, and fuzzy logic theory has been presented in section 1 of this thesis. This chapter introduces the second section of the thesis starting with a summary of the main conclusions from the chapters in section 1. The motivation for a case study using a diesel generator set as a test bed is then derived from these conclusions. The aims of the study are outlined in terms of evaluation of fuzzy systems in a CMFD role and development of practical low cost CMFD techniques for diesel engine systems.

5.2 A REVIEW OF SECTION 1

A wide-ranging review of condition monitoring and fault diagnosis has been undertaken in chapter 1. The need for on-board CMFD has been clearly established with the aims of maximising the availability of the engine and early detection of faults which cause an increase in engine emissions levels. The issues involved in specifying a cost-effective solution in terms of required instrumentation have also been considered. A number of CMFD techniques have been reviewed during the course of chapter one, and their strengths and limitations have been discussed.

Based on the limited successes of these individual CMFD techniques, the conclusion has been reached that combining evidence from different knowledge sources using a suitable data fusion system represents the best potential solution to the problem of CMFD in diesel engines. Typical knowledge sources for diesel engine fault diagnosis comprise systems models for parameter and state estimation, along with techniques for data classification and reasoning. The literature review has also shown that fuzzy systems are a possible common methodology for implementation of such knowledge sources, and are therefore worthy of more detailed evaluation.

Chapter 2 described the formalisation of logical methods and the application of logical propositions to predict or deduce conclusions where those conclusions may not be drawn from direct observation. Classical set theory was also reviewed showing how sets may be made to be the subjects of logical statements. From these foundations in classical theory the development of fuzzy set theory was then described. The benefits of using fuzzy sets to classify continuous variables were then outlined.

Fuzzy systems were further discussed in chapter 3, which focused on the possible structures and design options for fuzzy systems. It is clear from this chapter, that although a multitude of design parameters are available to the fuzzy systems engineer, a key consideration for a real-time CMFD system is to minimise the complexity and hence the computational cost, of the fuzzy system, whilst maintaining an adequate representation of the physical system being modelled.

Having identified a role for fuzzy systems in CMFD and carried out a review of the theories of fuzzy logic and fuzzy systems, chapter 4 presented a review of techniques for identification and training of fuzzy models. The aim of this section was to find practical *low-cost* approaches to the identification of suitable models for the CMFD scheme. By *low cost*, what is meant is that the techniques should be straightforward to apply, using easily obtainable data to train the fuzzy systems within a CMFD framework. The chosen techniques for identification should also aim to capitalise on the advantages offered by fuzzy systems for grey-box modelling, allowing the systems designer opportunity to incorporate *a priori* knowledge of the physical system being modelled.

5.3 THE APPLICABILITY OF FUZZY SYSTEMS TO CMFD.

Based on the review of fuzzy systems theory it is possible to summarise the properties of fuzzy systems with respect to their proposed role in fault diagnosis. Fuzzy systems have been shown to be capable of representing non-linear relationships to an arbitrary degree of accuracy and of having benefit in dealing with measurement noise. Detailed knowledge of the physical system being modelled is not a pre-requisite, although fuzzy systems allow the designer to incorporate *a priori* knowledge or heuristics. It is reasonable to assume that suitable training data will be available from testing of the engine in its normal fault free state, however training data for certain fault states may not be available. The rule-based format of the fuzzy systems means that the evaluation of the output from the system is an explicit process, thus allowing the relationships between the inputs and outputs to be easily visualised so that diagnostic results may be easily interpreted.

The chief disadvantage of fuzzy systems identified from test data is that they are by their nature empirical and no guarantees can be made about their robustness or generality.

Where the fuzzy systems are identified and trained entirely from training data, the defined input space is bounded by the maximum and minimum values of the data. Further to this, if only limited training data is available it may result in the fuzzy mapping being poorly defined in certain sub-regions of the input space. This may present

particular difficulties in a CMFD scheme should a fault condition occur which causes the input variables to migrate outside of the pre-defined input space. Therefore some form of limit checking on the input variables is recommended so that an estimate of confidence may be produced and used in association with the fuzzy state estimations.

Therefore in terms of reference model development for CMFD, it is expected that fuzzy systems may be most effectively applied in modelling a specific class of systems where the states are constrained within certain bounds, even under fault conditions. In diesel engine systems, for example, this could include speed and load estimates or fluid flow rate through restrictions, such as valves or compressors. However, it is unlikely to include estimates of engine temperature, as fault conditions are likely to cause overheating causing the engine temperatures to migrate outside the normal range of values.

5.4 THE CASE STUDY: OBJECTIVES

Two main points have been established thus far;

- Fuzzy systems have been shown to have a number of properties which are known to be useful in diagnostic systems, however fuzzy systems are also known to have certain limitations which raise questions concerning their suitability.
- There is a clearly stated requirement for development of on-board CMFD for diesel engine systems.

It is therefore proposed to undertake a case study which will encompass the development of fuzzy model-based diagnostic systems as knowledge sources suitable for incorporation into an on-board CMFD system.

The diesel engine represents an excellent test-bed for evaluation of fuzzy systems in fault diagnosis because of its complexity, its inherently non-linear dynamics, and the problems involving measurement noise associated with 'real' data. CMFD systems developed during the course of the case study, though primarily designed to be applicable to diesel

engine systems, should be also be structured to be generic and portable to other sorts of plant. Clearly, any positive results will contribute toward meeting the need for development of on-board CMFD techniques, and will therefore be of benefit to the industrial sponsors of the project.

This evaluation of the role of fuzzy systems in CMFD is designed to assess their capabilities in a number of areas; firstly, as systems modelling for parameter and state estimation in dynamic, non-linear systems subject to noise and uncertainty, and also as systems for reasoning and classification. Thus, fuzzy systems are proposed as a common methodology for these different aspects of a CMFD system and the conclusions drawn from the case study will be given in terms of their suitability in each of these roles.

5.5 THE CASE STUDY: A JUSTIFICATION

It has already been reported that a substantial body of research has been undertaken in both fuzzy systems theory and that of CMFD. Therefore it is valid to question whether this case study will offer any unique contribution to this body of work. This section aims to respond to that question.

In these examples, fuzzy models have often been assessed in the context of a direct comparison with other approaches to non-linear modelling. For example Jang [Jang 93a] and Chiu [Chiu 94] compare auto-regressive, neural and fuzzy models in non-linear time-series modelling. Laukonen [Laukonen 95] compares the use of dynamic fuzzy models of engine systems with the results obtained from a non-linear auto-regressive moving average (NARMAX) model structure. Several other researchers employ fuzzy systems to analyse engine data without recourse to state estimation [Zhang 98], [Lu 98], [Howlett 98].

The application of fuzzy systems in roles which allow a direct comparison to be made with other model structures, may not fully demonstrate the benefits of fuzzy systems. It has already been reported that non-linear models can be expressed as a common structure (equation 4.1), therefore given that sufficient information or data is available to identify

the structure parameters then it might be expected that model errors from each of the structures will be of a similar magnitude. This view is supported by Laukonen [Laukonen 95], who shows that the fuzzy model-based approach to state estimation, when compared with a NARMAX structure, performs similarly in terms of their model error although NARMAX systems incur greater development costs.

The full benefit of fuzzy modelling may only be realised when using combinations of *a priori* knowledge and system identification from acquired data to develop more appropriate model structures, specific to individual tasks. Therefore this study aims to test this aspect of fuzzy systems theory by modelling highly non-linear physical systems using a 'grey box' approach. Whilst it may be equally possible to identify such models with other structures, none offer the combination of non-linear capabilities and incorporation of heuristics.

A further benefit of the proposed scheme is the development of systems which output high level results to the engine user. Jewitt [Jewitt 85], Freestone [Freestone 85], Laukonen [Laukonen 95], Molteburg [Molteburg 91] etc. present results as raw parameter and state estimates. The use of appropriate classification and reasoning in such cases would benefit the engine operator by automating the process of identifying the engine condition from the output state or parameter estimations and presenting this result as a linguistic variable.

Therefore in the development of a fuzzy model-based CMFD scheme for a complex system, it may be seen that useful information can be made available from state estimates produced from models of any of the sub-systems or components which comprise the plant. If the state estimations and diagnostic reasoning elements of the CMFD system are held in separate modules, then information such as state estimates may be communicated between different modules of that system.

Applying this philosophy to the structural design of the CMFD system is intended to demonstrate the capabilities of fuzzy systems within an expert system framework for

fault diagnosis of complex systems. Again, this expert system structure is intended to be generic and appropriate for use with any suitable technique for state or parameter estimation.

5.6 SUMMARY

This chapter has presented a brief review of section 1 of the thesis and extracted a number of issues which demonstrate the need for a case study and highlight the novel aspects of this exercise. This case study has the aims of producing fuzzy model-based CMFD systems suitable for on-board diagnosis of diesel engine systems.

CHAPTER 6.

Experimental Arrangements

6. EXPERIMENTAL ARRANGEMENTS

6.1 INTRODUCTION

The following set of procedures are intended to outline the objectives, theory, and practical arrangements required for acquisition of data to identify a number of fuzzy models and estimators, which may subsequently be implemented as real-time systems and deployed in a software-based condition monitoring and fault diagnosis (CMFD) system. The aim of this system is to provide the operator of the diesel engine with information regarding the operating condition of the engine based on data acquired by an array of appropriate instrumentation.

Sjoberg et al [Sjoberg 95a] present an overview of different possible model structures for use in non-linear black box modelling. Sjoberg defines the model structure as being a map from the observed data to the regressor (or input variable) and a map from the regressor to the output space. Thus, the task of the systems designer is to choose both a suitable non-linear mapping and suitable regressors for development of appropriate reference models for use in residual generation and fault diagnosis. This task will be simplified to some extent by use of *a priori* knowledge of the engine systems based on reviews of relevant literature.

Essentially, the data acquisition procedures outlined here are designed to provide suitable data for the grey-box approach to fuzzy modelling proposed in chapter 5. However, in acquiring the data it is important to remember that fuzzy modelling from acquired training data results in models which may only be well-defined over certain regions in the state-space. Therefore the test programs will need to be designed to maximise this valid state-space. It will be shown in later chapters that that the extent of this space may be increased by inclusion of additional fuzzy sets and rules based on *a priori* knowledge of the system under consideration. Even with the knowledge available from the literature survey, some trial and error is likely to be necessary before suitable models are finalised.

The sources of the *a priori* knowledge required for such an approach include research by other authors and information obtained experimentally during the course of the test

program. This chapter will briefly review results obtained by other authors concerning the development of models representing the physics of diesel engine systems. Many authors have produced thermodynamic models of diesel engine systems for a number of different purposes including Molteburg [Molteburg 91], Filipi and Assansis [Filipi 97], Watson and Janota [Watson 82], Heywood [Heywood 88]. Chow and Wyszynski [Chow 99] present a useful review of papers concerning engine systems modelling by first and second law thermodynamic analysis.

6.2 DIESEL GENERATOR TEST-BED DESCRIPTION

A diesel generator set (see appendix 1 for detail) has been acquired and provided for the purpose of development and testing of the CMFD schemes under consideration here. A set of instrumentation for the generator set has also been supplied by Perkins Technology Ltd. for use on the test bed (see calibration sheet, appendix A2.2). The generator consists of a Perkins TG1004 diesel engine (see 'Electropak' data sheet, appendix A1.2, for details) attached to a Newage a.c. generator and packaged into a generator set by FG Wilson (see appendix A1.3 for details). The electrical load from this set is dissipated as heat from a Crestchic resistive load bank (see appendix A1.4 for details). The electrical loads may be varied by switching the resistors contained in the load bank into and out of the circuit, giving load range between 0 and 65kW with 1kW resolution. The generator set is controlled to a fixed speed of 1500 r.p.m.

6.3 SUB-DIVISION OF DIESEL ENGINE INTO APPROPRIATE SUB-SYSTEMS.

Having set out the model requirements for the CMFD system in sections 1.6 and 1.7, we may now consider the general approach to the development of a successful solution. The engine will be considered as a number of sub-systems and lower level sub-systems down to an appropriate level of detail. Thus the overall CMFD system is intended to be of hierarchical structure, with a number of knowledge sources representing the different levels of engine sub-systems outputting high-level information to an expert diagnostic system. The lowest level of detail for each knowledge source should be based on the intended maintenance policy for the engine. i.e. the lowest level of the diagnostic is the smallest replaceable component in the system.

The first task in the CMFD system design is therefore to divide the diesel into a number of appropriate sub-systems. These are presented in table 6.1.

Table 6.1 List of diesel engine sub-systems and components

Sub-system	Components
Combustion	fuel injectors, cylinders, valves.
Fuel	filters, lift pump, distribution pump, supply pipe-work.
Cooling	coolant pump, thermostatic valve, radiators, cooling fans, heat transfer, surfaces, pipe-work.
Lubrication	filters, oil pump, bearings.
Aspiration	filters, compressor, air inlet manifold, pipe-work
Exhaust	exhaust manifold, turbine, pipe-work
Control	speed sensor, control unit, actuator
Electrical	alternator, battery, starter motor.
Mechanical	con-rods, crank-shaft, cam shaft, gear train, bearings, valves, rockers, pistons.

6.4 PRIORITISATION OF THE CASE STUDY

As with any project, this study has a finite time-scale, thus some prioritisation of the work is necessary in order that important and useful findings may be reached in the time available. Further to this, where sub-systems have similar characteristics, the diagnostic techniques which are developed may be easily portable to other sub-systems. Thus the sub-systems which are to be the subject of this study are chosen to be those where the results are of particular benefit to engine operators and also where the systems are seen to have different characteristics from each other.

The characteristics of the combustion, cooling, aspiration and exhaust systems are discussed in sections 6.1 – 6.3. Considering the other systems listed in table 1, the lubrication system has some similar features to the cooling system i.e. it is a closed cycle

thermo-fluid system characterised by flow-rate, pressure and temperature. The electrical system on the diesel engine is only comprised of an alternator, battery and starter motor. Its function is to supply power to the controller and to the starter motor at start-up of the engine. A simple voltmeter supplied with the generator set to indicate loss of charge in the battery, and therefore provides convenient indication of a fault occurring in that system, therefore CMFD of this system will not be considered here.

The mechanical system converts the power from the reciprocating motion of the pistons to the rotating motion of the crankshaft. The power is then transmitted to drive both the internal and external loads on the engine. Faults in this system may be associated with mechanical wear, and therefore there are interactions between this system and the lubrication system. Diagnosis of the mechanical system may also be undertaken by spectral analysis of the vibration signal (see section 1.6.2). Whilst CMFD of the mechanical system is an interesting task, testing with simulated faults may require time consuming mechanical modifications to the engine. Therefore in view of limited time available it is proposed to give higher priority to sub-systems a) – c) as listed below.

Diagnosis of the control system was planned as part of a controller design project to run in parallel with this project in fault diagnosis. There is strong potential to extend this work to include diagnosis of the fuel system, therefore CMFD for these systems will not be considered here.

Considering the diesel engine sub-systems in terms of the prioritisation criteria, the sub-systems chosen for study are as follows;

- a) The *combustion system* is chosen because of its fast dynamics, periodicity, and strong influence on emissions, which means that effective CMFD techniques will be of benefit to the engines operators.
- b) The *cooling system*. A closed cycle system, involving transfer of heat and mass, with relatively slow dynamics. It seen to share these characteristics with lubrication system and therefore diagnostic techniques may be common to both systems.

- c) The *aspiration and exhaust systems*. Correct operation of these systems is important for performance and emissions. CMFD development of these systems also provides potential to explore the strong interactions between combustion system aspiration and exhaust.

6.5 DIESEL ENGINE SUB-SYSTEM CHARACTERISTICS

This section presents a description of the selected diesel engine sub-systems in terms of their function within the engine and considers the measurable properties which may be monitored to provide a useful indication of the system condition within the fuzzy-model based CMFD framework. System diagrams showing instrumentation schematics and system boundaries of the fuel, aspiration, combustion, exhaust and cooling systems are presented in appendix 2.1

6.5.1 THE COMBUSTION SYSTEM.

This sub-system is characterised by fast dynamics and periodicity driven by discrete combustion events in the engine's four cylinders. The operation of this system has significant effects on power output, efficiency and emissions performance, all of which are of particular interest to engine operators.

From the point of view of diagnosing combustion faults it may be argued that the thermal conversion efficiency, η_t , is the key indicator of performance;

$$\eta_t = \frac{W_c}{\eta_c m_f Q_{HV}} \quad \dots \quad 6.1 \quad [\text{Heywood 88 pp85}]$$

This relates the useful work done on the piston by the combustion of the fuel with fuel flow rate to the cylinder. The fuel flow rate may be easily measured however it is difficult to obtain an indication of work done on the piston. If the engine is to be tested off-line then a dynamometer may be used to indicate the total brake load on the engine and hence the useful work. However, this is clearly not a practical approach for an on-board system so alternatives must be sought. One possibility is to employ in-cylinder

pressure transducers to indicate mean effective cylinder pressures. To include a cylinder pressure transducer in each cylinder will prove expensive (e.g. Kistler 6053C sp30-60 in-cylinder transducer £1,701 each (1998 price)). Also Molteburg [Molteburg 91] reports that he experienced problems in obtaining reliable measurements of cylinder pressure. Molteburg goes on to recommend using alternative means, such as crank friction parameter or instantaneous engine speed measurements, to test for combustion system faults which are otherwise indicated by cylinder pressure.

Research has also been undertaken to estimate cylinder pressures based on signals obtained from an accelerometer mounted on the cylinder head. [Ordubadi 82], [Lynch 92]. This approach is preferable to the cylinder pressure transducer approach in that only one lower cost transducer is required. Data from the accelerometer may be utilised to indicate cylinder pressure discrepancies which may be symptomatic of a fault. Alternatively accelerometer data may be analysed using appropriate classifiers to indicate misfire [Li 99].

Filipi and Assansis [Filipi 97] have produced a detailed non-linear thermodynamic model of a single cylinder diesel engine. This models the in-cylinder combustion as a series of discrete events with respect to crank-angle, showing the resulting fluctuations of torque under steady load and transient conditions. Fluctuations in engine speed have also been analysed by Jewitt [Jewitt 85] and Freestone [Freestone 85] as variation in the periodicity of these fluctuations is symptomatic of certain faults in the combustion system.

In terms of instrumentation, speed signal analysis is preferable to accelerometer signal analysis, as engine speed is usually available in the standard instrumentation set. In the case of the diesel generator set test-bed, the speed signal used in the closed loop speed control algorithm and is obtained by converting pulse frequency from a magnetic proximity sensor used to detect the flywheel gear teeth.

The pulses from the flywheel gear tooth proximity sensor may also be integrated to provide a measure of crank angle. To relate this measure to the four-stroke engine cycle

a datum signal must be recorded once per 720° of crank angle. For the purpose of this test work a pair of gears with a 2:1 ratio were driven from the crankshaft and an infra-red detector used to detect the passage of a hole drilled in the idler gear aligned with top dead centre (TDC) on cylinder 1 (see appendix A2.6 for detail). Possible alternatives to this cycle datum are obtainable from the fuel pump timing, or injector needle lift transducers or fuel line pressure signals, however for the diesel generator set each of these possibilities are more expensive options.

Air/fuel ratio is also known to be a key factor in the formation of certain emissions [Heywood 88 pp589] and it will be shown that the air fuel ratio may also be used as a basis for a useful estimate of engine load.

Therefore a small number of signals have been identified as necessary to diagnose significant faults within the combustion system. These are;

- fuel flow rate [see appendix A2.3]
- air flow rate [see appendix A2.4]
- crank angle increments [see appendix A2.6]
- 4 stroke cycle datum point [see appendix A2.6]

6.5.2 THE COOLING SYSTEM.

This closed cycle thermo-fluid system consists of a number of components listed in table 6.1 and presented as a schematic in appendix 2.1. The successful operation of the system results in effective heat dissipation from the engine block, ensuring that the engine is maintained at proper temperature, thereby reducing the rate of mechanical wear. The flow of coolant around the cycle is controlled by a thermostatic valve which opens at a prescribed temperature to allow coolant to flow to the radiator. The system has mixed dynamics, in that the operation of the thermostatic valve is relatively fast compared with the heat transfer to the coolant.

Chiang et al [Chiang 82] develop a thermodynamic model of a truck cooling system for the purposes of improving thermal control of the engine, and consequently improve fuel efficiency and reduce wear rates. The models described in this paper are used as a basis for the development of a non-linear model of the cooling system. The parameters of the model have been estimated using the *series-parallel* model with data obtained from the test-bed. This parameter estimation process is presented in appendix 3. The aim of developing this model is to increase the understanding of the cooling system operation and to provide parameter estimates for the development of a sliding mode observer-based diagnostic for the radiator [Bhatti 99], [Jones 00].

Coolant temperatures may be measured at several points in the cooling system by use of thermocouples and platinum resistance thermometers (PRT's). Coolant flow rates however are difficult and impractical to measure directly. A turbine flow meter (TFM) is one possible technique which can be employed, though this is an expensive item, is intrusive and adds complexity to the system, it is also impractical in that a TFM may only conveniently be fitted between the thermostatic valve and the radiator. Thus, the coolant flow rate through the engine block cannot be measured directly when the thermostatic valve is not fully open. The use of pressure differential measurements to provide an estimate of coolant flow has also been explored, (see appendix 2.8) however this approach was found to give somewhat unreliable results. Therefore, the TFM has been employed to obtain initial data for modelling the operation of the thermostat valve in response to changes in temperature. It will also be shown that the valve position may be successfully estimated from appropriate temperature measurements using a fuzzy system, thereby eliminating the need for the permanently fitted TFM.

The system has been instrumented to allow development of appropriate models and estimators for diagnosis of faults. The instrumentation required for this process is listed below; (see appendix A2.1 for detail)

- coolant flow meter
- engine block surface temperature transducers – 2 on each side of engine

- ambient air temperature transducers at the radiator inlet and outlet
- coolant temperature and pressure transducers inlet and outlet of engine block and inlet and outlet of radiator.

6.5.3 THE ASPIRATION AND EXHAUST SYSTEMS.

These two systems are strongly inter-connected in the same gas flow path and mechanically, by means of the turbocharger, so they are considered jointly in this study. These two systems also have strong interactions with the combustion system. The systems are characterised by the pressure, temperature and flow-rate of inlet air and exhaust gas through the system. The efficiency of the aspiration process and removal of exhaust gas is crucial in maintaining the combustion processes and maximising the thermal efficiency of the engine.

Watson and Janota [Watson 82] present a text detailing the theory and application of turbo-chargers in internal combustion engine systems. Turbine and compressor operating characteristics can be plotted on a *performance map* as dimensionless groups;

$$\frac{\dot{m}_a \sqrt{T_{0,ii}}}{P_{0,ii}}, \eta, \frac{\Delta T_0}{T_{0,ii}} = f\left(\frac{ND}{\sqrt{RT_{0,ii}}}, \frac{P_{0,to}}{P_{0,ii}}\right)$$

D and R are fixed for a particular turbocharger and gas, respectively therefore the performance maps are usually expressed as;

$$\frac{\dot{m}_a \sqrt{T_{0,ii}}}{P_{0,ii}}, \eta, \frac{\Delta T_0}{T_{0,ii}} = f\left(\frac{N}{\sqrt{T_{0,ii}}}, \frac{P_{0,to}}{P_{0,ii}}\right) \quad \dots 6.2$$

Clearly the mass flow rates of air and fuel will therefore need to be measured to monitor the performance along with temperatures and pressures at inlet and outlet of the turbocharger, compressor and air filter.

Molteburg [Molteburg 91] uses an air filter model of the form;

$$\Delta P_{af} = k_{af} \frac{\dot{m}_a^2}{\rho_{amb}} \quad \dots 6.3$$

There is an advantage in using differential pressure gauges, especially for the filter model, namely that use of two transducers to measure input and output pressure can incur an error due to small differences in calibration between the two transducers. However for the purposes of this case study and in order to minimise the instrumentation in the aspiration system, it is advantageous to use a gauge at each measurement point. This means that the signal may be read for more than one model, e.g. air inlet manifold pressure and compressor outlet pressure.

Therefore, from equations 6.2 and 6.3, the required instrumentation for the aspiration and exhaust systems is itemised below (see appendix A2.1 for detail);

- pressure and temperature transducers;
 - filter inlet
 - compressor inlet, (=filter outlet)
 - air inlet manifold pressure
 - exhaust manifold pressure
 - turbocharger outlet pressure
- Air inlet mass flow
- Fuel flow transducer

6.6 ADDITIONAL INSTRUMENTATION: CELESCO SMOKE DETECTOR.

This instrument was fitted primarily as an aid to controller development work undertaken as part of a separate study. The system operates with a light emitting diode and receiver to indicate the opacity of the smoke (see appendix A2.5). The smoke detector is a somewhat impractical device for on-board CMFD systems, as it is large and requires compressed air supplies to maintain its lenses in a soot free state. However smoke

readings are of interest in the qualitative assessment of certain faults and are occasionally referred to in the course of the text.

6.7 DATA ACQUISITION AND SIGNAL PROCESSING FOR FUZZY MODEL IDENTIFICATION.

Techniques for sampling of signals, digital signal processing and system identification are widely reported elsewhere (e.g. [Oppenheim 89], [Ljung 87]). Choice of appropriate signal processing techniques and sample rates for these data acquisition procedures is an important issue. Factors affecting this choice are as follows;

- i) A priori knowledge of the dynamics of the system to be modelled.
- ii) The numbers and density of data pairs required for effective identification of the fuzzy models.
- iii) The frequency spectra of the data and knowledge of the bandwidths which will be of interest.
- iv) Sources of noise and the requirements for anti-aliasing filters.

Point i), above, refers to knowledge concerning which variables to record in order to effectively undertake the desired program of CMFD this has already been discussed in section 5. The second point refers to the way in which the fuzzy systems are identified. The fuzzy model is trained from input/output data pairs as described in chapter 4. If the density of data points in a particular region of the state-space is low than the input/output sets for that region may not be well defined. This problem may occur in systems where individual events occur at different rates. For example in the cooling system, the rate of change of the thermostat valve position is relatively fast, compared to the rise time of the coolant temperature, in response to a step change in load. Therefore the sample rate for the data should be determined, based upon the sampling theorem [Oppenheim pp86] to be suitable for the component in the system with the fastest dynamics.

The structure of the intended model is also a consideration in determination of appropriate data sampling processes. For instance in the case of the thermostat valve

model, the model input is a temperature measurement and the output is a prediction of volume flow rate. Therefore, due to the fact that data sampling for the thermostat model is carried out at specific time rather than temperature intervals, the density of the data around the regions where the valves are opening and closing is relatively low. Therefore it may be appropriate to initially over-sample the data and then re-sample with respect to temperature, rather than time. The issue of data density in certain regions of the input space is similar the work carried out by Parikh et al, [Parikh 99] who studied the effects of relative availability of training data in for each class on the performance of neural network classifiers.

In a black-box system where the relationships between the possible inputs and outputs of the system are not well known, a number of techniques are available to analyse data to increase the knowledge of the system to improve ones chances of making good choices for regressors and mapping functions. These techniques include; correlation of potential inputs and outputs to assess their inter-dependencies, excitation of the system with a certain prescribed inputs such as step, impulse, sine wave or ramp to assess its responses and spectral analysis of data sets acquired from the system. These three techniques may be employed here to help define sample rates for data acquisition.

The step response of the system reveals information allowing the time constant of the system to be estimated. As an example, an analysis of the dynamics of the diesel engine cooling system has been undertaken to recommend sample rates for data acquisition (see appendix 2.7). In this example, the response of the coolant temperature at the outlet to the engine block T_2 to 20kW increase in engine load has been observed and the time response estimated at 330s This suggests that quite low sample rates will be adequate to acquire temperature data suitable for training the fuzzy model. Additionally spectral analysis of the data acquired from thermocouples placed in the coolant system, show that if the sample rates are set to 10Hz, then any aliasing effects will be negligible. This is because the signals of interest have a narrow bandwidth and have frequencies considerably lower than 5Hz, whilst frequency components higher than 5Hz, have a relatively low power levels. This is not true for the signals from pressure transducers in

the system, which are affected by vibrations originating from combustion events within the engine, particularly at 25 and 50Hz, which means that suitable anti-aliasing filters will be required.

6.8 DATA ACQUISITION HARDWARE AND SOFTWARE

The data acquisition processes are undertaken using the dSpace™ [dSpace 99] DS1103 PPC Controller Board through sixteen 16 bit ADC channels. The signal processing routines for this board are prepared using Simulink™ [Mathworks 99] version 3.0 and Matlab™ version 5.3 [Mathworks 99]. The Matlab Real-Time workshop may be used to generate code automatically from the data acquisition system parameters generated in Matlab and system block diagrams created in Simulink. The code is then directly downloaded onto the DS1103 Controller and may run from the dSpace graphical user interface known as 'Control desk'.

6.9 MODELS AND ESTIMATORS: DEFINITIONS

In this thesis reference is made to fuzzy systems which will be employed as 'models' or 'estimators'. Not all the variables in a particular sub-system system are measurable due to considerations in terms of cost and practicality. However, in a model-based system where variables are not directly measurable, the problem arises of how to generate a residual. Where the variable is directly measurable, a residual may be calculated simply by taking the difference between the measured and modelled variable. Where no measured variable is available it becomes necessary to estimate that variable based on other plant measurements, thereby allowing a comparison to be made between the modelled and the estimated variable. Essentially, we may state that a *model* is defined to predict the value of a state associated with a component assuming that component is *functioning correctly*, and an *estimator* provides an estimation of the *actual value* of the state. This approach is therefore comparable with that of the parity space approach reported in section 1.6.4.4.

6.10 CONCLUDING REMARKS

The diesel engine generator set which is to be the subject of this case study has been described in this section with reference to its detailed specification contained as appendices. The engine's subsystems have been considered in terms of their function within the engine and prioritised for the purposes of case study. Thus, fuzzy model-based CMFD systems will be developed for a number of the defined sub-systems. Each of these CMFD systems may be viewed as a *knowledge source* for the overall engine CMFD system. Their outputs are intended as a source of evidence to be communicated to an expert or blackboard-type reasoning algorithm for diagnosis of the overall engine condition.

The sources of a priori information available for each engine subsystems under consideration have been briefly reviewed. Based on this information and consideration of cost and functionality, suitable instrumentation has been described and installed for the case study. The general considerations for specifying the data acquisition process have been considered and suitable hardware and software has been installed.

CHAPTER 7.

**Fuzzy model based condition monitoring and fault
diagnosis of a diesel engine cooling system**

7.1 INTRODUCTION

The overall aims of this case study outlined in section 5.4, provide the context for the development of the fuzzy-model based diagnostic scheme for the cooling system described in this chapter. This diagnostic scheme could represent one knowledge source for a blackboard-type CMFD system used to monitor the condition of the engine as a whole.

Fuzzy models of the systems described in this chapter have been developed from both *a priori* knowledge of the physical system, and by fuzzy systems identification using the ANFIS algorithm [Jang 93a] [Mathworks 99]. The architecture of the fuzzy model-based diagnostic system employed here is based on the generation and analysis of residuals [Isermann 97], and has been designed and implemented for real-time fault diagnosis using Matlab™, Simulink™ and dSpace™.

This chapter describes the structure and function of the models and diagnostic systems (section 7.4) and presents techniques for assignment of a ‘confidence weighting’ (section 7.8) to the model outputs. A number of target faults have been defined to test the diagnostic systems. The target fault conditions are such that they may be easily simulated on the engine, allowing test data to be acquired for the diagnostic systems without risk to the test-bed. These faults and the results obtained from them are described in detail in (section 7.9).

7.2 FUZZY MODEL FORMAT

Fuzzy models in this chapter have been implemented using the Takagi-Sugeno format [Takagi 85] for a M.I.S.O. system, i.e. for a j dimensional input vector \mathbf{X} , and a one dimensional output vector Y ;

$$\mathbf{X} = [x_1 \cdots x_j]$$

$$Y = [y]$$

The fuzzy system has R^i ($i = 1, \dots, n$) rules of the form;

$$R: \text{ If } x_1 \text{ is } A_1 \text{ and } \dots x_j \text{ is } A_j \text{ then } y = g(x_1, \dots, x_j) \\ = p_0 + p_1 x_1 + \dots + p_j x_j$$

Where A_1, \dots, A_j are fuzzy sets defined in the input space and, p_0, p_1, \dots, p_j are scalars.

For each rule, R^i , the “truth value” of the proposition $y = y^i$ is denoted by $|y = y^i|$, so for a given vector of input data $[x_1^0 \dots x_j^0]$ the truth-value of the proposition is obtained from;

$$|y = y^i| = \min(A_1^i(x_1^0), \dots, A_j^i(x_j^0))$$

where $A_j^i(x_j^0)$ is the membership function A_j^i evaluated at point x_j^0 .

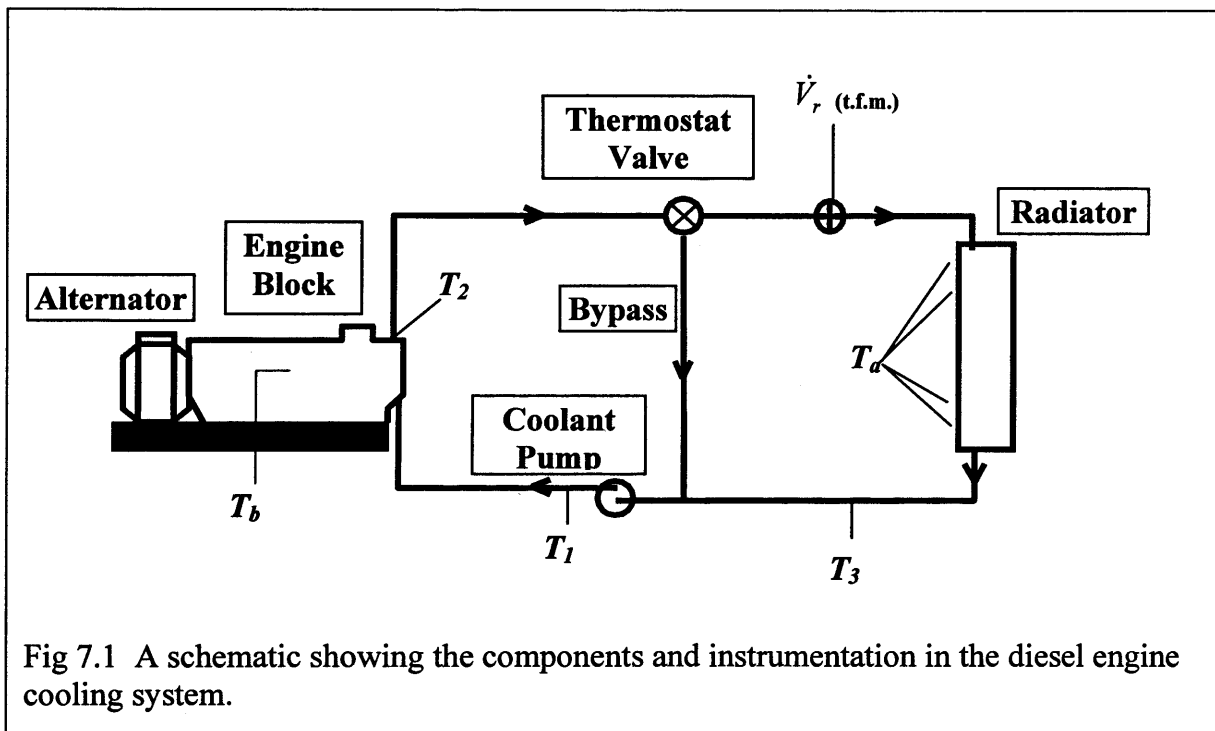
The output from the fuzzy system, y , is given as the average of y^i from R^i weighted by the “truth value” for each of the rules so that;

$$y = \frac{\sum |y = y^i| \times y^i}{\sum |y = y^i|}$$

7.3 COOLING SYSTEM DESCRIPTION

The test bed for the condition monitoring and fault diagnosis (CMFD) project work is described in detail in appendix 2. The diesel engine cooling system (see figure 7.1) is designed to maintain the engine at an appropriate working temperature thereby reducing the wear rates of mechanical components. The primary source of heat into the coolant system is the combustion of fuel in the engine cylinders, and, to a lesser extent, from internal friction of engine components. Heat is transferred from cylinder gas to the cylinder head and engine block, and from the block to the coolant. A small percentage of heat is dissipated via convection and radiation from the engine block to ambient, however, approximately 30% of the heat energy from the fuel is removed from the engine block via the coolant. Heat dissipation to atmosphere from the coolant is carried out via forced convection from a radiator.

The cooling system is controlled by a thermostatic valve, which allows the engine block to quickly warm up to a predefined coolant temperature. When the coolant reaches this set temperature, the thermostatic valve opens to allow the coolant flow to the radiator. The coolant is circulated through the system by a gear driven centrifugal coolant pump.



A non-linear mathematical model of a diesel engine cooling system has been developed (see appendix 3). The benefit of such a model is that the responses of the physical system to a particular fault may be predicted in a qualitative way by adjustment of certain parameters in the model. This provides additional information to that obtained by experimental simulation of faults. This approach is of particular use where the fault is potentially damaging to the engine.

Two first order differential equations originally developed by Chiang et al [Chiang 82], have been used in the development of the non-linear model. Equation 7.1, describes heat transfer by convection from the engine block to the coolant. The second equation is a

modification of the approach made by Chiang in that heat dissipation from the radiator is modelled as forced convection to air blown by a cooling fan over the radiator's finned surface [Kays 55].

$$m_b C p_c \frac{dT_2}{dt} = h_b A_b (T_b - T_2) - \dot{m}_b C p_c (T_2 - T_1) \quad \dots \quad 7.1$$

$$m_r C p_c \frac{dT_3}{dt} = \dot{m}_r C p_c (T_2 - T_3) - h_r A_r (T_3 - T_a) \quad \dots \quad 7.2$$

The parameters for equations 7.1 and 7.2 have been estimated experimentally by the employing the *series-parallel* model [Ioannu 96]. Results of this process are presented in appendix 3.

7.4 FUZZY MODEL BASED CMFD FOR A DIESEL ENGINE COOLING SYSTEM: AN OVERVIEW

The two stage fault diagnosis system described in this section, is designed to map the residual vector to one of a number of prescribed system conditions (see figure 7.2) where;

$$X = [X_1, X_2, X_3]^T$$

and;

$$X_1 = [T_{2(t)}, \hat{V}_{r(t-k)}]^T, \quad X_2 = [\frac{\Delta T_2}{\Delta t}, \hat{V}_r, \Delta T_{b2}]^T, \quad X_3 = [\frac{\Delta T_3}{\Delta t}, \hat{V}_r, \Delta T_{2a}]^T$$

represents the input vectors to the three fuzzy models,

$$\hat{Y} = [\hat{y}_1, \hat{y}_2, \hat{y}_3]^T$$

are the model outputs and;

$$Y = [y_1, y_2, y_3]^T$$

and

$$y_1 = \hat{V}_{r(t)}, y_2 = [\Delta T_{21}], y_3 = [\Delta T_{23}]$$

are the corresponding measured variables. The choices of inputs and outputs for the are described in sections 7.5, 7.6 and 7.7.

The residual vector is defined to be the measured (or estimated) variable minus the output from the corresponding fuzzy model. Therefore;

$$R = Y - \hat{Y} \quad \dots 7.3$$

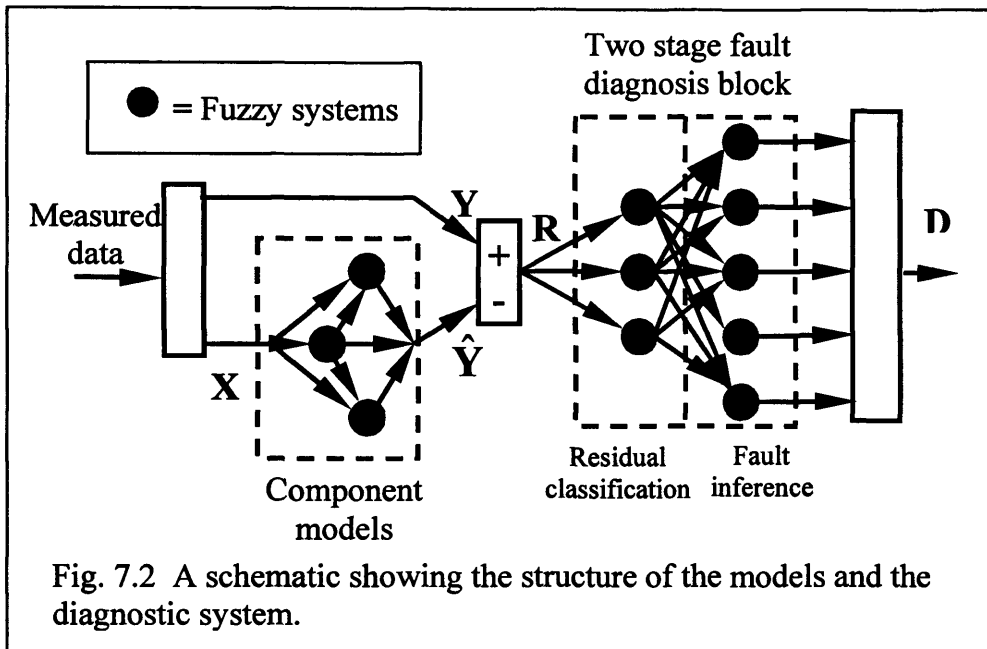
So that;

$$R = [r_1, r_2, r_3]^T$$

Based on R and its associated confidence weighting vector, C , (see section 7.8) the diagnostic system is designed to output a vector of numbers, D . Vector D represents the likelihood of a number of possible conditions of the diesel engine cooling system. The magnitude and sign of the three components of R , along with other information regarding the state of the system, are used to diagnose the system condition.

Components of R are each classified into one of five fuzzy sets defined with respect to the normal condition of the system (see figure 7.3).

Taking r_2 as an example, the '*Normal Residual*' set with membership function (m.f.), $\mu_N(r_2)$, is defined by analysis of the model error vector generated from a set of unseen test data obtained with the engine running in the normal condition. The mean and standard deviation of the model errors are calculated for samples of the test data where



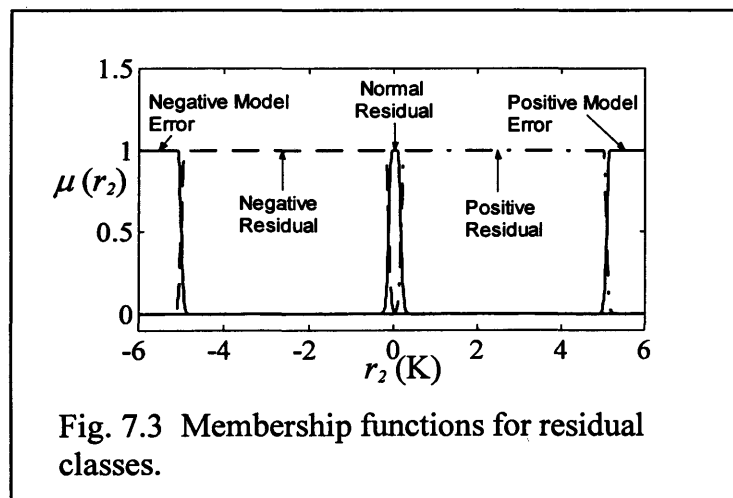
the confidence weighting is a maximum. The key design criteria for $\mu_N(r_2)$, is that it provides a good trade-off between sensitivity to fault conditions whilst maintaining a low ‘false alarm’ rate. With this in mind the $\mu_N(r_2)$ is defined as follows;

$$\mu_N(r_2) = \begin{cases} \exp\left(\frac{-(r_2 - (\bar{r}_2 + \sigma_{r_2}))^2}{2\sigma_{r_2}^2}\right) & \text{if } -\infty < r_2 \leq -\sigma_{r_2} \\ 1 & \text{if } -\sigma_{r_2} < r_2 \leq \sigma_{r_2} \\ \exp\left(\frac{-(r_2 - (\bar{r}_2 - \sigma_{r_2}))^2}{2\sigma_{r_2}^2}\right) & \text{if } \sigma_{r_2} < r_2 \leq \infty \end{cases} \dots 7.4$$

The m.f.’s for positive and negative residuals are defined using the same piecewise approach. The gradients of the m.f.’s are identical to those for $\mu_N(r_2)$ with the intersection at $\mu_N(r_2)=0.5$. Two additional m.f.’s are defined to indicate unfeasibly high residuals which are presumed to be caused by a error in the model. These two m.f.’s are defined arbitrarily where the residual is +/- 100% (approximately +/- 5K) of the range for y_2 .

Each target fault causes a characteristic pattern in the residual classes in terms of their sign and magnitude. The patterns are predicted from *a priori* knowledge of the systems or by making appropriate adjustments to the parameters of the non-linear cooling system models (equations 7.1 and 7.2) and simulating with appropriate sets of test data.

The benefit of this approach to design of the residual classifiers is that the process may be carried out using only data obtained from tests carried out with the cooling system in its 'normal' or 'fault-free' mode of operation. 'Normal' data is most easily available and may be obtained without risk of damage to the test-bed. The availability of a mathematical model (see appendix 3) to test the assumptions is a further benefit in this respect.



The results from stage 1 are then analysed by a number of fuzzy systems that are each designed to infer a particular condition or fault in the system. This stage employs a set of rules to infer each fault from the pattern of the residuals. The residual patterns for the range of target faults are shown in table 7.1.

For example, the rule to infer a fault in the radiator caused by a reduction in the heat transfer coefficient due to a fault condition;

If r_1 is *Normal* and r_2 is *Negative* and r_3 is *Positive* and Thermostatic Valve is *Open*, then Radiator fault is *True*

Clearly, diagnosis of faults in the radiator using this model-based technique are only possible when the thermostatic valve is in the open position. The low values of the confidence weights occurring when the thermostatic valve is in its transient state mean that it is only sensible to attempt a diagnosis when the thermostatic valve is in its fully open position.

Table 7.1 Residual classes for stage 2 diagnostic rules.

Component	Residual Condition	Valve Position					
		Open			Closed		
		r_1	r_2	r_3	r_1	r_2	r_3
All	Normal	<i>Normal</i>	<i>Normal</i>	<i>Normal</i>	<i>Normal</i>	<i>Normal</i>	<i>Any</i>
Thermostatic valve	Open w.s.b. ¹ closed	<i>Any</i>	<i>Any</i>	<i>Any</i>	<i>Positive</i>	<i>Any</i>	<i>Any</i>
	Closed w.s.b. ¹ open	<i>Negative</i>	<i>Any</i>	<i>Any</i>	<i>Any</i>	<i>Any</i>	<i>Any</i>
	Stuck partially open	<i>Negative</i>	<i>Any</i>	<i>Any</i>	<i>Positive</i>	<i>Any</i>	<i>Any</i>
Radiator	Reduced h_{rad}	<i>Normal</i>	<i>Negative</i>	<i>Positive</i>	<i>Any</i>	<i>Any</i>	<i>Any</i>
Pump (Coolant flow rate)	Low flow	<i>Normal</i>	<i>Negative</i>	<i>Negative</i>	<i>Normal</i>	<i>Negative</i>	<i>Any</i>
Engine block	Reduced h_{block}	<i>Normal</i>	<i>Negative</i>	<i>Normal</i>	<i>Normal</i>	<i>Negative</i>	<i>Any</i>

¹ w.s.b. 'when should be'

Residual classes are denoted by;

Negative Negative Residual

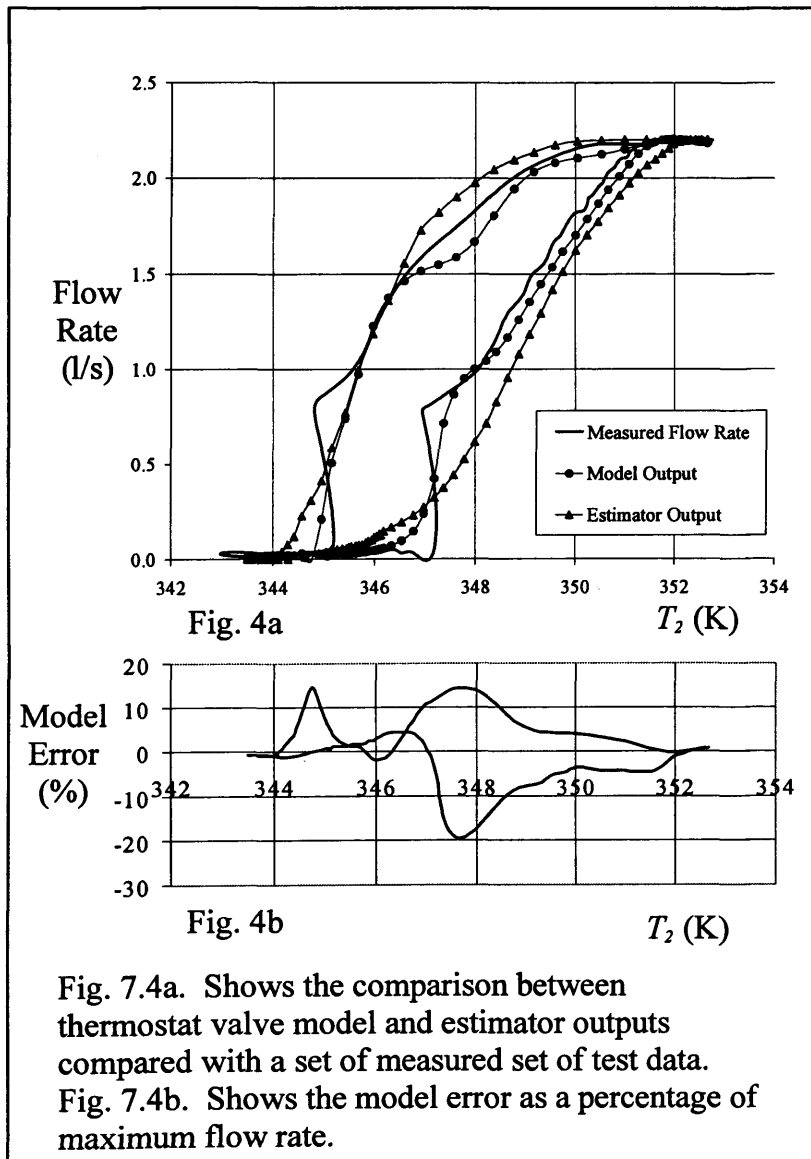
Positive Positive Residual

Normal Normal Residual

Any Any residual

7.5. DEVELOPMENT OF THE FUZZY THERMOSTATIC VALVE MODEL.

The objective of this modelling exercise is to relate the flow-rate through the radiator, \dot{V}_r , to the temperature at the thermostatic valve, T_2 . The thermostatic valve operates due to the expansion of melting wax inside the valve body pushing against a plunger, which opens and closes the valve. For the purposes of obtaining data for model identification, the coolant flow rate through the radiator is measured with a turbine flow meter (t.f.m.) situated between the thermostatic valve and the radiator inlet. The valve is designed to begin to open at a pre-set temperature of 74 °C and be fully open at 82 °C. Some hysteresis effects are seen to occur in the operation of the valve. (See figure 7.4)



There are a number of possible options at each stage of modelling the system. Initial analysis of the data suggests a number of candidate structures for the model. The models identified were of the format outlined in section 7.2, for a M.I.S.O. system. A recursive fuzzy model was selected as the most suitable structure since it is capable of modelling the hysteresis effects. The inputs and outputs for this model are as follows;

$$X_I = [T_{2(t)}, \hat{V}_{r(t-k)}]; \quad \hat{y}_1 = \hat{V}_{r(t)};$$

The advantage of this recursive model structure is that the information regarding previous state of the system is contained in a single input thus minimising the size of the fuzzy system required. However, the structure has the disadvantage that model errors are fed back as an input, and can cause instability in the model. This may be dealt with using a 'grey box' approach to modify the parameters of the fuzzy model in order to reduce the instability.

A general rule in system modelling is *do not try to estimate what you already know* [Sjoberg 95b]. Where *a priori* knowledge of the system exists it should be used in the development of the model. This is termed 'grey-box' modelling as opposed to 'black-box' modelling, where only input and output data from the system are used to identify the model. Applying this principle to the estimation of the parameters that define the fuzzy model of a system, the problem becomes one of how to incorporate *a priori* knowledge into the model.

Incorporating the results of the system identification from input-output data pairs with some rule-based knowledge of the system gives an improved model of valve operation.

\dot{V}_r is bounded such that;

$$0 \text{ (1/s)} \leq \dot{V}_r \leq 2.2 \text{ (1/s)} \Big|_{\text{all } T_2}$$

The identification process from input/output data pairs results in a model which is only defined over the range of the sampled data points, however applying knowledge of the system bounds allows the addition of the following general rules;

- i) If $T_2 > 82$ (°C) or $\hat{V}_{r(t-k)} > 2.2$ (l/s) then $\hat{V}_{r(t)} = 2.2$ (l/s)
- ii) If $T_2 < 74$ (°C) or $\hat{V}_{r(t-k)} < 0$ (l/s) then $\hat{V}_{r(t)} = 0$ (l/s)

Implementation of these rules with suitably defined membership functions reduces the problems caused by instability in the recursive model

7.6. ESTIMATION OF RADIATOR COOLANT FLOW RATE FROM TEMPERATURE MEASUREMENTS

A turbine flow meter (t.f.m.) has been employed to obtain data for development of the diagnostic system, however, this instrument is costly and impractical to fit in some parts of the coolant system. Therefore this section of the chapter describes a knowledge-based approach to estimation of the coolant flow rate through the radiator, based on easily obtainable temperature measurements.

Consider an energy balance with the system boundary defined at the inlet of the coolant pump where the coolant flows from the bypass and the radiator are conjoined. Then, assuming there is no heat transfer from the system pipe-work between thermostatic valve, radiator outlet and the inlet to the pump we have;

$$\dot{m}_b C_p T_1 = (1 - \alpha) \dot{m}_b C_p T_2 + \alpha \dot{m}_b C_p T_3 \quad \dots 7.5$$

Therefore in terms of volume flow rate;

$$\rho \dot{V}_b C_p T_1 = (1 - \alpha) \rho \dot{V}_b C_p T_2 + \alpha \rho \dot{V}_b C_p T_3 \quad \dots 7.6$$

Where;

ρ = coolant density

$\rho\dot{V}_b = \dot{m}$ = Coolant mass flow rate at pump outlet.

$\alpha\rho\dot{V}_b = \rho\dot{V}_r = \dot{m}_r$ = Coolant mass flow rate at the radiator inlet.

i.e. α is the proportion of the maximum coolant volume flow rate to the radiator which is controlled by the thermostatic valve. Therefore;

$$\alpha = \frac{\dot{V}_r}{\dot{V}_r|_{\max}} \quad \dots 7.7$$

Further to this, assume that ρ and C_p are constant, over the temperature range observed in the system. Therefore;

$$T_1 = (1 - \alpha).T_2 + \alpha.T_3 \quad \dots 7.8$$

and;

$$\alpha = \frac{(T_1 - T_2)}{(T_3 - T_2)} \quad \dots 7.9$$

Observations of the recorded temperature data show that these assumptions do not hold for all states of the system. The relationship for α is seen to hold when $\alpha > 50\%$ but when the thermostatic valve is closed errors are seen to be very high. This effect is thought to be due to change in dominant mode of heat transfer to the transducer which is used to measure, T_3 , when there is zero or low flow through the radiator. When the valve is open, heat transfer is due to convection from coolant flow. However, when the valve is closed, the proximity of the transducer to the engine block causes heat transfer by conduction and convection to the transducer.

It is therefore possible to make two statements regarding the flow-rate through the radiator;

- i) When the thermostatic valve is open above a certain limit the flow rate may be estimated using;

$$\hat{V}_r = f \left\{ \frac{(T_1 - T_2)}{(T_3 - T_2)} \right\} \quad \dots 7.10$$

- ii) When the valve is closed the relationship in i) does not hold and;

$$\hat{V}_r = 0;$$

Therefore a further indicator is required to distinguish between the two states. Clearly when the thermostatic valve is open, the coolant temperature is reduced as it passes through the radiator. This fact may be used along with i) and ii) above to produce a set of rules for the estimation of \dot{V}_r . Observation of the data shows that when the valve is closed $T_2 \approx T_1$. Therefore ΔT_{21} may be used as an additional input to differentiate between the valve states 'open' and 'closed'. This done by implementation of the following additional general rules;

- i) If $\Delta T_{21} > \delta$ then $\dot{V}_r = f \left\{ \frac{(T_1 - T_2)}{(T_3 - T_2)} \right\}$
- ii) If $\Delta T_{21} < \delta$ then $\dot{V}_r = 0$

Where δ is an appropriately fixed threshold.

Based on the knowledge of the system, a fuzzy system has been developed to act as an estimator for \dot{V}_r , with the output defined as the estimated value, \tilde{V}_r , and the input vector U is given by;

$$U = [\alpha, \Delta T_{21}];$$

In the context of the diagnostic system, \tilde{V}_r is substituted for a directly measured version of \dot{V}_r , therefore;

$$y_1 = \tilde{V}_r$$

7.7 FUZZY MODELS FOR COOLANT TEMPERATURE DIFFERENCES ACROSS ENGINE BLOCK AND RADIATOR

The fuzzy model inputs and outputs described in this section have been selected to be representative of the physical system, whilst the outputs are also suitable reference values for generation of residuals.

The selection of inputs and outputs for the fuzzy model representing heat flow to the coolant in the engine block and dissipation to atmosphere via the radiator are based on the states and parameters of the non-linear models for T_2 and T_3 (equations 7.1 and 7.2). The non-linear model parameters associated with heat transfer coefficient have not been included as inputs to the fuzzy model. These parameters were found to be effectively constant over the usual temperature range of the coolant, therefore their estimation will be implicit in the fuzzy identification process.

Volume flow rate through the engine block has proven difficult to measure directly however differential pressure measurements suggest that the flow rate through the engine block varies with the position of the thermostatic valve, due to the change in overall resistance to the coolant flow when this valve is operated. Therefore, the estimated

volume flow rate through the radiator from the fuzzy model is chosen as an input in X_2 to indicate the operation of the thermostatic valve.

The inputs X_2 and output, \hat{y}_2 are chosen to be;

$$X_2 = \left[\frac{\Delta T_2}{\Delta t}, \hat{V}_r, \Delta T_{b2} \right]; \quad \hat{y}_2 = [\Delta T_{21}];$$

where ΔT_{b2} is defined as $T_b - T_2$, and ΔT_{21} is defined as $T_2 - T_1$

Similarly, the inputs, X_3 , and output \hat{y}_3 , are chosen to be;

$$X_3 = \left[\frac{\Delta T_3}{\Delta t}, \hat{V}_r, \Delta T_{2a} \right]; \quad \hat{y}_3 = [\Delta T_{23}]$$

where ΔT_{2a} is defined as $T_2 - T_a$ and ΔT_{23} is defined as $T_2 - T_3$.

The inputs, $\frac{\Delta T_2}{\Delta t}$ and $\frac{\Delta T_3}{\Delta t}$, are calculated by incorporating a suitable delay into the system and subtracting the delayed value from the current value, for example;

$$\frac{\Delta T_2}{\Delta t} = T_{2(t)} - T_{2(t-k)}$$

The value of the delay, k , is chosen with respect to a number of criteria. k should be small with respect to the time constant of the system, but large enough so that $\frac{\Delta T_2}{\Delta t}$ is large with respect to measurement error in the signal. For this model the value $k = 20$ is found to be effective

The choices of inputs and outputs for the fuzzy models have been made from *a priori* knowledge of the system. In this case the knowledge is contained within the non-linear model. The parameters of the non-linear model have been estimated and tested, demonstrating that the model relationship between the inputs and outputs is appropriate.

Taking the outputs of the fuzzy models to be the temperature differences across the components results in a smaller range of output values, compared with estimating the states T_2 or T_3 . This choice produces benefits in terms of residual analysis. Deviations in the states T_2 and T_3 due to a fault condition are small (approx. 1% of normal range), however, because the ranges for y_2 and y_3 are 0 – 5 K the deviations are larger with respect for this range (approx. 20%). Therefore, this choice of model output results in a model with greater sensitivity to fault conditions.

7.8 ESTIMATION OF CONFIDENCE WEIGHTS

This section describes how confidence weights are assigned to the outputs from the fuzzy models.

Remembering that the fuzzy models are simply a mapping from sets defined in the input space to a set of first order linear functions, then confidence may be defined in terms of the knowledge of the accuracy of the mapping. To explain this further, there may be some regions in the input/output space where the fuzzy model is not well defined. Clearly model errors will result in erroneous diagnosis. With this in mind, the confidence weights are defined to be high in regions where it may be shown that the model is representative of the physical system and low elsewhere.

In using data to train a fuzzy model the input space for the model is defined only over the range of the input data. This implies that if, at any subsequent time, the model inputs are outside the pre-defined input space, then the confidence value assigned to the model output should be low.

An overview of the procedure for developing an estimator to assign confidence weights to outputs from the various fuzzy models is shown in figure 7.5. The regions outside the defined input space are easily identified by observation of the training data ranges. So this procedure focusses on identifying regions within the input space where the training errors are seen to be high.

The first stage of the process is to train the fuzzy models with suitable input/output $[X_T, Y_T]$ data pairs. The resulting fuzzy model is then retested using the input components of the training data, X_T . The outputs obtained \hat{Y}_T may be compared with Y so that the training error vector, e_T , may be simply defined as;

$$e_T = Y - \hat{Y}_T$$

The training error vector is then classified with respect to the size of the error into two classes denoted “*High*” and “*Low*”. The classification is carried out using a fuzzy system based on the mean, \bar{e}_T and standard deviation, σ_{e_T} , of the error vector. Two membership functions are defined; a Gaussian membership function, μ , is defined for *Low* and *High* is defined as its complement so that;

$$\mu_{Low}(e_T) = \exp\left(\frac{-(e_T - \bar{e}_T)^2}{2\sigma_{e_T}^2}\right)$$

$$\mu_{High}(e_T) = 1 - \mu_{Low}(e_T)$$

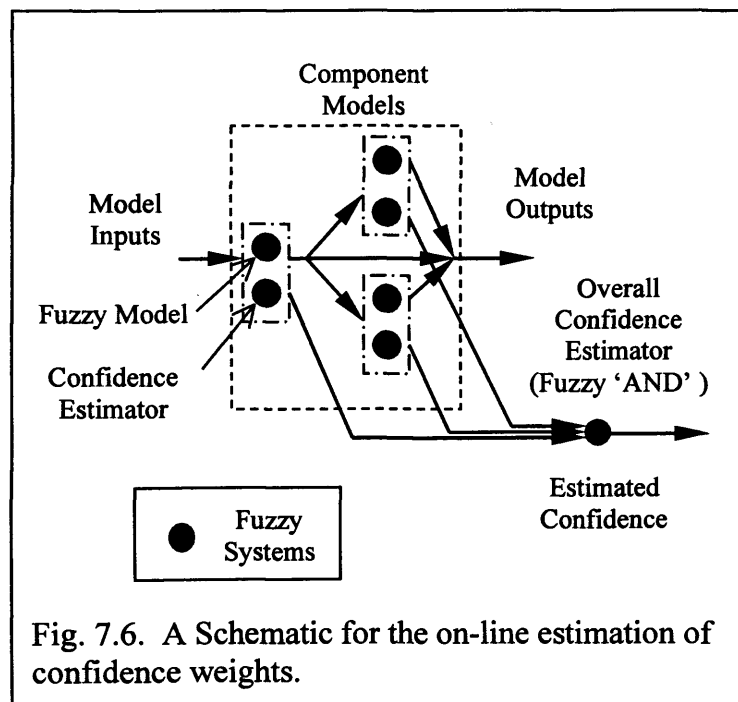
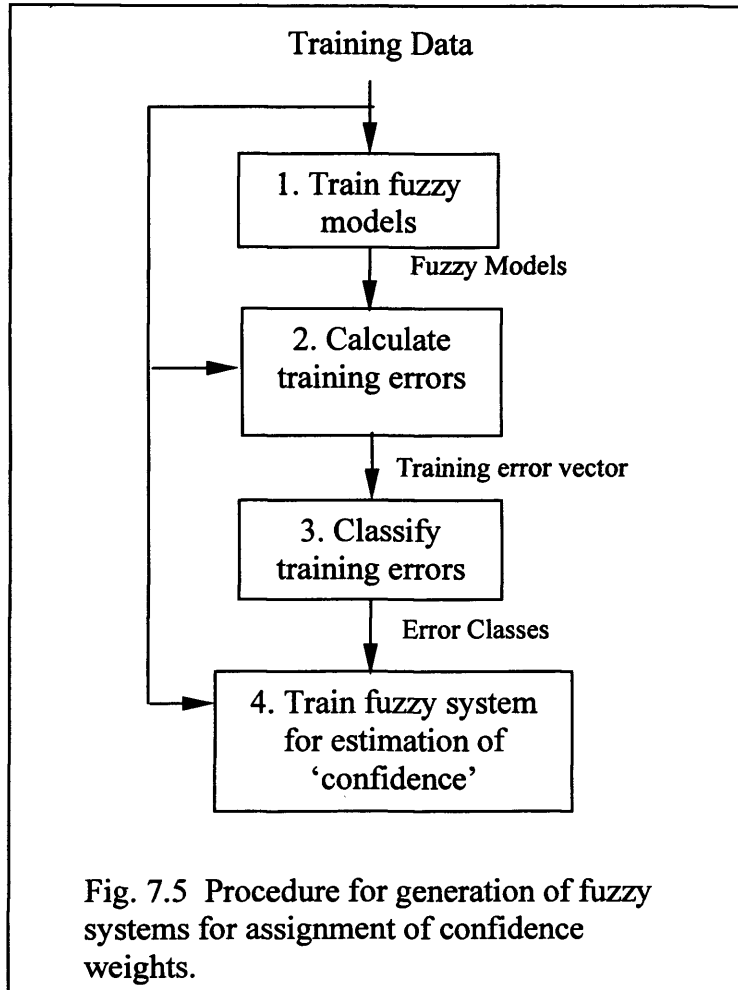
Intuitively therefore, the membership of the *low* training error class is equivalent to the membership of a class representing a high confidence level in subsequent use of the model. Therefore the confidence weighting C_i , for model i , (where $i = 1, 2, 3$ in this case) may be defined as;

$$C_i = \mu_{Low}(e_{Ti})$$

The training errors are thus classified into two fuzzy classes. Using this convention, a vector of data pairs, T_{Ci} , may be defined in order to train a fuzzy system for estimating the confidence level

$$T_{Ci} = [X_i, C_i]$$

Where outputs from more than one model are combined to infer a fault, then the confidence weights are combined using a logical, 'AND', operator in order to assign an overall confidence level to the diagnosis (See figure 7.6).



7.9 RESULTS

In order to test the model-based diagnostic system the engine has been tested with the cooling system in a number of different conditions. These are as denoted A-D as follows;

A. Normal: The engine is run in a fault-free condition. (See figure 7.7)

B. Thermostatic valves (TSV) fault: Failed in closed position.

The Perkins 1004TG engine employs two thermostatic valves operating in parallel. For the purposes of this test, the two valves were replaced with two valves of identical design but with a higher opening set point: 82°C as opposed to 74°C. The valves rarely fail in practice but when this occurs they tend to fail in the closed position. This presents the diagnostic system with a set of data within this temperature range $74^{\circ}\text{C} < T_2 < 82^{\circ}\text{C}$ corresponding to a fault, whilst protecting the engine from possible damage due to overheating which may arise from using valves fixed in the closed position

C. Radiator Fault: Reduced heat transfer performance.

This fault is simulated by partially covering the frontal area of the radiator i.e. obstructing the airflow from the cooling fan using a strip of card. This closely simulates clogging of the radiator heat transfer surfaces, which sometimes occurs in dusty environments. Two different sizes of obstructions were made to cover 10% then 25% of radiator frontal area.

D. Low Coolant Flow-Rate

A system bypass has been introduced to the circuit in the form of a 25mm diameter return pipe with isolation valve from pump outlet to pump inlet. This simulates the effect of reduced pump performance. Opening the isolation valve returns a proportion of the coolant flow to the inlet of the pump, which is noted to reduce the coolant volume flow rate through the system by approximately 10%. N.B. it should be noted that this fault should not be detected using the expression developed for the

radiator flow rate estimator, \tilde{V}_r , as introducing the bypass pipe-work artificially alters the configuration of the system such that the relationship for α no longer holds.

The test runs for A - D consisted of applying a step load change to the engine, to increase the heat input into the cooling system, resulting in the opening of the thermostatic valve. Temperature data was acquired at a sample rate of 1Hz for a period of up to 30 minutes to allow the engine to reach a steady operating temperature. The diagnostic scheme requires five input variables, $U=[T_l, T_2, T_3, T_b, T_a]$

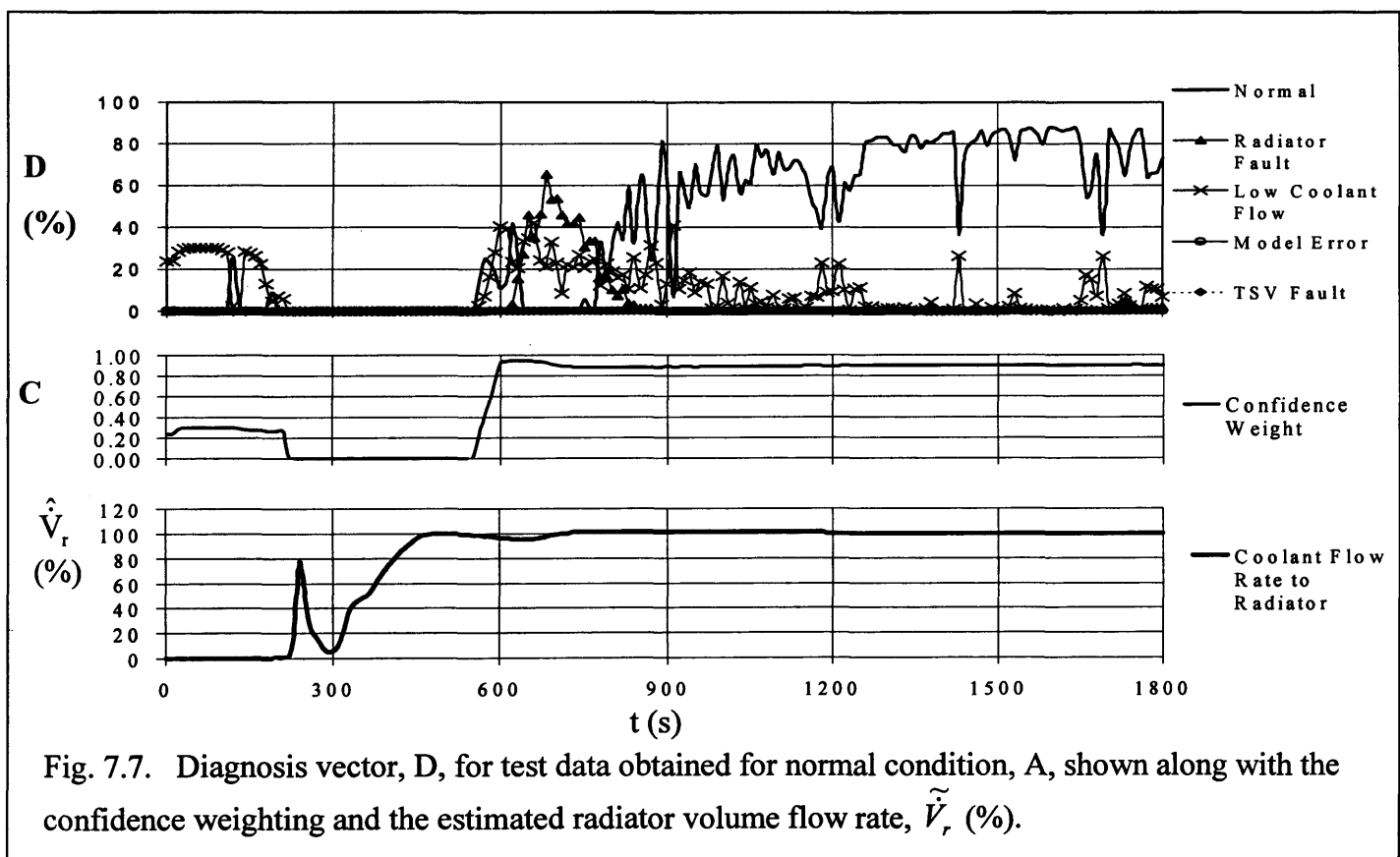


Fig. 7.7. Diagnosis vector, D , for test data obtained for normal condition, A , shown along with the confidence weighting and the estimated radiator volume flow rate, \hat{V}_r (%).

7.10 DISCUSSION

The success rate is defined as the percentage of data samples for which the diagnosis of the systems condition matches the actual condition and the system diagnosis is defined to be the outcome with the highest truth value. The results presented in table 7.1 and figure 7.7 show that the fuzzy model based CMFD system has a success rate ranging between 56.7% and 82.5%. The success rate of the system is low when the thermostatic valve is

closed, but improves when the system warms-up and the thermostatic valve opens to allow coolant flow through the radiator. This is illustrated in figure 7.7, which shows the increase in confidence levels associated with the opening of the thermostatic valve.

Results for A* in table 7.1 show the improvement in the diagnostic success rate from 59.1% to 76.4% as the thermostatic valve opens. However, figure 7.7 shows that after ≈ 1000 s the success rate is actually 100%. From these results it may be seen that the confidence weightings could be modified to give a zero value up until the point at which the valve opens, thereby further reducing the number of misclassifications.

The confidence weights are seen to be at a minimum during the periods in which the thermostatic valve is in transition, the reasons for this may be seen in figure 7.4b, which shows that the TSV model errors are relatively high in the transition region. The confidence weights are also low in the regions where the valve is closed and the engine cold, just after start up. Although the confidence weighting reduces the period in which the diagnostic system produces a conclusive result, it provides benefits in increasing the degree of belief in the result when it is available

The fuzzy systems approach has provided a flexible means for incorporating heuristics into both models and diagnostic systems. This has facilitated the 'grey-box' approach to modelling, demonstrated by the fuzzy systems developed to represent the action of the thermostatic valve. Encapsulating *a priori* knowledge of the cooling system in this way has allowed an effective diagnostic system to be developed based on a small number of cheap and reliable temperature sensors.

The structure of the diagnostic system (see figure 7.2) has been designed to be generic in the sense that it may be applied to other diesel engine systems, and also that it could be applied with different model formats. Although the architecture of the system bears a marked similarity with that of an artificial neural network, the model based system is transparent in that, meaningful data may be extracted from any level of the system. Also the diagnostic system may be interrogated to provide the reasoning for a given output.

Therefore as diagnostic systems for additional diesel engine systems are developed, information may be easily shared. This will allow cross-referencing of models to detect faults with symptoms that appear in more than one engine system.

Diagnoses of faults are based on deviations from the normal operation condition of the system. This provides the benefits over other forms of classifier [Parikh 98] in that the only data from the diesel engine system in its normal operating condition is required for the diagnostic development. Clearly however, data from selected fault conditions are required to test the diagnostics. In this case the target faults which have been used to test the systems, produce symptoms which may be predicted from knowledge of the system and the mathematical models which are available. However, in other systems, unknown fault conditions may be indicated by assignment of additional 'unknown' classes for unrecognised residual patterns.

Table 7.2. Results table for conditions A – D.

System Condition	Diagnosis (% of samples)					
	A	B	C	D	Model Error	No Diagnosis
A	59.1	0	6.9	15.4	0.2	18.4
A*	76.4	0	9.1	6.0	0.1	8.3
B	0	60.0	0	1.2	4.6	34.2
C	0	0	56.7	2.2	41.1	0
D	0	0	0	71.5	0.1	28.5
D*	0	0	0	82.5	0	17.5

Notes on table

- i) The system diagnosis is taken to be the highest value in the diagnosis vector, i.e. $\max(D)$

- ii) System condition rows A* and D* refer to diagnosis results subsequent to opening of the thermostatic valve.
- iii) The percentage of correct diagnoses for the radiator fault is calculated from the point in time at which the thermostatic valve is fully open.
- iv) The percentage of correct diagnoses for the thermostatic valve fault is calculated over the temperature range, $74^{\circ}\text{C} < T_2 < 84^{\circ}\text{C}$.
- v) Column 6, 'No Diagnosis', refers to regions where confidence levels are zero, and therefore, $D=[0,0,0,0,0]$.

7.11 CONCLUSIONS

Fuzzy systems have been developed which offer benefits in terms of providing a CMFD system for an engine cooling system based on a small number of low cost sensors.

In four test cases, for separate cooling system operating conditions, the diagnostic system's success rate ranged between 56.7% and 82.5%. Misclassifications of fault conditions B, C, and D, were reduced to, 1.2%, 2.2% and 0%, respectively by use of 'model error' class and confidence weights on the diagnosis output.

The results obtained from the cooling system working in its normal condition, show that the performance of the diagnostic system improves from a 59.1% success rate to one of 76.4% as the thermostatic valve opens and the cooling system warms-up to its normal operating temperatures.

Recursive fuzzy models have been shown to be an effective technique for modelling of hysteresis in the thermostatic valve system.

The development of this diagnostic system represents a generic approach to fault diagnosis that may readily be applied to other engine systems and other model formats.

As such, this type of diagnostic system may be employed as a knowledge source for 'blackboard'-type fault diagnosis structures.

CHAPTER 8.

**A High Level Technique For Engine Combustion System
Condition Monitoring and Fault Diagnosis**

8.1. INTRODUCTION.

The combustion system has been identified in chapter 6 as a high priority for CMFD due to its strong influence on both power output and emissions of the engine. This chapter will describe the development of a fuzzy model-based CMFD approach for this engine subsystem.

The performance of a diesel engine may be described in terms of its *thermal conversion efficiency* [Heywood 88 pp85] defined as;

$$\eta_t = \frac{W_c}{\eta_c m_f Q_{HV}} \quad \dots 8.1$$

From the point of view of performance monitoring this is very useful, because a reduction in efficiency of the engine due to a fault in the combustion system will result in increased fuel consumption for a particular load. However, it is well known that engine load is difficult to measure on-line, and therefore obtaining information regarding the fuel consumption with respect to engine load for an on-board diagnostic system represents a problem. This document presents a possible solution to the problem of diagnosis of engine faults which adversely affect the thermal conversion efficiency by combining evidence from two separate estimations of engine load, based on air fuel ratio and the power spectrum of the speed signal, and a predictive model of engine speed.

Certain faults affect the periodicity of the fluctuations in the engine speed signal. This property has been exploited by other researchers [Freestone 85], [Jewitt 85] who have developed techniques for analytical interpretation of engine speed and torque fluctuations for fault detection.

The variation in periodicity under fault conditions means that an estimation of load based on the power spectral density of the speed signal is not robust. This problem is countered by implementing a reference model to predict speed fluctuations with respect to crank angle. This model has a further benefit that may be used to detect periodic fault

symptoms in the speed signal leading to identification of the individual cylinder affected by the fault.

The system is demonstrated using data from a diesel generator set test bed. Data has been obtained with three different operating conditions imposed on the engine. The first condition is normal, i.e. fault-free operation. Two combustion fault conditions have also been imposed on the engine described as follows;

C1 Fuel injector fault. This fault simulates a damaged injector by removing a packing washer from the injection valve spring. This introduces backlash into the valve system and means that the valve will open and inject fuel into the cylinder at a very much lower pressure than would normally be the case. The implications for combustion are presumed to be that the atomisation performance of the nozzle is reduced and therefore the efficiency of the combustion process is reduced due to the larger droplet size. This presumption is difficult to confirm in the laboratory, but is reinforced by the subsequent loss of power and increase in smoke levels of the engine.

C2 Air inlet valve fault. A valve-seating problem was simulated on an air inlet valve on one of the cylinders by inserting a copper shim of 0.9mm between the rocker arm and the valve stem. This results in the valve not closing properly during the combustion, compression and exhaust strokes of the engine cycle. Therefore, cylinder pressures are reduced causing a fall in combustion efficiency. Other symptoms of this fault are high-pressure pulses in the air-inlet manifold, loss of power and drastically increased levels of smoke.

Five input signals to the overall system are required. The transducers are listed as follows (see also appendix 2);

- i) Magnetic pick-up: To measure the rotational speed and angular increments from flywheel gear teeth.

- ii) IR sensor: To provide a datum for the four stroke engine cycle from a crankshaft mounted 2:1 gear-wheel arrangement designed to provide 1 pulse/720° of crank-angle.
- iii) Fuel meter
- iv) Air flow meter
- v) Air inlet manifold pressure transducer

8.2 DEVELOPMENT OF FUZZY SYSTEMS FOR ESTIMATION OF ENGINE LOAD.

8.2.1 LOAD ESTIMATION FROM FREQUENCY ANALYSIS OF THE SPEED SIGNAL.

Force on the pistons, generated by gas pressure due to combustion events in the engine's four cylinders is periodically transferred to the crankshaft via the pistons and connecting rods. The total load torque ($T_b + T_f$) acts on the engine as a resistance to the rotation of the crankshaft, therefore small speed fluctuations occur in the engine speed. The amplitude of these fluctuations is seen to depend on the engine load. (See figure 8.1). Jewitt and Lawton [Jewitt 85] develop an expression from which the instantaneous engine speed may be calculated;

$$\frac{d\omega}{dt} = \frac{1}{I} \left\{ P_c A r \left(\sin(\phi) + \frac{\sin(2\phi)}{2n} \right) - (T_B + T_f) \right\} \quad \dots \quad 8.2$$

Clearly the speed fluctuations are a function of crank angle rather than time, therefore the frequency analysis undertaken in this study is carried out with respect to crank angle. Freestone's [Freestone 85] treatment of engine speed data was also undertaken with respect to crank angle rather than time. Chin [Chin 86] reports that use of crank-angle as the independent variable has shown benefit in terms of reducing the errors in parameter estimation for engine models used in speed controller development. Therefore, it is proposed to calculate the power spectral density (PSD) of engine speed with respect to crank angle over one engine cycle, i.e. 720° of crank-angle, ($^\circ\phi$). This approach should eliminate any errors in the observed PSD caused by small changes in engine speed.

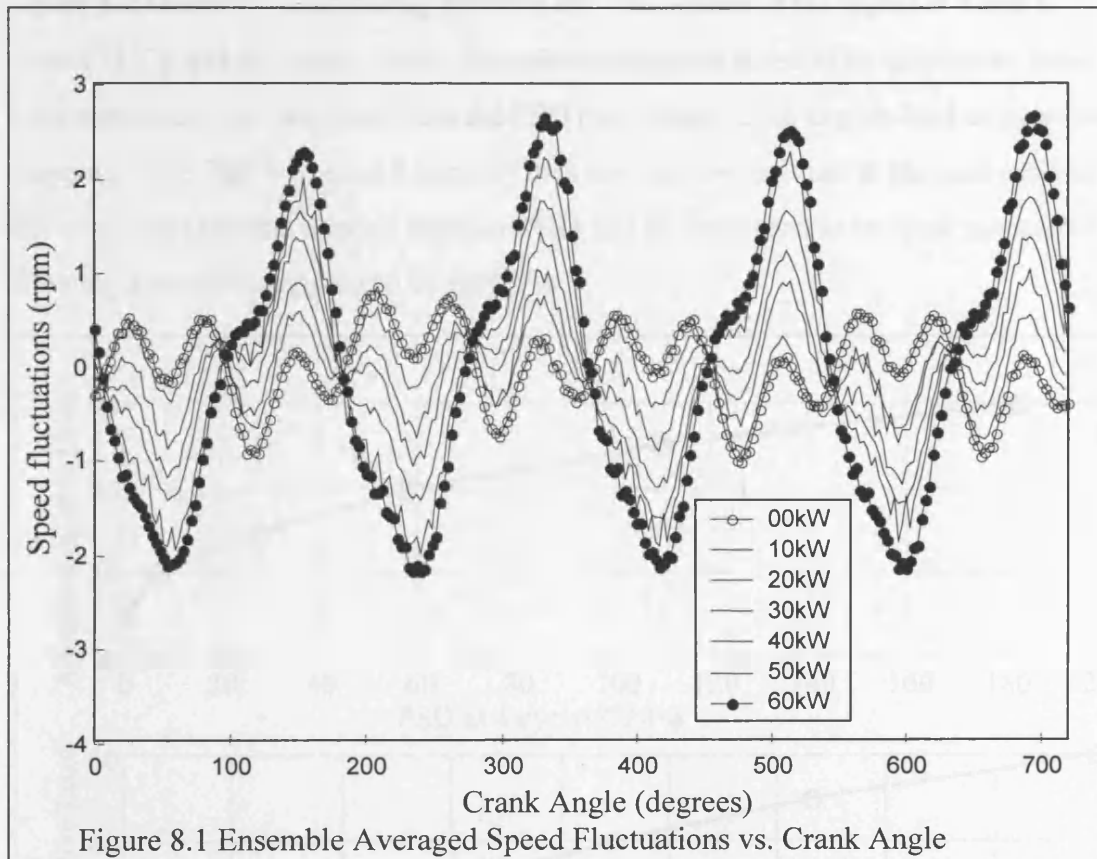


Figure 8.1 Ensemble Averaged Speed Fluctuations vs. Crank Angle

From observation of the speed fluctuations with respect to crank angle in figure 1, (sampled at 252 samples/ $720^\circ\phi$) the main frequency components of interest are 4 and 8 cycles/ $720^\circ\phi$. Thus an appropriate sampling interval is chosen to be 18° of crank (40 samples/ $720^\circ\phi$).

The PSD calculation is as follows

$$G(j\omega) = \sum_{m=0}^{M-1} N e^{-j2\pi\omega m / M} \quad \dots 8.3$$

The power spectral density may then be obtained from;

$$P_{xx}(\omega) = |G(j\omega)|^2 \quad \dots 8.4$$

Figure 8.2 shows the relationship between the PSD values of the signal at 4 and 8 cycles/ $720^\circ\phi$ and the engine load. The relationships are noted to be non-linear, however information may be extracted from the PSD and related to the engine load using a fuzzy mapping. The PSD values at 8 cycles/ $720^\circ\phi$ are used as the input to the load estimator due to the fact that the relation between PSD and load are seen to increase monotonically, allowing a simpler mapping to be employed.

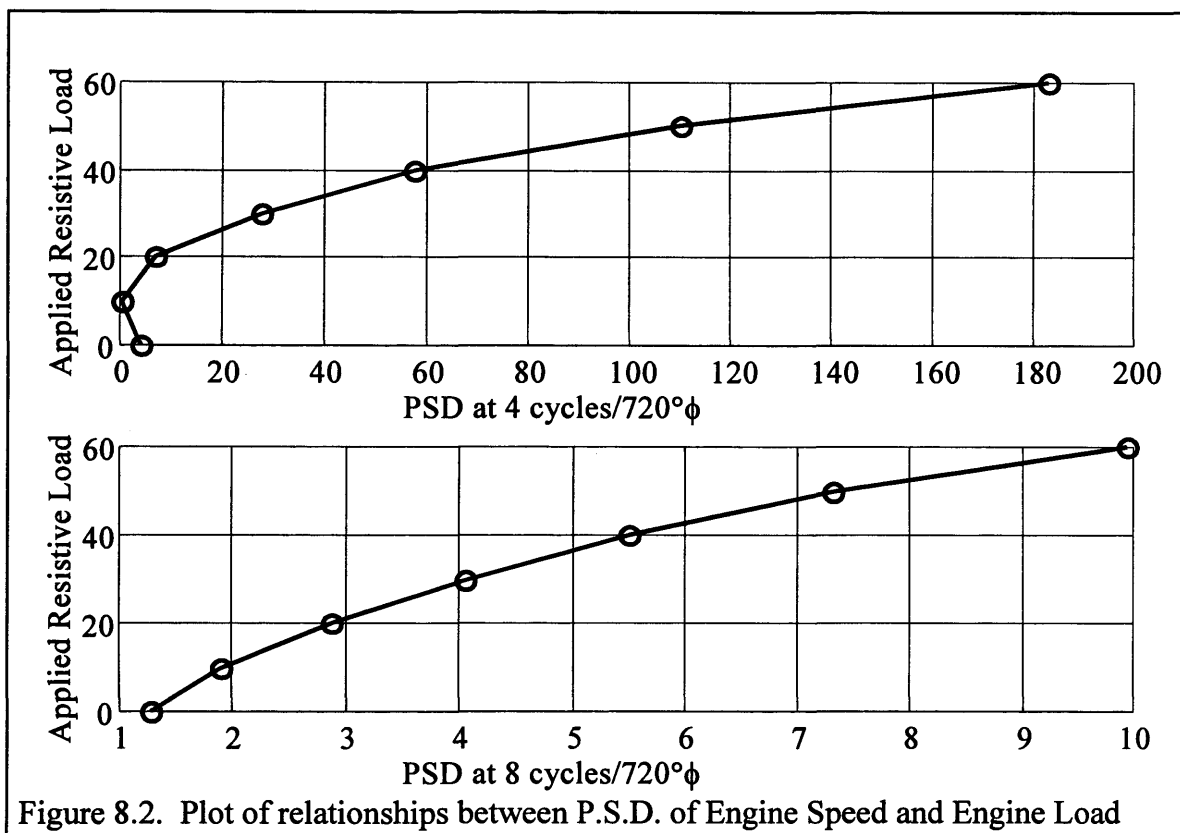
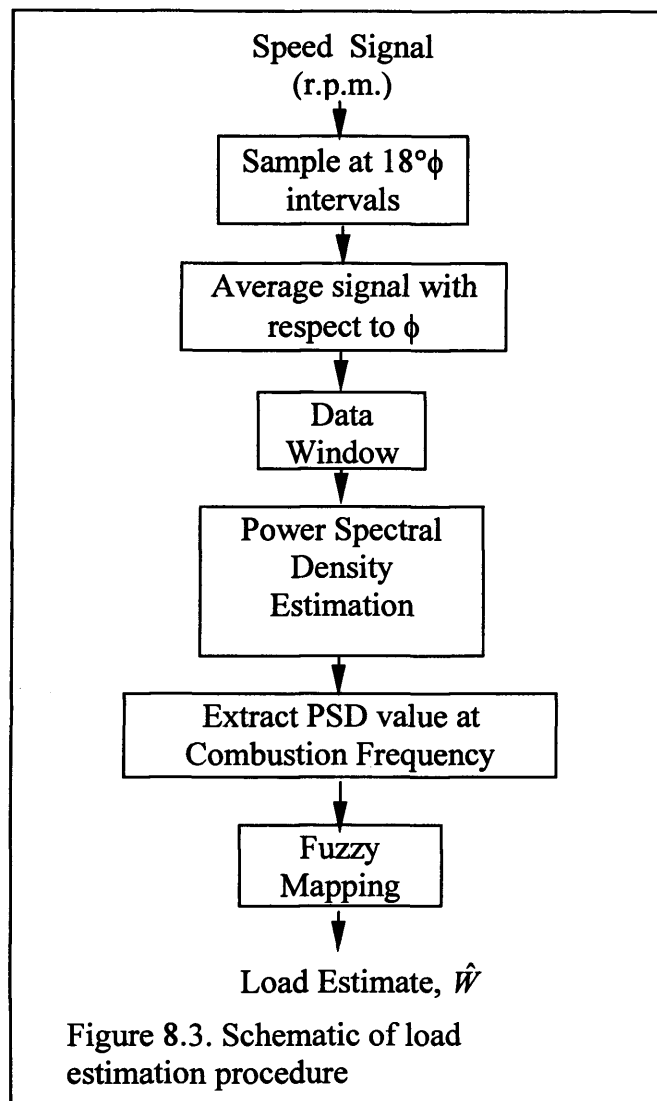


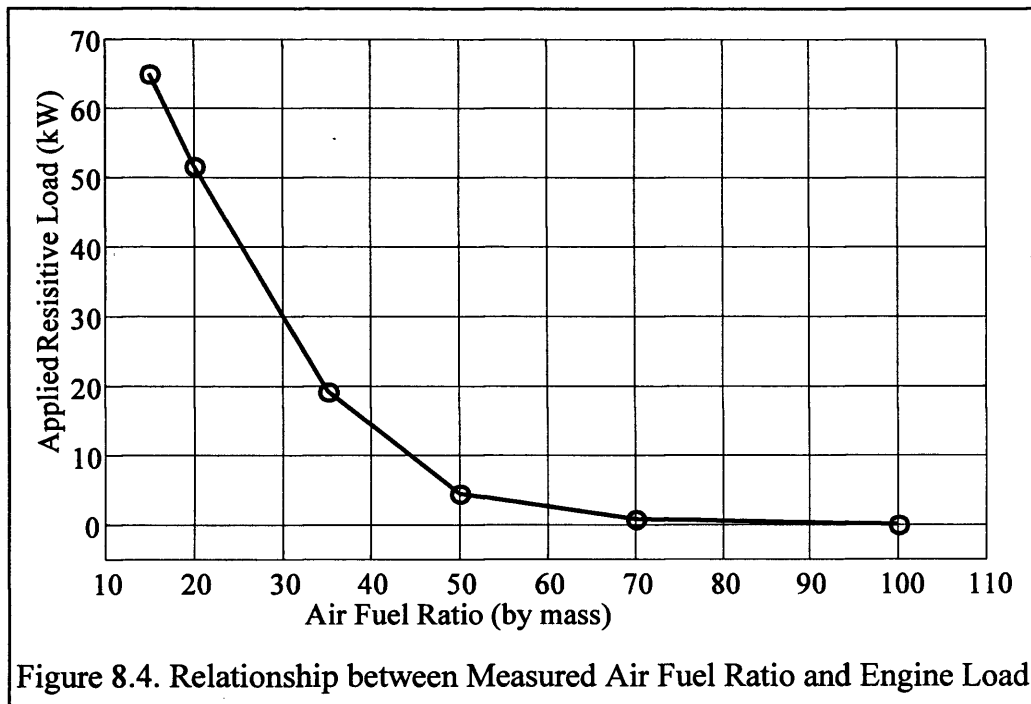
Figure 8.2. Plot of relationships between P.S.D. of Engine Speed and Engine Load

An engine load estimator is proposed as presented in the schematic, figure 3. A magnetic pick-up device is used to obtain pulses from the engine's flywheel gear teeth at 126 pulses/revolution. These pulses are converted to a d.c. voltage, proportional to the engine speed, using a suitable frequency-voltage card. The resulting speed signal is pre-processed with an appropriate high-pass digital filter designed to remove the d.c. component of engine speed. Ensemble averaging of the speed fluctuations is carried out with respect to ϕ in order to help eliminate signal noise. A Hanning data window is then applied prior to calculation of the PSD estimate.



8.2.2 LOAD ESTIMATION FROM AIR FUEL RATIO

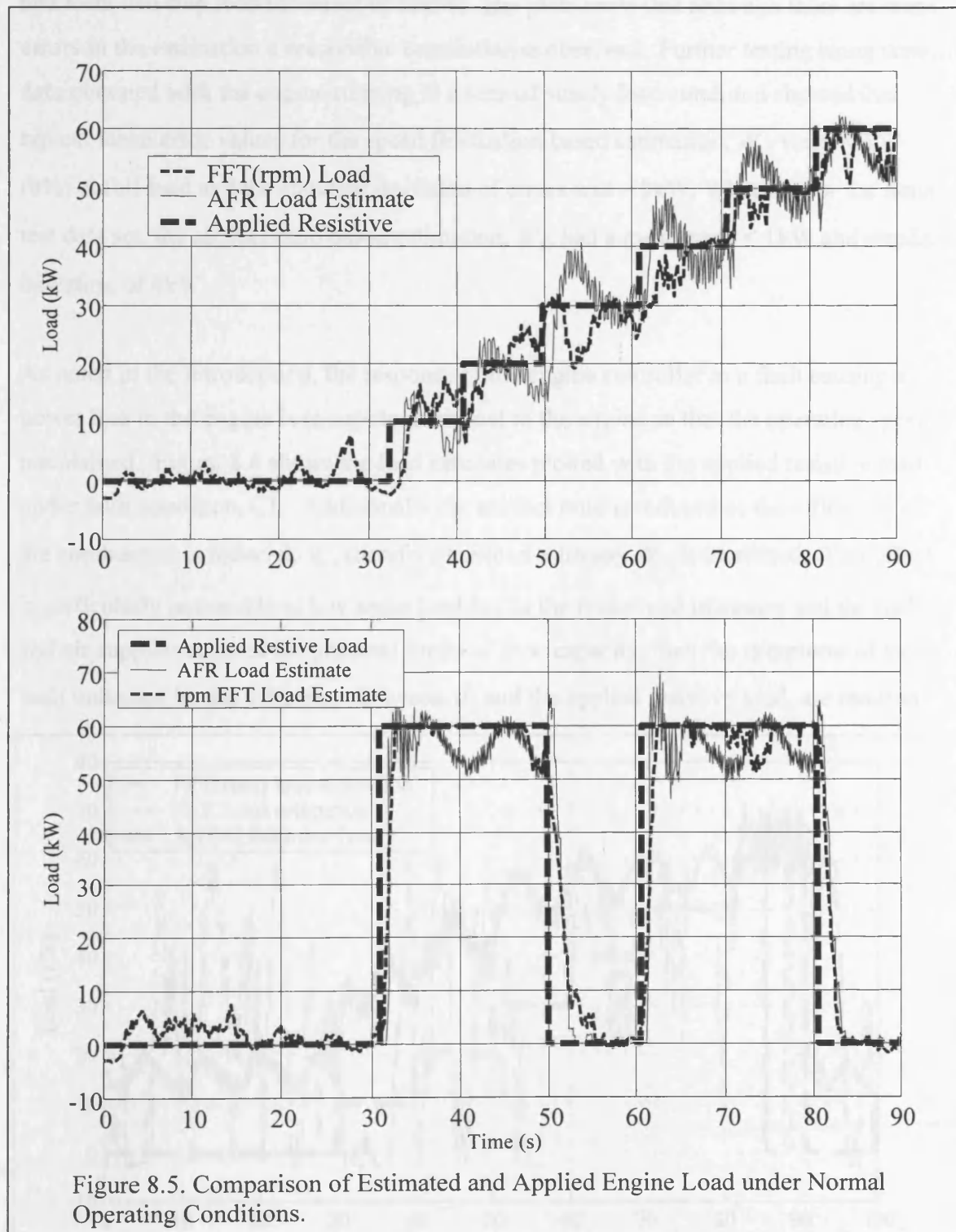
Combustion in a diesel engine always takes place with lean fuel mixtures and at part load with very low mixtures, i.e. air/fuel ratio is always greater than stoichiometric, which is typically 14.9 for hydrocarbon fuels [Challen 00]. If the load on the engine is increased the controller responds by increasing the mass flow rate of the fuel to the engine. Mass flow rate of the aspiration air to the cylinder also increases in this event, but due to flow restrictions imposed by the geometrical constraints within the aspiration system, the flow rate cannot increase to the same extent as the fuel flow rate. Thus, a reduction in air/fuel ratio occurs at high engine load with the limiting value being the stoichiometric ratio. This relation may be observed in figure 8.4.



8.3 IMPLEMENTATION AND TESTING OF LOAD ESTIMATOR UNDER NORMAL AND FAULT CONDITIONS

The load estimators have been developed using training data obtained from the diesel generator set test bed, trained using the ANFIS algorithm available in the Matlab™ Fuzzy Logic Toolbox and implemented in Simulink™. A number of sets of test data have been acquired, both with the engine running in its normal, fault-free state and with two separate fault conditions imposed on the engine.

Figure 8.5 shows the applied and estimated loads obtained from evaluating the load estimators with inputs from unseen test data (i.e. a separate set to the data used for training the fuzzy mappings) obtained with the engine in its normal operating condition.



The system was tested using data acquired both from a 'staircase' load test on the engine, and from two step load increases of 60kW. The plots show that although there are some errors in the estimation a reasonable correlation is observed. Further testing using unseen data obtained with the engine running in a normal steady load condition showed that typical mean error values for the speed fluctuation based estimation, \hat{W}_1 , were <5kW (8%) at full load and the standard deviation of errors was ~9kW. Whereas, for the same test data set, the air/fuel ratio based estimation, \hat{W}_2 , had a mean error <1kW and standard deviation of 4kW.

As noted in the introduction, the response of the engine controller to a fault causing a power loss in the engine is to supply more fuel to the engine so that the operating speed is maintained. Figure 8.6 shows the load estimates plotted with the applied resistive load under fault condition, C1. Additionally the air/fuel ratio is reduced as the efficiency of the combustion is reduced, η_c , therefore the load estimate, \hat{W}_2 , is increased. This effect is particularly noticeable at low brake load but as the brake load increases and the fuel and air supplies reaches the physical limits of their capacity, then the symptoms of the fault indicated by the difference between \hat{W}_2 and the applied resistive load, are reduced.

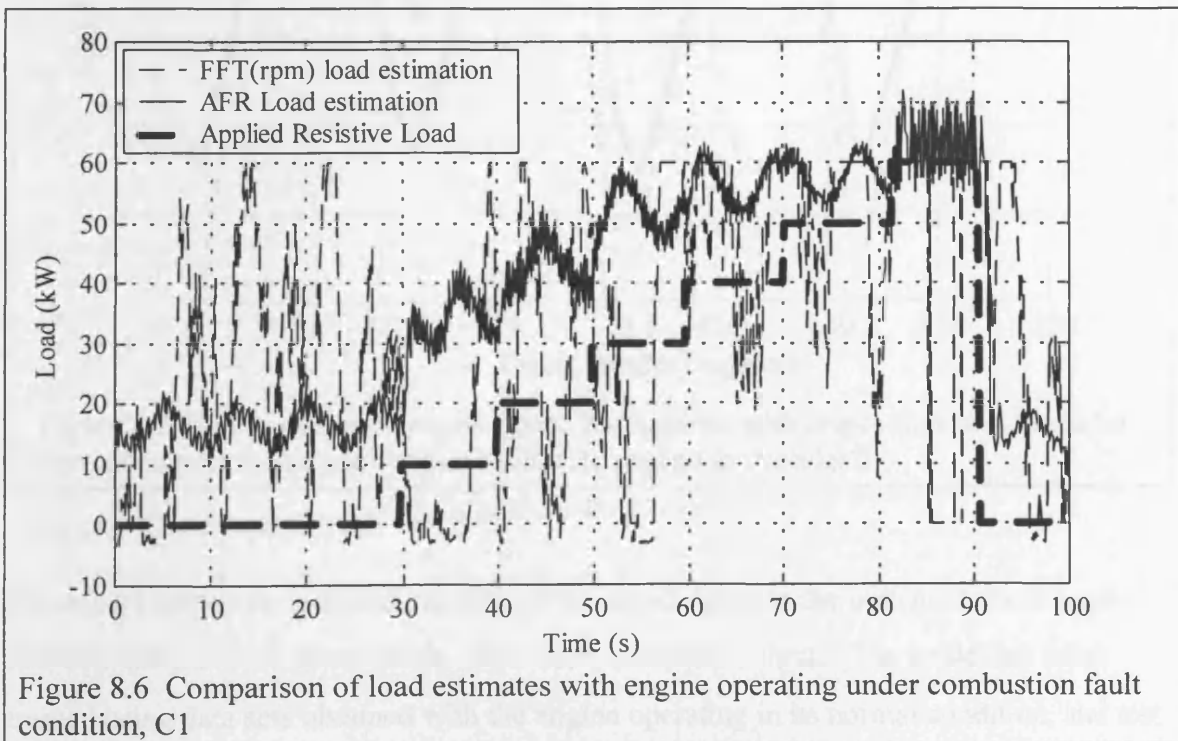
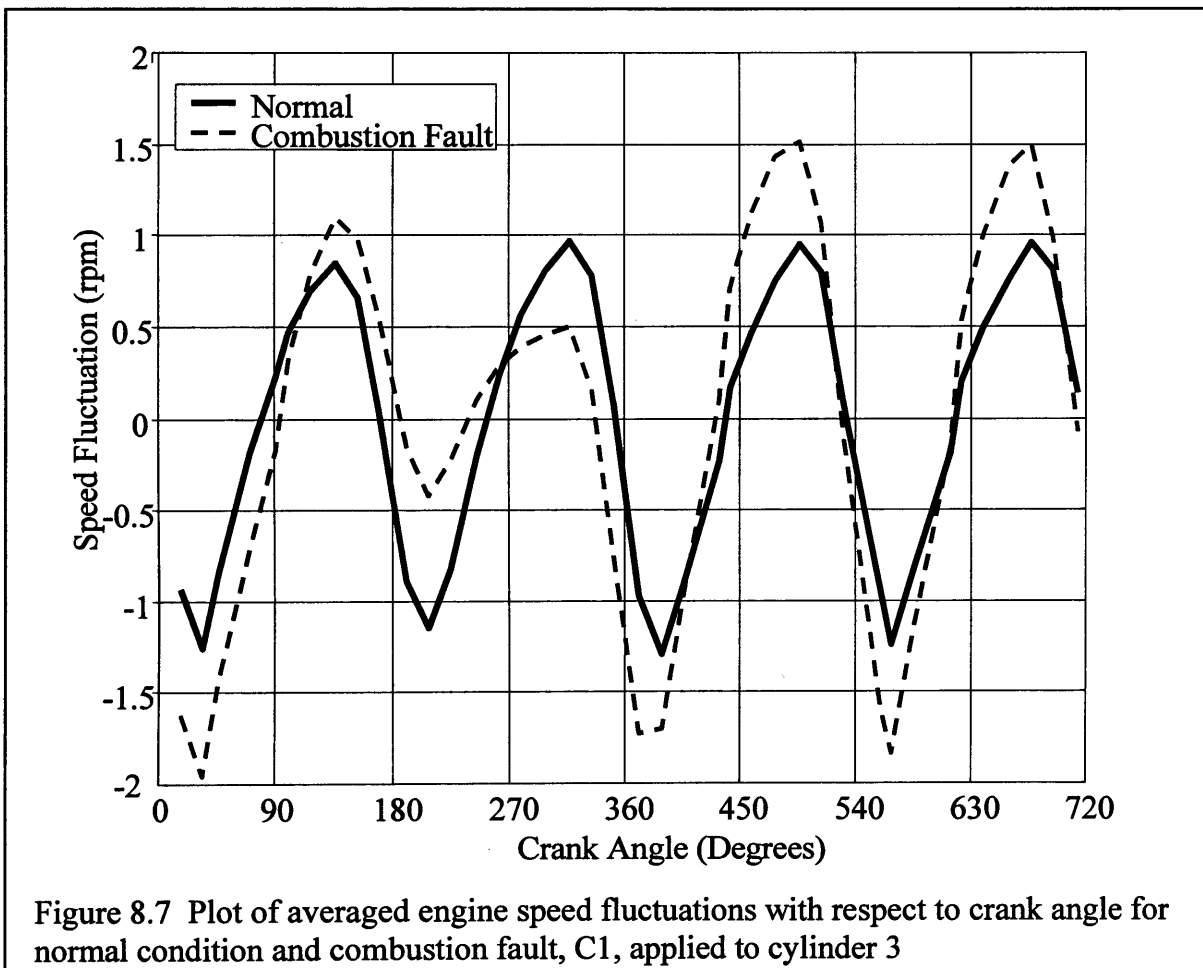


Figure 8.6 Comparison of load estimates with engine operating under combustion fault condition, C1

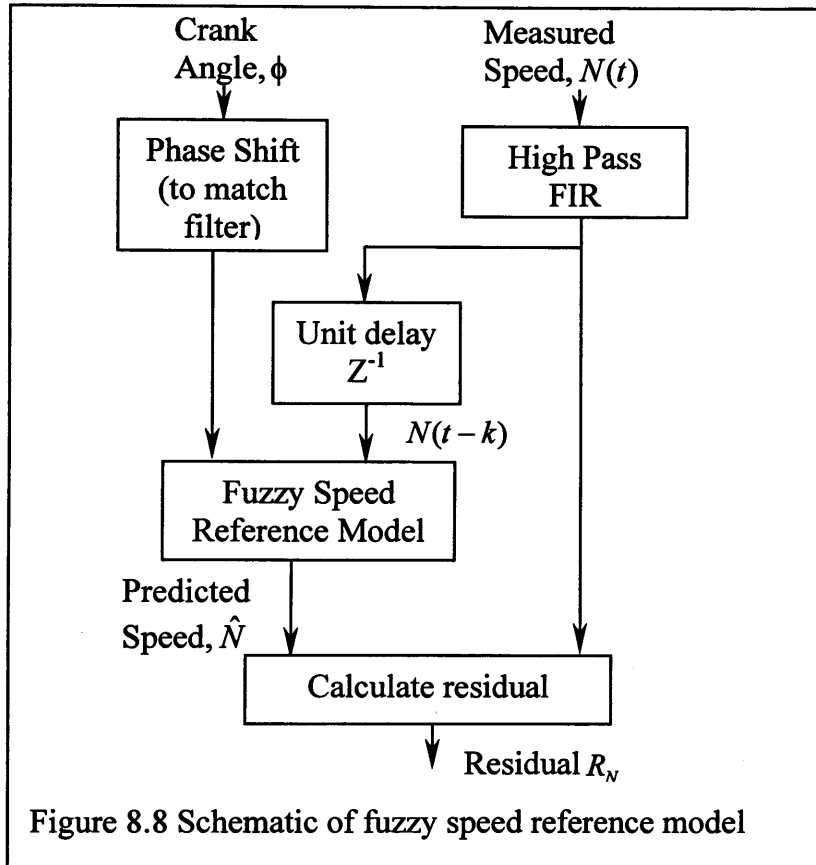
8.4 DEVELOPMENT OF A FUZZY REFERENCE MODEL FOR ENGINE SPEED FLUCTUATIONS.

The purpose of the predictive model for engine speed is to provide a cross-reference for the load estimators in the fault diagnosis scheme. Faults associated with individual cylinders, for instance, faults C1 and C2, will affect the periodicity of the engine speed signal (see figure 8.8), leading to inaccuracies in the load estimation, \hat{W}_1 . For this reason a reference model has been developed to complement the load estimator not only by providing an indication of confidence in the estimate but also to detect periodic fault symptoms in the engine speed signal (see schematic, figure 8.7).



The model relates periodic fluctuations of the speed signal to the indicated crank angle and uses the previous speed value, $N(t-k)$, to scale the output. The model has been trained using data sets obtained with the engine operating in its normal condition, and test

results obtained from testing the model with unseen data in both the normal and fault conditions are shown in figures 8.9 and 8.10.



8.5 DEVELOPMENT OF A FUZZY REFERENCE MODEL FOR BOOST PRESSURE FLUCTUATIONS.

Air inlet manifold or *boost* pressure measurements exhibit similar properties to the engine speed signal in that pressure, fluctuations occur which are periodic with crank angle and the amplitude is related to the load on the engine. The pressure fluctuations are associated with the opening and closing of the air inlet valves to the cylinder. Therefore a model has been developed with identical structure to that shown in figure 8.8 with the exception that the inputs are crank angle and boost pressure.

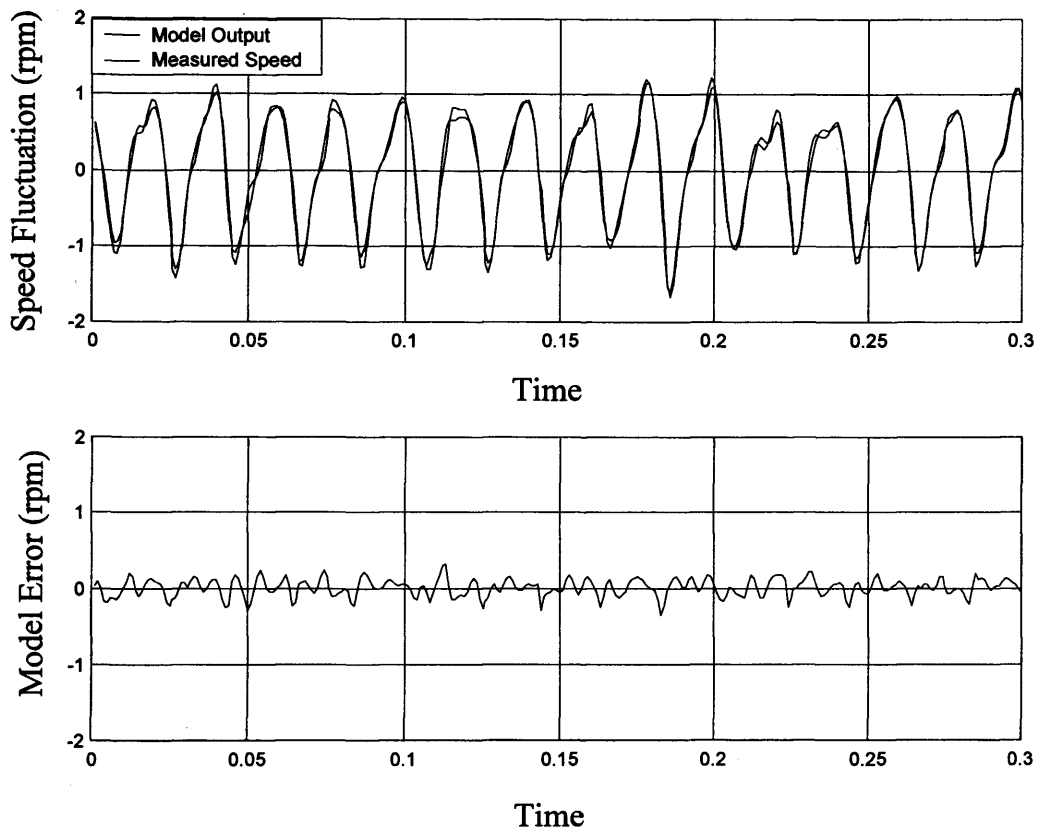


Figure 8.9 Comparison of predictive speed model outputs and measured speed fluctuations

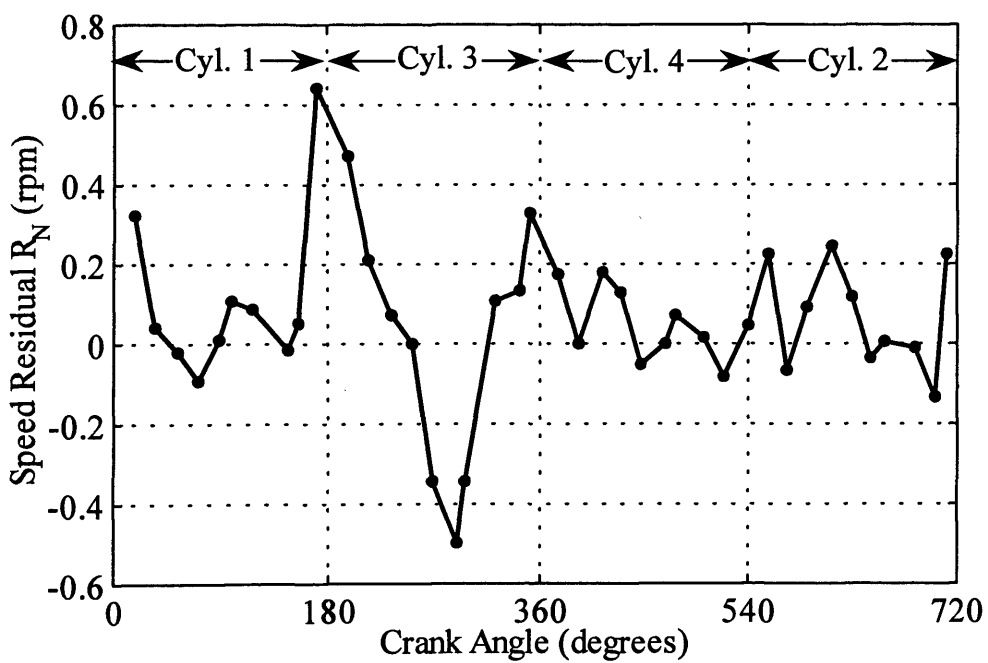
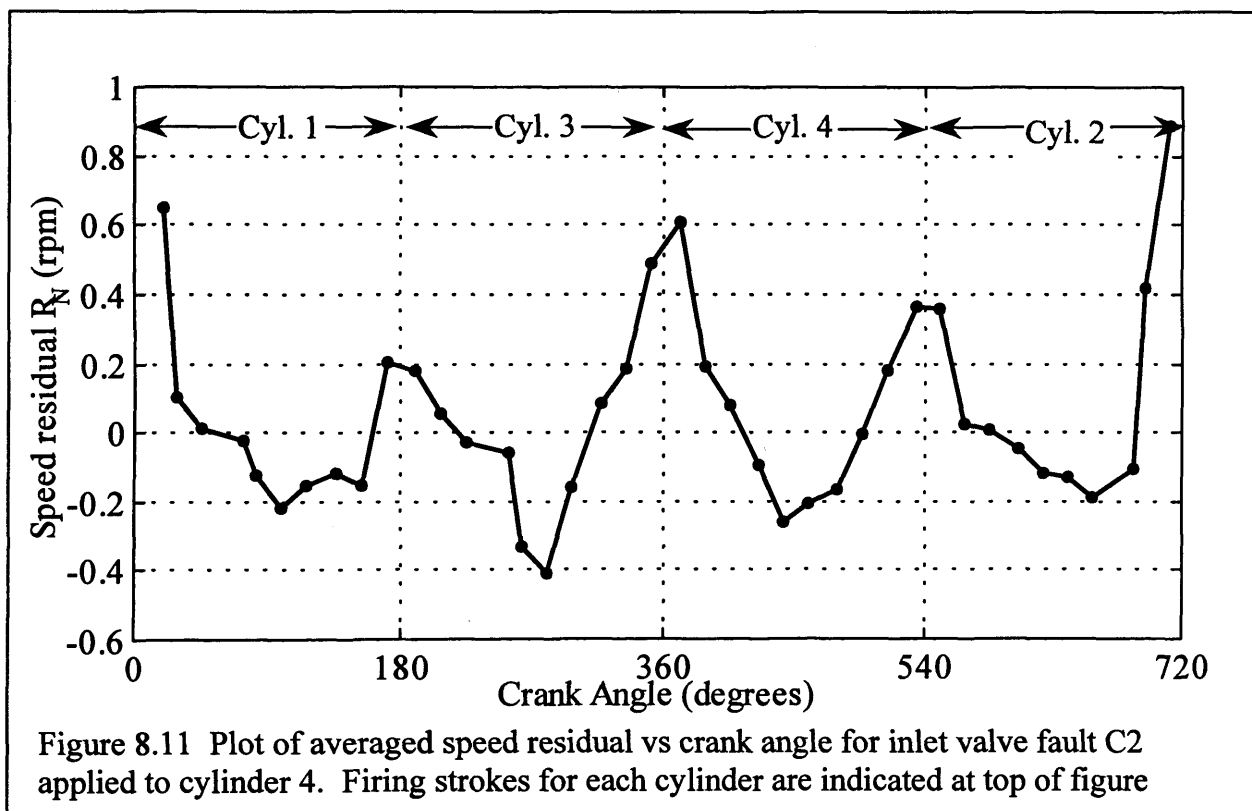


Figure 8.10. Plot of averaged speed residual vs crank angle for combustion fault C1 applied to cylinder 3. Firing strokes for each cylinder are indicated at top of figure

8.6 IMPLEMENTATION AND TESTING OF ENGINE SPEED AND BOOST PRESSURE REFERENCE MODELS UNDER NORMAL AND FAULT CONDITIONS.

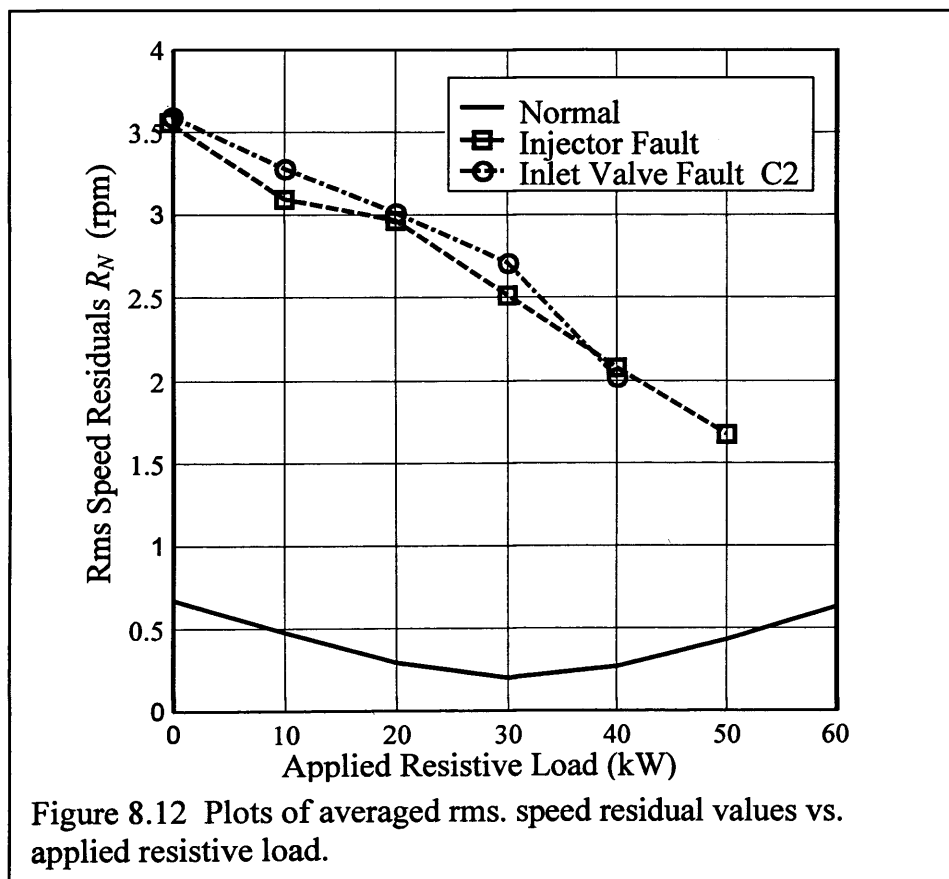
The models described in sections 8.4 and 8.5 have been implemented in Simulink™ and tested with data obtained with the engine in the normal condition and also in conditions C1 and C2. A comparison of predicted and measured engine speed fluctuations is presented in figures 8.8 and 8.9. Figures 8.10 and 8.11 show the effects on the R_N due to imposition of the fault conditions C1 and C2 on the engine. In figure 8.10, the effects of imposing fault C1 on cylinder three is clearly visible in R_N . However, the effect of the inlet valve fault on the engine speed when applied to cylinder 4 does not leave such a clear signature with respect to crank angle. This is due to the fact that high-pressure pulses of combustion gases passing back through the open inlet valve into the air inlet manifold, affect combustion processes in other cylinders.

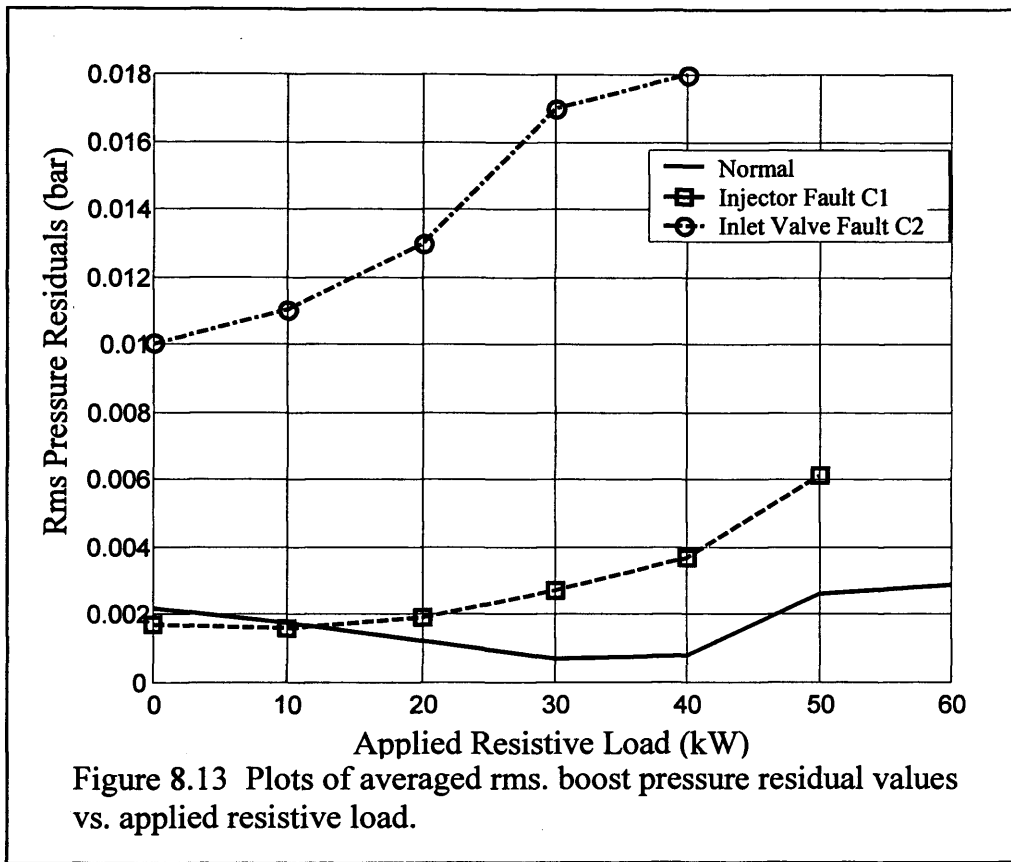


Figures 8.12 and 8.13 show the results obtained by calculating the root mean square (rms.) error values with respect to crank angle increments as follows;

$$\text{rms of speed residual, } \bar{R}_N = \left[\frac{\sum_{\phi_i=\phi_1}^{\phi_40} [R_N(\phi_i)]^2}{40} \right]^{0.5} \dots 8.5$$

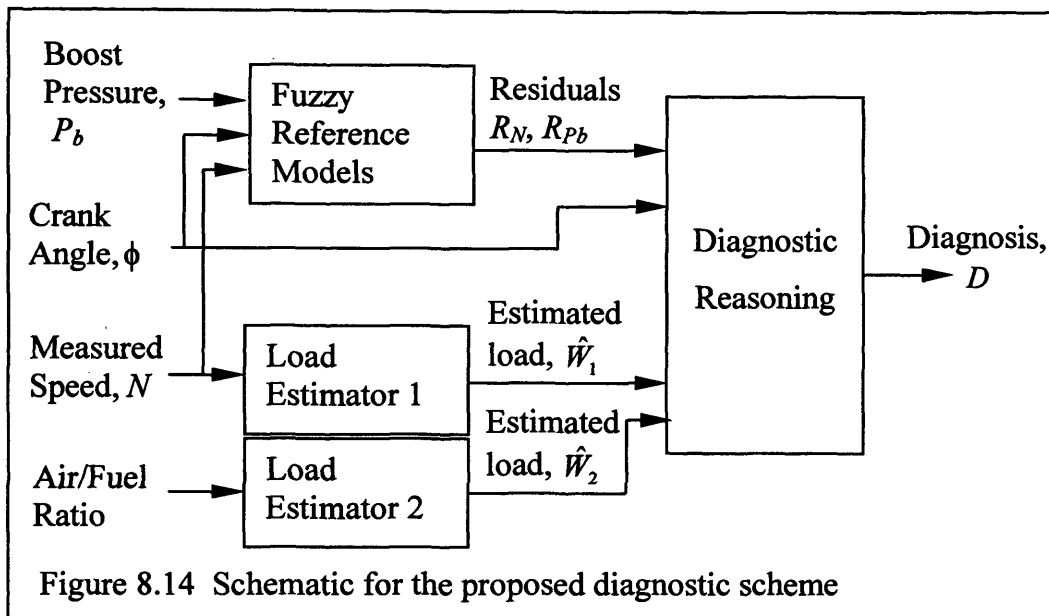
The rms. values of the speed residual R_N and the boost pressure residual R_{pb} are plotted with respect to applied resistive load for the normal, C1 and C2 conditions. These plots show the clear difference between the rms. values from the normal condition and from the two fault conditions.





8.7 THE PROPOSED HIGH-LEVEL DIAGNOSTIC SYSTEM.

The task of the diagnostic reasoning system is to combine the information from the models and estimators to infer the condition of the combustion system. The proposed diagnostic scheme (figure 8.14) is high level in that, discrepancies from the normal class may be the result of a number of different faults that have an effect on the combustion efficiency of the system. The robustness of the system is increased by use of the speed reference model, which has also been shown to be capable of generating residuals that indicate the periodic symptoms of combustion system faults.



The total load on the engine is the sum of the brake load i.e. the total power available at the drive-shaft, and the ‘pumping work’ [Heywood 88], this is the work required to pump various fluids, air, fuel, coolant water, and lubricating oil around the engine. This factor is also defined to include internal friction. Total load on the engine W is given by;

$$W = W_B + W_P \quad \dots 8.6$$

The effect of certain faults is to increase the pumping work required to maintain the engine power output at the given speed. Therefore the load on the engine under these fault conditions is given by;

$$W = W_B + W_P + \Delta W_f \quad \dots 8.7$$

where ΔW_f is the additional pumping work caused by the fault. Fluctuations in engine speed and the relationship between air/fuel ratio and engine load are indicators of the total load on the engine, so that \hat{W}_1 and \hat{W}_2 are estimations of $W = W_B + W_P + \Delta W_f$.

Therefore the class of faults which may be detected using the proposed diagnostic system

are those which affect either the periodicity of the speed signal or the magnitude of the combustion efficiency, η_c , and hence the air/fuel ratio with respect to W .

The diagnostic reasoning system is developed using a two-stage fuzzy rule based approach (see figure 7.2) with the first stage used to classify the residuals from the knowledge sources. The sets, *Normal*, and *High* may be defined using data from the engine in a fault-free condition.

The eight rules for system are presented in table 8.2. The rules have been defined by observation of the relations between the magnitude of the residuals and the existence of fault conditions, exemplified in figures 8.5, 8.6, 8.12 and 8.13;

The diagnostic system described has been implemented in Simulink and tested with unseen data sets obtained from the diesel generator set test-bed. The data files referred to contain data resulting from ‘staircase’ increases in resistive load on the engine, as shown in figures 8.5 and 8.6.

The confusion matrix shows that the diagnostic system correctly classifies over 90% of the samples in each of the test data sets. The results show few misclassifications, with the exception of fault, C1, which has a 9% misclassification as C2. Reviewing the diagnostic rules suggests that this misclassification and the misclassifications of C1 are probably due to model errors in the boost pressure reference model.

Table 8.1 Confusion matrix of diagnostic results

Engine Condition	Diagnosis (% of samples)			
	Normal	Combustion Fault C1	Inlet Valve Fault C2	Unknown
Normal	96.95	0.00	0.00	3.05
Combustion Fault, C1	0.34	90.43	9.24	0.00
Inlet Valve Fault, C2	0.00	0.00	93.03	6.97

1. If (\bar{R}_N is *Normal*) and (\bar{R}_{pb} is *Normal*) and ($R_{\hat{w}}$ is *Normal*) then (Normal is *True*)(C1 is *False*)(C2 is *False*)(Unknown is *False*)
2. If (\bar{R}_N is *Normal*) and (\bar{R}_{pb} is *Normal*) and ($R_{\hat{w}}$ is *High*) then (Normal is *True*)(C1 is *False*)(C2 is *False*)(Unknown is *False*)
3. If (\bar{R}_N is *Normal*) and (\bar{R}_{pb} is *High*) and ($R_{\hat{w}}$ is *High*) then (Normal is *False*)(C1 is *False*)(C2 is *True*)(Unknown is *False*)
4. If (\bar{R}_N is *Normal*) and (\bar{R}_{pb} is *High*) and ($R_{\hat{w}}$ is *Normal*) then (Normal is *False*)(C1 is *False*)(C2 is *False*)(Unknown is *True*)
5. If (\bar{R}_N is *High*) and (\bar{R}_{pb} is *Normal*) and ($R_{\hat{w}}$ is *Normal*) then (Normal is *False*)(C1 is *True*)(C2 is *False*)(Unknown is *False*)
6. If (\bar{R}_N is *High*) and (\bar{R}_{pb} is *Normal*) and ($R_{\hat{w}}$ is *High*) then (Normal is *False*)(C1 is *True*)(C2 is *False*)(Unknown is *False*)
7. If (\bar{R}_N is *High*) and (\bar{R}_{pb} is *High*) and ($R_{\hat{w}}$ is *High*) then (Normal is *False*)(C1 is *False*)(C2 is *True*)(Unknown is *False*)
8. If (\bar{R}_N is *High*) and (\bar{R}_{pb} is *High*) and ($R_{\hat{w}}$ is *Normal*) then (Normal is *False*)(C1 is *False*)(C2 is *True*)(Unknown is *False*)

Table 8.2: Fuzzy rules for diagnostic reasoning.

8.8 DISCUSSION.

The proposed high level diagnostic system combines information from these separate, but complementary knowledge sources, from which, a range of faults in the combustion system of an isochronous diesel generator set may be inferred with a high success rate, based on signal analysis from five robust, low-cost transducers.

The models and load estimators that have been developed may be regarded as knowledge sources containing information about the characteristics of the signals in the normal operating condition. Compared with the physical modelling approach undertaken by both Freestone [Freestone 85] and Jewitt [Jewitt 85], the process of fuzzy model structure identification and training from data shows two benefits whilst maintaining a high success rate in condition diagnosis. Firstly, in terms of both the ease of development of the diagnostic system, the process encapsulates qualitative information regarding the combustion system from the engine designer, but requires much less work in terms of mathematical analysis and estimation of physical engine parameters. The second benefit of the fuzzy rule-based diagnostic system is the high level nature of its outputs. The consequents, Condition is *Normal*, *Combustion fault, C1* and *inlet valve fault, C2*, are the highest level results from this system. Additional lower level rules, involving results from additional instruments, models and classifiers, could be used to add further detail to the conclusion.

The system has been demonstrated to effectively detect a class of faults that cause a change in the air/fuel ratio with respect to engine load. This is an important function, because air/fuel ratio has a strong influence on the emissions levels from the engine. The validated load estimation could also provide the basis for a number of other lower level diagnostic systems. For example, heat transfer to the engine's cooling system is closely related to its load.

Results from the speed reference model show that classification of the residuals with respect to crank angle should allow a faulty cylinder to be identified. Figure 10 shows residuals for cylinder 3. The firing order of the engine is 1, 3, 4, 2, therefore the maximum values of the residuals are seen to occur during the firing stroke of the faulty cylinder. The residual peaks for the air inlet valve fault, C2, are not so clearly aligned, suggesting a more complex relationship between the fault and the variation in engine speed. The explanation for this may be that the high-pressure pulses of combustion gases from the faulty cylinder during combustion and exhaust strokes, are returned to the air inlet manifold causing knock-on effects for the induction processes of the other cylinders. Classification of the boost pressure residuals is used to successfully discriminate between the combustion faults in the cylinder and air inlet valve faults. Clearly, this same principle could also be applied to detect similar faults in the exhaust valves.

Classification of residuals using fuzzy sets in this case study has benefited from the availability of fault condition test data. In situations where these data are not available it should still be possible to classify residuals from normal condition data only. This may be achieved by carrying out appropriate statistical analysis of model error to define a definition of a *Normal* class and definition of a fault condition outside this class. This approach will result in a less detailed conclusion e.g. it may not be possible to differentiate between different faults which cause variation in engine periodicity. However benefit to the engine operator still exists in having some indication of an engine fault, albeit more general.

8.9 CONCLUSIONS

The high-level fault diagnosis system has been shown to be an effective technique for detection of a class of faults that show the common symptom of a reduction in combustion efficiency of the isochronous diesel generator set. The results from testing the diagnostic system with unseen data obtained from three separate engine conditions,

showed that the success rate of the diagnostic scheme was greater than 90% for each of the three conditions.

Although the load estimation based on engine speed fluctuation may not be robust to certain faults, the periodicity in the speed fluctuations with respect to crank angle may be modelled. Variations in this periodicity are strong indicators of faults in individual cylinders and may be detected by comparison with the reference model, thereby also providing an estimate of confidence in the load estimation.

CHAPTER 9.

Fuzzy model-based condition monitoring and fault diagnosis for the aspiration and exhaust systems of a turbocharged diesel engine.

9.1 INTRODUCTION

The aspiration and exhaust systems are strongly inter-connected in the same gas flow path and mechanically, by means of the turbocharger, so they are considered jointly in this study. A schematic of the systems, showing their components and system boundaries, is presented in appendix 2, figure 2.1.

The systems also have strong interactions with the combustion system. The function of the aspiration system is to supply sufficient air for efficient combustion of fuel in the cylinders, whilst the exhaust system directs the exhaust gases away to the atmosphere. The key components in the systems are itemised in chapter 6, table 6.1.

The efficiency of the aspiration process, and removal, of exhaust gas is crucial in maintaining the combustion processes and maximising the thermal efficiency of the engine. The following chapter will firstly consider the individual components of the system in some detail, with reviews of relevant literature. The function of the components will be explained and a table of potential faults and their impact on engine operation will be drawn. With reference to these potential faults and the theoretical review, a fuzzy model-based diagnostic system is developed using *a priori* knowledge of the system and readily available data acquired from the diesel engine test bed operated in its normal condition only. The diagnostic system is then tested with data obtained from the diesel generator set test-bed in a series of simulated fault conditions.

9.2 THEORETICAL REVIEW

9.2.1 THE AIR FILTER

The function of the air filter is to prevent dust, dirt or other airborne particles from entering the engine. Such particles are likely to cause increased friction on moving parts such as bearings, or to increase abrasion and wear rates on pipe-work, turbocharger blades, cylinder liners etc. The filter itself is a dry type, with a paper element of large surface area for long life, folded into a wide-cylindrical housing. Mahon [Mahon 93

pp12] outlines the need for effective air filtration and recommends that a filter should have approximately 0.5m^2 of surface area for each m^3 per minute of induction air, and also that a differential pressure-based alarm should be fitted to indicate when a new filter element is required.

An air filter model may be derived from the Bernoulli equation as follows;

$$\frac{P_{amb}}{\rho_{amb}g} + \frac{\dot{V}_{a1}^2}{2gA_1^2} + z_1 = \frac{P_{ci}}{\rho_{amb}g} + \frac{\dot{V}_{a2}^2}{2gA_2^2} + z_2 \quad \dots 9.1 \text{ [Massey pp95]}$$

Assuming that there is no change in air density through the filter, inlet and outlet of the filter are in the same horizontal plane then $z_2 - z_1 = 0$ and there is no leakage of air from filter;

$$\frac{P_{ci}}{\rho_{amb}} - \frac{P_{amb}}{\rho_{amb}} = \frac{\dot{V}_{a1}^2}{2A_1^2} - \frac{\dot{V}_{a2}^2}{2A_2^2} \quad \dots 9.2$$

The filter causes friction on the flow of air so that, some kinetic energy is lost, so introducing a coefficient, C , to denote this;

$$\frac{P_{ci}}{\rho_{amb}} - \frac{P_{amb}}{\rho_{amb}} = \frac{\dot{m}_{a1}^2}{2\rho_{amb}A_1^2} - \frac{C\dot{m}_{a1}^2}{2\rho_{amb}A_2^2} = \frac{(A_2^2 - CA_1^2)}{2A_2^2A_1^2} \frac{\dot{m}_a^2}{\rho_{amb}} \quad \dots 9.3$$

renaming the constant term gives;

$$\Delta P_{af} = k_{af} \frac{\dot{m}_a^2}{\rho_{amb}} \quad \dots 9.4$$

Where \dot{m}_a^2 , and ρ_{amb} are the aspiration air mass flow-rate and density respectively, k_{af} is a scalar coefficient and $\Delta P_{af} = P_{amb} - P_{ci}$.

The coefficient, k_{af} , is characteristic of the condition of the air filter, so that if the filter becomes blocked with particles during a period of use then, the flow is restricted so that coefficient, C, is reduced. Consequently, for a particular mass flow rate of air, the value for, k_{af} , and hence the pressure difference, ΔP_{af} , will increase.

9.2.2 THE TURBOCHARGER

The maximum power which may be generated by an engine of fixed capacity and hence size, is limited by the amount of fuel which may be efficiently burned in the cylinders. This in turn is restricted by the amount of air which can be supplied to the combustion process. Clearly, if more air can be delivered to the cylinder during the combustion cycle then more fuel can be burned and more power produced. One approach to increasing the availability of induction air is to fit a turbocharger. A turbocharger consists of two components see (figure 1, appendix 2) a turbine and a compressor. The compressor is used to increase the density of the air as it enters the air inlet manifold so that more air may be forced into the cylinder during the combustion cycle. The turbine is used to extract the energy required to drive the compressor from the exhaust stream. The two are connected mechanically by a drive shaft and turn at very high rotational speeds (up to approximately 100,000 r.p.m.).

Watson and Janota [Watson 82] present a text detailing the theory and application of turbo-chargers in internal combustion engine systems. Turbine and compressor operating characteristics can be plotted on a *performance map* as dimensionless groups;

$$\frac{\dot{m}_a \sqrt{T_{0,ii}}}{P_{0,ii}}, \eta, \frac{\Delta T_0}{T_{0,ii}} = f \left(\frac{ND}{\sqrt{RT_{0,ii}}}, \frac{P_{0,io}}{P_{0,ii}} \right)$$

D and R are fixed for a particular turbocharger and gas, respectively therefore the performance maps are usually expressed;

$$\frac{\dot{m}_a \sqrt{T_{0,ti}}}{P_{0,ti}}, \eta, \frac{\Delta T_0}{T_{0,ti}} = f\left(\frac{N}{\sqrt{T_{0,ti}}}, \frac{P_{0,ti}}{P_{0,ti}}\right) \quad \dots 9.5$$

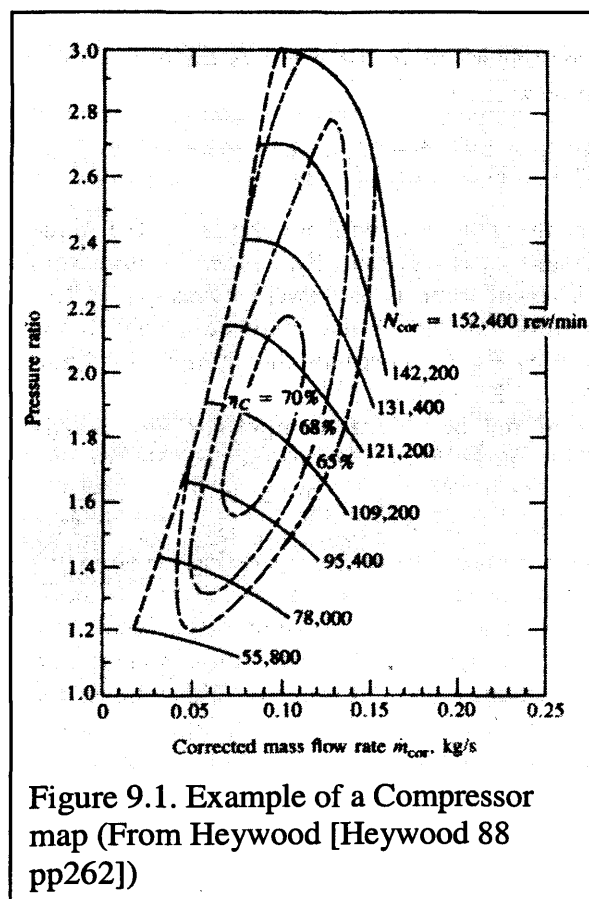
The example performance map shown in figure 9.1, indicates the operating regions of the compressor. The region is bounded to the left by the *surge line*, the point at which localised flow reversal begins to occur in the compressor for a reduction in mass flow at constant pressure ratio. Continued reduction in mass flow will lead to a complete flow reversal and fall in pressure ratio. To the right of the map the stable operating region is bounded by the *choking*, where the mass flow rate is increased to the point where the localised flow velocities become supersonic, at which point any additional increase in angular velocity causes only a small increase in mass flow rate. The region of highest operating efficiency is centred between these two limits and parallel to the surge line.

9.2.3 EXHAUST SYSTEM PIPEWORK

The exhaust from the outlet of the turbine is vented to atmosphere via suitable pipe-work. The nature of this pipe-work varies between applications, but it may contain other components such as silencers, particulate traps, smoke detection equipment etc. Ideally, the pressure difference between the outlet of the turbocharger and the atmosphere, ΔP_{eo} , should be minimised to allow the maximum amount of useful work to be reclaimed from the exhaust flow to drive the compressor. Components acting as a restriction to the gas flow may be given a similar mathematical treatment to that of the air filter in section 9.2.1. Bends are also noted to be the cause of energy losses in pipe flows. Massey [Massey pp 210] expresses these losses as;

$$\Delta h = \frac{ku^2}{2g} \quad \dots 9.6$$

Where Δh is the loss of head, u is the flow velocity and k is a constant proportional to the ratio of the bend radius and the pipe diameter. Thus, any of these components or other flow restrictions in the exhaust, will cause a back-pressure on the turbine outlet and consequently have an adverse effect on the efficiency of the turbocharger and the engine generally.



9.3 POTENTIAL FAULTS AND SYMPTOMS IN ASPIRATION AND EXHAUST SYSTEMS

Based on the theoretical knowledge presented in section 9.2 a table of eleven potential conditions has been drawn up (see table 9.1). The table includes the normal condition

and ten potential faults and their symptoms. The third column 'Experimental Simulation' indicates the seven engine conditions which have been simulated on the engine by various means. Reasons for the omission of four of the conditions from this list are presented in this column.

Table 9.1. Aspiration system condition descriptions.

CONDITION	DESCRIPTION	EXPERIMENTAL SIMULATION
d01. Normal	All states are operating in the expected operating condition for the given engine load.	Yes
d02. Combustion fault	This fault is defined to be a loss in engine power output due to a fault occurring in the combustion system. This is a general term defined to include loss of fuel to the cylinder, misfire, blow by or other cylinder condition which may cause the power loss. i.e. any of the faults which are detectable by the diagnostic systems described in chapter 8.	Yes
d03. Exhaust leak (outlet side of turbine)	Diesel engines fitted in certain locations may require exhaust gases to be directed away from the engine to atmosphere via ducting or via a particulate trap to remove pollutants. However, a leak occurring on the outlet side of the turbine, will cause the turbine pressure to fall to a value closer to atmospheric increasing the power available, but allowing potentially harmful exhaust gas to escape to the environment.	No Siting of engine in confined laboratory space prevents this on health and safety grounds
d04. Exhaust restriction (outlet side of turbine)	A blockage in this part of the exhaust system could be due to soot filling a particulate trap if fitted, or some other obstruction. If the exhaust is blocked after the turbine the outlet pressure of the turbine will rise and therefore the useful power available to the turbocharger will be reduced	Yes
d05. Air inlet leak (compressor side of filter)	The inlet air-flow into the aspiration system passes through a filter unit. A small pressure differential is created across the filter by the pumping action of the pistons and the compressor or blower if fitted. If an air leak occurs in this section of the aspiration system the air that enters the aspiration system will be unfiltered and airborne particulates could cause damage directly to the system components or increase wear rates due to abrasion.	Yes
d06. Air inlet restriction (blocked air filter)	Should the air filter become blocked the engine will need to expend extra energy as pumping work in order to maintain the necessary flow of air required to maintain the appropriate air/fuel ratio. A severely blocked filter will clearly have an adverse effect on engine efficiency.	Yes
d07. Air inlet valve fault.	This fault is specifically defined to be when the valve fails to seat properly, this usually occurs due to wear on the engine. The effect of this is that the combustion chamber is ineffectively sealed during the power stroke causing a loss in cylinder pressure and hence a drop in engine power output. (see also chapter 8)	Yes
d08. Exhaust leak	This fault could be caused by corrosion of components or poor sealing of joints in the exhaust and will cause a loss of pressure in	No Siting of engine in

(manifold side of turbine)	the exhaust manifold, allowing a fraction of the exhaust gases to escape to atmosphere thereby bypassing the turbine. This will clearly cause a drop in the work available to compress the inlet air and hence cause power loss in the engine, as well as allowing potentially harmful exhaust gas to escape to the environment.	confined laboratory space prevents this on health and safety grounds
d09. Turbocharger fault	Increased friction in the bearings possibly due to the condition (or lack of) lubricating oil, or due to mechanical wear or failure will cause a drop in efficiency of the turbine system. This will result in a reduction in mass flow rate through the compressor for a given turbine pressure ratio.	No There is a possibility of permanent damage to turbocharger components, combined with time and practicality of obtaining and fitting replacements
d10. Exhaust valve fault	This fault is defined similarly to fault d07. i.e. the exhaust valve fails to seat properly. The effect of this is that the combustion chamber is ineffectively sealed during the power stroke causing a loss in cylinder pressure and hence a drop in engine power output.	No The main diagnostic technique is the same as that for condition 7, and is described in chapter 8
d11. Air Inlet Manifold Leak	As with the exhaust manifold leak, this fault could be caused by corrosion of components or ineffectively sealed joints between components. A fall in inlet manifold pressure will result in reduced engine power	Yes

9.4 SPECIFICATION OF REFERENCE MODELS FOR FAULT DIAGNOSIS

Suitable instrumentation has been defined in chapter 6 for the monitoring of appropriate signals from the aspiration and exhaust systems. Sections 9.1 to 9.3 have presented a study of the function and theory of the aspiration system and its components, resulting in a list of potential faults which cause either loss of engine efficiency or emission of harmful exhaust gases. This section will present a description of the reference models required to diagnose the faults noted in table 9.1. The models are then used to generate residuals which are classified and used in a fuzzy reasoning algorithm to diagnose faults.

9.4.1 AIR INLET FILTER MODEL

In his thesis Molteburg [Molteburg 91] uses a model of the form 9.1 and acquires sufficient data to estimate the parameter, k_{af} . In the approach outlined here a fuzzy model

is proposed to estimate the pressure drop, ΔP_{af} . Thus the parameter, k_{af} , is encapsulated within the rules of the fuzzy model trained from acquired data and the model is a fuzzy mapping of the form;

$$\text{Air filter model, } \Delta \hat{P}_{af} = f(\dot{m}_a, T_{amb}) \quad \dots 9.7$$

The temperature measurement, T_{amb} , is included as an input because the air density is strongly related to temperature and inclusion of T_{amb} was found to reduce model training and checking errors.

9.4.2 TURBINE MASS FLOW ESTIMATOR

This estimator is based on the turbine map relations presented in 9.3.2. Its purpose is to estimate the total mass flow rate through the turbine. Since the aspiration air and fuel flow rates are measured, the estimation of mass flow rate through the turbine may be used in performing a mass balance in order to check for leaks of air or exhaust gases in the system between the air flow meter, fuel meter and turbine. The exhaust mass flow estimation is identified as fuzzy system of the form;

$$\text{Turbine mass flow estimator, } \hat{m}_{exh} = f\left(\frac{\sqrt{T_{ii}}}{P_{ii}}, \frac{P_{to}}{P_{ii}}\right) \quad \dots 9.8$$

Where subscripts ii and to denote turbine inlet and turbine outlet respectively.

9.4.3 EXHAUST PIPE-WORK DIFFERENTIAL PRESSURE MODEL

In a pipe-work system of fixed cross sectional area with a given mass flow rate and hence gas velocity, the pressure difference, ΔP_{eo} , between the inlet to the pipe-work (in this case the outlet from the turbocharger) and the pipe-work outlet to atmosphere will be

constant. However in the exhaust system the wide range in temperatures of the gases has an effect on the density of the gas.

In section 9.4.2 the mass flow rate for the exhaust gases passing through the turbocharger is estimated using a fuzzy system. This estimation is validated in a mass balance with input fuel and air rates. Therefore it is proposed to use this mass flow estimation as an input, along with exhaust temperature to allow a relationship to be identified for the exhaust gas density, so that the fuzzy model for the pressure drop is in the form;

$$\text{Exhaust differential pressure model, } \Delta \hat{P}_{eo} = f(\hat{m}_{exh}, T_{exh}) \dots 9.9$$

Where some restriction acts on the exhaust system, ΔP_{eo} will increase allowing the generation of a residual between the measured and predicted values for ΔP_{eo} .

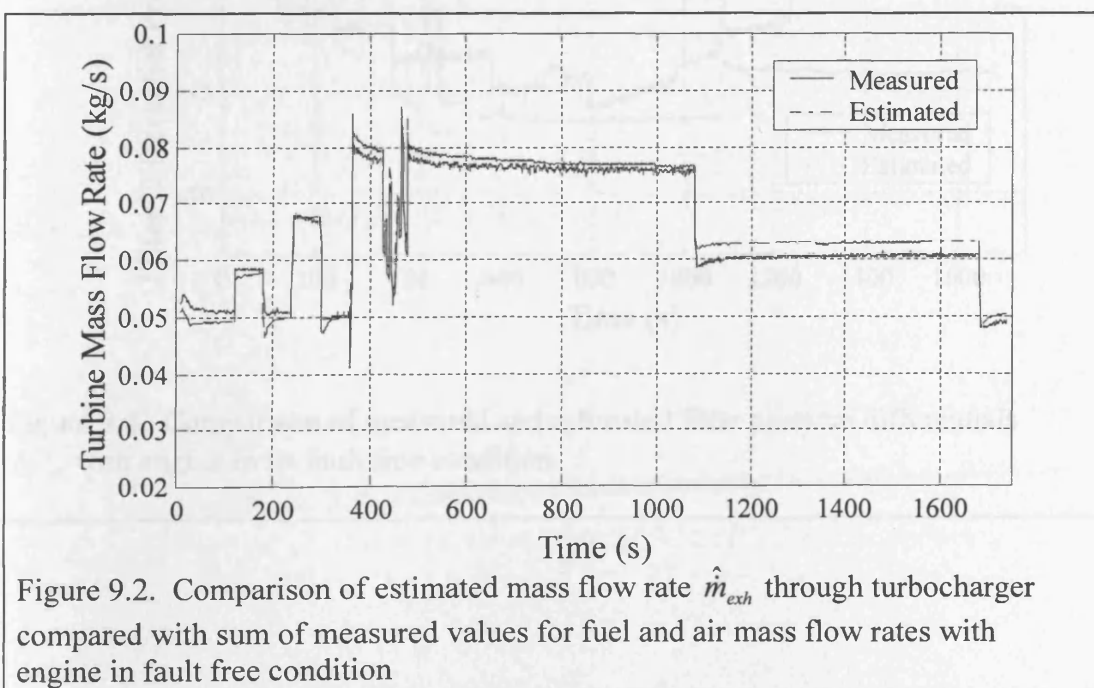
9.5 GENERATION OF REFERENCE MODELS

The three models described in section 9.4 have been tested using a training data set obtained with the engine operated in the normal condition. The test program included data from a series of step load changes on the engine intended to maximise the range of the training data so that the valid range of the fuzzy model inputs are maximised. The step change data was supplemented with a sets of data obtained with the engine running in the steady state condition having had sufficient time for temperatures to reach their maximum normal values. The training process was undertaken using ANFIS in Matlab™, using two data sets, for training and checking respectively. The training process minimises the model errors with respect to the training data and tests the resulting fuzzy system with the checking data set to ensure some degree of generality in the fuzzy system.

The reference models are based on the steady state values for pressures and temperatures in the aspiration and exhaust systems. However, significant pressure fluctuations in air

inlet and exhaust manifold pressure signals are observed in the raw data with fundamental frequencies of 50 Hz, a frequency which corresponds to that of the combustion events in the diesel engine. Therefore it is desirable to filter out noise originating from these periodic processes whilst avoiding aliasing errors. The data was initially captured at ten times the fundamental frequency, i.e. 500Hz, and filtered using a low pass, FIR filter designed with a cut-off frequency of 1Hz. This filter provides sufficient attenuation at 10Hz for the data to be safely re-sampled at 20Hz with no significant aliasing effects. All training and test data sets were acquired using this process.

The models have been tested with a third unseen set of data and the results plotted in figures 9.2 to 9.4. The test data consists of data obtained with the engine in its normal fault-free condition. The engine speed is controlled to 1500 rpm and the brake load is applied to the generator set by a resistive load bank (see appendix 1.4). The applied resistive load is initially set at 0kW, then three successive step load changes are applied for approximately 60 seconds each, at 20, 40 and 60 kW respectively. A series of 12 rapid changes in load are then applied for approximately 5 seconds each. Finally the engine is run with a 60kW applied load for approximately 10 minutes and 30kW for 10 minutes to allow the systems to reach a steady state (see figure 9.9).



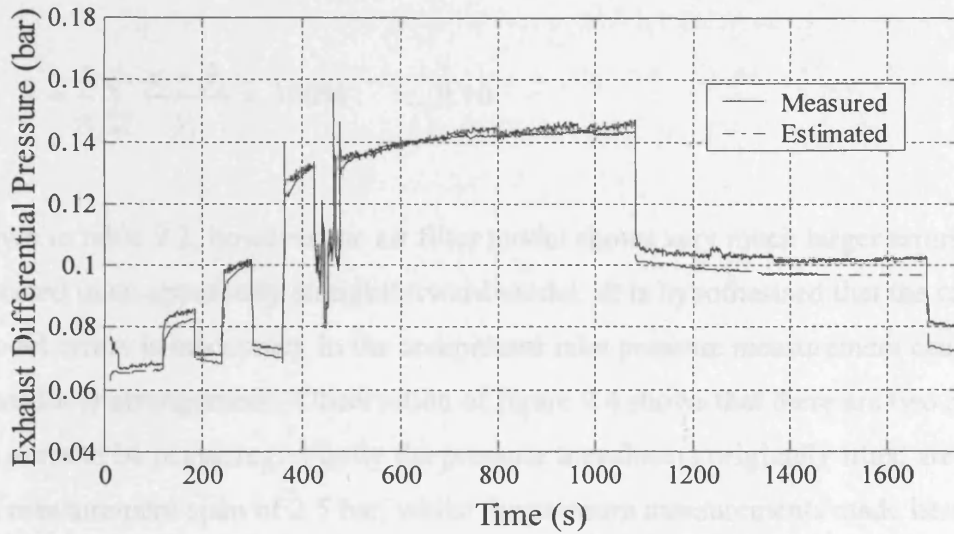


Figure 9.3. Comparison of measured and estimated exhaust pressure differential ΔP_{eo} with engine in fault free condition

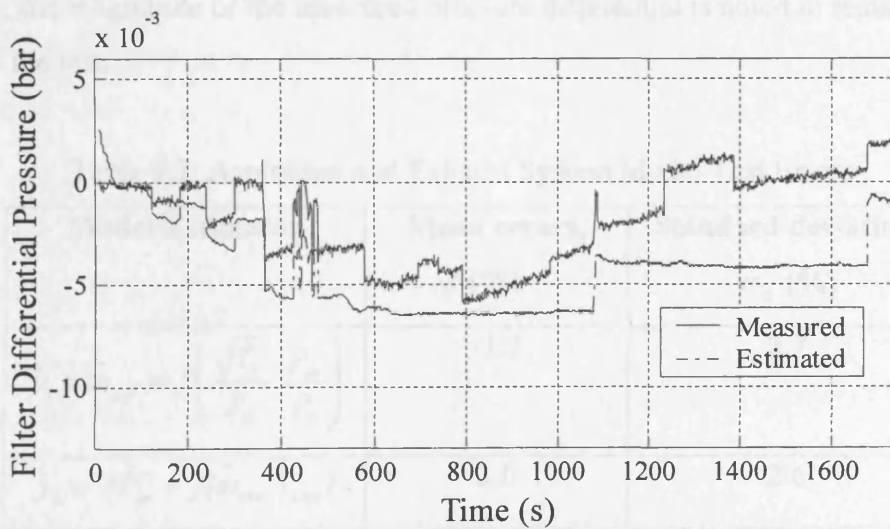


Figure 9.4. Comparison of measured and estimated filter pressure differentials ΔP_{af} with engine in its fault free condition.

Test results for the turbine mass flow estimator and the exhaust differential pressure model are seen to show low percentage model errors, ε , calculated from;

$$\bar{\varepsilon} = \frac{1}{n} \sum_{i=1}^n \frac{y_i - \hat{y}_i}{y_i} \times 100\% \quad \dots 9.10$$

as shown in table 9.2, however the air filter model shows very much larger errors. This is unexpected in an apparently straightforward model. It is hypothesised that the cause of the model errors is inaccuracy in the compressor inlet pressure measurement caused by the transducer arrangement. Observation of figure 9.4 shows that there are two effects which seem to be occurring. Firstly the pressure transducers originally fitted are scaled with a measurement span of 2.5 bar, whilst the pressure measurements made here are of the order of 10^{-3} bar suggesting that a pressure transducer with more suitable measurement range would be appropriate. It is also noticeable that certain ‘jumps’ occur in the measurement of ambient pressure which could be due to vibration from the engine. Secondly, the magnitude of the measured pressure differential is noted to reduce over the course of the test.

Table 9.2. Aspiration and Exhaust System Model Test Errors

Model/Estimator	Mean errors, $\bar{\varepsilon}$ (%)	Standard deviation, σ_{ε} (%)
$\hat{y}_1 = \hat{m}_{exh} = f\left(\frac{\sqrt{T_{ii}}}{P_{ii}}, \frac{P_{to}}{P_{ii}}\right)$	-1.7	2.7
$\hat{y}_2 = \Delta\hat{P}_{eo} = f(\hat{m}_{exh}, T_{exh})$	3.0	2.6
$\hat{y}_3 = \Delta\hat{P}_{af} = f(\hat{m}_a, T_{amb})$	8.8	127.2

The physical arrangement of the pressure transducers is that the transducers are mounted on a panel outside of the generator set canopy and connected to the tapping point on the

engine by the use of small bore pipe-work which is routed under the engine. Again, because the magnitudes of the pressure differentials are so small in this instance, heating effects on the pipe-work from the engine may have had a significant effect on the pressure measurement. As the temperature in the pipe-work increased over the course of the test, the indicated pressure from the compressor inlet appeared to rise from a small vacuum to a value close to atmospheric, thereby reducing the pressure differential.

9.6 RULES FOR CLASSIFICATION AND REASONING.

Three reference models have now been developed for producing residuals for fault diagnosis in the aspiration and exhaust systems and a number of potential faults have been described, six of which may be experimentally simulated on the generator set test bed. This section will detail how, based on *a priori* knowledge of the engine systems and reference models, the residuals may be classified and used to diagnose those fault conditions.

9.6.1 RESIDUAL CLASSIFIERS

The fuzzy classifiers described here are used to analyse the residual, R , calculated from the difference between the measured state vector, Y , and the estimated or predicted state vector, \hat{Y} , by;

$$R = Y - \hat{Y}$$

Where $R = [r_1, r_2, r_3]^T$; $Y = [y_1, y_2, y_3]^T$; $\hat{Y} = [\hat{y}_1, \hat{y}_2, \hat{y}_3]^T$ in this example.

An effective classifier for a residual should be capable of differentiating between model errors as shown in table 9.2 and residuals caused by a prescribed deviation in operating condition of the system under study, thereby providing an effective trade-off between sensitivity to fault conditions and a low false alarm rate.

Classifiers are defined using the approach taken in chapter 7, section 4. The membership functions are defined based on the model error distributions obtained from a set of normal test data. The ‘*Normal*’, membership functions $\mu_N(r_i)$ are defined, based on the mean and standard deviation of the model errors, using the ‘*Gaussian2mf*’ functions available in the Matlab™ Fuzzy Logic Toolbox. These are defined for each residual, r_i , as shown in equation 9.11. The membership functions obtained from this design process are illustrated in figure 9.5.

The membership functions for *Positive* and *Negative* are also designed using the ‘*Gaussian2mf*’ function. These are defined using the standard deviation of the model error, σ_{r_i} , to set the gradient parameter for the membership function, with the centre parameters, \bar{r}_i , defined such that the membership functions for *Positive*, $\mu_{Pos}(r_i)$, and *Negative*, $\mu_{Neg}(r_i)$, intersect with $\mu_N(r_i)$ at $\mu_{Pos}(r_i) = \mu_N(r_i) = 0.5$ and $\mu_{Neg}(r_i) = \mu_N(r_i) = 0.5$ respectively.

$$\mu_N(r_i) = \begin{cases} \exp\left(\frac{-(r_i - (\bar{r}_i + \sigma_{r_i}))^2}{2\sigma_{r_i}^2}\right) & \text{if } -\infty < r_i \leq -\sigma_{r_i} \\ 1 & \text{if } -\sigma_{r_i} < r_i \leq \sigma_{r_i} \\ \exp\left(\frac{-(r_i - (\bar{r}_i - \sigma_{r_i}))^2}{2\sigma_{r_i}^2}\right) & \text{if } \sigma_{r_i} < r_i \leq \infty \end{cases} \quad \dots 9.11$$

9.6.2 DEVELOPMENT OF DIAGNOSTIC REASONING

Two fundamental approaches are used as the basis for this process; the mass balance and the energy balance. The measured fuel and air-flow rates represent the only mass flows into the combustion, and hence the exhaust system (neglecting any small consumption of lubricating oil). Therefore the estimated mass flow through the turbine may be compared with the measured values for air and fuel flow to detect leaks into and out of the system

bounded by the air and fuel meters and the turbine. As has been described in section 9.2.1 the models for the exhaust pipe-work and air filter are based on the steady flow energy equation and therefore any additional work which is required to overcome.

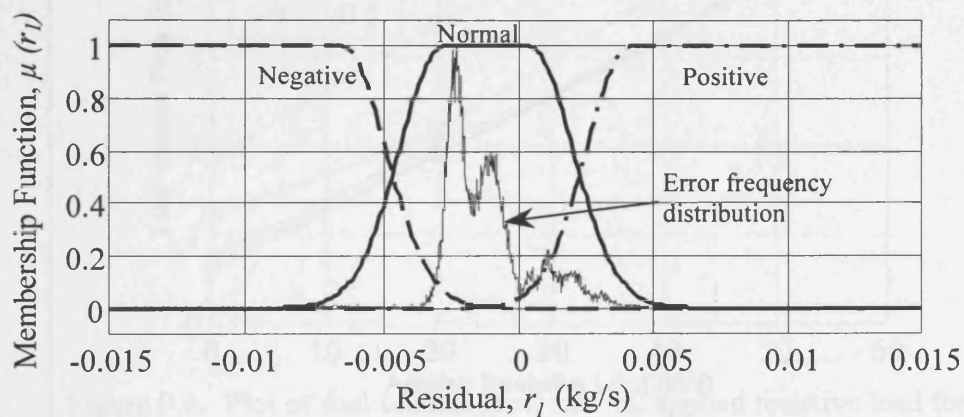


Figure 9.5. Plot of fuzzy classifier membership functions for *Negative*, *Normal* and *Positive* residual classes. A scaled frequency distribution for normal model error is shown for comparison.

restrictions in exhaust or inlet air filter will show as a residual when compared with the measured pressure difference.

From figures 9.6, 9.7 and 9.8, it is noted that faults occurring in the combustion system cause effects in the aspiration and exhaust systems. However, techniques for diagnosing those combustion system faults have been developed and described in chapter 8. The success rates for diagnoses of these faults was seen to be greater than 90% in each case (see table 8.1). Because of the interaction between the three systems, these results must be considered when developing these diagnostic rules.

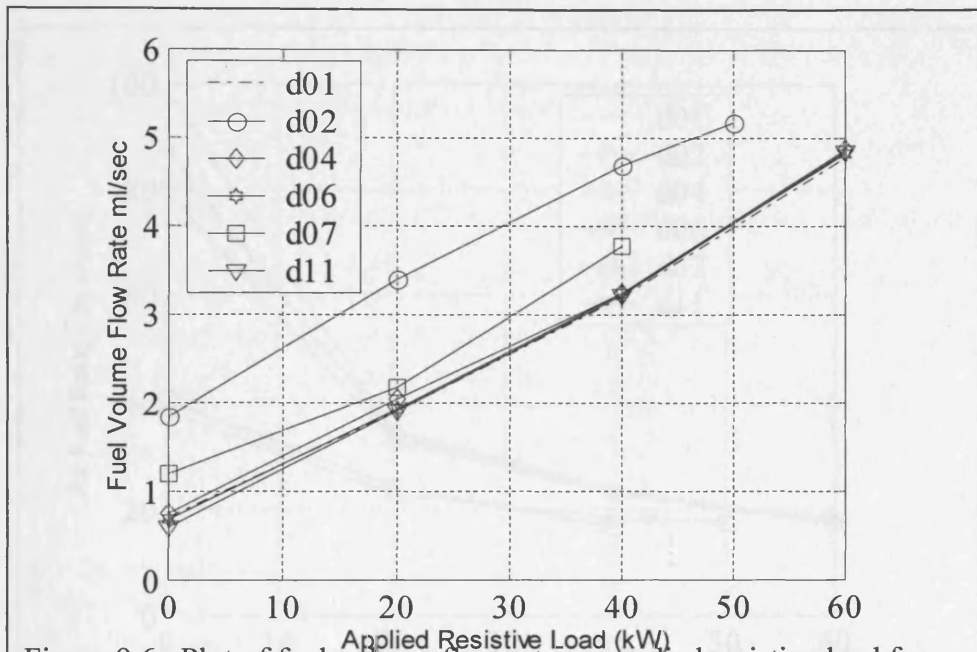


Figure 9.6. Plot of fuel volume flow rate vs. applied resistive load for six engine conditions

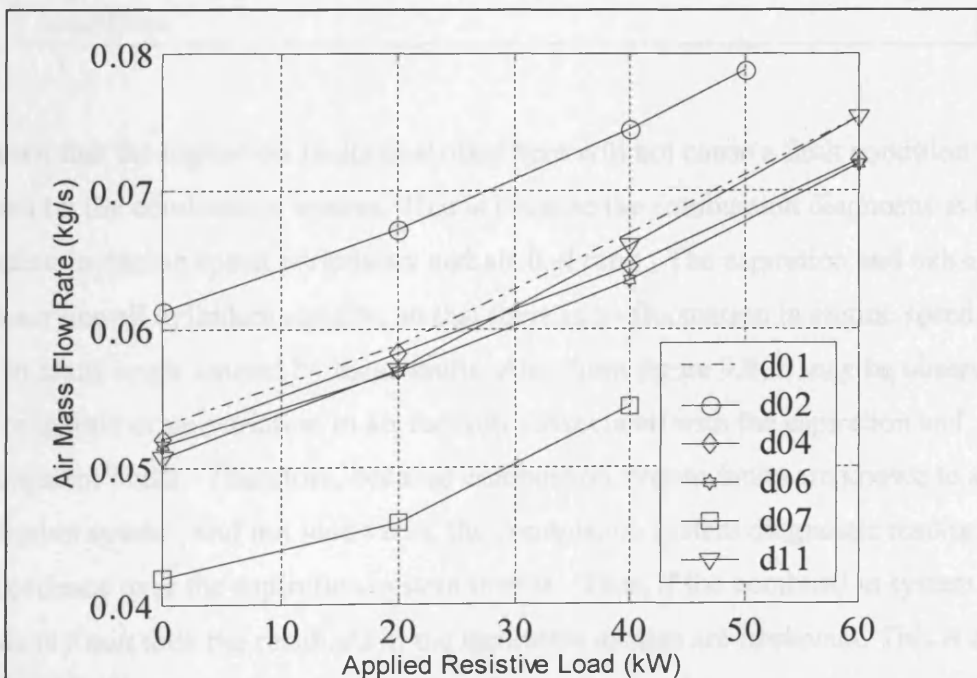
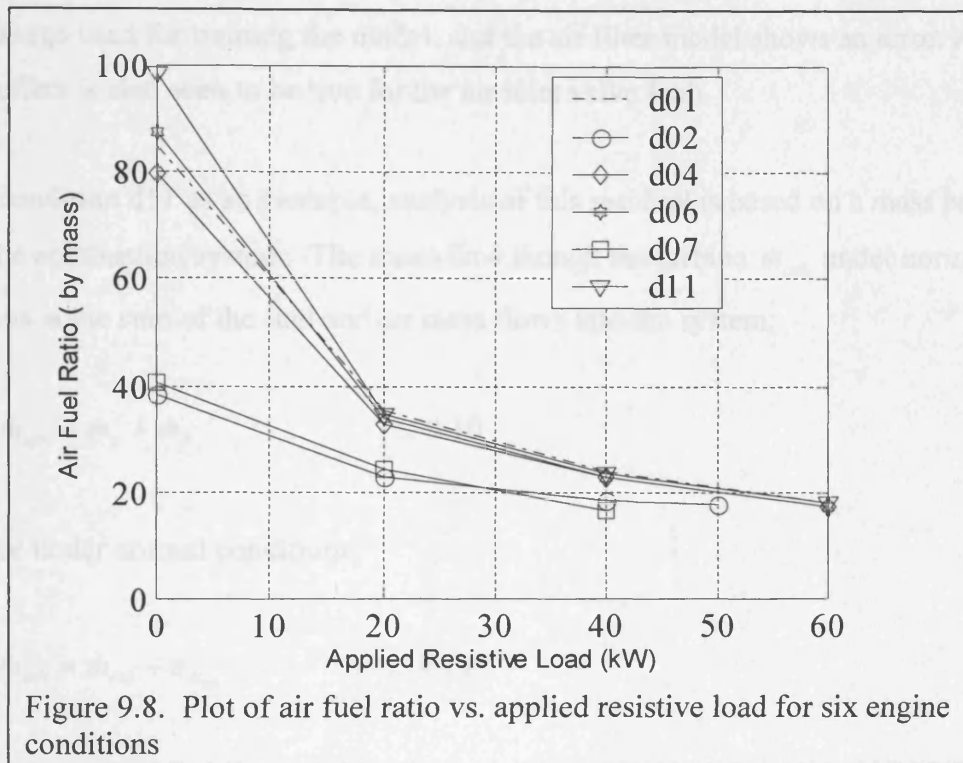


Figure 9.7. Plot of air mass flow rate vs. applied resistive load for six engine conditions



It is known that the aspiration faults described here will not cause a fault condition to be diagnosed by the combustion system. This is because the combustion diagnostic is based on variation in engine speed periodicity and air fuel ratio. The aspiration and exhaust systems service all cylinders equally, so that there is no fluctuation in engine speed with respect to crank angle caused by these faults. Also from figure 9.8, it may be observed that there is little or no variation in air fuel ratio associated with the aspiration and exhaust system faults. Therefore, because combustion system faults are known to affect the aspiration system, and not vice versa, the combustion system diagnostic results must take precedence over the aspiration system results. Thus, if the combustion system diagnosis is *Fault* then the residuals in the aspiration system are irrelevant. This is an important fact in defining the rules for fault diagnosis as problems may be caused due to the bounded nature of the fuzzy models in the system. For example, figure 9.7 showed how the combustion fault causes an increase in \dot{m}_a so that the air-flow rate is outside the

normal range used for training the model, and the air filter model shows an error. A similar effect is also seen to be true for the air inlet valve fault.

Taking condition d11 as an example, analysis of this residual is based on a mass balance across the combustion system. The mass-flow through the turbine \dot{m}_{exh} under normal conditions is the sum of the fuel and air mass flows into the system;

$$\dot{m}_{exh} = \dot{m}_a + \dot{m}_f \quad \dots 9.10$$

Therefore under normal conditions;

$$\hat{\dot{m}}_{exh} = \dot{m}_{exh} + \varepsilon_{\dot{m}_{exh}} \quad \dots 9.11$$

where $\varepsilon_{\dot{m}_{exh}}$ is the model error. Residuals have been defined as, $R = Y - \hat{Y}$, so in this case;

$$r_{\dot{m}_{exh}} = r_1 = \dot{m}_{exh} - \hat{\dot{m}}_{exh} + \varepsilon_{\dot{m}_{exh}} \quad \dots 9.12$$

Therefore, given that the normal classes have been defined to include the expected magnitudes of model error, it is clear that a residual in r_1 classified as *Positive, P*, by the fuzzy classifier indicates that;

$$\dot{m}_a + \dot{m}_f > \hat{\dot{m}}_{exh} \quad \dots 9.13$$

It is therefore inferred that mass is lost from the system bounded by the flow meters and the turbine, thereby providing a clear indication of a leak.

Therefore based on the knowledge of the physical systems, models and diagnostics the rules for fault detection and isolation in the aspiration and exhaust systems are listed in the table 9.3.

Table 9.3 Aspiration and Exhaust System Diagnostic Rules

Condition	Combustion System Diagnosis	Residual		
		r_1	r_2	r_3
d01. Normal	<i>Normal</i>	<i>Normal</i>	<i>Normal</i>	<i>Normal</i>
d02. Combustion fault	<i>Fault</i>	<i>any</i>	<i>any</i>	<i>any</i>
d03. Exhaust leak (outlet side of turbine)	<i>Normal</i>	<i>Normal</i>	<i>Negative</i>	<i>Normal</i>
d04. Exhaust restriction (outlet side of turbine)	<i>Normal</i>	<i>Normal</i>	<i>Positive</i>	<i>Normal</i>
d05. Air inlet leak (compressor side of filter)	<i>Normal</i>	<i>Positive</i>	<i>Normal</i>	<i>Positive</i>
d06. Air inlet restriction (blocked air filter)	<i>Normal</i>	<i>Normal</i>	<i>Normal</i>	<i>Negative</i>
d07. Air inlet valve fault.	<i>Fault</i>	<i>any</i>	<i>any</i>	<i>any</i>
d08. Exhaust leak (manifold side of turbine)	<i>Normal</i>	<i>Negative</i>	<i>Normal</i>	<i>Normal</i>
d09. Turbocharger fault	<i>Normal</i>	<i>Negative</i>	<i>Negative</i>	<i>Normal</i>
d10. Exhaust valve fault	<i>Fault</i>	<i>any</i>	<i>any</i>	<i>any</i>
d11. Air Inlet Manifold Leak	<i>Normal</i>	<i>Positive</i>	<i>Normal</i>	<i>Normal</i>

From the table, a fuzzy system has been generated to contain the diagnostic reasoning for each fault, using two rules. For example;

1. If (r_1 is *Normal*) and (r_2 is *Normal*) and (r_3 is *Normal*) then (*Normal*, *d01* is *True*)
2. If (r_1 is not *Normal*) or (r_2 is not *Normal*) or (r_3 is not *Normal*) or (*Normal*, *d01* is *False*)

9.6.3 CONCLUDING REMARKS

The diagnostic structure has been defined using *a priori* knowledge of the aspiration and exhaust systems and data readily available from running the engine in its normal condition. The resulting structure contains a three-stage process consisting of residual

generation, classification and reasoning, similar in structure to that presented in figure 7.2. The following section will test this structure with data obtained from a series of fault conditions which have been experimentally simulated on the engine.

9.7 ASPIRATION AND EXHAUST SYSTEM TEST RESULTS

A series of tests have been carried out to provide data with which to test the fuzzy model based diagnostic structure. The test conditions are those which are indicated to be practical in table 9.1. Table 9.4 provides a set of descriptions of the individual sets of fault data and the modifications to the aspiration and exhaust system components which have been made in order to obtain the data.

The data sets were obtained with the engine operated under a series of applied resistive loads, which were generally of the same profile as described in section 9.5 and figure 9.9. This load profile is intended to test the models with the engine running in steady state at full and part load, in response to step changes of varying magnitude, and also in response to a set of rapid step changes.

Table 9.4 Aspiration and Exhaust System Fault Data File Descriptions

Test No.	Filenames (.mat file)	Description	P_{amb} mmHg	T_{amb} °C
1	d01_t1_0112	Normal. Fault-free operation.	742.75	20.0
2	d01_t1_0712	Normal. Fault-free operation	745.45	20.5
3	d02_f1_1303	Combustion fault. Faulty injector (spring removed) cylinder 4. (See also fault description C1 in section 7.1)	743.30	22.0
4	d04_f1_3110	Exhaust restriction. 45mm diameter exhaust orifice plate. An orifice plate has been incorporated into the exhaust pipe-work, downstream of the silencer, reducing the internal diameter of the exhaust from 55mm. This raised the turbine outlet pressure at 60kW by 1%. and having no measurable effect on the boost pressure.	737.00	21.0
5	d04_f1_0111	Exhaust restriction. 35mm diameter exhaust orifice plate. With the exhaust system modifications as described above, the orifice size for this test was reduced to 35mm, This configuration had the effect of raising the turbine outlet pressure at 60kW by approximately 6% and consequently reducing the compressor pressure ratio by 1.6%.	736.40	18.0
6	d05_f3_3011	Air inlet leak. Air inlet vent 4x20mm at inlet to air flow meter. Four holes were cut into were cut into a specially fitted insert in	750.00	20.5

		the air inlet pipe-work between the air filter and compressor inlet to simulate an air inlet leak.		
7	d06_f3_2610	Air inlet restriction valve cap set to 14.3mm aperture A variable inlet valve with screw-down cap, was fitted to the inlet side of the air filter. In this test the air gap was set to 14mm increasing the measured filter pressure differential at 60kW load by 36 % from 0.0049 bar to 0.0067	753.25	21.0
8	d06_f3_2710	Air inlet restriction valve cap set to 4.25mm aperture. With the experimental arrangement as above, the air gap was set to approximately 4.25 mm, increasing the the filter pressure differential at 60kW load by over 500% from 0.0049 bar to 0.0025. Neither (test 7 nor test 8) of these inlet restriction valve settings caused a measurable reduction in measured air-flow rate.	749.00	20.0
9	d06_f4_2710	Intermittent air inlet restriction fault. The restriction valve cap was lowered to 4.25mm for 2 minutes each at 0kW load, 30kW load and 60kW load. Total test length was approximately 25 minutes.	749.00	21.0
10	d07_f1_0503	Inlet valve fault, cylinder 1 valve shimmed open (See also fault description C2 in section 7.1)	757.25	20.5
11	d11_f1_1511	Air inlet manifold leak: 7mm manifold vent. A threaded connection was fitted into the inlet manifold port normally used for the inlet air pre-heater, adjacent to the compressor outlet. The connection was fitted with a centre-drilled insert of vent diameter 7mm. This arrangement allowed a fraction of the induction air to escape. This caused a pressure drop of approximately 5% in the air inlet manifold at 60kW, and rendered the engine incapable of being step loaded from 0-60kW.	750.00	18.5
12	d11_f1_0112	Air inlet manifold leak: 3mm manifold vent. Arrangement as above with smaller vent diameter	742.30	22.0
13	d11_f2_0112	Air inlet manifold leak. Intermittent fault. The valve fitted to inlet manifold heater port was opened and closed. Maximum opening was restricted to 7mm. Valve opened for one minute at 0kW load, one minute at 30kW load and one minute at 60kW load. Total test length is 12 minutes.	742.30	22.0

There is some variation on the relative impact of the various test conditions on the engine. Some of the main effects are seen in the plots of air and fuel flow rates in figures 9.6 – 9.8 and described in the table 9.4. These plots show that the fault conditions had little effect on the ability of the engine to produce sufficient power to meet the applied load. The most significant fault was the air inlet manifold leak, with the orifice diameter set to 7mm. This fault slowed the rate at which boost pressure could be built up in the manifold and prevented the engine being step loaded from 0 to 60kW although full power could be attained by incrementally increasing the load with smaller steps.

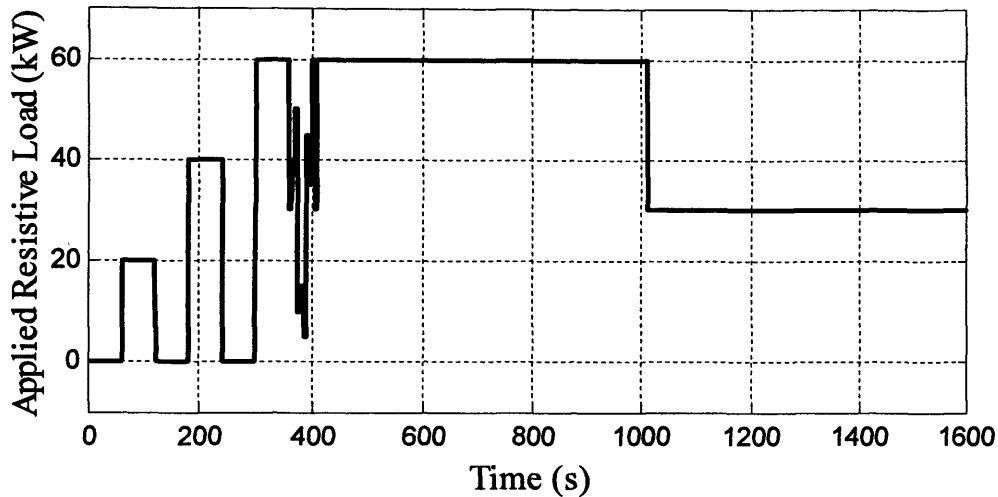


Figure 9.9. Aspiration and exhaust system diagnosis tests: Typical profile of typical applied resistive load.

A total of thirteen data sets have been used in testing diagnostic systems. The results are shown in a confusion matrix, table 9.5. The test numbers in column 1 of table 9.5 correspond to the test numbers for the fault descriptions given in table 9.4. The rows of this matrix contain the data for a given test whilst the columns contain the outcome of the diagnostic reasoning, expressed as a percentage of the sampled data points. Thus, the success rates for correct diagnoses of the various conditions are highlighted along the leading diagonal of the matrix. The conclusion of the diagnostic reasoning is defined as the outcome indicated by the maximum value of the diagnostic vector, $\max(D)$, where D is as defined in section 7.4, and illustrated in figure 7.2

Where practical, some fault conditions have been applied intermittently i.e. the fault is simulated and the system subsequently returned to the normal condition. An example of this is presented graphically in figure 9.10, showing how the diagnosis result changes from normal, d01, to air inlet manifold fault, d11, as the residual classification changes, with the diagnosis subsequently returning to normal after the fault is removed.

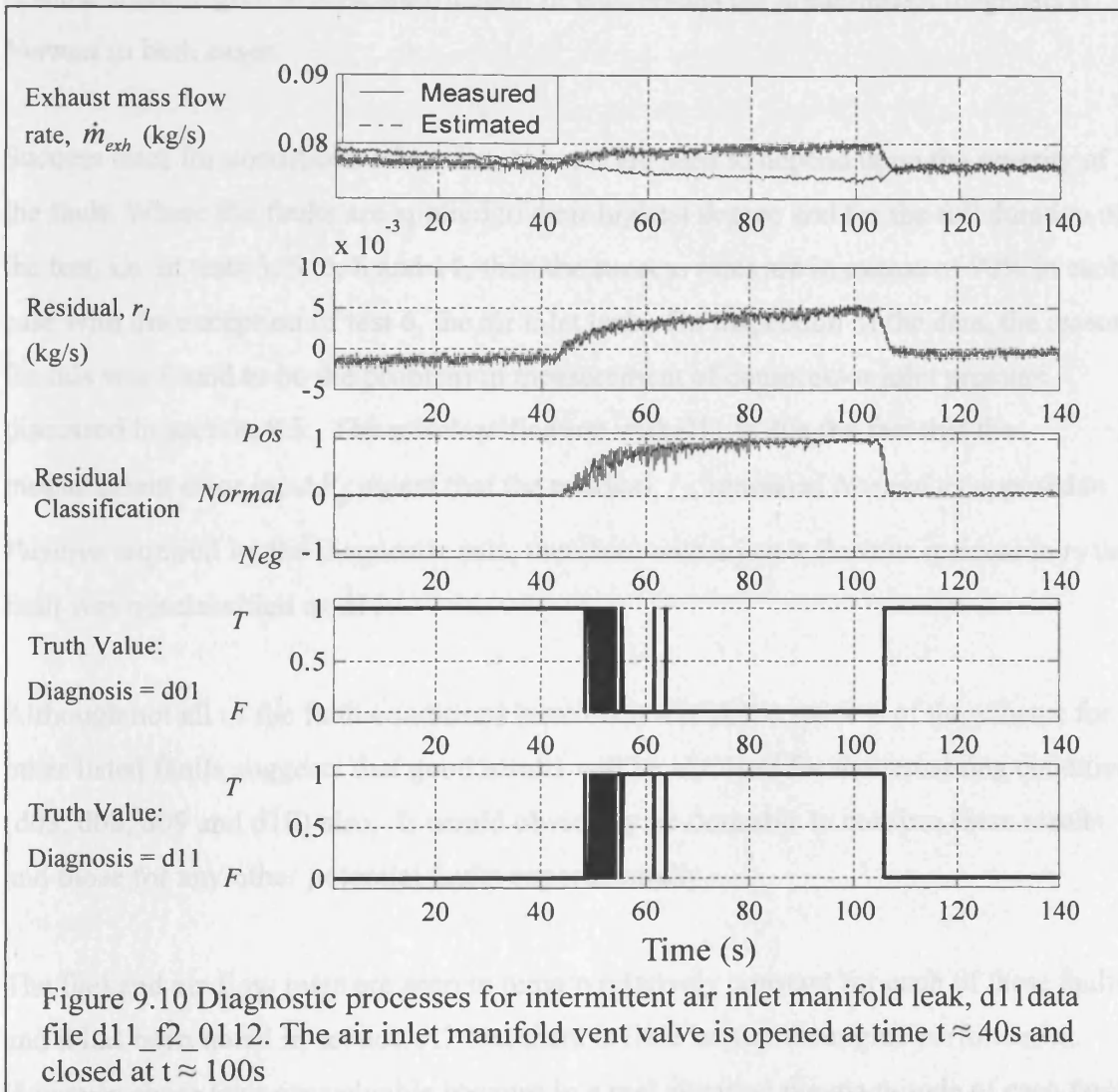
Table 9.5. Aspiration and exhaust system test results confusion matrix.

Test No.	Condition	Diagnosis (% of sample data points)						
		d01	d02	d04	d05	d06	d07	d11
1	d01	96.2	0.0	0.7	0.0	0.0	0.0	3.0
2	d01	96.4	0.0	0.1	0.0	0.15	0.40	2.9
3	d02 ¹	0.0	99.3	0.0	0.1	0.6	0.0	0.0
4	d04	14.6	0.0	60	0.0	24.2	0.0	0.6
5	d04	0.0	0.0	100	0.0	0.0	0.0	0.0
6	d05	1.6	0.0	0.1	21.4	0.0	0.0	76.9
7	d06	57.5	0.0	0.1	0.0	41.5	0.0	0.8
8	d06	0.1	0.0	0.0	0.0	99.9	0.0	0.0
9	d06 ²	62.6	0.0	3.2	0.0	25.9	0.0	8.2
10	d07 ¹	0.4	0.0	6.6	0.0	0.0	92.9	0.0
11	d11	0.0	0.0	0.0	0.0	0.0	0.0	100
12	d11	90.8	0.0	4.6	0.0	0.2	0.0	4.4
13	d11 ²	86.7	0.8	3.8	0.0	0.0	0.4	8.3

¹Assuming combustion diagnosis system gives results as per table 7.1, i.e. 99.3 % of sample data diagnosed as combustion fault or inlet valve fault and 93% of sample data correctly diagnosed as an inlet valve fault.

² Data file shows intermittent faults.

The effects of the combustion system faults, d02 and d07, are classified taking into account the reported diagnosis success rates from the combustion system (see table 7.1). The fact that these success rates are generally not 100% leaves some room for misclassification by the aspiration and exhaust system diagnosis.



9.8 DISCUSSION

The confusion matrix in table 9.5 shows that the diagnosis success rates are generally good. One key ability of any diagnostic system is to correctly indicate when the system is in its normal condition and thereby to minimise the rate of false alarms or *false positive* diagnoses. The confusion matrix shows that for the two sets of normal condition data the false positive rate is less than 4%. The intermittent faults in tests 9 and 13 have fault durations of approximately 24% and 25% of total test time respectively. Although there

is some small degree of misclassification in both results the predominant diagnosis is *Normal* in both cases.

Success rates for conditions other than *Normal* are seen to depend upon the severity of the fault. Where the faults are applied to their highest degree and for the full duration of the test, i.e. in tests 3, 5, 6, 8 and 11, then the success rates are in excess of 90% in each case with the exception of test 6, the air inlet leak. On inspection of the data, the reason for this was found to be the problem in measurement of compressor inlet pressure discussed in section 9.5. The misclassification with d11 is due the fact that the measurement error in, ΔP_{af} meant that the residual, r_3 , remained *Normal* as opposed to *Positive* required by the diagnostic rule, therefore with a just a *Positive* residual in r_1 the fault was misclassified as d11.

Although not all of the fault conditions have been tested, the success of the scheme for other listed faults suggests that good results will be obtained for the remaining conditions (d03, d08, d09 and d10) also. It would obviously be desirable to confirm these results and those for any other potential faults experimentally.

The fuel and air-flow rates are seen to remain relatively constant for each of these faults and it has been noted in section 9.7 that there is little impact on engine performance. However, these tests are valuable because in a real situation the magnitude of each fault has the potential to increase, for example by further blockage of filters or exhaust. Thus the tests have shown that the fuzzy systems are capable of detecting the faults before serious consequences occur.

It should be emphasised that the results obtained in these tests have been obtained from a diagnostic using only *a priori* knowledge and normal data. Therefore it is suggested that diagnostic rates could be further improved if fault data had been used in the design. For instance the thresholds between normal and fault data could have been further optimised

to increase the sensitivity of the diagnostic system. However restricting the design process to use of normal data only, demonstrates a benefit of fuzzy systems over other forms of classifier, which need data from the various fault conditions for training. In other cases, where such extensive *a priori* knowledge is not available for definition of diagnostic reasoning, it is suggested that a diagnostic system with a more general output consisting of two classes, *Normal* and *Not Normal* could be designed.

The fact that the fuzzy models for state estimation and prediction are not necessarily robust to faults in other parts of the system infers that they may only be suitable for fault diagnosis and isolation of small perturbations from the *Normal* class. However for a more serious fault, the lack of robustness means that values for R would be uncertain. Approaches to dealing with this robustness problem have been dealt with in preceding chapters. One approach is to define an *Unknown* class to include unknown combinations of residuals such as that developed in the combustion system diagnosis (see section 8.5). Similarly a *Model Error* class could be incorporated to accommodate unfeasibly high values (see section 7.4).

The problem caused by the lack of robustness in the models can be overcome in certain cases if sufficient knowledge is available to predict the behaviour of the systems. For instance the diagnostic rules for condition d05 in table 9.5 show that for diagnosis d05 to be true, positive residuals must exist in r_1 and r_3 . This is because the compressor has to do less work to overcome the flow resistance normally offered by the filter, therefore the air mass flow rate is greater than would be expected for the pressure ratio across the turbine. The pressure ratio is an input to the turbine mass flow rate estimator, resulting in an underestimate of the mass flow rate and the generation of a residual in r_1 . Similarly a fall in turbocharger mechanical efficiency will result in an over estimation of \hat{m}_{exh} as \hat{m}_a will be reduced for a given pressure ratio. Therefore, the $\Delta\hat{P}_{af}$ will also be an overestimate resulting in a *Negative* classification for residual, r_2 . However, suitable *a priori* knowledge is not always available. For instance the effects of the combustion and

inlet valve faults cause input values to migrate outside the valid input ranges of the fuzzy models, therefore residuals are unpredictable.

The use of the estimated value, \hat{m}_{exh} , as an input for the exhaust differential pressure model means that the differential pressure, ΔP_{eo} , may be predicted without the need for a second mass flow meter in the exhaust. The mass flow rate could of course be obtained directly from $\dot{m}_a + \dot{m}_f$, however the model would then clearly not be robust to leaks in the system. Hence, the complexity of the diagnostic reasoning would need to be further increased, in that the rules for classification of the leak conditions would need to take account of the residual in r_3 .

The use of energy and mass balances as the basis for the diagnostic logic employed here has proven to be an effective approach. It is also postulated as an afterthought that the mass balance approach could detect coolant leaks into the combustion system or leaks from the fuel system. In the case of the coolant leak a small ingress of coolant via the head gasket, into the cylinder would then be emitted from the exhaust system as steam causing a *positive* residual in r_1 and r_2 . In the case of the fuel leak the engine controller would increase the rate of fuel supply to the engine but the airflow rate would stay constant therefore the air fuel ratio would change indicating a fault in the combustion system diagnosis. Thus the symptoms in the aspiration system would again be a *positive* residual in r_1 and r_2 . The location of the fuel leak would also have implications for the diagnosis. If the leak were upstream of the distribution pump, then there would be no effect on the periodicity of the speed signal, whereas a leak between the pump and the injectors would cause a reduction in the performance of an individual cylinder and hence affect the periodicity of the speed signal. These two additional faults serve to emphasise the need for firstly, a more rigorous cause-effect analysis of the system and its interactions with other engine systems, and secondly, the need for a 'catch-all' *Unknown* fault class, as previously discussed, to indicate unknown combinations of residuals.

A fuzzy technique for estimation of confidence in the fuzzy model outputs has been incorporated in the coolant system diagnostic. However this has not been attempted for this system as the scheme depends on the availability of model errors for training the fuzzy confidence estimators. This is a problem due to the fact that training errors from the air filter model are compounded with the measurement errors in compressor inlet pressure discussed in section 9.5. The measurement errors have a dynamic nature associated with the heating of the connecting pressure pipe-work, therefore an identification of a relationship between input values and model errors gave very poor results.

A further issue in identifying the air inlet filter model is raised by the fact that the input variables are dependent on ambient conditions. Therefore input variables may prove difficult to control in certain environments, i.e. anywhere where climate control is not available. Elsewhere, if the systems designer is restricted to training a given model from data, then the model will only be valid over the range of ambient conditions experienced during the course of the test. This has not proved to be a problem during the course of the case study due to the fact that the laboratory conditions are quite similar (see table 9.4) and also the fact that the modelled variables are differential pressures dependent on mass flow rates rather than absolute pressures values. However should such a model be required to work over a wider range of temperature then suitable correction factors or theoretical extrapolation would be required for the input variables. For instance in this case, available information for the relationship between ambient air conditions and density could be incorporated into the model.

Although Molteburg [Molteburg 91 pp96] proposes techniques for condition monitoring of a number of engine components based on parameter estimation, results are not presented for estimation of air filter or turbocharger parameters. Other components are successfully diagnosed, however certain parameters are found to be load dependent and therefore testing is only carried out at fixed loads and speeds and therefore parameters

may only be valid around certain operating points for the engine. The results from these tests show that in comparison with parameter estimation process undertaken by Molteburg, these fuzzy techniques offer benefit in terms of their application to an on-board systems, in that good results are obtained from a wide range of applied loads in both steady state and transient conditions.

9.9 CONCLUSIONS

A fuzzy model-based CMFD system has been developed for the aspiration and exhaust system of the diesel generator set test bed. The diagnostic system has been based on *a priori* knowledge of the engine systems and components, and easily obtainable data from the engine running in its normal fault-free condition.

The CMFD system has been tested with a total of 13 test data sets comprising 7 separate engine conditions. The success rate of the diagnostic is seen to exceed 90% of samples in 7 of the 13 test sets of test data, (test data sets 1,2,3,5,8,10,11). In two sets of test data (sets 9 and 13) intermittent faults were applied to the engine, and the test results are seen to reflect the change in operating condition. In a further three tests (4,7,12) the magnitudes of the applied faults were reduced below the sensitivity of the diagnostic system, and the proportion of samples diagnosed as faults to the proportion of samples diagnosed as normal was reduced.

One set of test data (6) was found to have a 76.9% misclassification rate. This was explained to be problem in the measurement of compressor inlet pressure.

None of the aspiration or exhaust system faults was found to have a significant impact on the performance of the engine, though the largest air inlet manifold leak imposed reduced the rate at which the resistive load could be applied. Therefore, the high success rates in these tests have shown that the fuzzy systems are capable of detecting the faults before serious consequences occur.

Robustness of the fuzzy models used in this diagnostic system has been discussed. The models have been found to be generally effective at generating residuals where deviations from the normal condition are small, though for larger deviations robustness of models is not guaranteed or expected. In some cases this lack of robustness may be predicted and compensated for by inclusion of additional diagnostic rules. However in other cases model outputs are unpredictable, which, given the high success rates for diagnosis of the normal condition, could still be used to produce a less detailed diagnosis. i.e. instead of a detailed description of the fault e.g. '*Air inlet manifold leak*', the level of detail is reduced to '*Not Normal*'.

Combustion system faults were found to have a significant effect on the aspiration and exhaust systems; therefore cross-referencing of diagnostic results was a necessity in order to effectively identify faults occurring in a component of the aspiration or exhaust system.

The process of producing a comprehensive cause and effect analysis for faults in such interactive sub-systems is a complex task. The fact that two further fault conditions have been postulated subsequent to completion of the test work, suggests that a more rigorous approach to this analysis task should be adopted for future work.

SECTION 3.
Analysis of the results
from the case study

CHAPTER 10.

Discussion

10.1. INTRODUCTION

A wide-ranging review of condition monitoring and fault diagnosis has been undertaken in chapter 1, establishing the need for effective on-board CMFD. Typical knowledge sources for diesel engine fault diagnosis comprise systems models for parameter and state estimation, along with techniques for data classification and reasoning. The literature review has also shown that fuzzy systems are a possible common methodology for implementing systems in each of those areas, and are therefore worthy of more detailed evaluation.

A more detailed study of theory relevant to the design and application of fuzzy systems is carried out in chapters 2, and 3. Chapter 4 presented a review of techniques for identification and training of fuzzy models, recommending that the chosen techniques for identification should also aim to capitalise on the advantages offered by fuzzy systems for grey-box modelling, allowing the systems designer opportunity to incorporate *a priori* knowledge of the physical system being modelled.

Chapter 5 set out the motivations and objectives for the diesel engine case study, summarising the properties of fuzzy systems with respect to their proposed role in fault diagnosis. Fuzzy systems were shown to be capable of representing non-linear systems where detailed knowledge of the physical system being modelled is not a pre-requisite. The assumption was stated that suitable training data will be available from testing of the engine in its normal fault free state, however training data for certain fault states may not be available. The rule-based format of the fuzzy systems allows the relationships between the inputs and outputs to be easily visualised with the benefit that diagnostic results may be easily interpreted. The chief disadvantage of fuzzy systems identified from test data is that they are by their nature empirical and no guarantees can be made about their robustness or generality. Therefore in terms of reference model development for CMFD, it was hypothesised that fuzzy systems may be most effectively applied in modelling a specific class of systems where the input states are constrained within certain bounds, even under fault conditions.

Given the stated need for on-board CMFD systems, combined with the inherent qualities of fuzzy systems, a case study was proposed to develop fuzzy model-based CMFD systems as knowledge sources using a diesel generator set as an appropriate test case. This evaluation of the role of fuzzy systems in CMFD is designed to assess their capabilities as a common methodology for state estimation, classification, and reasoning.

Chapter 6, described the experimental arrangements for the test-bed, setting out a justification of the approach to development of the CMFD systems and division of the engine into sub-systems. The issue of instrumentation, data acquisition and signal processing was also addressed. Chapters 7, 8 and 9 present results from the development of fuzzy model-based CMFD systems from the cooling, combustion, aspiration and exhaust systems respectively.

This chapter will discuss the results obtained in chapters 7, 8 and 9 in terms of the aims and objectives of the case study. The discussion is divided into two sections, the first dealing with general issues concerning use of fuzzy systems in CMFD and the second with results specific to the diagnosis of faults in diesel engine systems.

10.2. APPLICATION OF FUZZY SYSTEMS IN CMFD.

The following section contains a discussion of fuzzy systems and their application in CMFD with reference to the results presented in chapters 7, 8 and 9, along with comparable studies or relevant studies by other researchers. Fuzzy systems used in the study have been applied as a common methodology in three distinct roles, as models or state estimators, as classifiers and in reasoning processes.

A common structure for fuzzy model-based CMFD has been employed with some degree of success in all of the diesel engine systems considered in the study. The structure consists of residual generation by comparison of measured states with the output from appropriate reference models or state estimators. The residuals are then classified into a number of fuzzy sets defined in terms of the magnitude and sign of the residual. Each sub-system is monitored using a number of reference models, thus a vector of residuals is formed. The pattern of the residuals contained within this vector is analysed by a diagnostic reasoning process, consisting of a number of fuzzy systems containing rules which associate the pattern of residuals with a linguistic variable representing a number of possible diagnoses which have been identified for the system.

The fuzzy model structures employed have not been subjected to rigorous analysis or comparison. The models and estimators have all been trained using the ANFIS algorithm in Matlab™ with appropriate data vectors. The fuzzy model structures employed have been of the *Sugeno* type as defined in section 7.2, with ‘generalised bell’ input membership functions. The output membership functions are first order linear functions of the inputs. Where the fuzzy system represent a relation, $y=f(x)$, then first order linear output membership functions are an intuitively appealing approach. Use of the first order output membership functions allow *weighted average* defuzzification which offers benefit in computational cost. The function for the fuzzy set-operator *AND* (the *t-norm*) has been defined to be the product operator. As noted in section 3.2.2.4 this is intuitively appealing because use of the product *t-norm* allows the membership value of all fuzzy sets in the premise to influence the outcome. Comparison of checking data results obtained from the training of two versions of the exhaust mass flow estimator

(section 9.4.2) using the *min* and *product* t-norms showed that the product operator gave marginally better results with mean and standard deviation of errors of -0.4% and 1.7% respectively (using formula given in equation 9.10). This is compared with a mean and standard deviation using the *min* t-norm of -0.5% and 1.8% respectively. It is concluded that this similarity in results should be expected where systems are trained from data using an error-based objective function, as the fuzzy systems parameters will be adapted to compensate for any differences in the structure. With the exception of the recursive thermostatic valve model all systems employed have been designed with a feed-forward structure.

The application of fuzzy systems as models, classifiers and in the diagnostic reasoning process will be considered in the following sections.

10.2.1 AN ASSESSMENT OF FUZZY SYSTEMS AS MODELS OR STATE ESTIMATORS

A number of different fuzzy models and state estimators have been employed as appropriate in the three diesel engine subsystems. Fuzzy systems have been successfully used to approximate non-linear relations, for example;

- i) As an estimator coolant flow rate through the thermostat valve (see section 7.5), from appropriate temperature measurements.
- ii) As an estimator engine load, based on power spectral density of speed signal (see section 8.2.1).
- iii) As an estimator for mass flow rate through a turbine based on the pressure and temperature measurements (section 9.4.2)
- iv) A recursive fuzzy model has been used to predict coolant flow rate through the thermostat valve with respect to temperature; a highly non-linear system exhibiting hysteresis (see section 7.5).
- v) Time-series models incorporating appropriate delays in the inputs have been employed to predict periodic fluctuations in speed and boost pressure signals with respect to crank angle (see sections 8.4 and 8.5).

The use of the coolant flow rate estimator in conjunction with the recursive fuzzy model provides a good example of the benefit of the capacity of fuzzy models for the incorporation of heuristics. Knowledge of the heat transfer model for the cooling system allowed an approximate expression for the coolant flow rate as a non-linear function of three temperature measurements to be written (equation 7.10), based on an energy balance through the sub-system. Observation of the test data showed that this relationship does not hold in all engine conditions, specifically when the thermostat valve is closed, due to a change in mode of heat transfer one of the temperature transducers. Therefore in order to improve the performance of the estimator the following simple rule was added to the system;

If the temperature difference across the radiator is not *Zero*, then the thermostat valve is *Open*.

where *Zero* is appropriately defined as a fuzzy set.

This demonstrates the way in which fuzzy systems may be used to complement mathematical techniques. Firstly, the mathematical relationship is only approximate as the heat balance was based on a number of assumptions concerning heat losses and fluid properties. Secondly, to mathematically model the change in mode of heat transfer to the temperature transducer in this example is a difficult task. Therefore, the task of developing a mathematical model of this relationship is difficult and prone to error due to the assumptions involved. Incorporation of the approximate mathematical relation and the general rule for thermostat valve position, allows an effective estimator to be produced relatively easily by training the fuzzy system with appropriate data.

The thermostat valve exhibits hysteresis and whilst this is a useful property allowing smooth operation of the valve, it poses a challenging prediction problem, due to the fact that the relationship of inputs to outputs is not one-to-one over the full range of inputs. The recursive fuzzy model for prediction of coolant flow rate is shown to provide an

effective solution to this problem. Once again the incorporation of heuristics was found to be beneficial, in this case to improve the stability of the model by incorporation of additional membership functions.

Comparison of the outputs from the coolant flow rate estimator and model allow a residual to be generated. The benefit of this approach is clearly that the operation of the valve can be monitored based on output signals from three temperature transducers only. Compared with fitting a turbine flow meter into the cooling system, this has benefit in terms of cost and practicality. The turbine flow meter is a costly and intrusive instrument for flow measurement, which may only be conveniently fitted between the thermostat valve and the radiator. Coolant temperature is usually measured at the outlet from the engine block to provide a warning of over heating, thus only two temperature transducers are required in addition to the normal set to provide a diagnosis. Further to this, the set of temperature transducers would be required irrespective of the fitting of the turbine flow meter, or any other direct flow measurement technique, for condition monitoring of the radiator.

Therefore the development of the fuzzy models for CMFD of the thermostat valve has met the objectives of the case study in the following ways;

- i) A fuzzy model has been developed, based on acquired data and heuristics, capable of predicting outputs from a highly non-linear system exhibiting hysteresis.
- ii) A state estimator has been developed, exploiting an approximate non-linear mathematical relationship, and incorporating a simple heuristic to improve the estimation performance.
- iii) Comparison of the outputs from these fuzzy systems provides valuable information for condition monitoring thermostat valve operation in the diesel engine test-bed.
- iv) The model and estimator are based on signals from a small number of low cost transducers.

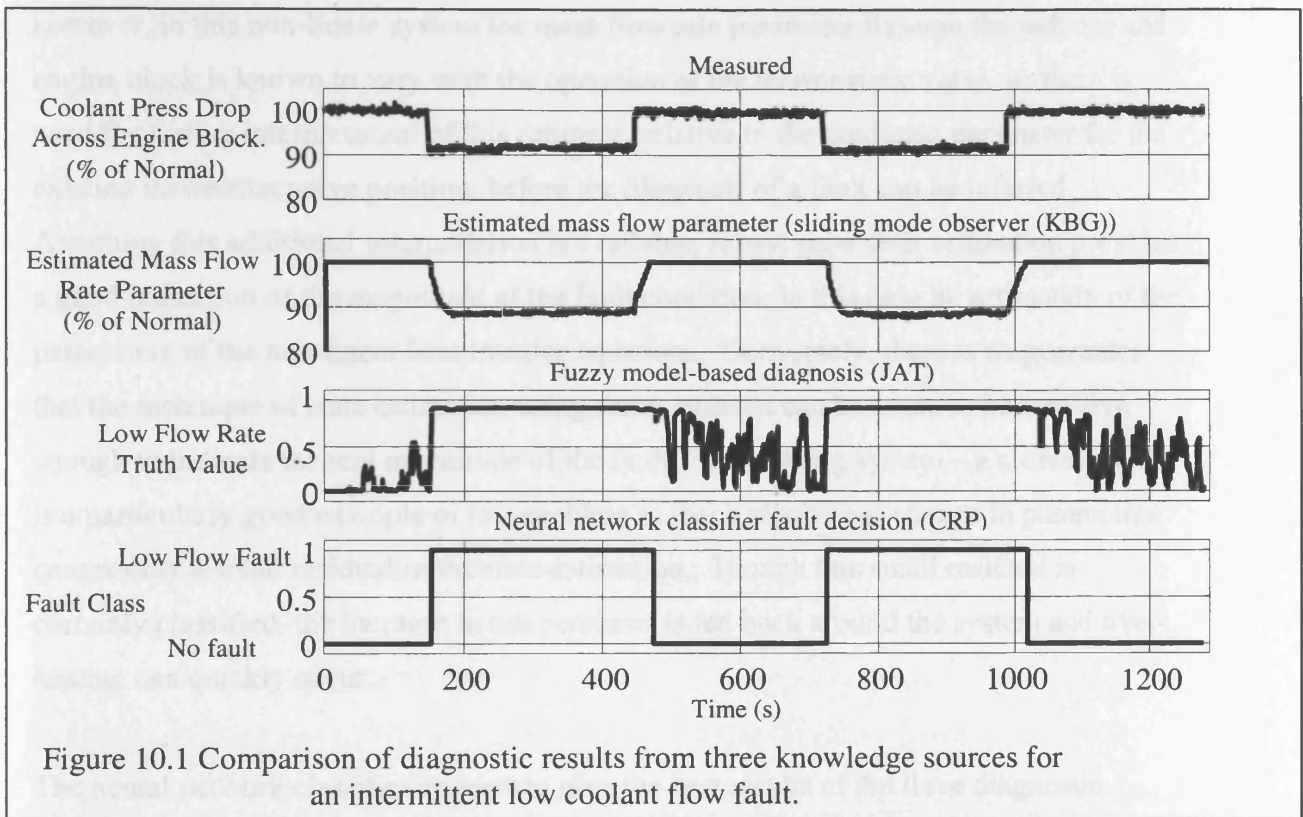
A number of similar examples where fuzzy models and estimators have been employed to meet these objectives have been presented in chapters 7, 8 and 9. For example, the speed and boost pressure reference models proposed in chapter 8 to detect fluctuations in the periodicity of the engine speed and boost pressure caused by faults in individual cylinders and inlet valves respectively. Frequency domain analysis of fluctuations in the speed signal provides a low-cost estimate of applied generator set load. Pressure and temperature measurements at the inlet and outlet of the turbine provide an alternative to the addition of a mass flow meter in indicating exhaust mass flow rate.

10.2.2 A QUALITATIVE COMPARISON WITH OTHER TECHNIQUES FOR MODELLING AND STATE ESTIMATION

It is valid to question whether fuzzy systems offer any benefit over other approaches to encapsulating diagnostic knowledge about the subject system. Although this thesis does not aim to rigorously compare knowledge sources for fault diagnosis, the opportunity to undertake a small study comparing results from three different techniques has been taken. Based on this study and relevant results by other researchers, this section will discuss the benefits or otherwise in the use fuzzy systems for fault diagnosis applications.

A variety of fault diagnosis techniques have been described in Chapter 1, section 6. Fuzzy systems have been compared with two of these techniques, namely a neural network classifier and a sliding mode observer-based approach, in a diagnostic scheme designed to directly compare their performance in fault diagnosis using the same test data. The results are used to highlight some of the qualitative differences between the individual techniques [M.o.M.'s 27/07/2000].

The data obtained is from the cooling system and the applied low flow fault condition is described in section 7.9. The fault condition was applied intermittently to the system by opening and closing a bypass valve. A plot of differential pressure provides an indication of the change in coolant flow rate through the engine created by operation of the valve. Results are plotted in figure 10.1.



The first point which is obvious from figure 10.1 is the fact that the diagnostic outputs from different techniques are each in a different form. This is because of the nature of the techniques. The sliding mode observer technique is described in detail by Bhatti et al [Bhatti 99]. The model parameters are assumed constant and any change in parameters may then be expressed as a function of the discontinuous signal which is used to maintain the sliding mode condition. Therefore, a robust parameter estimation is obtainable on-line from the observer. The neural network classifier technique applied on this example, [Parikh 98] has been developed using training data previously obtained by running the engine in a number of fault conditions (including this one) and the normal condition. The fuzzy model-based system is as described in chapter 7, based on prediction and estimation of system states. Thus, the three techniques are fundamentally different in their approach to the fault diagnosis; yet figure 10.1 shows that each is capable of some degree of success in diagnosing the fault condition.

The sliding mode observer produces a good estimate of the mass flow rate parameter, however, in this non-linear system the mass flow rate parameter through the radiator and engine block is known to vary with the operation of the thermostatic valve, so there is need for further interpretation of this estimate, relative to the predicted parameter for the existing thermostat valve position, before the diagnosis of a fault can be inferred.

Assuming this additional interpretation is available, robust parameter estimation provides a good indication of the magnitude of the fault condition; in this case by estimation of the parameters of the non-linear heat transfer equations. Conversely, there is no guarantee that the technique of state estimation using fuzzy systems can be made to be sensitive enough to indicate the real magnitude of the fault. The cooling system – a closed cycle – is a particularly good example of this problem in that a significant change in parameters causes only a small residual in the state estimation. Though this small residual is correctly classified, the increase in temperatures is fed back around the system and over-heating can quickly occur.

The neural network classifier appears to give the best results of the three diagnostic systems. However the chief disadvantage is that data must be obtained from the fault condition to train the network, also the fault class is defined for the specific magnitude of the fault, i.e. a 10% flow reduction, so additional data must be acquired to broaden the range of fault magnitudes which may be successfully diagnosed. It has also been noted that both fuzzy systems and neural networks are universal approximators and are functionally equivalent. Therefore it is expected that a fuzzy classifier designed with similar training data could perform equally well in terms of the diagnostic process, although the curse of dimensionality associated with fuzzy systems may mean that the neural network is more computationally efficient.

The low coolant flow example shows that each technique is capable of producing good results, in their respective formats, given that sufficient information is available for the development of each individual technique. In this case the required information is a mathematical model, used in the design of the sliding mode observer, normal data and appropriate heuristics for the fuzzy system and normal and the fault condition data from

the neural network. Therefore it may be concluded that the choice of technique for a given system depends on the type of information available and/or the nature of the desired output.

The amount of effort required in design and development of knowledge sources for the CMFD system is also an issue. The work involved producing the systems in the context of a research project is not necessarily a good indicator of the costs associated with producing the systems commercially. Certain tasks will only need to be undertaken in the first instance such as development of models and diagnostic structures. Once these have been generated the task is one of estimating parameters of the system and tuning or calibrating the system as appropriate for the subject plant. The estimate of initial parameters for fuzzy or mathematical models is a relatively straightforward process which could be based on the normal performance testing of the system. However, the acquisition of fault data for training of classifiers would require a more specialised program of testing involving experimental simulation of the target faults. In a comparison of black box modelling techniques, Laukonen [Laukonen 95] compares the use of dynamic fuzzy models of engine systems with the results obtained from a non-linear auto-regressive moving average (NARMAX) model structure. The conclusion was drawn that the techniques gave similar results but that the general approach to fuzzy system identification was more straightforward and reduced the cost in terms of development time. This finding is supported by comparison of the fuzzy system identification for the radiator in chapter 7, with the development of a non-linear radiator models and estimation of parameters presented in appendix 3. A substantial amount of mathematical analysis is required for non-linear model development and estimation of a large number of parameters describing the various fluid properties of air and coolant. Whilst some knowledge of the physics of the heat-transfer was necessary for production of the fuzzy model, once suitable inputs and outputs for the system had been finalised then the model identification process was relatively straightforward.

It is important to reiterate that fuzzy systems are not a unique solution to any of the modelling and estimation applications which have been produced. The functional

equivalence between neural networks and fuzzy systems has already been discussed as has their application in fault diagnosis. The structure of the recursive fuzzy model employed to predict the flow rate through the thermostat valve, for instance, is comparable with the neural network structures proposed for output prediction in systems with backlash proposed by Schenker and Agarwal [Schenker 98].

Comparison of the use of the fuzzy system with the use of a look-up table to estimate the applied resistive load on the generator set from the air-fuel ratio shows the benefits of the filtering effects of fuzzy mappings noted in section 3.2.1. The look-up table used in the example is based on a first order linear interpolation of the data points used for training the fuzzy system, with the mean values of the data points calculated for 10kW load intervals. The results obtained from this comparison are shown in figure 10.2. The air fuel ratio is noted to be a noisy signal particularly due to measurement errors in the fuel flow rate. The mean and standard deviation of the fuzzy estimation error are 0.72kW and 4.02kW respectively compared with 4.4kW and 8.3kW for the look-up table estimation. The fuzzy mapping is seen to reduce transmission of this noise, particularly at low applied loads where the inherent signal noise means that a many-to-one mapping is more appropriate than a linear interpolation. Training a fuzzy system to represent this mapping is therefore an appropriate solution.

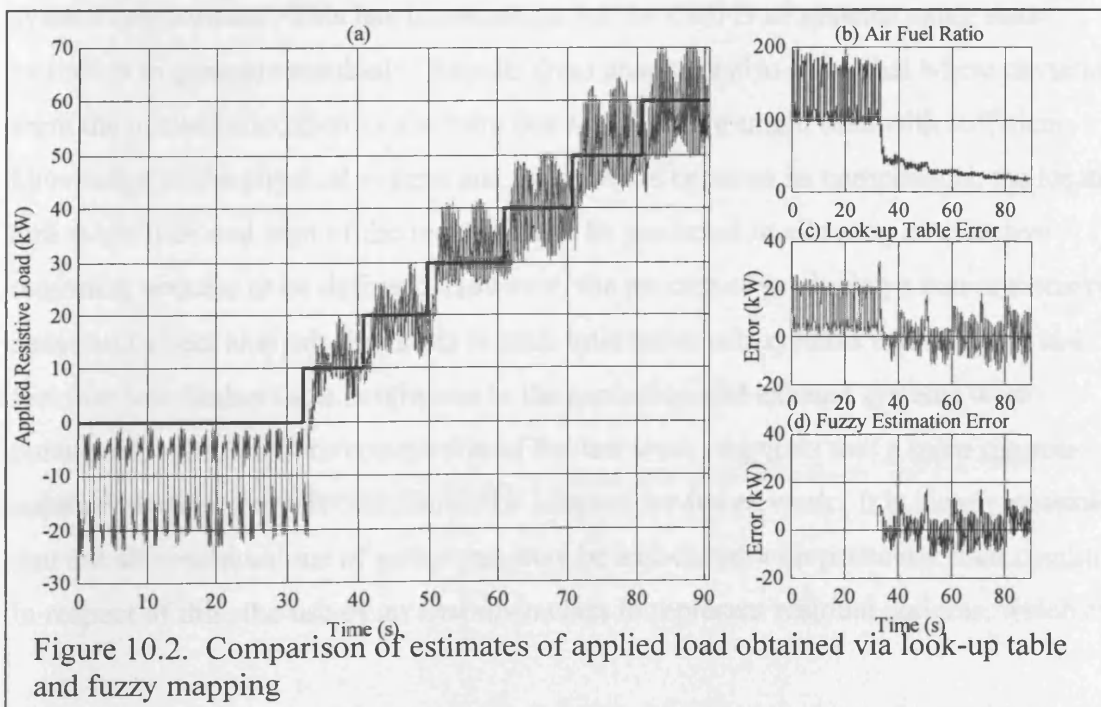


Figure 10.2. Comparison of estimates of applied load obtained via look-up table and fuzzy mapping

10.2.3 ROBUSTNESS ISSUES IN FUZZY MODELS FOR CMFD

The robustness of fuzzy systems is a key question in their use as models and state estimators. With some understanding of the nature of fuzzy systems, it is clear that robustness can neither be guaranteed nor expected outside the range of the training data because of the bounded nature of the input space, and the fact that identified models are only empirically validated by use of checking data.

The issues raised by these limitations have implications for the use of fuzzy models for residual generation by state estimation in multi-component systems, for example the aspiration and exhaust system as reported in chapter 9. The results presented in this chapter show that fuzzy models were found to be generally effective at generating residuals where deviations from the normal condition are small, though for larger deviations robustness of models is not guaranteed or expected. Certain faults cause symptoms which affect the system in such a way that deviations from the normal condition were large, and the reliability of fault inference based on model outputs was therefore lost.

In a multi-component system, faults in one component may affect the states of other system components. This has implications for the CMFD of systems using state estimates to generate residuals. Results from chapter 9 also show that where deviations from the normal condition in a system due to a fault are small, then with sufficient knowledge of the physical system and interactions between its components, the location and magnitude and sign of the residuals can be predicted in allowing an effective reasoning process to be defined. However, the process of producing a comprehensive cause and effect analysis for faults in such interactive sub-systems is a complex task. The fact that two further fault conditions in the aspiration and exhaust systems were postulated, subsequent to completion of the test work, suggests that a more rigorous approach to this analysis task should be adopted for future work. It is clearly possible that not all combinations of symptoms may be associated with particular fault conditions. In respect of this, the use of an *Unknown* class to represent residual patterns, which are

not associated with known system conditions, may be of benefit. This approach has been incorporated into the classification and reasoning process for the combustion system faults presented in chapter 8. The implication of the *Unknown* condition class is that further investigation of the fault is required. In this way the *Unknown* class provides additional information to the operator or to a data fusion system.

In addition to the *Unknown* class, further approaches have been attempted to reduce the problems associated with lack of robustness in fuzzy models. In chapter 7 *Model Error* classes and confidence estimates have been used to provide additional information for use in the diagnostic reasoning process where evidence from knowledge sources is combined. The *Model Error* class is defined in terms of the residual R and is based on the idea that very large residuals (with respect to the magnitude of the estimated state), are very likely to be caused by model error, due to the inputs having migrated outside the valid input space. Whereas confidence estimates provide a technique for producing a map of the training errors in the fuzzy model so that regions in the input space where the relationships between the inputs and outputs have not been well defined by the training process for whatever reason are identified. This knowledge may be used as a weighting for the final diagnosis. Results obtained in chapter 7 show that as with the *Unknown* class, these techniques can be used to reduce misclassifications and provide extra information to a data fusion system to improve decision making when combining evidence.

Comparing the use of state estimation with a robust parameter estimation approach for multi-component systems, it seems that where the parameter estimate is indicative of the condition of the performance of an individual component, then the complexity of the diagnostic reasoning process could be significantly reduced. This assumes that suitable classification algorithms are also available to indicate the deviation of the parameter from the predicted norm. Isermann [Isermann 91] also compares the use of state and parameter estimates in process fault diagnosis, noting that although both approaches may produce good results, parameter estimation may be preferable, as state estimation using models requires knowledge of the process parameters in any case. In the case of fuzzy models

the parameters of the physical system are encapsulated within the parameters of the fuzzy model, the membership functions and rules. Therefore to attempt a parameter estimation procedure using a fuzzy modelling approach would entail an on-line fuzzy identification of the system and an algorithm to detect changes in those parameters. This provides scope for further work firstly in comparing fuzzy techniques with robust parameter estimation techniques to assess where each may be most successfully applied (or combined) and secondly to assess the potential of on-line identification of fuzzy systems in a parameter estimation procedure.

The bounded nature of the input space for fuzzy systems has implications for the data acquisition process. Tests programs for acquisition of training data should be designed to maximise the range of input data and try and ensure an appropriate distribution of data points for effective training process. However there are certain problems where inputs are not controllable, for instance, where ambient temperature is an input. For example, the air inlet filter model in 9.4.1, the air inlet temperature is used as the theoretical treatment of the air filter indicates that the pressure difference across the filter is a function of air density, which in turn is related to ambient air temperature. In cases such as this, additional theoretical analysis may need to be incorporated into the fuzzy system to attempt to predict the effects of inputs outside the range of the training data and therefore extend this range.

10.2.4 FUZZY SYSTEMS IN CLASSIFICATION AND REASONING

In the model-based fault diagnosis structures which have been described, residuals are produced by comparison of measured states with predicted or estimated states. The residuals are then classified into a number of fuzzy sets defined in terms of the magnitude and sign of the residual. A common structure for the fuzzy model-based diagnostic is illustrated in figure 7.2.

The fuzzy systems which have been used for the classification of residuals have been produced, based on the testing errors of the model as described in section 9.6.1 with illustration in figures 7.3 and 9.5. Input membership functions for the classifiers have

been chosen as 'Gaussian2mf' as this form of membership function allows easy incorporation of statistical information regarding the distribution of model testing errors. It may be observed from figure 9.5 that the frequency distribution of the model errors is not strictly normal or Gaussian, as defined by;

$$y = \frac{1}{\sigma\sqrt{2\pi}} e^{-\frac{1}{2}[(x-\bar{x})/\sigma]^2}$$

However the intuitive notion that, for the test data set, there should be a *Normal* class defined in R , such that the data is regarded as normal over the range defined between the +/- the average model error magnitude, gradually becoming *less normal* outside that range is shown to produce good results in practice. This approach to the classification of residuals is shown in chapter 9, to be of particular benefit where fault data has not been used in the definition of *Normal*, *Negative* and *Positive* residual classes.

The fuzzy systems employed in classification use constants as output membership functions. Constant membership functions are easy to manipulate and effectively map the continuous residual variable onto the bounded class membership value (see figure 9.10 for an example of this). A fuzzy rule base is defined for each specified condition (and also for unknown residual patterns) of the form described in section 9.6.2. Breaking the rule base for diagnostic reasoning down from a multi-input, multi-output system into a number of multi-input, single-output systems makes manipulation of the individual diagnostic rules more straightforward.

The architecture of the classification and reasoning process (figure 7.2) is similar to that of a neural network with one hidden layer. However the main benefit of the fuzzy structure over the neural network architecture is one of transparency. In event of an unknown condition the fuzzy system provides meaningful information at each layer, e.g. it can be interrogated to obtain raw data, residuals, and importantly, the residual classes. For instance if residual classes are made available to an expert operator then even though the diagnostic system may not recognise the fault symptoms and infer a fault, an

experienced engine operator may be able to do so. The classification and reasoning structure is intended to be generic and could clearly be used with other techniques for residual generation. For instance a fuzzy system has been used with a sliding mode observer technique [Bhatti 99] to infer the system condition.

10.3. A DISCUSSION OF DIESEL ENGINE CMFD

The previous section has considered issues concerning the use of fuzzy systems in fault diagnosis. The following section will consider issues more specific to the CMFD of diesel engine systems. The results from the individual diagnostic techniques will be discussed along with the applicability of the techniques to diesel engine applications other than the isochronous generator set. Section 10.2.3 and 10.2.4 have commented on the proposed architecture for a generic a classification and reasoning system. The diagnostic structure will be reviewed in section 3.3 in terms of the interactions between diesel engine subsystems.

10.3.1 A DISCUSSION OF DIESEL ENGINE SUB-SYSTEM CMFD RESULTS.

Development of CMFD systems using fuzzy logic techniques has been undertaken for three diesel engine sub-systems. The selection of the sub-systems was chosen to test the applicability of the fuzzy approach to CMFD on sub-systems with differing characteristics as outlined in sections 6.3-6.5.

Results obtained from testing of cooling system fuzzy model based CMFD system (see table 7.1 and figure 7.7) show a diagnostic success rate ranging between 56.7% and 82.5%. The success rate of the system is low when the thermostatic valve is closed, but improves when the system warms-up and the thermostatic valve opens to allow coolant flow through the radiator. Confidence weights are an important factor in reducing misclassifications, particularly due to model error where the thermostatic valve is closed or in a transient state. This is confirmed by the results for A* in table 7.1 which show the improvement in the diagnostic success rate from 59.1% to 76.4% as the thermostatic valve opens. Figure 7.7 shows that after $t \approx 1000s$ the success rate is actually 100%.

Chapter 8 describes a high level CMFD system for the diesel engine combustion system. This fuzzy model based CMFD system combines information from four separate, but complementary knowledge sources. These consist of two independent estimates of generator set load and two reference models used to predict fluctuations in speed and boost pressure signals. By comparing results from these knowledge sources, a range of faults in the combustion system of the isochronous diesel generator set can be inferred based on signal analysis from five robust, low-cost transducers. The system has been demonstrated to effectively detect a class of faults that cause a change in the air/fuel ratio with respect to engine load. The confusion matrix in table 7.1 shows that the diagnostic system correctly classifies over 90% of the samples in each of the test data sets. The results show few misclassifications, with the exception of fault, C1, which has a 9% misclassification as C2. Reviewing the diagnostic rules suggests that this misclassification and the misclassifications of C1 are probably due to model errors in the boost pressure reference model.

Section 9.5 presents results from the development and testing of a diagnostic scheme for the aspiration and exhaust systems of the engine. The confusion matrix in table 9.5 shows that the diagnosis success rates are generally good. The confusion matrix shows that for the two sets of normal condition data the misclassification rate is less than 4%.

Success rates for conditions other than *Normal* are seen to depend upon the severity of the fault. Where the faults are applied to their highest experimental magnitude and for the full duration of the test, i.e. in tests 3, 5, 6, 8 and 11, then the success rates are in excess of 90% in each case with the exception of test 6, the air inlet leak. On inspection of the data, the reason for this was found to be the problem in measurement of compressor inlet pressure discussed in section 9.5. The misclassification with d11 is due the fact that the measurement error in, ΔP_{af} meant that the residual, r_3 , remained *Normal* as opposed to *Positive* required by the diagnostic rule, therefore with a just a *Positive* residual in r_1 the fault was misclassified as d11.

The success rates for the diagnosis of the various fault conditions are therefore seen to be generally good. However, it is difficult to directly compare the performance of these fuzzy techniques with other techniques for fault diagnosis in engines. Although a small study to qualitatively compare three diagnostic techniques is reported in section 10.2.2., large scale comparisons have not been undertaken. A number of other authors have produced CMFD systems for engine systems [Freestone 85], [Jewitt 85], [Uchida 89], [Dabbar 89], [Molteburg 91], [Zhong 93], [Krishnaswami 94], [Luh 94], [Constantinescu 95], [Laukonen 95], [Meiler 97], [Li 99]. Typically, results from the respective diagnostics techniques are presented qualitatively or graphically rather than statistically, as percentages of correct samples obtained from test data. The two exceptions to this in the stated examples, are papers by Li *et al* [Li 99] and Meiler [Meiler 97] which both report neural network classifier approaches to diagnosis of combustion system faults.

Meiler uses neural networks to recognise fault patterns in the torsional vibration of a marine diesel engine reporting successful diagnosis rates of between 75 and 100% for individual and combinations of faults affecting the cylinders in the combustion system. Symptoms for certain combinations of faults were also noted to be unrecognisable, as the classifiers could not be trained successfully. Li *et al* also use a series of classifiers to interpret time and frequency domain data sampled from an accelerometer to detect misfire in a spark ignition (SI) engine with a success rate of between 65% and 80%. The faults and techniques for diagnosis of the combustion system faults using the speed reference model are similar in nature to these techniques and show equally good or better results. Fuzzy systems have already been shown to offer certain benefits over neural network techniques. In comparison with Li *et al*, as well as demonstrating a higher success rates, the benefits of the fuzzy model-based, over the neural network approach to misfire detection are seen in figure 7.10. That is, information regarding the cylinder affected by the combustion fault, may be obtained from analysing the residual with respect to crank-angle

A fuzzy model-based diagnostic has been developed by [Laukonen 95] for a V6 automotive SI engine undertaking the United States standard Inspection and Maintenance

IM240 test cycle under laboratory conditions on a dynamometer test bed. Use of the dynamometer allows brake torque to be used as an input to the fuzzy models along with air and fuel mass flow, engine speed and throttle angle. Residuals are generated using dynamic fuzzy models with an ARX type structure incorporating appropriate delays in the inputs. A diagnostic reasoning process is described based on residual patterns. Results from a number of tests comprising calibration faults of throttle, fuel mass flow rate sensor and speed sensor, are presented graphically as residuals extracted from a short period of the test duration. A residual is defined to be an instance where the difference between the predicted state and the measured state exceed a prescribed threshold. i.e. where

$$|\hat{y} - y| > t \quad \dots 10.1$$

The residuals show the expected patterns over a high proportion of the time period for which the results are plotted. Thus, results appear to be good for this technique, although there is no indication of how the individual threshold for each residual has been defined and there is no statistical analysis of the successful diagnoses over the full range of test samples. This technique has clear similarities with those employed in chapters 7-9 of this thesis. However, by comparison the results obtained in this thesis are for a much wider range of components and systems, have a well-defined approach to setting of fuzzy thresholds in residual classification and produce a high level diagnostic output in the form of a linguistic variable. The fuzzy model-based CMFD proposed in this thesis is also more appropriate to an on-board system as measurement of load torque is not a requirement.

It has already been noted that engine torque or load measurements are difficult to arrange for an on-board CMFD system [Jewitt 85]. This is also reported by Molteburg [Molteburg 91] in his Ph.D. thesis, where he develops a set of mathematical models for components of the engine system as follows;

- i) Air filter
- ii) Compressor

- iii) Air Receiver
- iv) Cylinder model (incorporating various sub-models)
- v) Crank
- vi) Speed Controller
- vii) Exhaust Receiver
- viii) Turbine

A number of parameter estimation techniques of the above models are then assessed including Gauss-Newton, Kalman filter, Prediction error, NARMAX and maximum likelihood methods.

A series of faults are simulated experimentally on the test engine. The simulated faults are;

- a) Flow restriction applied air filter
- b) Faulty air cooler (inter-cooler) induced by limiting flow of water to the cooler,
- c) Faulty injector. Fuel flow to a particular cylinder reduced by blocking a fuel injector nozzle hole.
- d) Faulty injection pump, simulated by increasing the delay in the injection timing mechanism

Tests are also carried out with the engine in the normal condition and with some multiple fault conditions comprising combinations of a) – d) (above). Faults are detected using by using an on-line implementation of the Gauss-Newton technique to estimate a series of parameters associated with models 1-8 (above). Parameter estimations are compared with those obtained whilst the engine was running in the normal state to infer a fault condition.

Although the estimated parameters are shown to be a good indicator of fault conditions, again a direct statistical comparison between Molteburg's work and the results obtained in this thesis is not possible. Molteburg's data acquisition work was carried out under

conditions of fixed load and engine speed for a time period sufficient to acquire enough data for the parameter estimation. He also notes that some of the parameters are coupled to engine load as might be expected. Both these two facts expose limitations in the applicability of this approach to on-board CMFD fault diagnosis. The fuzzy models are generally seen to be effective in estimating states under various and rapidly changing loads (for example see figures 9.2 and 9.3) showing benefit over this parameter estimation approach. Once again the high level linguistic output from the fuzzy model based CMFD system is a further benefit.

10.3.2 APPLICABILITY OF RESULTS TO VARIABLE SPEED DIESEL ENGINES

The diagnostic techniques which have been developed in this thesis have only been tested with data from the isochronous diesel generator set. Whilst this is a suitable test-bed in many respects, many potential applications for on-board CMFD are engines of variable speed. It is therefore desirable that the techniques should be portable to variable speed applications with modifications where necessary. Clearly some further work is required in order to accomplish this task but this section will consider some of the issues involved.

Whilst it is true that none of the diagnostic systems depend explicitly on the magnitude of the speed signal, the physical parameters of the subsystems may be coupled in some way. The combustion system diagnosis is likely to be most affected. However, other systems such as the cooling system will also be affected, for example by variation in radiator fan speed or coolant pump speed.

Fuzzy techniques for estimation of engine load in an isochronous diesel generator set have been demonstrated in chapter 8. The two techniques are complementary, in that one is based on air-fuel ratio and one is based on frequency analysis of engine speed. Whilst these estimates are not robust to certain fault conditions, comparison of the estimations in what may be regarded as a parity vector, can either validate the load estimate, where the estimates are within the bounds of the estimation errors, or indicate a fault where they are not. The estimate of load from engine speed may only be practical in medium to low

speed isochronous engines with a small number of cylinders, as for higher speed engines particularly those with larger numbers of cylinders the amplitude of the speed fluctuations will be reduced as more cylinders are contributing to the load torque within the cycle and there is a greater flywheel effect, smoothing out the speed variations. It is possible that the techniques could be adapted for use for variable speed engines, as speed is sampled with respect to crank angle rather than time. However, the limitations for engine speed and number of cylinders would still apply. This speculation clearly provides the basis for possible future work. Even though the speed-based load estimate may not be universally applicable, a possible alternative knowledge source is a robust sliding mode observer technique for load estimation of the form proposed by Kao and Moskwa [Kao 94]

10.3.3 STRUCTURAL ISSUES IN DIESEL ENGINE CMFD

Chapter 9 concludes that combustion system faults were found to have a significant effect on the aspiration and exhaust systems therefore cross-referencing of diagnostic results was a necessity in order to correctly identify faults occurring in a component of the aspiration or exhaust system. Whilst the results in chapter 9 provide an example of effect of the interactions between certain sub-systems, if additional CMFD systems were added then the interactions would clearly become more complex. This emphasises the need for a more rigorous cause and effect analysis of the faults and their symptoms occurring in each of the engine sub-systems. It has been noted in section 10.2 that the cause and effect analysis is of particular importance where fuzzy model-based state estimations and predictions are used for residual generation in a multi-component system because of their lack of robustness to certain fault conditions. This process could be avoided if robust parameter estimation techniques were employed as an alternative. Although it has been demonstrated that fuzzy model based diagnostic systems may be produced without the need for acquisition of fault data, increased knowledge of the behaviour of interacting subsystems will allow a greater degree of detail to be incorporated in the diagnosis.

The results from chapter 9 also indicate the need for a hierarchical CMFD structure. In this example results from the CMFD system for the combustion system must take precedence over those from the aspiration systems. This is due firstly to the magnitude of their impact, secondly to the reliability with which they may be diagnosed (ie >90% success) and thirdly to the fact that the combustion system CMFD was seen to be robust to the simulated faults in the aspiration system. Based on this example, the highest level of the diesel engine CMFD system would be the combustion system. This is supported by the fact that faults in combustion system affect most other systems either directly, e.g. aspiration system and exhaust system in terms of mass and heat flow, or indirectly, e.g. the cooling and lubrications systems, as a source of heat and potential leakage.

Additional work is clearly required to further investigate the interactions between systems and based on the results to finalise the design of the hierarchical CMFD structure. Chapter 9 shows that cause and effect analysis is a complex issue. The idea of a system-by-system approach is probably not the right one for this, as fault conditions have to be replicated a number of times to obtain equivalent fault data for each system. Ideally what is required is a modular approach to data acquisition with sufficient instrumentation and computational power for data acquisition so that time spent on experimental fault simulation tests may be minimised. This data acquisition system should be designed to reflect the requirements of the specified engine CMFD system. However if sufficient instrumentation and computational power for the data acquisition system required by such a proposal is not available then a top-down approach may be an appropriate alternative i.e. simulate faults and obtain data from the combustion system first, then repeat tests for other systems.

10.3.4. APPLICATIONS: PRACTICAL ISSUES

The results in this thesis have mainly been with development of appropriate techniques for CMFD of diesel engine systems, there are also other practical issues which would need to be considered prior to implementation of the scheme. It is likely that some parameters will undergo a natural variation with time, and example of this is noted in appendix 3, section 4, where oil and grime is noted to have formed a coating on the

radiator surface resulting in a change in the heat transfer coefficient. However the generator set has only been run for a total of 160 hours, a small fraction of its design life, therefore significant changes in system parameters should not perhaps not be expected. Effects such as this will have implications for the classification of residuals, or parameters. The three-layer structure offers the possibilities that the fuzzy sets used to classify the system could be simply redefined or re-calibrated to accommodate this parameter change. Alternatively with suitable *a priori* knowledge then the normal classification could be initially defined to give a wider normal class, based on the safe working limits of the system. For example, where the estimated state is the temperature drop across the radiator the normal class could be defined based on the minimum allowable temperature drop. A further possibility is that the adaptive nature of fuzzy systems could be exploited to re-train the fuzzy models within their existing structure as part of the regular maintenance schedule. i.e. After maintenance has been carried out and the fault free operation of the engine has been confirmed then a retraining of the models could be undertaken using some automated approach, incorporated into the CMFD system.

Whilst consideration has been made to specifying the system with low-cost, robust and 'tried and tested' instrumentation, calculation of a true 'cost benefit' can only be obtained with commercially sensitive statistics, to compare the costs of the CMFD system with the expected savings in terms of engine availability. The cost benefit would require information such as the mean time between failure (m.t.b.f.) for various components and the costs of failure for a particular engine specification and application. This would then be compared with the cost of installation of the required instrumentation, hardware and software required by the overall CMFD system. The high level CMFD such as those proposed for the combustion system capable of indicating serious faults from a limited number of instruments may provide the best value fault diagnosis, with CMFD for lower level systems only being cost effective on larger more expensive or safety critical applications.

10.4. CONCLUDING REMARKS

The use of fuzzy systems as techniques for storing information about a system has been shown to be effective. The theme of this thesis is what sort of information may be usefully stored, and how may this be used in condition monitoring and fault diagnosis. Three distinct roles for fuzzy systems in CMFD architecture have been identified; namely, as models or state estimators, as classifiers and in the reasoning process used to infer faults. These techniques have met the objectives of the case study in number of ways. Fuzzy models and estimators have been developed, capable of predicting outputs from highly non-linear systems. Knowledge of the system has been incorporated as heuristics and approximate non-linear mathematical relationships, to improve the estimation and prediction performance. Comparison of the outputs from these fuzzy systems provides valuable information for condition monitoring of components the diesel engine test-bed. The model and estimators are based on signals from a small number of low cost transducers based. Predicted and estimated states from the models are communicated between models and the classification and reasoning process within the CMFD structures.

A qualitative comparison was undertaken with a number of other diagnostic techniques generally fuzzy systems were noted to be more straightforward to develop than mathematical or NARMAX type models. The fuzzy model-based diagnostic system was seen to have benefits over neural network classifier approaches in that fault condition data was not necessarily required in the development of the diagnostic system and the diagnostic system structure also had advantages in terms of transparency.

The chief drawback of the state estimation approach to diagnosis using fuzzy models and estimators is the lack of robustness in the models. Models were found to be effective in residual generation where the deviation from the normal system condition was small but for larger deviations, robustness could not be guaranteed or expected. This was seen to cause particular problems in multi-component systems. A number of techniques including the incorporation of further diagnostic rules, use of confidence estimates, an *Unknown* class and a *Model Error* class in the diagnostic classification and reasoning

process where seen to reduce the number of misclassifications in the result and provide additional useful information to the operator or to a data fusion system. A further consequence of this lack of lack of robustness in the situation where data availability is restricted to the *normal* condition only, is that the detail of the diagnosis may be reduced. i.e. the diagnosis is '*Not Normal*' rather than a specific fault.

A comparison between fault diagnosis via state and parameter estimations was considered concluding that, though both were capable of diagnosing faults, robust parameter estimation offers the benefit of providing a better indication of the magnitude of the fault. Use of fuzzy systems for classification and reasoning in combination with robust parameter estimation as a knowledge source was reported to represent a useful approach.

A generic reasoning and diagnosis architecture was proposed and techniques outlined for specifying residual classes without need for fault condition data. In general for a complex system where the diagnostic reasoning process combines results from a number of models, a general rule seems to be; the greater the robustness of the models the lower the complexity of the diagnostic reasoning.

Qualitative, and in two cases, quantitative results by other researchers were used to emphasis the effectiveness and benefits of the proposed fuzzy model based CMFD systems.

A number of practical issues were also considered including the design of a hierarchical structure for fault diagnosis of engine systems, the applicability of the proposed CMFD systems to variable speed applications, the potential cost benefit of CMFD systems and the definition of residual classes in order to cope with a natural change in engine parameters associated with wear over time. All these issues have not been fully addressed as part of this thesis and will be itemised in chapter 12, Further Work.

CHAPTER 11.

Conclusions

11. CONCLUSIONS

The literature review presented in section 1 of this thesis concluded firstly that fuzzy systems are a possible common methodology for CMFD systems, and secondly, that fuzzy systems are of benefit over other non-linear modelling techniques in providing a suitable approach to grey box modelling. This case study has been undertaken with the aims of assessing the capabilities in a number of areas; firstly, as systems modelling for parameter and state estimation in dynamic, non-linear systems subject to noise and uncertainty, and also as systems for reasoning and classification. The conclusions are presented below with the section 11.1 containing a number of general statements concerning the applicability of fuzzy systems in CMFD. Section 11.2 focuses on points more specific to the diagnosis of diesel engine systems.

11.1 THE APPLICABILITY OF FUZZY SYSTEMS TO CMFD

11.1.2 A common structure for fuzzy model based CMFD has been developed and tested with data from a number of sub-systems of the diesel generator set test-bed. The structure is comprised of three layers. The first layer is residual generation with fuzzy reference models and estimators for state estimation. Residuals are classified using a fuzzy classifier and diagnostic conclusions are inferred from the pattern of residual classes via a fuzzy rule base. Output from the diagnostic system is a linguistic variable. The diagnostic results obtained for three diesel engine sub-systems developed during the case study, show this approach to be a powerful technique for CMFD system design which may be generalised, both for other types of plant and other forms of reference model.

11.1.2 The rule-based structure of fuzzy systems, which allows the incorporation of *a priori* knowledge or heuristics, has been shown to be of benefit in estimation of states where relationships between input and output states are only approximately known.

11.1.3 The fuzzy model based approach to CMFD has been demonstrated to be of benefit in comparison to neural network classification techniques, by the development of diagnostic system structures, using only *Normal* condition data and *a priori* knowledge.

11.1.4 The robustness of the fuzzy models used in state estimation is a key issue. The fuzzy models were found to be generally effective at generating residuals where deviations from the normal condition are small. For larger deviations robustness of models is not guaranteed or expected.

11.1.5 The complexity of defining the diagnostic rule-base for multi-component systems in a model-based technique is strongly coupled to the robustness of the individual models. Good diagnostic results have been obtained using the fuzzy model based structure and sufficient *a priori* knowledge to fully predict the behaviour of the system under certain fault conditions. Also at issue however, is the use of state estimation rather than parameter estimation to predict faults. Due to the robustness limitations of fuzzy models themselves, and the relationship between the complexity of the diagnostic rule-base and the robustness of the models then, where sufficient theoretical knowledge of the system is available, robust parameter estimation, using a sliding mode observer for instance, would be the preferred choice of reference model.

11.1.6 In order to improve the diagnostic performance of the fuzzy model-based systems in the face of the stated robustness problems, an *Unknown* class for unrecognised residual patterns, a *Model Error* class for unfeasibly high residual magnitudes and a confidence weighting, based on mapping the input space to identify regions of high model error, have been demonstrated for the fuzzy model-based CMFD system. These techniques have been shown to reduce misclassifications and provide additional information to the operator or data fusion engine.

11.2 FUZZY MODEL BASED CMFD OF DIESEL ENGINE SYSTEMS

11.2.1 The structure has been applied to three diesel engine subsystems resulting in a high percentage of correct diagnoses for a range of simulated faults. A comprehensive quantitative comparison with other fault diagnostic techniques was not possible, however comparison of success rates for combustion system diagnosis showed that the fuzzy model based systems performed equally well or better than two neural network techniques. In contrast to the neural network classifiers approach the fuzzy systems offer

the benefit that a fuzzy model based CMFD system can be developed without the need for fault condition data.

11.2.2 The correct diagnosis of individual fault conditions was seen to vary with the magnitude of the fault condition as would be expected. The correct diagnosis of the *Normal* condition was 59.1% for the cooling system over all sample points, but 76.4% for the cooling system for all sample points recorded whilst the thermostat valve was open. In the combustion, aspiration and exhaust systems the *Normal* condition was correctly diagnosed for more than 96% of sample data.

11.2.3 A qualitative comparison between the techniques showed that the fuzzy CMFD systems offered benefit over other model-based strategies in representing the results as high-level linguistic variables.

11.2.4 In contrast to a Gauss-Newton parameter estimation technique for estimation of component parameters, the fuzzy-model based CMFD system was shown to be effective over the full range of applied engine brake loads, and could effectively diagnose fault conditions even during periods of rapid load changes, thereby demonstrating a higher degree of applicability for on-board CMFD.

11.2.5 Direct measurement of brake load is a difficult to achieve in practice for an on-board system. Two independent fuzzy model based techniques for estimation of applied load on the isochronous diesel generator set have been developed. A comparison of the load estimations may be used to test their validity, so that the validated load estimate could be used elsewhere in the diagnostic structure. Conversely, a discrepancy between the two estimates can be used to provide a strong indication of the presence of a combustion system fault.

11.2.6 Results for the aspiration and exhaust system indicate the need for a hierarchical diagnostic structure, with the combustion system CMFD process at its highest level. The need for a more rigorous cause and effect analysis was also identified.

CHAPTER 12.

Further Work

12. FURTHER WORK

The work undertaken during this thesis has raised questions which provide the motivation for further work in a number of areas. These areas are itemised as follows;

12.1 A COST BENEFIT ANALYSIS.

A cost benefit analysis should be carried out with the aim of evaluating the potential commercial and operational benefits for on-board CMFD systems. The study should aim to provide a formula for estimating the cost to the operator of lost engine availability for a comprehensive list of known potential faults. This formula will allow the costs of lost availability, to be balanced against the cost and practicality of fitting a CMFD system. The potential cost benefit is obtained from implementation of a CMFD system capable of detecting faults at an early enough stage for preventative action to be taken to minimise this loss of availability. Thus the aim of the formula is to provide an indication of diesel engine applications where it may be cost effective to fit some form of on-board CMFD.

Factors to be considered in estimating the costs to the operators due to loss of availability include the engine application (e.g. lost production time), the mean time between failures for engine components and the time taken for their repair or replacement. This will need to be balanced against factors including the cost of installation and maintenance of diagnostic system and the success rates in fault detection.

12.2 DEVELOPMENT OF KNOWLEDGE SOURCES FOR ADDITIONAL SYSTEMS AND COMPONENTS.

There is a clear need to develop additional knowledge sources and for systems and components which have been itemised in table 6.1 but not included in this thesis. This work could be extended to items which are not listed in table 6.1 but are sometimes used in the diesel engine design, for instance charge cooling or exhaust gas recirculation.

12.3 EXPLORE THE INTER-ACTION BETWEEN DIESEL ENGINE CONTROLLER CMFD

Although CMFD techniques for a number of diesel engine sub-systems have been successfully developed. A potentially useful knowledge source is the engine controller. It is intended that a sliding mode controller will be developed as part of the project and interactions between the controller and the fuel, combustion system and indicated engine speed are expected to provide valuable information concerning the state of the engine.

12.4 A CAUSE AND EFFECT ANALYSIS.

Once a comprehensive set of knowledge sources has been developed then a more rigorous cause and effect analysis could be attempted for a wide range of faults. The question of how to approach such a cause and effect analysis also need to considered. The process should also aim to incorporate other types of knowledge source particularly robust parameter estimation techniques, where conclusion 11.1.5 indicates these to be appropriate.

12.5 TEST THE APPLICABILITY OF DIESEL ENGINE CMFD SYSTEMS TO VARIABLE SPEED ENGINES.

The isochronous diesel generator set is an appropriate test bed in many respects. However, many potential diesel engine applications are variable speed. Therefore, it is desirable to evaluate the applicability of fuzzy CMFD techniques developed here to variable speed applications. Particularly the load estimators and CMFD techniques which have been developed for the combustion system.

12.6 EXPLORE OTHER TECHNIQUES FOR FUZZY SET DEFINITION IN RESIDUAL CLASSIFIERS

A thorough study to find appropriate techniques for fuzzy set definitions in the classification layer of the structure should be carried out. Good results have been obtained using *Normal* condition model error as a basis for the definition. Other approaches could include use of engine design and specification data to indicate safe working limits, or some form of model to predict the allowable 'drift' in the system

parameters which may occur over time. A further development in this area could include an automated system for on-line re-calibration of the diagnostic system.

12.7 ESTIMATION OF MECHANICAL EFFICIENCY IN GENERATOR SETS

In certain applications where an indication of the brake load is available, (such as a generator set where the electrical power output is a measure of the brake load), a validated load estimation (see chapter 8) may be useful as an indicator of the mechanical efficiency of the engine. Where W_B is known, then the mechanical efficiency, μ_m , defined as the useful work available divided by the total work, may be estimated by (from equation 8.6);

$$\hat{\mu}_m = \frac{W_B}{\hat{W}} = \left(1 - \frac{W_P}{\hat{W}}\right) \quad \dots 8.8$$

Therefore, where a fault condition exists which results in increased pumping work, such as an aspiration system fault, or other mechanical fault such as increased bearing friction, then;

$$\hat{\mu}_m = \frac{W_B}{\hat{W}} = \left(1 - \frac{W_P + \Delta W_{Pf}}{\hat{W}}\right) \quad \dots 8.9$$

Therefore, the relationship between the indicated brake load and the estimated total load could be used to detect a class of faults which result in a reduction in mechanical efficiency.

Use of the reference models to predict speed and pressure fluctuations with respect to crank angle has been demonstrated for the isochronous diesel generator set. However there is much scope for development of this type of reference model to be suitable for diagnostics applications in variable speed engines.

Plotting the residual from the speed reference model with respect to crank angle, (figure 8.10) shows that there is clear potential for development of a suitable classifier with the purpose of identifying individual cylinders affected by this class of combustion fault.

References

REFERENCES

- [Abate 90] Abate, M.; Dosio, N., *Use of fuzzy logic for engine idle speed control*, SAE Paper 900564
- [Bajpai 1974] Bajpai, AC; Mustoe, L.R., *Engineering Mathematics*, John Wiley and Sons, 1974.
- [Bezdek 81] Bezdek, J.C., *Pattern Recognition with Fuzzy Objective Function Algorithms*, Plenum Press 1981
- [Bezdek 94] Bezdek, J.C., *Editorial: Fuzziness vs. Probability. Again (!?)*, IEEE Transactions on Fuzzy Systems, Special Edition Fuzziness vs. Probability. Feb 1994 Vol. 2. No.1 pp1-3. ISSN 1063-6702.
- [Bhatti 99] Bhatti, A.I.; Twiddle, J.A.; Spurgeon, S.K.; Jones, N.B., *Engine cooling system fault diagnostics with sliding mode observers and a fuzzy analyser*, Proceedings of 1999 IASTED conference on Modelling, Identification and Control, Innsbruck, Austria 1999.
- [Bochenski, 51] , Bochenski, IM , *Ancient formal logic*, North Holland Publishing Company, Amsterdam, 1951.
- [Boole 1854] Boole, G, *An Investigation of The Laws of Thought*, Dover Publications Inc., 1854.
- [Challen 99] Challen, B; Baranescu, Rodica, (Editors), *Diesel Engine Reference Book (Second edition)*, Butterworth Heinemann 1999.
- [Chiang 82] Chiang, E.C.; Ursini, V.J.; Johnson, J.H., *Development and evaluation of a diesel powered truck cooling system computer simulation program*, SAE Paper 821048, 1982.

- [Chin 86] Chin, Y-K; Coats, F.E, *Engine dynamics: Time-based versus crank-angle based*, SAE Paper 860412. 1986.
- [Chiu 94] Chiu S, *Fuzzy model identification based on cluster estimation*, Journal of Intelligent and Fuzzy Systems September 1994. Vol. 2 number 3.
- [Cho 96] Cho,K.B.; Wang, B.H., *Radial basis function based adaptive fuzzy systems and their adaptations to system identification and prediction*, Fuzzy Sets and Systems 83 (1996) 325-339.
- [Chow 84] Chow, E.Y.; Wilsky,A.S., *Analytical redundancy and the design of robust failure detection systems*, IEEE Transactions on Automatic Control.Vol AC29 No7 July 1984.
- [Chow 99] Chow, A.; Wyszynski, M.L., *Thermodynamic modelling of complete systems – a review*, Proc. I.Mech.E., Part D, Vol. 213. pp403-415, 1999.
- [Constantinescu 95] Constantinescu, R.F. ;Lawrence, P.D.; Hill, P.G.; Brown, T.S., *Model-based fault diagnosis of a two-stroke diesel engine*, 1995 International Conference On Systems man and Cybernetics, Vol. 3, pp2216-2220 Oct 22-25, 1995.
- [Cox 94] Cox, E., *The fuzzy systems hand book.*, Academic Press Ltd., 24-28 Oval Road, London. NW1 7DX. 1994.
- [Dabbar 89] Dabbar, J.M.; Ward, D.A ; Logan, K.P., *Expert performance diagnosis system for marine diesel engines.*, 14th Ship Technology and Research STAR symposium 12-15 Apr, 1989 pp3-2-1 to 3-2-18.
- [dSpace 99] , *dSpace Installation and Configuration Guide*, , dSpace, GmbH, Technologiepark 25-D-33100 Paderborn, Germany.

- [Dubois 85] Dubois, D., *A review of fuzzy set aggregation connectives*, Information Science, 36, no 1-2, pp85-121.
- [Durkin 94] Durkin, J, *Expert Systems: Design and Development*, Macmillan Publishing Company 1994.
- [Eastwood 00] Eastwood, P., *Critical topics in exhaust gas aftertreatment*, Research Studies Press Ltd., Baldock, Herts, UK. 2000.
- [Englemore 88] Englemore, R.; Morgan, T., *Blackboard systems.*, Addison Wesley UK 1988.
- [Filipi 97] Filipi, Z.S.; Assansis, D.N., *Non-linear, transient, single cylinder diesel engine simulation for prediction of engine speed and torque*, 1997 Spring Conference of the ASME internal Combustion Engine Division, ICE-Vol. 28-1, pp61-70, ASME 1997.
- [Fitch 99] Fitch, J.C., *Best practice in maximising fault detection in rotating equipment using wear debris analysis*, Condition Monitoring'99, Jones, M.H. and Sleeman, D.G. (eds.), Coxmoor Publishing, ISBN: 901892115, pp. 65-76.
- [Freestone 85] Freestone, J.W.; Jenkins, E.G., *The diagnosis of cylinder power faults in diesel engines from flywheel speed measurements*, International Conference on Vehicle Condition Monitoring and Fault Diagnosis, I.Mech.E. Conference publications 1985-2, C33/85, pp15-25 ISBN 0 85298 558 4.
- [Gardner 58] Gardner, M., *Logic machines, diagrams and Boolean algebra*, New York: Dover, 1958.
- [Gelgele 98] Gelgele, H.L.; Wang, K., *An expert system for engine fault diagnosis: development and application*, Journal of intelligent manufacturing (1998), 9, 539-545

- [Green 88] Green, J.A., *Sets and Groups*, Green J.A. Routledge and Kegan Paul, 2nd Edition, 1988.
- [Heywood 88] Heywood, J.B., *Internal Combustion Engine Fundamentals*, McGraw-Hill International Editions 1988.
- [Horikawa 92] Horikawa, S.; Furuhashi, T.; Uchikawa, Y., *On fuzzy modelling using fuzzy neural networks with the back-propagation algorithm*, IEEE Transactions on Neural Networks. Vol. 3, No 5. September 1992 pp801-806.
- [Howlett 98] Howlett, R.J. , *Monitoring and control of an internal combustion engine using neural and fuzzy techniques* , Conference on the Engineering of Intelligent Systems, EIS '98 .
- [Hoyt 67] Hoyt, J.P., *A brief introduction to probability theory*, Scranton, Pa. : International Textbook Company, 1967.
- [Huang 00] Huang, S-J.; Lee, T-H, *Fuzzy logic controller for a retrofitted closed loop injection moulding machine*, Proc. I.Mech.E., Part I, Vol. 214. pp9-21, 2000.
- [Ioannou 96] Ioannou, P.A.; Sun, J., *Robust Adaptive Control*, Prentice-Hall 1996
- [Isermann 91] Isermann, R.; Freyermouth, B, *Process Fault Diagnosis Based on Process Model Knowledge - Part 1: Principles for Fault Diagnosis with Parameter estimation*, Journal of Dynamic Systems, Measurement and Control. December 1991, Vol 113 pp 620 – 633.
- [Isermann 97] Isermann, R; Balle, P., *Trends in the application of model based fault detection and diagnosis of technical processes*, Control Eng. Practice Vol. 5, No 5 pp709-719 1997.

- [Jang 93a]** Jang J-S.R., *ANFIS adaptive network-based fuzzy inference system*, IEEE Transactions on Systems Man And Cybernetics, Vol. 23, No3., pp665-685 May/June 1993.
- [Jang 93b]** Jang, J-S.R.; Sun, C-T., *The functional equivalence between radial basis function networks and fuzzy inference systems*, IEEE Transactions on Neural Networks 4, pp156-159, 1993.
- [Jewitt 85]** Jewitt, T.H.B.; Lawton, B., *The use of speed sensing for monitoring the condition of military vehicle engines*, International Conference on Vehicle Condition Monitoring and Fault Diagnosis, I.Mech.E. Conference publications 1985-2, C39/85, pp67-75 ISBN 0 85298 558 4.
- [Jones 00]** Jones N.B., Spurgeon S.K., Pont M.J., Twiddle J.A., Lim C.L., Parikh C.H. & Goh K.B., *Aspects of diagnostic schemes for biomedical and engineering systems*. , Proc. IEE. Science, Measurement and Technology, 147, 2000, 357 – 362.
- [Kao 95]** Kao, M; Moskwa, J.J., *Turbocharged diesel engine modelling for non-linear engine control and state estimation*, Transactions of ASME, Journal of Dynamic Systems, Measurement and Control, March 1995 Vol. 117 pp20-30.
- [Karpman 85]** Kapman, G.;Dubuisson, B., *Complexity index for system diagnosability*, IEEE Transactions on Systems Man And Cybernetics, Vol. SMC-15 No2., March/April 1985.
- [Karray 95]** Karray, F; Natarajan, K; Mansour, S, *Hierarchical rule-based control of a diesel engine system*, 1995 International Conference On Systems man and Cybernetics, Vol. 4, pp3000-3004 Oct 22-25, 1995.
- [Kays 55]** Kays W.M.; London A.L., *Compact Heat Exchangers*, McGraw-Hill 1955.

[Kosko 94a] Kosko, B., *Fuzzy systems as universal approximators*, IEEE Transactions on Computers, Vol. 43, No11, pp13-29, Nov 1994.

[Kosko 94b] Kosko, B., *Fuzzy thinking. The new science of fuzzy logic*, HarperCollins Publishers 77-85 Fulham Palace Road, Hammersmith, London.1994.

[Krishnaswami 94] Krishnaswami, V; Luh, G-C.; Rizzoni, G., *Fault detection in IC engines using nonlinear parity equations*, Proceedings of the American Control Conference, American Automatic Control Council, Jun29 -Jul1 1994, Vol2, pp2001-2005.

[Laukonen 95] Laukonen, E.G.; Passino, K.M.; Krishnaswami, V.; Luh G-C., Rizzoni, G., *Fault detection and isolation for an experimental internal combustion engine via fuzzy identification*, IEEE Transactions on Control Systems Technology, Vol3, No3, pp347-355, Sept 1995.

[Leontaritis 85a] Leontaritis, I.J.; Billings, S.A., *Input-output parametric models for non-linear systems. Part1: Deterministic non-linear systems*, International Journal of Control, 41 pp 329-344.

[Li 99] Li, Y.; Pont, M.J.; Jones, N.B.; Twiddle, J.A., *Using MLP and RBF classifiers in embedded condition monitoring and fault diagnosis applications*, Condition Monitoring'99, Jones, M.H. and Sleeman, D.G. (eds.), Coxmoor Publishing, ISBN: 901892115, pp. 237-243.

[Lilly 84] Lilly, L.C.R.; (Editor), *Diesel Engine Reference Book*, Butterworth and Co Ltd. 1984.

[Ljung L] Ljung, L., *System Identification: Theory for the user*, P T R Prentice Hall Information and System Science Series 1987.

- [Long 96] Long, B.R.; Boutin K.B., *Enhancing the process of Diesel engine condition monitoring*, 18th Annual Fall Conference of the ASME internal Combustion Engine Division, ICE-Vol. 27-1, pp61-68, ASME 1996.
- [Lu 98] Lu, Y.; Chen, T.Q.; Hamilton, B.; , *A fuzzy diagnostic model and its application in automotive engine diagnosis*, Journal of Applied Intelligence, 9 231-243 (1998), Kluwer Academic Publishers.
- [Luenberger 71] Luenberger, D.G., *An introduction to observers*, IEEE Transactions Vol. A.C. -16 596-602, Dec. 1971
- [Luh 94] Luh, G-C.; Rizzoni, G., *Identification of a nonlinear MIMO ic engine model during I/M240 driving cycle for on board diagnosis*, Proceedings of the American Control Conference, June 1994, pp1581-1584.
- [Lukasiewicz 51] Lukasiewicz, J, *Aristotle's syllogistic from the standpoint of modern formal logic*, Oxford Clarendon Press 1951.
- [Lynch 92] Lynch, M., *Cylinder pressure reconstruction from external structural vibrations using digital signal processing techniques*, M.Sc. Thesis, Department Of Engineering University of Leicester, 1992.
- [Mahon 92] Mahon, L., *Diesel generator set handbook*, Butterworth Heinemann 1992.
- [Massey 68] Massey, B.S., *Mechanics of Fluids*, Van Nostrand Reinhold (UK) Co. Ltd 1968.
- [Mathworks 99] , *Using Matlab v5.3*, The MathWorks Inc. 24, Prime Park Way, Natick, MA 01760.

- [Matlab 97] **Jang, J-S.R.; Gulley, N.**, *Fuzzy Logic Toolbox, User's Guide (second printing)*, The MathWorks Inc. 24, Prime Park Way, Natick, MA 01760.
- [Meiler 97] **Meiler, P.P.; Maas, H.L.M.M.**, *Condition monitoring of a diesel engine by analysing its torsional vibration using modern information technology*, Proc. 11th Ship Control System Symposium, Southampton April 1997 Part 2 Vol. 1, pp373-387.
- [Michie 82] **Michie, D.**, *Introductory readings in expert systems*, Gordon and Breach Science Publishers 1982.
- [M.o.M.'s 27/07/2000]. *Minutes of the quarterly diesel engine group project meeting*, Dept. of Engineering, University of Leicester, 27/07/2000
- [Molteberg 91] **Molteberg, G.A.**, *The application of system identification techniques to performance monitoring of four stroke turbocharged diesel engines*, Ph.D. Thesis, Division of Marine Engineering, Norwegian Institute of Technology, University of Trondheim. ISBN 82-7119-344-9. ISSN 0802-3271.
- [Montgomery 91] **Montgomery, D.C.**, *Design and Analysis of Experiments*, Wiley 1991.
- [Oppenheim 89] **Oppenheim, A.V.; Schaffer, R.W.**, *Discrete-time signal processing*, Prentice Hall International Signal Processing Series 1989.
- [Ordubadi 82] **Ordubadi, A.**, *Fault detection in internal combustion engines using an acoustic signal*, SAE International Congress and Exposition, Proceedings of Engine Noise Symposium 22-26 Feb 1982, pp 145-150.
- [Ozisik 85] **Ozisik M.N.**, *Heat transfer A basic approach*, McGraw-Hill International Editions 1988.

- [Parikh 98] Parikh, C.R.; Pont, M.J. ; Li, Y.; Jones, N.B.; Twiddle, J.A, *Towards a flexible application framework for data fusion using real time design patterns*, Proceedings of 6th European Congress on Intelligent Techniques and Soft Computing (EUFIT), Aachen, Germany, September 7-10,1998 pp.1131-1135.
- [Parikh 99] Parikh, C.R.; Pont, M.J.; Li, Y.H.; and Jones, N.B., , *Investigating the Performance of MLP Classifiers where Limited Training Data are Available for Some Classes*, Soft Computing Techniques and Applications, John, R., Birkenhead, R. (eds.), Physica-Verlag, ISBN: 3790812579, pp. 22-27.
- [Patton 89] Patton, R.; Frank, P.; Clark, R., *Fault diagnosis in dynamic systems: Theory and application*, Prentice Hall International Series in Systems and Control Engineering 1989.
- [Perkins 95] Perkins International Ltd., *Workshop manual Phaser and 1000 Series.*, Publication No. TPD 1312E Issue 1. Technical Publications, Perkins International Ltd., Peterborough PE1 5NA 1-04-1995.
- [Schenker 98] Schenker, B.; Agarwal M., *Output prediction in systems with backlash*, Proc. I.Mech.E., Part I, Vol. 212. pp17-26, 98.
- [Seng 99] Seng, T.L.; Khalid, M; Yusof, R., *Adaptive general regression neural network for modelling of dynamic plants*, Proc. I.Mech.E., Part I, Vol. 213. pp275-287, 98.
- [Simonsen 88] Simonsen, J.R., *Engineering Heat Transfer*, MacMillan Education 1988
- [Simulink 99] , *Using Simulink v3*, The MathWorks Inc. 24, Prime Park Way, Natick, MA 01760.

- [Sjoberg 95a] **Sjoberg, J.; Zhang, Q.; Ljung, L.; Benveniste, A.; Delyon, B.; Glorionec, P-Y.; Hjalmarsson, H.; Juditsky, A.,** *Non-linear black-box modeling in system identification: A unified overview*, Automatica 31, 1691-1724.
- [Sjoberg 95b] **Sjoberg, J.,** *Non-linear system identification with neural networks*, PhD Thesis, Dept of Electrical Engineering, Linkoping University, S-581 83 Linkoping Sweden ISBN 91-7871-534-2.
- [Takagi 85] **Takagi, T.; Sugeno, M.,** *Fuzzy identification of systems and its applications to modelling and control*, IEEE Transactions on Systems Man And Cybernetics, Vol. SMC-15 No1., January/February 1985.
- [Thiessen 82] **Theissen, F.; Dales, D.,** *Diesel fundamentals. Principles and service*, Reston publishing company, A Prentice Hall Company, Reston, Virginia USA. 1982.
- [Twiddle 99] **Twiddle, J.A.,** *Fuzzy model-based fault diagnosis of a diesel engine cooling system*, Leicester University Engineering Dept, Internal Paper, 99-1 Jan 99.
- [Uchida 89] **Uchida, K.; Hirota, K.,** *Trend understanding expert system (TRUSTEX) based on fuzzy-crisp hybrid reasoning.*, Proceedings of 29th SICE international Conference, Vol. 2, pp. 1355-1358, Jul 25-27 1989.
- [Vachkov 92] **Vachkov, G Matsuyama, H,** *Fault diagnosis by using fuzzy rule-based models*, 2nd International Conf. on fuzzy logic and neural networks, Iizuka Japan. 1992, pp385-388.
- [Wang 92] **Wang, L-X.; Mendel, J.M.,** *Fuzzy basis functions, universal approximation, and orthogonal least squares learning*, IEEE Transactions on Neural Networks Vol. 3, No 5, September 1992.

- [Wang 94] Wang J.T.; Jones N.B.; Sehmi A.S.; De Bono D.P., *A blackboard system for fuzzy ECG interpretation*, System Analysis Modelling and Simulation., 14, 1994 pp81-92.
- [Wang 97] Wang, L-X., *A Course In Fuzzy Systems and Control*, Prentice - Hall international 1997.
- [Watson 82] Watson, N.; Janota M.S., *Turbocharging the Internal Combustion Engine*, Macmillan Press Ltd. 1982.
- [Whitehead 10] Whitehead, A.N.; Russell, B., *Principia Mathematica*, Cambridge University Press, Vols. I,II,III, 1910 – 1913.
- [York 85] York, R.A., *Onboard Engine monitoring and diagnosis for heavy equipment and stationary power plant*, Earthmoving Industry Conference. 15-17 April, 1985. SAE Technical Paper Series 850773.
- [Zadeh 65] Zadeh, L.A., *Fuzzy sets*, Information and Control 8, 338-353.
- [Zhang 98] Zhang, Y.; Zhang, Z.P.; Zhou, Y.C., *Research on the fuzzy and dynamic monitoring of the diesel engine operating conditions*, Journal of automobile engineering 1998 Vol./Part: v212 n5 Pages: p421-427.
- [Zhong 93] Zhong, W.; Zongying, G., *Expert system for analysing the performance and diagnosing faults of D.I. diesel engines*, SAE International Congress and Exposition, SAE Special Publication, pp 51-55, March 1-5 1993.
- [Zimmerman 91] Zimmerman H.-J., *Fuzzy Set Theory and its Applications (second edition)*, Kluwer Academic Publishers 1991.

APPENDIX 1.

Details of Diesel Generator Test-bed

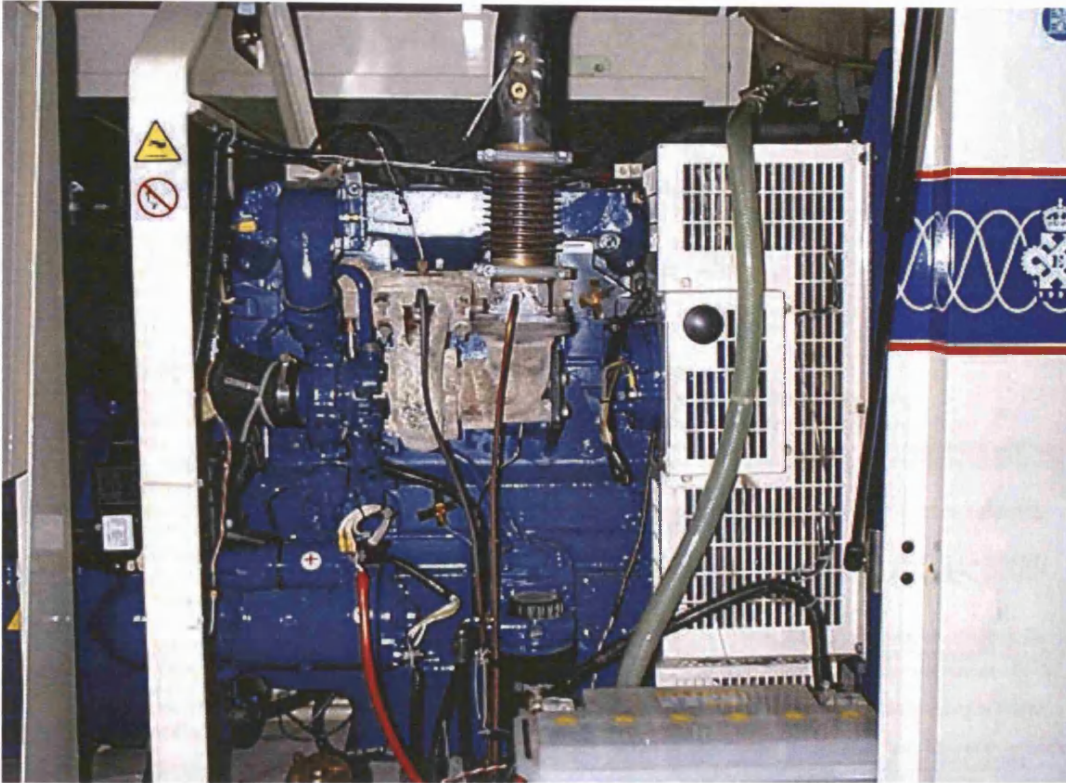
APPENDIX 1.1 GENERATOR SET TEST-BED PHOTOS



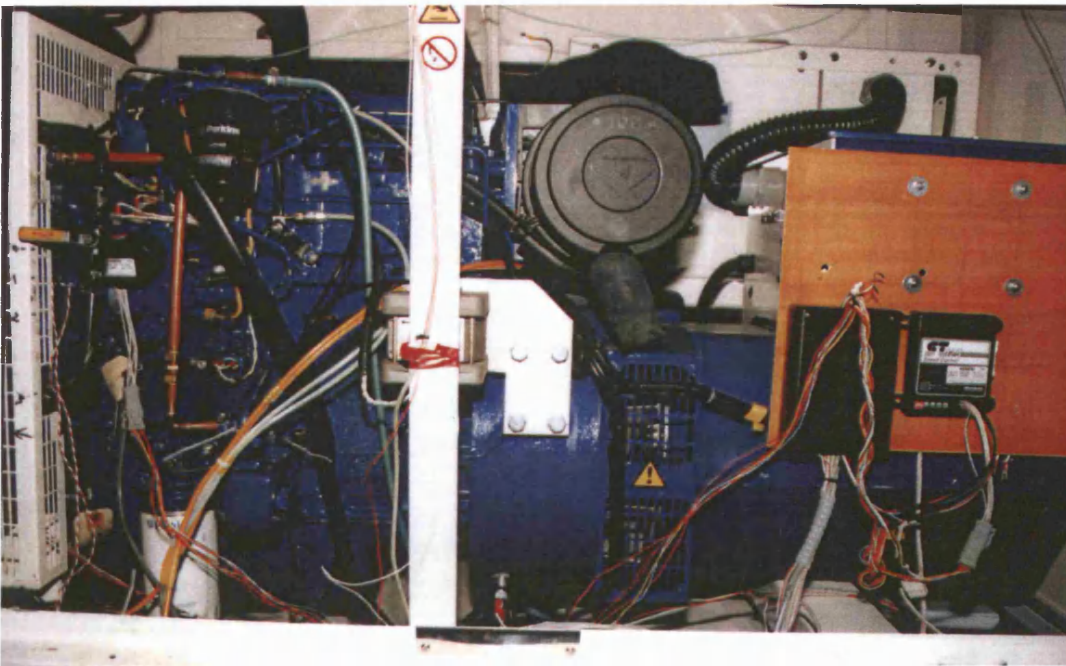
Picture 1. Diesel generator set test-bed installation in thermodynamics laboratory, showing the generator set, load bank and smoke detector.



Picture 2. Data acquisition equipment and PC in thermodynamics laboratory.



Picture 3. Generator set diesel engine, right hand side, showing turbo-charger, air-inlet pipe-work, air inlet and exhaust manifolds.



Picture 4. Diesel generator set, left hand side, showing air filter pipe-work, oil filter, controller, actuator and fuel pump.

SPECIAL NOTE

THE FOLLOWING
IMAGE IS OF POOR
QUALITY DUE TO THE
ORIGINAL DOCUMENT.

THE BEST AVAILABLE

IMAGE HAS BEEN

ACHIEVED.

APPENDIX 1.2 'ELECTROPAK' 1004TG DIESEL ENGINE DATA SHEETS

Perkins ELECTROPAKS 1004TG Technical Data

Basic technical data

Number of cylinders: 4
 Cylinder arrangement: Vertical, in line.
 Cycle: 4 stroke
 Induction system: Turbocharged.
 Combustion system: Direct injection.
 Bore: 100,0mm (3.937in).
 Stroke: 127,0mm (5.0in).
 Compression ratio: 16.0:1.
 Cubic capacity: 3.99 litres (243in³).
 Direction of rotation: Clockwise viewed from the front.
 Firing order: 1, 3, 4, 2.
 Total weight (dry): 434kg (956lb).
 Total weight (wet): 462kg (1018lb).
 Overall dimensions: Height 960mm (37.8in);
 Length 1242mm (48.9in); Width 647mm (25.4in).
 Moment of inertia (mk²): Engine 0,1254kg m² (428lb in²);
 Flywheel, (1)
 Cyclic irregularity for engine and flywheel at 110% standby
 power: 1500 rev/min 0,0050; 1800 rev/min 0,0030. (2)
 (1) For flywheel inertia, see flywheel option drawings.
 (2) Data shown applies to engine and flywheel only (D8001 or
 D8005).

Performance

Speed variation at constant load: ±0.8%.
 Maximum overspeed limit: 2860 rev/min.
 Average sound pressure level for bare engine (without inlet
 and exhaust) at 1 metre: 1500 rev/min 91.2 dBA; 1800 rev/min
 96.4 dBA.

Note: All data based on operation under BS 5514: 1982, ISO
 3046/1: 1982 and DIN 6271.

Test conditions: Air temperature 25°C (80.6°F), barometric
 pressure 100kPa (29.5in Hg), relative humidity 30%, air inlet
 restriction at maximum power 5.0.

All ratings certified within ±5%.

If the engine is to operate in ambient conditions other than the test
 conditions then suitable adjustments must be made for any change
 in inlet air temperature, barometric pressure or humidity. For full
 details refer to Perkins Engines.

Diesel fuel: To conform to BS 2869: 1983 Class A2 or ASTM
 D975 66T Number 2D.

Lubricating oil: A single or multigrade lubricating oil must be used
 which conforms with specification API CD/SE or CCMC D4.

Start load delay: Ninety percent of prime power rating can be
 applied 10 seconds after the starter motor is energised. The
 remaining 10% can be applied 15 seconds after start if the ambient
 temperature is not less than 15°C (59°F). If the ambient
 temperature is less than 15°C (59°F), an immersion heater is
 recommended. For specific information refer to Perkins Engines.

General installation data – typical installation conditions

Item	Units	Type of operation and application			
		Prime		Standby	
		50Hz	60Hz	50Hz	60Hz
Engine speed	rev/min	1500	1800	1500	1800
Gross engine power	kW (bhp)	67.4 (90.4)	78.2 (104.9)	74.2 (99.5)	86.0 (115.3)
Brake mean effective pressure	kPa (lbf/in ²)	1369 (198)	1320 (191)	1503 (218)	1453 (210)
Piston speed	m/s (ft/s)	6.35 (20.8)	7.62 (25.0)	6.35 (20.8)	7.62 (25.0)
Electropak nett engine power	kW (bhp)	65.7 (88.1)	75.6 (101.4)	72.3 (97.0)	83.2 (111.6)
Engine coolant flow	litre/min (UK gal/min)	80.0 (17.5)	97.0 (21.3)	80.0 (17.5)	97.0 (21.3)
Combustion air flow	m ³ /min (ft ³ /min)	4.52 (159)	5.85 (206)	4.71 (166)	6.16 (215)
Exhaust gas flow	m ³ /min (ft ³ /min)	13.1 (462)	15.9 (561)	14.0 (494)	17.0 (600)
Exhaust gas temperature	°C (°F)	561 (1041)	511 (951)	596 (1104)	548 (1018)
Cooling fan airflow (3)	m ³ /min (ft ³ /min)	100 (3539)	130 (4600)	100 (3539)	130 (4600)
Fan absorption	kW (bhp)	1.89 (2.53)	2.87 (3.85)	1.89 (2.53)	2.87 (3.85)
Total heat from fuel	kW (Btu/min)	181 (10293)	208 (11828)	199 (11317)	228 (12966)
Gross heat to power	kW (Btu/min)	68.2 (3678)	79.1 (4498)	75.0 (4265)	87.0 (4987)
Net heat to power	kW (Btu/min)	66.4 (3776)	75.3 (4282)	73.2 (4162)	83.2 (4731)
Heat to water and lubricating oil	kW (Btu/min)	43.0 (2445)	47.0 (2672)	47.0 (2672)	52.0 (2957)
Heat to exhaust	kW (Btu/min)	53.4 (3036)	63.3 (3600)	55.6 (3161)	66.7 (3793)
Heat to radiation	kW (Btu/min)	16.4 (932)	18.6 (1057)	21.4 (1217)	22.3 (1268)

(3) Caution: The airflows shown in this table, will provide acceptable cooling for an open power unit operating in ambient temperatures of up to 53°C (46°C if a canopy is fitted). If the power unit is to be enclosed totally, do a cooling test to check that the engine cooling is acceptable. If there is not sufficient cooling, contact Perkins Technical Service Department for further information.

 Perkins

1004TG Technical Data

Cooling system

Radiator:

Face area: 0,31m² (3.33ft²).
 Rows and material: 4 brass.
 Gills/inch and material: 12 copper.
 Width and height of matrix: 559mm (22.0in) × 560,0mm (22.04in).
 Pressure cap setting: 75kPa (10.8lbf/in²).
 Maximum top tank temperature: 103°C (207°F).
 Estimated cooling air flow reserve: 1500 rev/min 0,12kPa (0.47in H₂O); 1800 rev/min 0,15kPa (0.59in H₂O). (4)
 (4) **Caution:** See note 3 at the bottom of the table on front page.

Fan:

Diameter: 508mm (20.0in).
 Drive ratio: 1.25:1.
 Number of blades: 7.
 Twist angle: -.
 Material: Plastic.

Coolant:

Maximum static pressure head at pump: 1500 rev/min 6,2m (20.3ft); 1800 rev/min 4,3m (14.1ft).
 Total system coolant capacity: 22,2 litre (39.0 UK pt).
 Drain down capacity: 22 litre (38.7 UK pt).
 Minimum temperature to engine: 70°C (158°F).
 Temperature rise across engine: 7,7°C (13.8°F).
 Maximum permissible external system resistance: 35kPa (5.0lbf/in²).

Thermostat:

Operation range: 82-93°C (180-199°F).

Electrical system

Battery charging system:

Type: Negative ground.
 Alternator: 12V/24V options.
 Starter motor: 12V/24V options.

Cold start recommendations

Minimum starting temperature °C °F	Grade of engine lubricating oil	Battery specifications			
		BS3911 Cold start amps	SAE J537 Cold cranking amps	Number of batteries needed	Perkins type
-10 14	10W	395	600	1	A
-10 14	20W	520	800	1	B
-15 5	10W	520	800	1	B
-20 -4	5W	520	800	1	B

Exhaust system

Maximum permissible back pressure for total system: 6kPa (1.77in Hg).

Inside diameter of exhaust outlet flange: 57,6mm (2.26in).

Note: Changes to induction restriction, exhaust back pressure and fuel viscosity/temperature/specific gravity, can affect power output. For further details contact Perkins Technical Service Department.

Fuel system

Type of injection system: Direct.

Fuel injection pump: Rotary type.

Fuel atomiser:

Type: Multi-hole.

Injection pressure: 23,3 MPa (230 atm).

Fuel lift pump:

Delivery/hour: 1500 rev/min 98,1 litres (172.6 UK pt); 1800 rev/min 69,1 litres (156.7 UK pt).

Pressure: 30kPa (4.3lbf/in²).

Maximum suction head: 1,8m (6.0ft).

Maximum pressure head: 3,0m (9.8ft).

Governor type: Mechanical, integral with fuel injection pump.
 Speed control to BS 5514 Class A1.

Induction system

Maximum permissible air intake restriction at engine: Clean filter 3,0kPa (12in H₂O); Dirty filter 5,0kPa (20in H₂O).

Air filter type: Dry element type.

Minimum dirt capacity: 353g/m³/min.

Turbocharger type: Garrett Airesearch T31/45/1.06/57.

Lubrication system

Lubricating oil capacity: Total system 8,5 litres (15.0 UK pt); Sump only 6,9 litres (12.1 UK pt).

Normal operation angles: Front up 25°; Front down 25°; Side to side 25°.

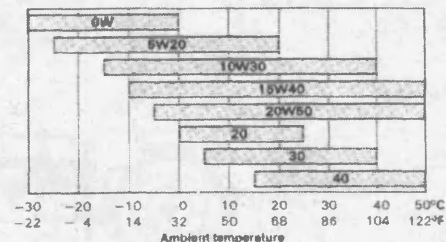
Pressure at which oil relief valve opens: 345-414kPa (50-59lbf/in²).

Lubricating oil pressure: At rated speed 310-390kPa (45-56lbf/in²); Minimum at idle speed 62-90kPa (8.9-13lbf/in²).

Lubricating oil temperature: At normal operation 105°C (221°F); Maximum 125°C (257°F).

Lubricating oil consumption as a percentage of fuel consumption: 0,2% maximum.

Recommended SAE viscosity grades:



Mountings

Maximum bending moment at rear face of engine block: 791Nm (583lbf ft).

Position of centre of gravity (wet engine): Forward from rear face of block 279mm (10.98in); Above crankshaft centre line 279mm (10.98in); Offset from vertical centreline 15mm (0.5in) right side.

Perkins Power Sales & Service Limited

Peterborough PE1 5NA, England

All information given in this leaflet is correct at the time of printing but may be changed subsequently by the Company.

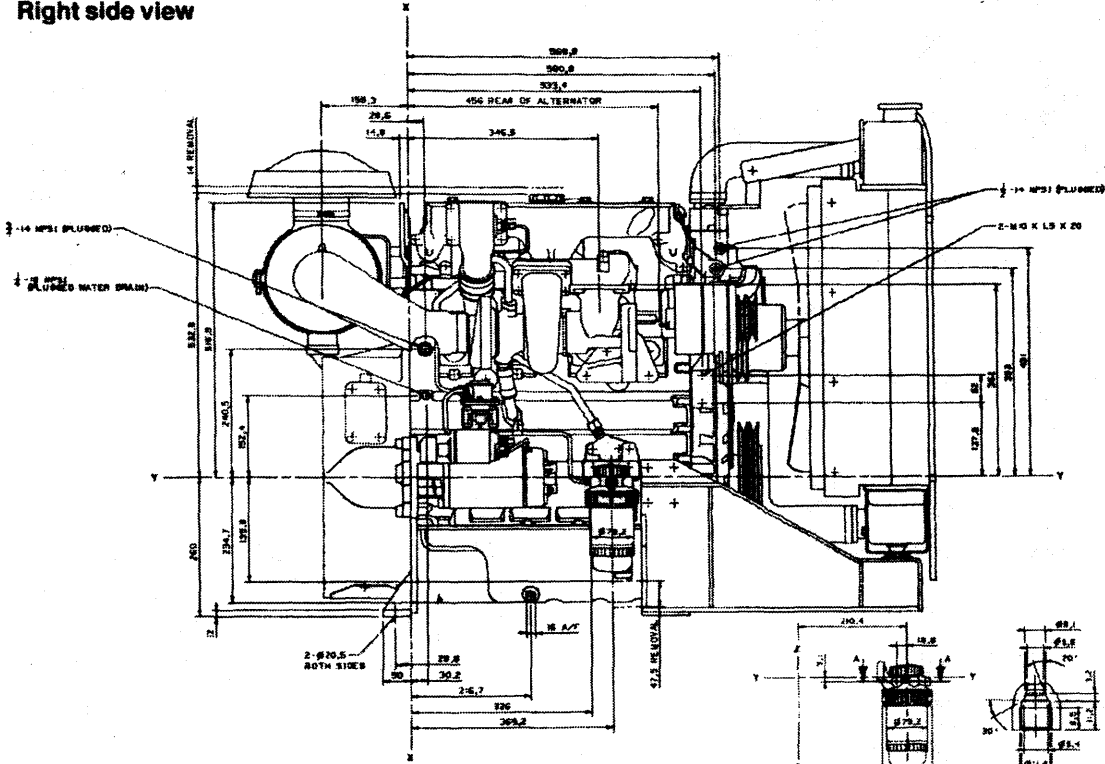
Printed in England by Fisherprint Ltd., Peterborough. Publication TPD 0993 1251/1004TG.

 Perkins

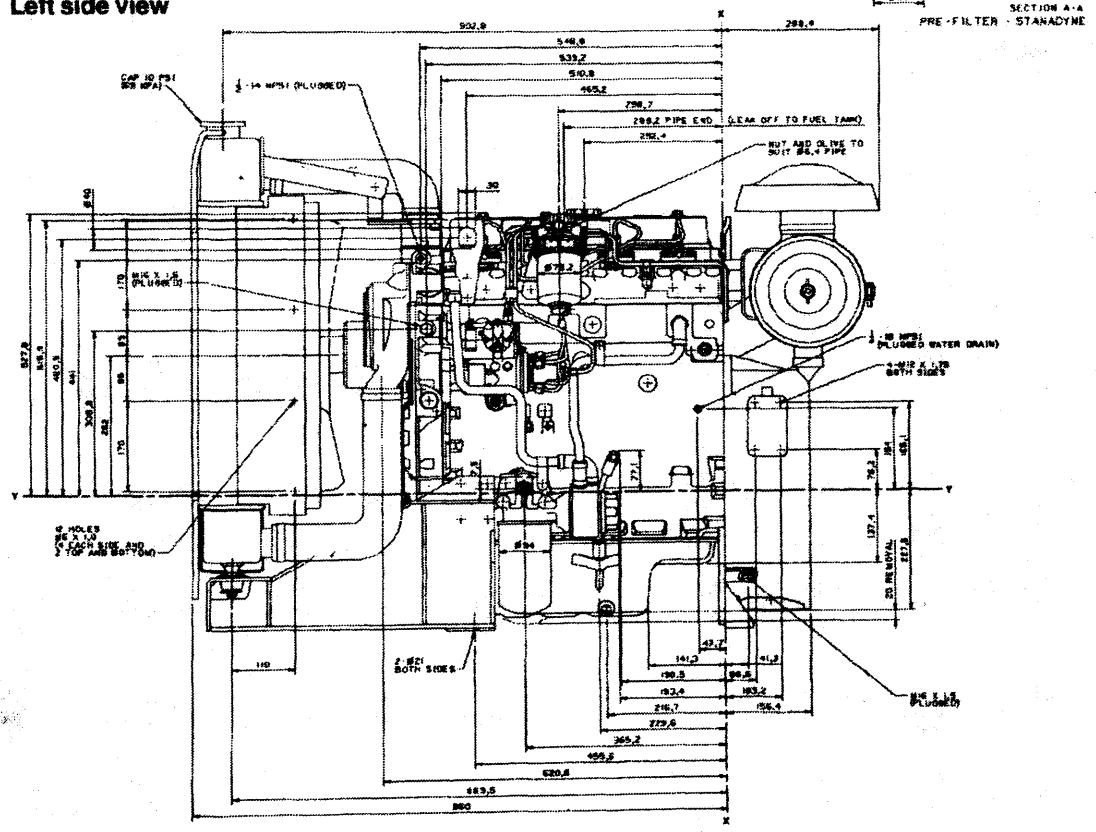
Perkins ELECTROPAKS December 1994

1004TG Electropak

Right side view

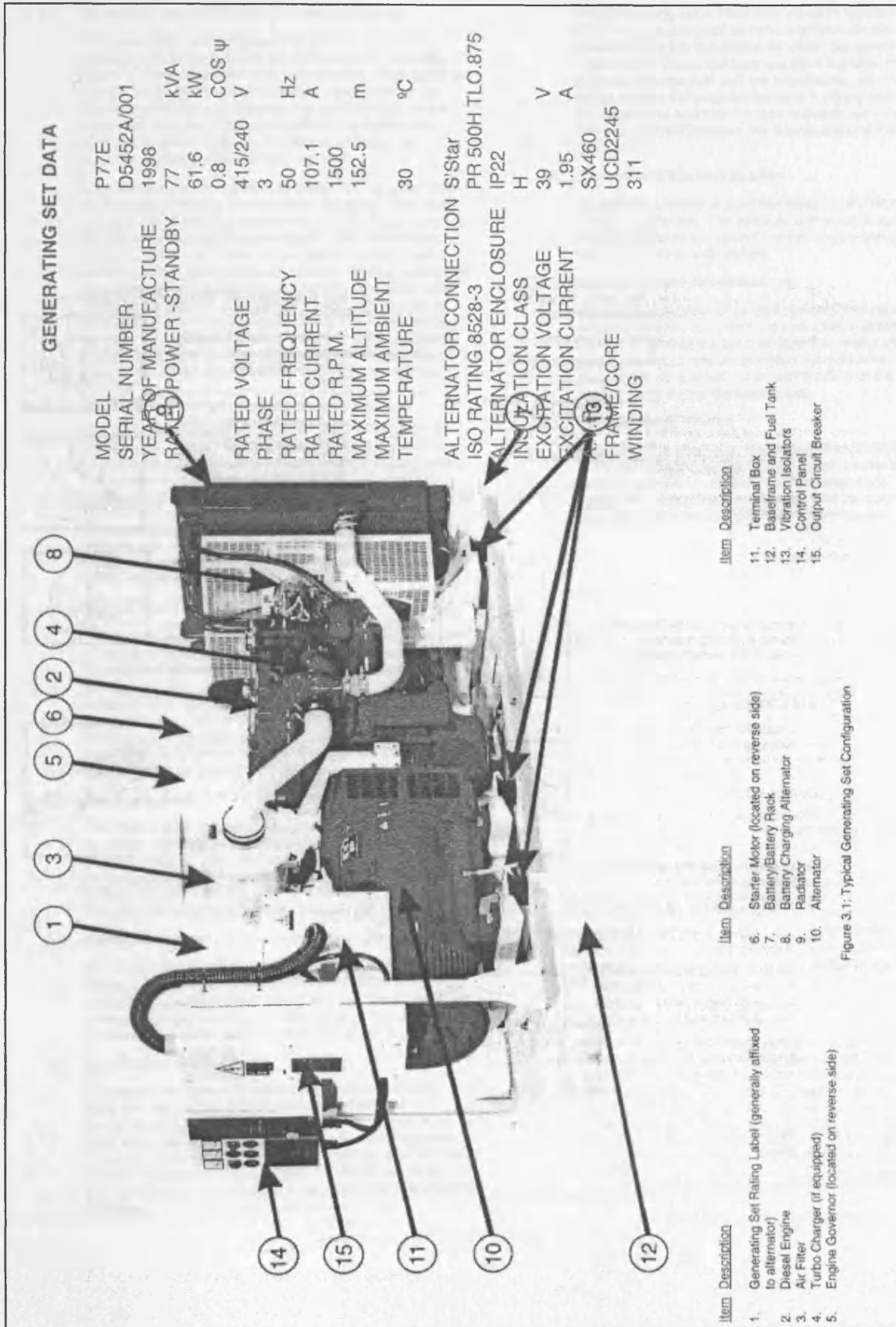


Left side view



Perkins ELECTROPAKS May 1993

APPENDIX 1.3 GENERATOR SET DATA SHEET AND DESCRIPTION



SPECIAL NOTE

THE FOLLOWING
IMAGE IS OF POOR
QUALITY DUE TO THE
ORIGINAL DOCUMENT.

THE BEST AVAILABLE

IMAGE HAS BEEN

ACHIEVED.

GENERAL DESCRIPTION

3.1 Generating Set Description and Identification

This generating set has been designed as a complete package to provide superior performance and reliability. Figure 3.1 identifies the major components. This figure is of a typical generating set. However, every set will be slightly different due to the size and configuration of the major components. This section briefly describes the parts of the generating set. Further information is provided in later sections of this manual.

Each generating set is provided with a Rating Label (item 1) generally affixed to the alternator housing. This label contains the information needed to identify the generating set and its operating characteristics. This information includes, but is not limited to, the model number, serial number, output characteristics such as voltage, phase and frequency, output rating in kVA and kW, and rating type (basis of the rating). For reference, this information is repeated on the Technical Data Sheet provided with this manual. The model and serial numbers uniquely identify the generating set and are needed when ordering spare parts or obtaining service or warranty work for the set.

3.2 Diesel Engine

The diesel engine powering the generating set (item 2) has been chosen for its reliability and the fact that it has been specifically designed for powering generating sets. The engine is of the heavy duty industrial type with 4 stroke or 2 stroke compression ignition and is fitted with all accessories to provide a reliable power supply. These accessories include, among others, a cartridge type dry air filter (item 3), a turbocharger fitted on some engines (item 4), and a mechanical or electronic close control engine speed governor (item 5).

3.3 Engine Electrical System

The engine electrical system is negative ground/earth and either 12 or 24 volts DC depending on the size of the set. This system includes an electric engine starter (item 6), battery and battery rack (item 7) which may also be located on the floor next to the set for some of the larger generating sets, and a battery charging alternator (item 8). Most sets are provided with lead-acid batteries which are discussed more fully in Section 10, however other types of batteries may be fitted if they had been specified.

3.4 Cooling System

The engine cooling system is comprised of a radiator (item 9), a high capacity pusher fan and a thermostat. The alternator has its own internal fan to cool the alternator components. Note that the air is "pushed" through the radiator so that the cooling air is drawn past the alternator, then past the engine and finally through the radiator.

3.5 Alternator

The output electrical power is normally produced by a screen protected and drip-proof, self-exciting, self-regulating, brushless alternator (item 10) fine tuned to the output of this generating set. Mounted on top of the alternator is a sheet steel terminal box (item 11).

3.6 Fuel Tank and Baseframe

The engine and alternator are coupled together and mounted on a heavy duty steel baseframe (item 12). Except for the largest sets, this baseframe includes a fuel tank with a capacity of approximately 8 hours operation at full load. An extended capacity fuel tank of approximately 24 hours operation may be fitted. Where a fuel tank is not provided with the baseframe, a separate fuel tank must be provided.

3.7 Vibration Isolation

The generating set is fitted with vibration isolators (item 13) which are designed to reduce engine vibration being transmitted to the foundation on which the generating set is mounted. These isolators are fitted between the engine/alternator feet and the baseframe. Alternately, on larger models the engine/alternator is rigidly mounted on the baseframe and the vibration isolators are supplied loose to be fitted between the baseframe and the foundation.

3.8 Silencer and Exhaust System

An exhaust silencer is provided loose for installation with the generating set. The silencer and exhaust system reduce the noise emission from the engine and can direct exhaust gases to safe outlets.

3.9 Control System (Identification)

One of several types of control systems and panels (item 14) may be fitted to control the operation and output of the set and to protect the set from possible malfunctions. Section 9 of this manual provides detailed information on these systems and will aid in identification of the control system fitted on the generating set.

3.10 Output Circuit Breaker

To protect the alternator, a suitably rated circuit breaker (item 15) selected for the generating set model and output rating is supplied mounted in a steel enclosure. In some cases the output circuit breaker may be incorporated in the automatic transfer system or control panel.

APPENDIX 1.4 CRESTCHIC LOAD BANK DATA SHEET

Crestchic Ltd.

EQUIPMENT	65kW LOAD MODULE
SUPPLY VOLTAGE	415V, 50Hz, 3-PHASE, 4-WIRE
AUXILIARY SUPPLY	240V, 50Hz, 1-PHASE (6-AMPS)
STEP RESOLUTION	1kW
CONTROL	REMOTE ACS100H
CONTROL CABLE	10M
CUSTOMER	PERKINS ENGINES LTD FRANK PERKINS WAY EASTFIELD PETERBOROUGH PE1 5NA
CRESTCHIC CONTRACT NUMBER	1674

APPENDIX 2.

Test Bed Instrumentation

APPENDIX A2.1 INSTRUMENTATION SCHEMATICS

Table A2.1 Key to components in figure A2.1.

No.	Component
1	Fuel Tank
2	Fuel Pre-filter
3	Fuel Lift Pump
4	Fuel Filter Canister
5	Fuel Delivery Pump
6	Fuel Leakage Return Line
7	Fuel Injector
8	Cylinder
9	Air Filter
10	Compressor
11	Air Inlet Manifold
12	Inlet Valve
13	Exhaust Valve
14	Exhaust Manifold
15	Turbine

Table A2.2 Key to instrumentation in figure A2.1.

Item	Component
A	Fuel Meter (Electronic)
B	Fuel Meter (Optical)
C	Air Inlet Temperature
D	Air Inlet Mass Flow
E	Compressor Outlet Air Temperature
F	Boost Pressure (Air Inlet Manifold Pressure)
G	Exhaust Temperature (Turbine Inlet)
H	Exhaust Pressure (Turbine Inlet)
I	Exhaust Pressure (Turbine Outlet)
J	Exhaust Temperature (Turbine Outlet)
K	Smoke Detector
L	Engine Speed/ Crank Angle increments (Flywheel gear teeth) 126 per rev.
M	Ambient Temperature
N	Ambient Pressure
O	Combustion Cycle Datum (2:1 gear mechanism from crankshaft) 1 per cycle

Figure A2.1 Schematic for Components and Instrumentation in Fuel, Aspiration, Combustion and Exhaust systems

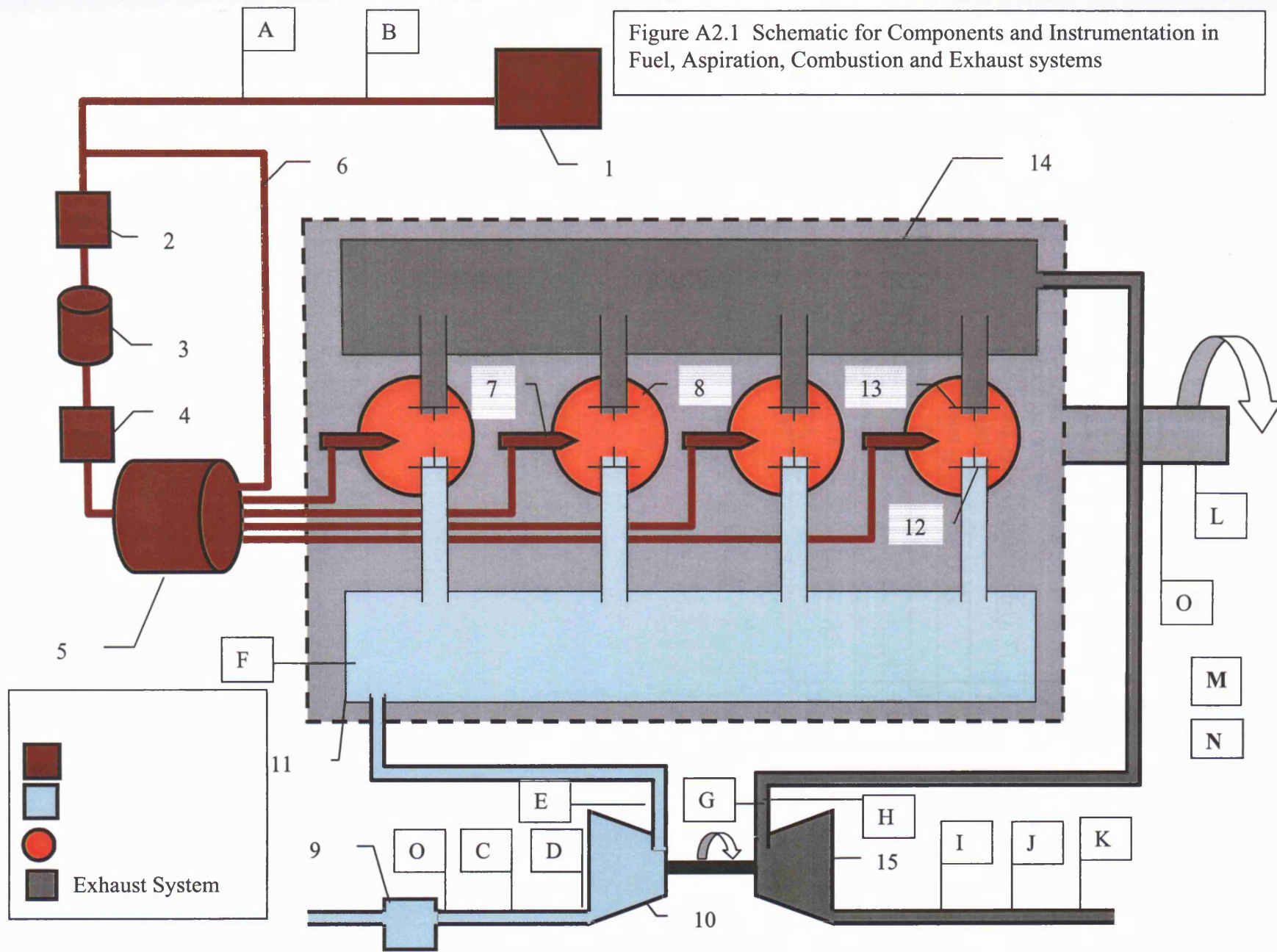
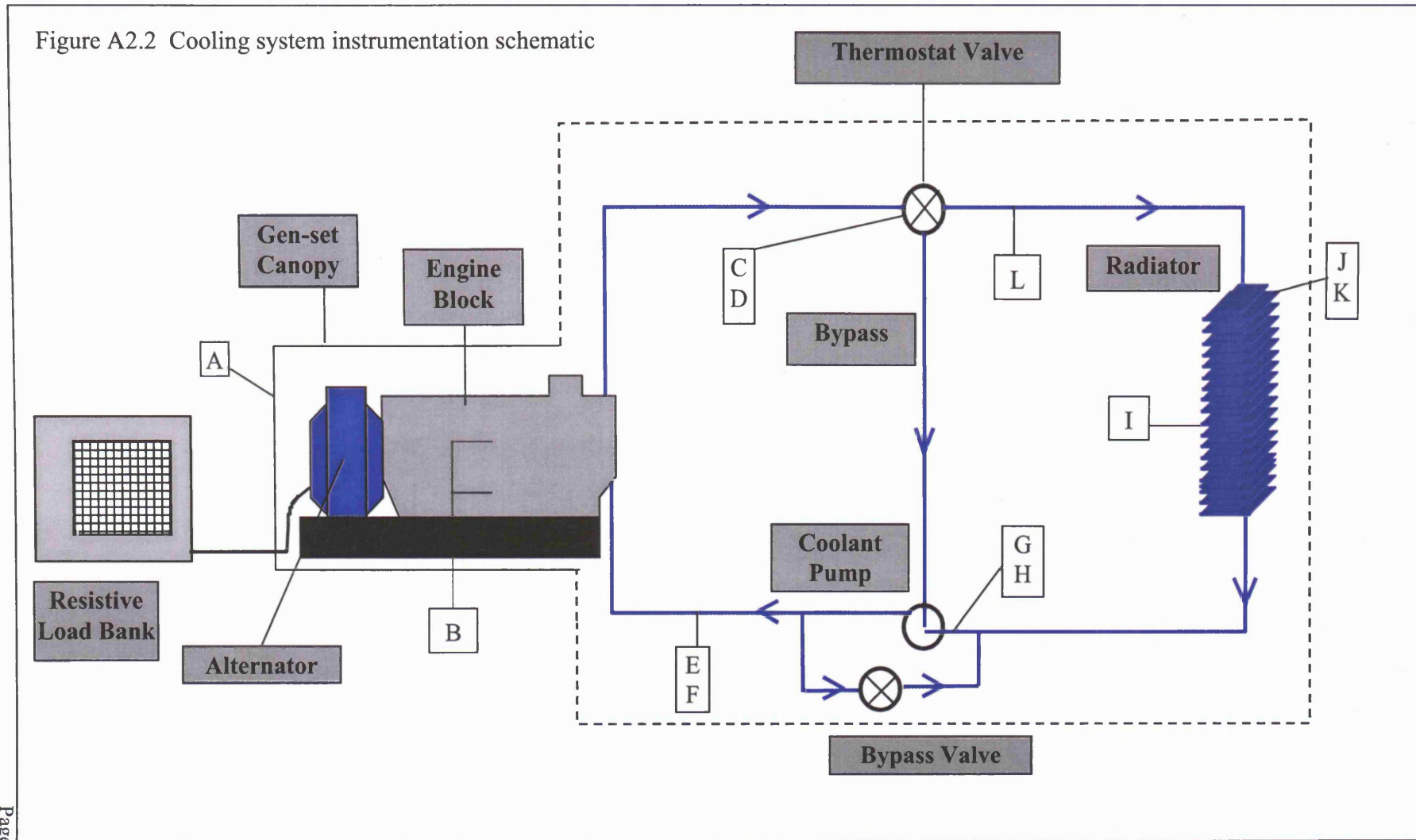


Table A2.3. Key to cooling system instrumentation in figure A2.2

A	Ambient Temperature, T_a	Thermocouple
B	Engine Block Temperature, T_b	4 Surface Temperature Transducers
C	Coolant Temperature at engine block outlet (thermostatic valve inlet), T_2	PRT
D	Coolant Pressure at engine block outlet, P_2	Pressure transducer
E	Coolant Temperature at engine block inlet (pump outlet), T_1	PRT
F	Coolant Pressure at engine block inlet, P_1	Pressure transducer
G	Coolant temperature at radiator outlet (pump inlet), T_3	PRT
H	Coolant pressure at radiator outlet, P_3	Pressure transducer
I	Air temperature at inlet to radiator, T_{amb}	4 thermocouples
J	Coolant temperature at inlet to radiator T_4	PRT
K	Coolant pressure at radiator outlet, P_4	Pressure transducer
L	Coolant volume flow rate to radiator, \dot{V}_{rad}	Turbine flow meter

Figure A2.2 Cooling system instrumentation schematic



SPECIAL NOTE

THE FOLLOWING
IMAGE IS OF POOR
QUALITY DUE TO THE
ORIGINAL DOCUMENT.

THE BEST AVAILABLE

IMAGE HAS BEEN

ACHIEVED.

APPENDIX A2.2 INSTRUMENTATION CALIBRATION REPORT

Memorandum



Date: 09 March 1999
 To: LUED
 From: David Wareing
 Subject: Gen-Set Calibration Report.

Engine Block Calibration:

Coolant Flow in l/min = $(0.023 * (\Delta P(\text{mmHg}) - \text{Static head}))^{0.5}$

Radiator Calibration:

Coolant flow in l/min = $(0.087 * (\Delta P(\text{mmHg}) - \text{Static head}))^{0.5}$

Chan #	Description	Calibration
1	Engine Speed	2000 rpm/V. Input 2 F-V at 126 teeth per rev
2	Coolant temp, pump inlet	Slope 17.540 degC/V, intercept 1.163 degC
3	Coolant temp, eng outlet under thermostat	Slope 17.562 degC/V, intercept 0.882 degC
4	Coolant temp, Radiator inlet	Slope 17.553 degC/V, intercept 1.828 degC
5	Air temp, inlet elbow	Slope 17.534 degC/V, intercept -1.166 degC
6	Air Temp, induction manifold	Slope 17.540 degC/V, intercept -0.408 degC
7	Spare	
8	Engine oil pressure, main gallery	0-10V = 0-6 bar
9	Air pressure, Induction manifold	0-10V = 0-2.5 bar
10	Coolant Pressure, pump inlet	0-10V = -1-1.5 bar
11	Coolant Pressure, pump outlet	0-10V = 0-2.5 bar
12	Coolant pressure, under thermostat	0-10V = 0-2.5 bar
13	Coolant pressure, radiator inlet	0-10V = 0-2.5 bar
14	Exhaust gas pressure, before turbo	0-10V = 0-6bar
15	Air pressure, inlet pipe	0-10V = -1-1.5 bar
16	Exhaust gas pressure, after turbo	0-10V = 0-2.5 bar
17	Spare	
18	Spare	
19	Spare	
20	Spare	
21	Surface temp cyl head LHS	I 0-200DegC = 0-1v
22	Surface temp cyl block LHS	J 0-200DegC = 0-1v
23	Surface temp cyl head RHS	K 0-200DegC = 0-1v
24	Surface temp cyl block RHS	L 0-200DegC = 0-1v
25	Oil temp, oil rail	M 0-200DegC = 0-1v
26	Exhaust temp front	N/A
27	Exhaust temp rear	N/A
28	Exhaust temp before turbo	N 0-1000 DegC = 0-5V
29	Exhaust temp after turbo	O 0-1000 DegC = 0-5V
30	Air temp, intake to enclosure	A 0-100 DegC = 0-1V
31	Air temp before rad, top LHS	B 0-100 DegC = 0-1V
32	Air temp before rad, bottom LHS	C 0-100 DegC = 0-1V
33	Air temp before rad, top RHS	D 0-100 DegC = 0-1V
34	Air temp before rad, bottom RHS	E 0-100 DegC = 0-1V
35	Air temp after rad, top LHS	F 0-100 DegC = 0-1V
36	Air temp after rad, bottom LHS	G 0-100 DegC = 0-1V
37	Air temp after rad, top RHS	H 0-100 DegC = 0-1V
38	Air temp after rad, bottom RHS	M 0-100 DegC = 0-1V

N.B all pressures are gauge. It is advisable to note ambient atmospheric conditions: pressure and humidity, during test work.

APPENDIX A2.3. ELECTRONIC FUEL METER CALIBRATION

ACKNOWLEDGEMENT

Thanks to Keng Boon Goh for his help in preparing this report

A2.3.1 OBJECTIVE:

To calibrate an electronic fuel meter for future benchmarking and controller design use.

A2.3.2 INTRODUCTION:

The Electronic Fuel Meter (provided by Perkins Engines Ltd) is produced by Enviro Systems Limited (see data sheet, section A2.9). It is typically used for monitoring fuel consumption on combustion engines and industrial boilers. There are two Hall-Effect sensors mounted inside an aluminium block. On the side of the aluminium block are two oval shape gears, one of them with a rod shape magnet mounted on it.

When the gears are moving, the sensors on the other side will pick up pulses due to changes in magnetic flux density. These pulses go through an integrated circuit within the sensor itself and produce a series of pulses at the output pin. The number of pulses over a certain time period will determine rate of fuel flow into the engine. So, the relationship between the pulses and fuel consumption rate can be written as:

$$\text{Fuel consumption rate} = f(\text{output pulse frequency}).$$

Note: At the beginning of this test, the two sensors (p/n: UGN3020) had been found to be not functioning as no pulses were detected. So, they have been replaced by UGN3503N which have the same function as the original sensor, but different electrical specification. The latter is more sensitive and is suitable for this test as the fuel rate is low. The following procedure has been proposed to carry out the calibration test.

Special Note

**Page 241 missing from
the original**

A2.3.3 MEASURANDS

Measurands are:

- a) Time taken ($T_{ss\#\#}$) for the diesel engine to burn a fixed volume of fuel at a series of load settings.
- b) Whilst recording, $T_{ss\#\#}$, simultaneously record the output signals from electronic fuel meter.
- c) Record ambient temperature near header fuel tank

There are two output pulse signals from the electronic meter (one from each of the sensors). Thus, assuming the sensors are diametrically opposed, then one pulse is recorded for each half-turn of the gear wheel. The pulses are recorded using the Matlab/Simulink/dSpace system. Data is recorded at a sampling rate of 100Hz.

A2.3.4 PROCEDURE

Installation of test equipment, electronic and optical fuel meter, header fuel tank to the engine is shown in Figure A2.3. The optical fuel meter is installed in series with the electronic flow meter so that the fuel rate can be measured simultaneously when data acquisition program is triggered to record the output from electronic meter. It is important to note that any leakage from the fuel distribution pump is returned to the supply line at a point after the fuel meter, so that the fuel measurement is net flow to the engine.

Perkins Diesel Engine 1000 series

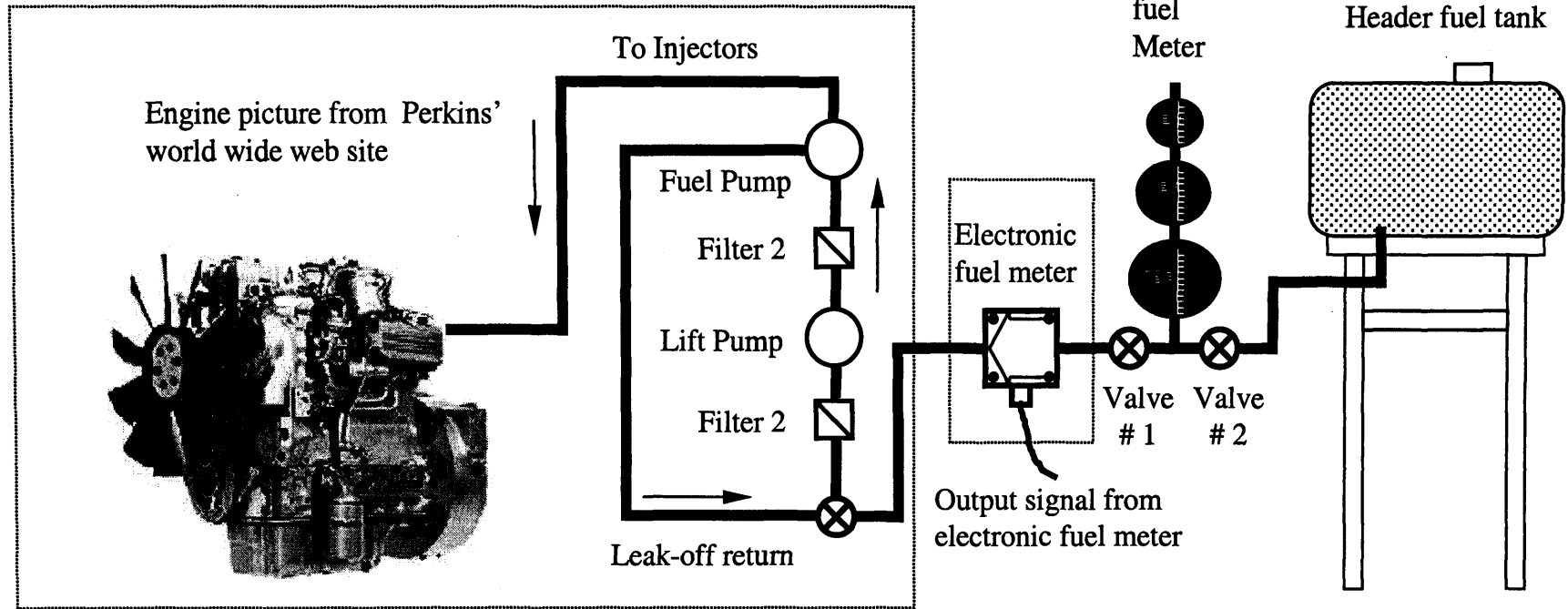


Figure A2.3: A schematic shows the installation and arrangement of the optical fuel meter and electronic fuel meter together with header fuel tank to the diesel engine

A2.3.5. RESULTS

The time taken for a fixed volume of fuel consumption were recorded in following table and the rate of fuel flow through the electronic fuel meter was calculated.

Table A2.4

Load applied (kW)	Measured Fuel Volume (ml)	Time taken (s)			Mean (s)	Flow rate (ml/s)	Mean Pulses per sec	Time per pulse
		1 st	2 nd	3 rd				
0	75	105.33	105.28	105.29	105.30	0.71	1.48	0.68
20	175	95.12	95.25	95.18	95.18	1.84	3.70	0.27
40	175	55.78	55.78	55.66	55.74	3.14	6.31	0.16
65	175	33.96	33.91	33.91	33.93	5.16	10.35	0.10

A2.3.6. FUEL SPECIFICATION

The fuel is from Texaco Gas Oil (see Fuel Specification Sheet, section A2.3.10.)

At ambient temperature at 24°C

Density = 0.866 kg/m³

A2.3.7. ASSUMPTIONS

1. Density of fuel does not change through out the test.
2. Fuel temperature is constant.

A2.3.8. FUEL FLOW RATE ESTIMATION FROM TRANSDUCER PULSE SIGNAL.

The fuel volume flow rate is calculated from the time period of the pulses. The number of time increments between the leading edge of each pulse is summed using a resettable integrator block in a Simulink™ block diagram (see figure A2.4 below). The point at which the integrator resets is used as a trigger point to estimate the average rate of fuel flow for the time period between the two pulses, from a look up table.

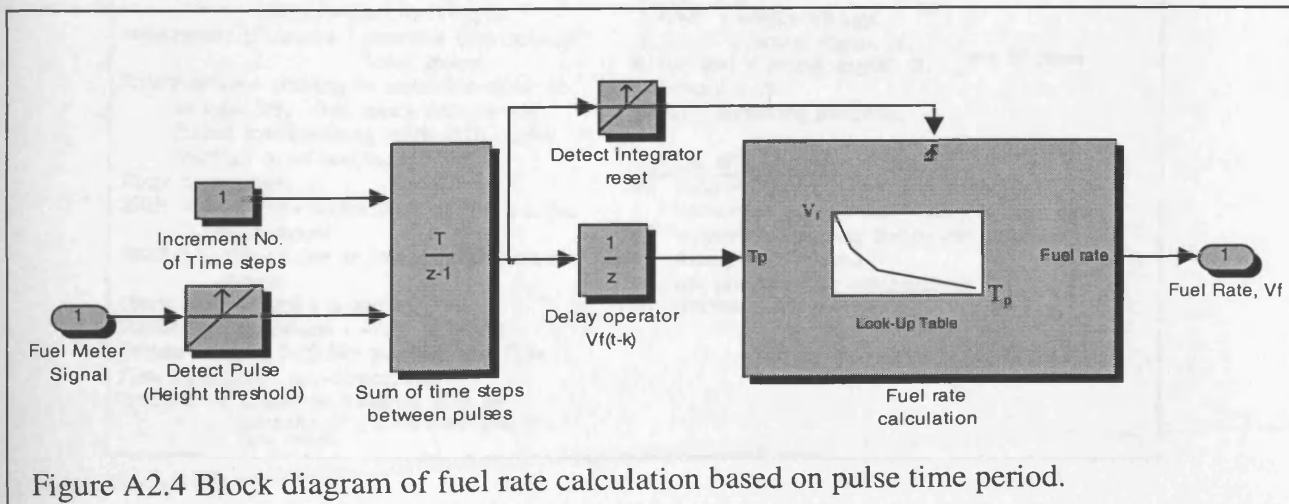


Figure A2.4 Block diagram of fuel rate calculation based on pulse time period.

SPECIAL NOTE

THE FOLLOWING

IMAGE IS OF POOR

QUALITY DUE TO THE

ORIGINAL DOCUMENT.

THE BEST AVAILABLE

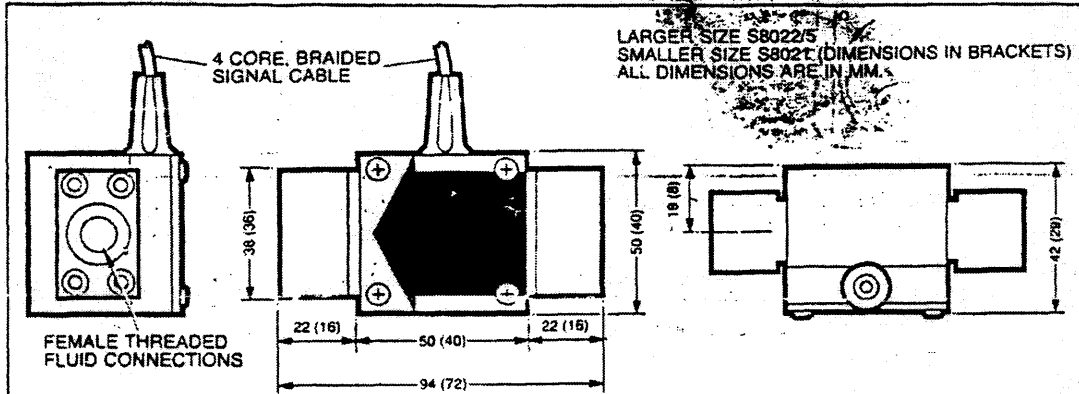
IMAGE HAS BEEN

ACHIEVED.

A2.2.9. ENVIROSYSTEMS FUEL FLOW TRANSDUCER DATA SHEET

EnviroSystems Ltd.		ES	Project GENERAL	Dwg S8021/S8022/5
Grange-over-Sands, Cumbria, England, LA11 6BE. Tel: 044 84 4233			Sheet	Rev 3
Title FLOW TRANSDUCER S8021 and S8022/5		This information is confidential		
Purpose CUSTOMER INFORMATION	Issued by MARKETING	© EnviroSystems Ltd.	Date 5.1.84	3422

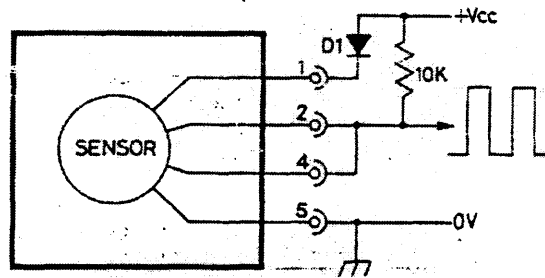
05395



ELECTRICAL SPECIFICATION

Power Supply : 4.5-24 volts (Vcc)
 Current consumption : 40 mA max
 Output : square wave pulses from open collector TTL, MSI and C-MOS compatible.
 Output high : supply voltage with 10K pull-up
 Output low : 100 mV typically
 Electrical terminations : unterminated 4-core screened cable 5.0 metres (16'5")
 Frequency : S8021 - 1 pulse/0.5cc
 S8022/5 - 1 pulse/1.25cc

ELECTRICAL CIRCUIT



D1 = IN 4001 or similar polarity reversal protection diode.

MECHANICAL SPECIFICATION

Minimum sensible flow : 0.025 L/hr (0.005g/h)
 Maximum flow : S8021 - 100 L/hr (22g/h)
 S8022/5 - 500 L/hr (110g/h)
 Measurement principle : positive displacement (oval gears)
 Construction : housing in aluminium alloy or ss type 316. Oval gears from carbon filled thermosetting resin with carbon bearings on ss shafts.
 Fluid connections :
 S8021 - 4mm hose connections or M13 x 1.0mm female thread
 S8022/5 - M18 x 1.5mm or M14 x 1.0mm female thread
 Operating Pressure : 6 bar max
 Operating Temperature : -15°C to +65°C
 Pressure drop : 0.03 bar at 50% of max flow
 Flow direction : uni-directional
 Precision : linear performance with an accuracy of ± 0.5% over 96% of flow range

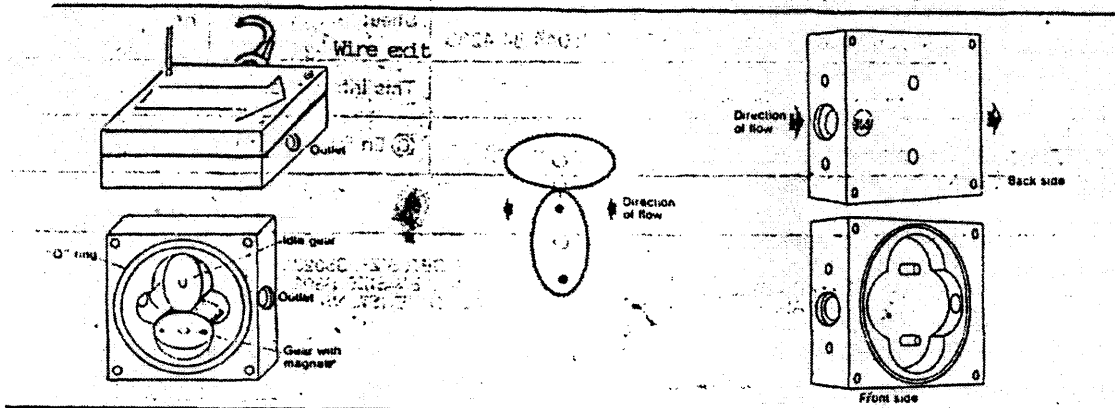
CONNECTIONS

- 1 (red) = supply voltage
 - 2 (blue) = output signal (A)
 - 4 (yellow) = output signal (B)
 - 5 (green) = 0V
- Braid = screening potential

TYPICAL APPLICATIONS

- a) accurate fuel consumption monitoring on combustion engines and heating boilers
- b) volumetric sampling device for batching/dosing applications
- c) low pressure drop applications
- d) process plant control

FLOW SENSOR MAINTENANCE - ASSEMBLY AND DISASSEMBLY 17/6/83



Should a foreign body manage to block the flow sensor the following procedure should be adhered to (see diagram).

- a) Unscrew the four screws, taking care not to drop them.
- b) Ease off the cover, being careful not to detach the oval gears in the process.
- c) Taking great care, remove the oval gears and clean them in fuel with the aid of a small brush.
- d) Clean the housing recess in the same way.
- e) Replace the oval gears taking care to relocate the gear containing the two magnets in the correct position as shown in the diagram, since the magnets must signal to the pick up area. The gear with the magnets must be underneath that part of the cover opposite the side which from which the wires leave.
- f) Check that the two oval gears mesh properly. A dislocated gear will cause an obstruction. If the unit is properly cleaned and assembled the two oval gears will rotate freely at the touch of a finger. NEVER FORCE.
- g) Replace the cover making sure that the arrow points in the direction of the liquid flow and that the gear with the two magnets is opposite the wire leaving the cover. To facilitate its relocation 'IN' is marked on the back of the sensor by the inflow aperture (see diagram).

PRECAUTIONS TO BE TAKEN DURING ASSEMBLY

- 1) Make absolutely sure that the direction of the liquid flow matches the direction of the arrow.
- 2) We prefer the orientation of the shafts on which the gears are mounted to be horizontal to reduce the risk of loosing fuel and parts during maintenance.
- 3) When mounting the unit take great care that no solid particle finds its way into the instrument or fuel supply tubing as any foreign body can cause the meter to malfunction, and may damage the gears.
- 4) Screw down the 4 screws holding the cover, but do not over-tighten.

A2.3.10. DIESEL GENERATOR SET TEST-BED FUEL SPECIFICATION

TEXACO GAS OIL

FUEL

Texaco Gas Oil is a distillate fuel manufactured to give clean burning, maximum heat output and efficient combustion in boilers and off-road diesel engines. It is a rebated gas oil, bearing a reduced rate of excise duty and as such is dyed red and contains chemical markers in accordance to Customs and Excise requirements, to prevent its use as a fuel in road vehicles.

Texaco Gas Oil is a "dual purpose" fuel and is recommended as a boiler fuel in domestic or light industrial installations with pressure jet burners and as a diesel fuel for off-the-highway equipment such as stationary diesel engines, farm tractors, construction equipment, railway and marine engines.

Texaco Gas Oil exceeds the latest requirements of relevant British Standard Specification BS 2869 Class A2 and D. Fuel properties are seasonally adjusted to maintain good low temperature operability.

	MINIMUM	MAXIMUM	TYPICAL
Appearance	Clear		Clear
Water Content, ppm		200	55
Density @ 15 °C, kg/m ³	820		866
Cetane Number	45		48
Strong Acid Number	Zero		Zero
Filterability (CFPP) °C	Winter Summer	-12 -4	-14 -9
Viscosity, Kinematic @ 40 °C, mm ² /s (cSt)	2.0	5.5	3.4
Sulphur, % Wt		0.20	0.12
Copper Corrosion, 3 hours @ 50 °C		Class 1	Class 1
Flash Point, (Closed Cup, PM) °C	55		80
Carbon Residue, on 10% distillation residue, % Wt		0.30	0.12
Sediment, % Wt		0.01	< 0.01
Ash Content, % Wt		0.01	< 0.01

Distillation Characteristics			
% Volume recovered @ 250 °C		65	30
% Volume recovered @ 350 °C	85		95

Gross Calorific Values			
KWh/rl			10.33
MJ/l			39.3
kcal/kg			10891

APPENDIX A2.4. ELECTRONIC AIR FLOW METER CALIBRATION

ACKNOWLEDGEMENT

Thanks to Keng Boon Goh for his help in preparing this report

A2.4.1 OBJECTIVE:

To calibrate an air flow meter for use in the aspiration system of the diesel generator set test-bed.

A2.4.2. INTRODUCTION.

A Lucas 4AM hot-wire air flow meter is used to measure mass flow rate of air into the engine. The transducer output is a d.c. voltage proportional to the air velocity through an orifice of fixed cross sectional area.

In order to calibrate the air flow meter, an air box is used to measure the actual air-flow rate into the engine. The air box allows the mass flow rate to be calculated, based on the Bernoulli effect and continuity equation as set out below.

A2.4.3. AIR BOX ORIFICE EQUATION INFORMATION

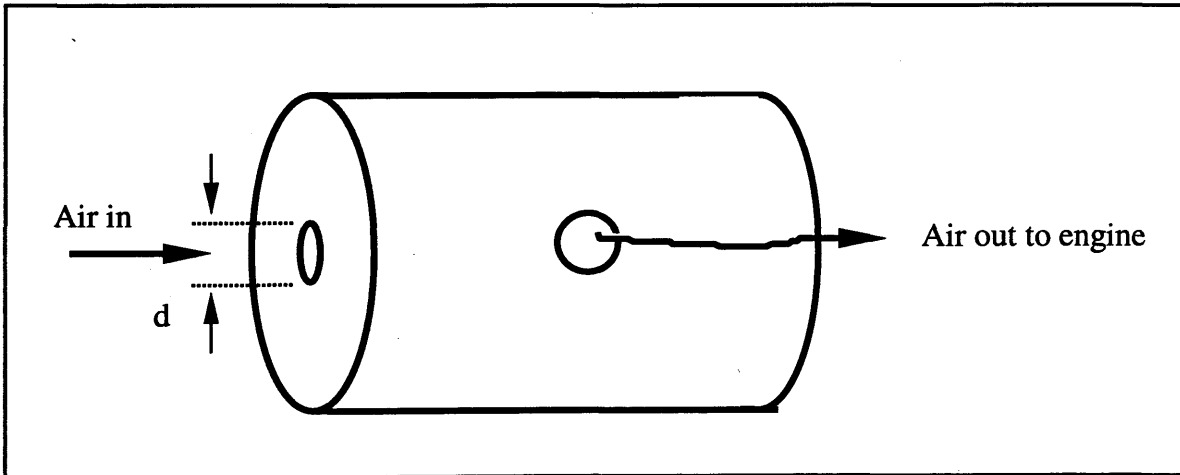


Figure A2.5 Sketch of air box.

A manometer inclined at 20° is used to indicate the pressure difference from measurement of the vertical change in water level (Δh). The formula to calculate the air mass flow, \dot{m}_a , is as follows.

$$\dot{m}_a = 1.4221 * 10^{-6} * d^2 \sqrt{\frac{P\Delta h}{T_{amb}}}$$

where, \dot{m}_a = air mass flow rate (kg/s)
 d = orifice diameter (mm)

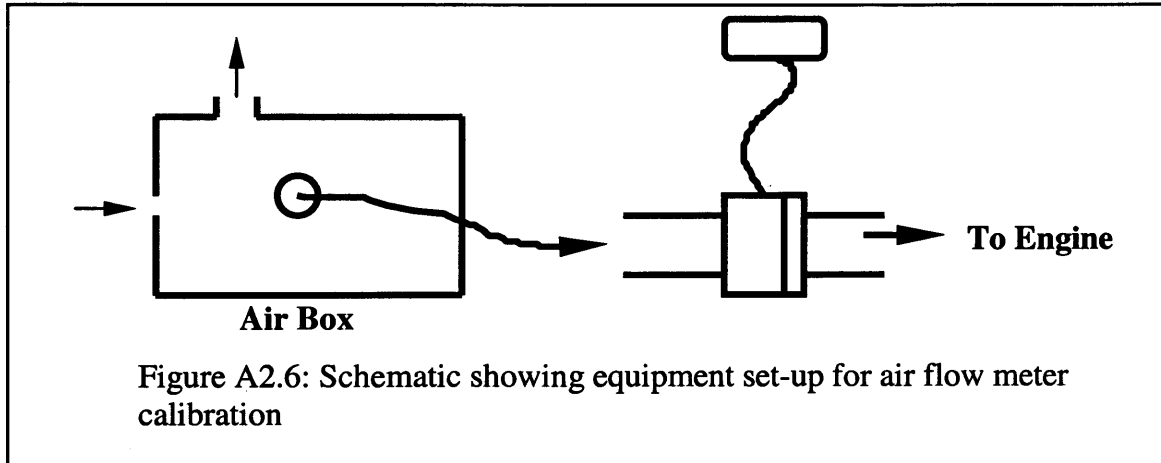
P = atmosphere pressure (mmHg)

T_{amb} = ambient temperature (K)

Δh = vertical change in water level (mm)

A2.4.4 TEST PROCEDURE:

Equipment set-up is as shown in Figure A2.6. The air box is connected before the air flow meter and the air flow meter is placed in between the air box and engine. Readings are recorded from both devices at various brake loads applied to the engine.



A2.4.5. MEASURANDS

Measurands are:

- a) Air flow meter reading (voltage, V)
- b) Engine speed reading (rpm)
- c) Manometer reading from drum (mm)
- d) Ambient temperature ($^{\circ}\text{C}$)
- e) Applied resistive load (kW)
- f) Air mass flow rate (kg/s) = m

A2.4.7. RESULTS

Atmospheric pressure at start, $P = 759.0\text{mmHg}$

Ambient temperature at start, $T_{amb} = 289\text{K}$

Δh at start = 0mm

Table A2.5. Air flow meter calibration data

Load (kW)	AFM (V)	Δh (mm)	Calculated air mass flow rate, \dot{m}_a (kg/s)
0	4.27	54	0.0553
20	4.42	67	0.0616
40	4.62	86	0.0698
50	4.72	98	0.0745
60	4.83	112	0.0797

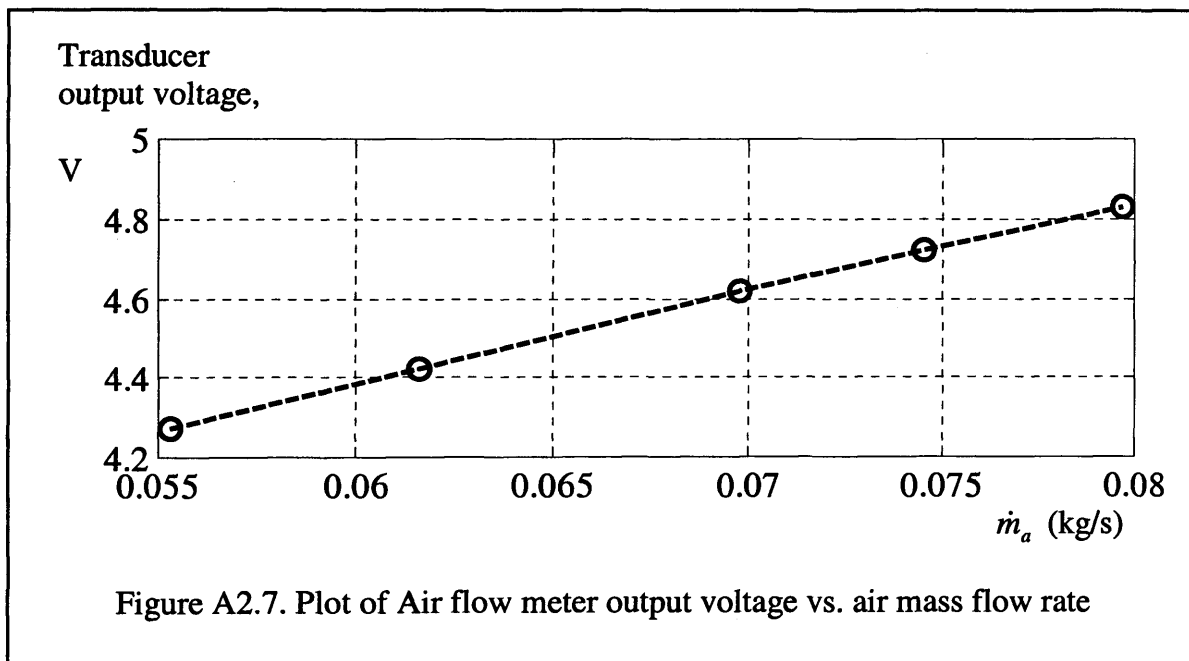


Figure A2.7. Plot of Air flow meter output voltage vs. air mass flow rate

Figure A2.7 shows the relationship of the transducer output, V , to air mass flow rate, \dot{m}_a , to be approximately linear over the working range of the engine. Using a least squares approach to establish a first order approximation for this relation yields;

$$\dot{m}_a = 0.0433V - 0.1300$$

Therefore, this relationship has been used to calculate air flow from transducer voltage.

APPENDIX A2.5 SMOKE METER CALIBRATION

ACKNOWLEDGEMENT

Thanks to Keng Boon Goh for his help in preparing this report

A2.5.1 OBJECTIVE:

To calibrate a smoke meter for use on diesel generator set test-bed.

A2.5.2 INTRODUCTION:

The smoke meter is manufactured by Telonic Berkeley Inc. The Opacity meter measures the relative light absorption of the smoke discharged from the diesel engine exhaust. Measurement is done by passing light pulses from a light emitting diode (LED) through the engine exhaust stream and using a photoelectric detector to detect the loss in light transmission due to smoke. The relative light energy loss is translated into both an opacity and a smoke density (k) value. Definition of opacity and smoke density are shown below.

Light intensity reduction can be expressed as, $\frac{I}{I_o} = e^{-naQL}$

where n = number density of smoke particles

a = average particle projected area

Q = average particle extinction coefficient

L = light beam path length within the smoke

k = naQ

I_o = intensity of LED source

I = intensity of light reaching photodiode

$$\frac{I}{I_o} = e^{-kL} = \frac{T}{100} = 1 - \frac{N}{100}$$

$$N = \left(1 - \frac{I}{I_o}\right) 100 = \text{Opacity}(\%), \quad k = \frac{\ln\left(1 - \frac{N}{100}\right)}{L} = \text{Smoke Density}(m^{-1})$$

A2.5.3 HARDWARE

The Celesco Model 107 consists of two basic units:

- i) The sensor unit, which is installed in-line in the engine exhaust gas flow line, contains a light source and photo-detector module.
- ii) A rack-mounted, all solid-state control unit contains the operating controls, digital display, power supplies and signal processing electronics.

A2.5.4 CALIBRATION OF SMOKE DETECTOR

Calibration of the smoke detector is performed by adjusting the span of the opacity scale on the control unit to 0 and 100%. This is done by adjustment of a potentiometer, firstly with a clear path between the LED and the photoelectric detector and setting the

potentiometer to read 0%, then blocking the path with an opaque obstruction and adjusting the potentiometer to read 100%.

A2.5.5 RESULTS

The calibrated smoke detector was used to record on-line smoke readings for a series of applied engine loads. Figure 1 shows how the smoke reading (opacity, %) changes with load (kW).

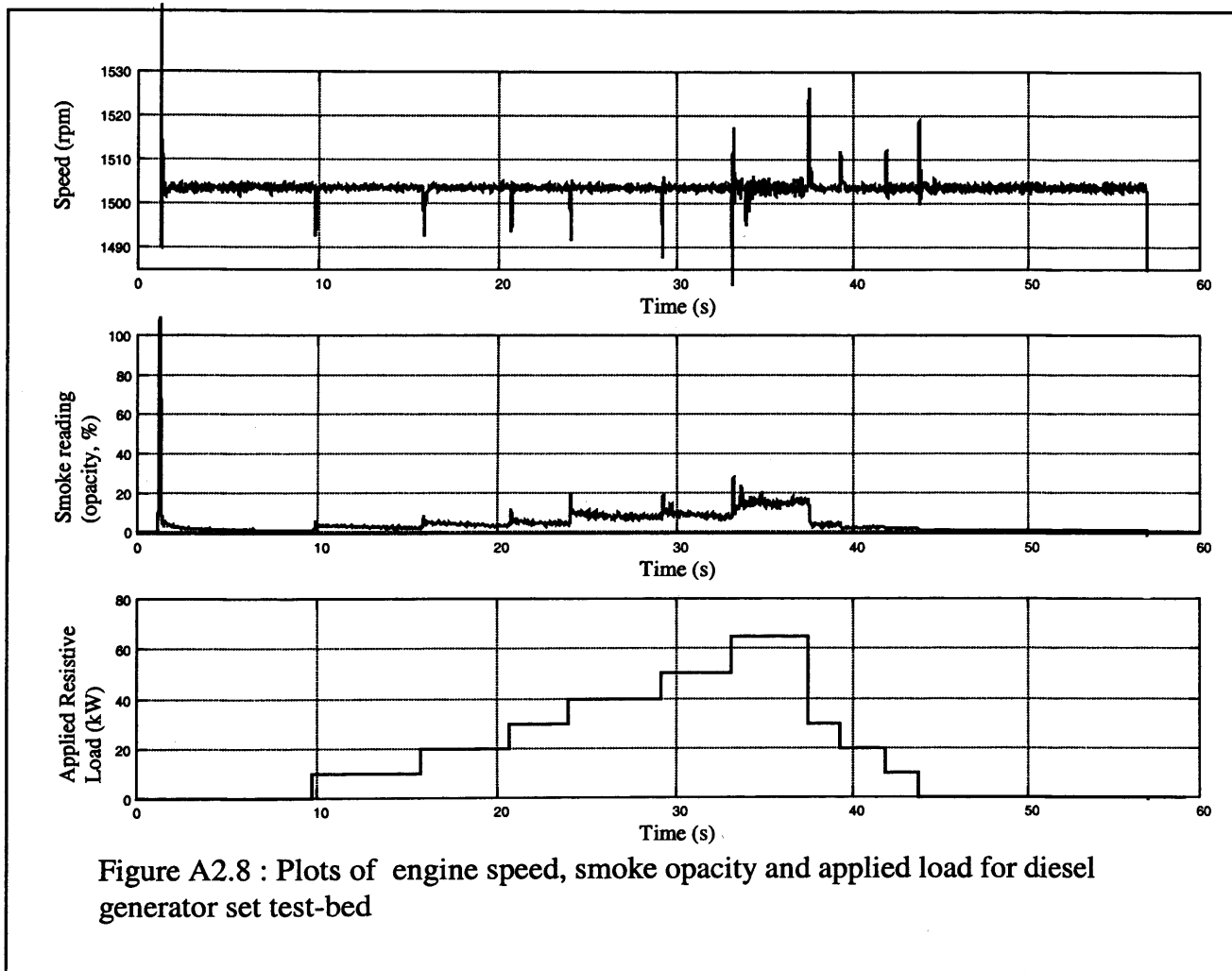


Figure A2.8 : Plots of engine speed, smoke opacity and applied load for diesel generator set test-bed

APPENDIX A2.6 INDICATION OF CRANK ANGLE WITH RESPECT TO FOUR-STROKE CYCLE.

A2.6.1 INTRODUCTION

This report describes the hardware and software techniques employed to produce an indication of crank angle to allow referencing of the four stroke diesel engine cycle.

A2.6.2 DATUM POINTS AND INSTRUMENTATION

The fly-wheel has 126 gear teeth, which mesh with the starter motor gear. A Hall effect transducer is mounted into the bell housing surrounding the flywheel. The gear teeth cut the magnetic flux of the transducer causing a small voltage to be induced across its terminals as an individual gear tooth passes the sensor.

A pair of gears has been fitted to the crankshaft pulley at the non-drive end of the engine. The gears have a 1:2 ratio between drive gear on the pulley wheel and the idler gear so that the idler gear rotates at half the engine speed (750 rpm). The four strokes of the engine cycle take two full revolutions so that a small hole may be drilled in the idler gear for use as a cycle datum, synchronised with top dead centre in the at the end of the compression stroke on cylinder 1. This means that a signal obtained from this datum may be used to indicate the start of the engine cycle. The procedure for obtaining the t.d.c. of cylinder 1 is described in the Perkins' engine manual [Perkins 95], operation 17A-01A/B.

An Infra-Red (IR) sensor is mounted on a frame attached the generator set canopy in order to detect the passage of the datum hole as the crankshaft rotates. A light emitting diode in the sensor emits a small beam of IR, the reflection of which from the gear wheel is detected by the transducer. As the datum hole passes the sensor the reflection is lost causing a small voltage pulse at the output terminals of the transducer.

A2.6.2 A SYSTEM FOR ON LINE INDICATION OF CRANK-ANGLE WITH RESPECT TO THE 4-STROKE ENGINE CYCLE.

So far two datum signals have been described;

- i) Angular increments of $126/360^\circ$ from the flywheel gear teeth.
- ii) One per cycle pulse obtained from the datum hole in idler gear

The aim of the next section is to describe a system which may be implemented on-line in real-time, capable of indicating the crank angle with respect to the four stroke engine cycle. Knowledge of the firing order will then allow this reference angle to be used as a basis for prediction of periodic events associated with any of the other cylinders.

A Simulink™ model has been produced see figure A2.9 which is used to detect the pulses from the flywheel gear tooth proximity sensor. This pulse indicates an increment in crank angle of $126/360$ degrees. These increments are summed using a re-settable discrete time integrator. The integrator is reset once per cycle using the pulse from the IR sensor as a trigger signal. The output from the integrator is then scaled with respect to the sample time to provide a output crank-angle indication in the range, $0 - 720^\circ$. The Simulink™ model has been converted to code suitable for use in real-time on the dSpace ds1103 microprocessor-based data acquisition hardware.

The system has been tested online and results showing crank-angle with respect to time are presented in figure A2.10.

APPENDIX A2. SPECIFICATION OF SAMPLE RATES FOR ACQUISITION

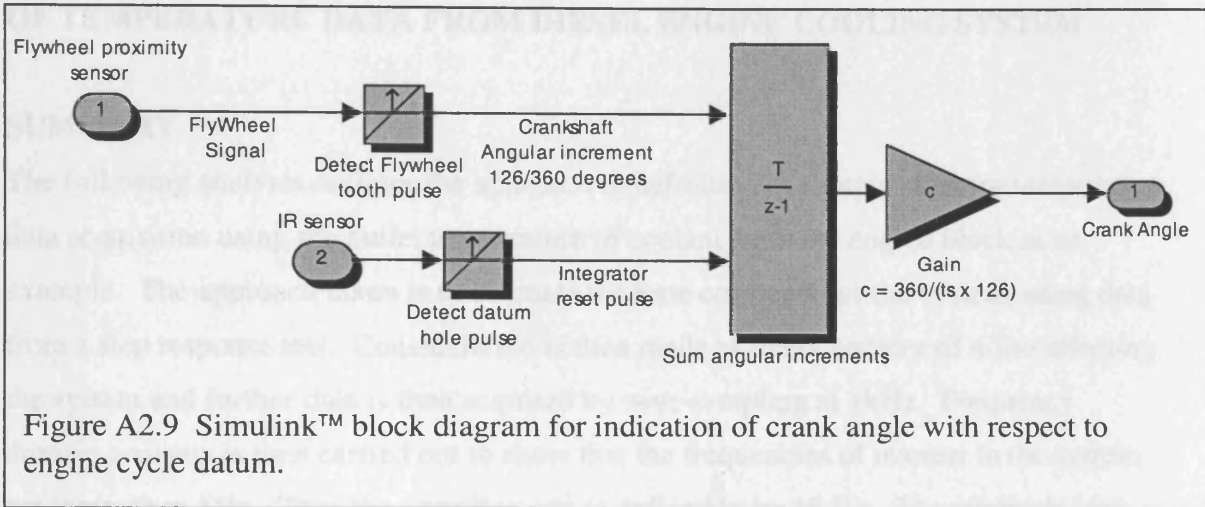


Figure A2.9 Simulink™ block diagram for indication of crank angle with respect to engine cycle datum.

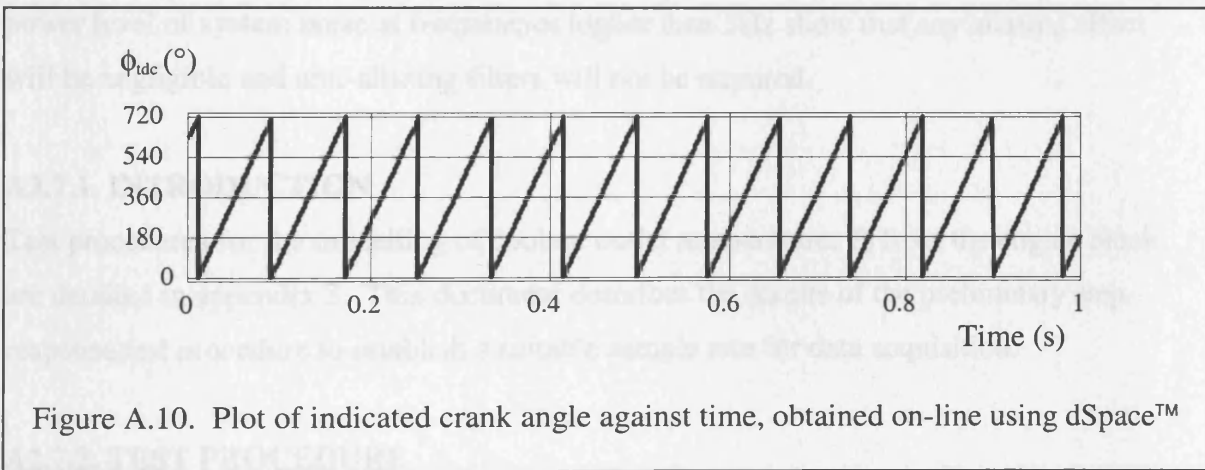


Figure A.10. Plot of indicated crank angle against time, obtained on-line using dSpace™

APPENDIX A2.7. SPECIFICATION OF SAMPLE RATES FOR ACQUISITION OF TEMPERATURE DATA FROM DIESEL ENGINE COOLING SYSTEM

SUMMARY

The following analysis outlines the approach to definition of sample rates for temperature data acquisition using the outlet temperature of coolant from the engine block as an example. The approach taken is to estimate the time constants for the system, using data from a step response test. Consideration is then made of likely sources of noise affecting the system and further data is then acquired by over-sampling at 1kHz. Frequency domain analysis is then carried out to show that the frequencies of interest in the system are lower than 5Hz. Thus the sampling rate is defined to be 10 Hz. The relatively low power level of system noise at frequencies higher than 5Hz show that any aliasing effect will be negligible and anti-aliasing filters will not be required.

A2.7.1. INTRODUCTION

Test procedures for the modelling of coolant outlet temperature, T_2 from the engine block are detailed in appendix 3. This document describes the results of the preliminary step-response test procedure to establish a suitable sample rate for data acquisition.

A2.7.2. TEST PROCEDURE

The time taken for the engine temperatures to reach a steady state temperature is known to be approximately 20-30 minutes. Figure A2.11 shows the response of the engine outlet temperature variable, T_2 , to a step change in engine load of 20kW, recorded at 10Hz for a period of approximately 17 minutes.

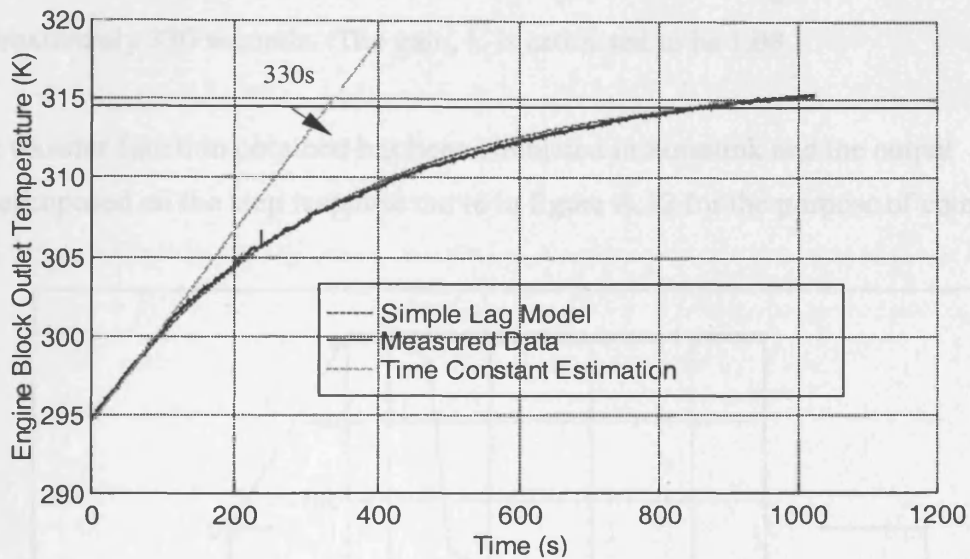


Figure A2.11. Step response data and model for T_2 with respect to 0-20kW step in engine load.

Likely sources of noise in the T_2 data series are thought to be;

- rotational frequency of the engine at 25Hz
- frequency of combustion events at 50Hz
- mains power supply frequency 50Hz

A further series of T_2 is then recorded at 1kHz for a period of approximately 20 seconds. Over-sampling at 1kHz will allow these noise frequencies to be observed by obtaining an estimate of the power spectral density up to 500Hz.

A2.7.3 ANALYSIS

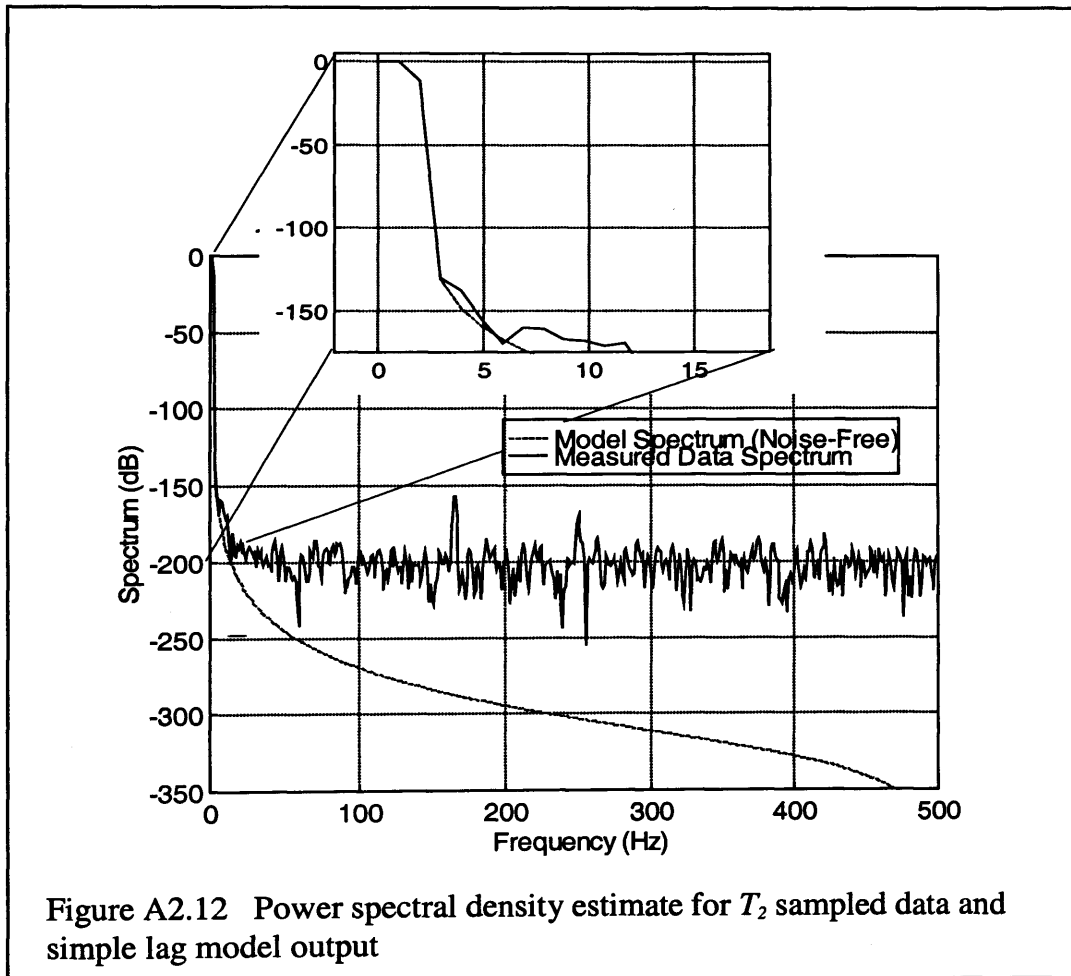
From the data presented in figure A2.11 it is possible to estimate a simple lag model for the step response with a transfer function of the form;

$$T_2(s) = \frac{k}{\tau s + 1} P(s)$$

Where k is a scalar, P is the engine load and τ is the time constant

The time constant, τ , is estimated from the response curve in figure A2.11 to be approximately 330 seconds. The gain, k , is estimated to be 1.08

The transfer function obtained has been simulated in Simulink and the output superimposed on the step response curve in figure A.12 for the purpose of comparison.



A spectral analysis has been carried out on the data series obtained at 1kHz as follows. 1024 data points were extracted from the series and a 1024 point Hanning window applied to the data series to avoid effects of 'leakage'. A 1024 point power spectral density estimation was obtained and is shown in figure A2.12.

For the purpose of comparison, a set of data has been obtained from the simulation, and the estimated power spectral density has been obtained using the same procedure as for the sampled data. Results have been superimposed onto figure A2.12.

A2.7.4. DISCUSSION

Results from the frequency domain analysis of the temperature data show that the frequencies of interest are contained within a narrow bandwidth, at frequencies lower than 5Hz. It is noted that frequencies outside this bandwidth are of relatively low power level lower than -100dB.

The expected sources of noise due to mains supply, frequency of rotation and frequency of combustion events are noted to be insignificant.

T_2 is measured using a platinum resistance thermometer (PRT), frequency analysis of other temperature variables measured using PRT's showed similar results. Temperature levels measured using thermocouples were seen to have higher noise levels at frequencies greater than 5Hz however these were still seen to be generally lower than -100dB.

The above results imply that 10Hz will be a suitable frequency for temperature data acquisition.

In specifying an anti-aliasing filter for use in data acquisition, the minimum stop-band attenuation, A_{\min} , would normally be set to a level equal to the expected quantisation error noise for a given ADC. This is given by the following relationship;

$$A_{\min} = 20\log_{10}(\sqrt{1.5} \times 2^{B+1})$$

where B is the number of bits in the ADC

Thus for a 16 bit ADC the minimum stop-band attenuation would be 104dB.

The relatively low power levels of the frequencies higher than 5Hz, imply that errors due to aliasing will be negligible and that anti-aliasing filters will not be required for the data, as no significant attenuation would be obtained.

A2.7.5. CONCLUSIONS

For the acquisition of the specified temperature data;

1. 10Hz represents a suitable sampling frequency.
2. Anti aliasing filters need not be employed for temperature measurements at this sampling frequency.

APPENDIX A2.8. CORRECTION FACTORS FOR RADIATOR COOLANT FLOW CALCULATION

A2.8.1. OBJECTIVE

To establish a relationship between pressure difference between radiator inlet and outlet and the coolant flow rate through the radiator.

A2.8.2. BACKGROUND

The radiator has been previously calibrated against a known orifice (see A2.8.7) and relationship identified as

$$\dot{V}_{rad} = 0.087\sqrt{\Delta P_{rad}} \quad (\text{l/min})$$

NB. ΔP_{rad} in mmHg

$$\Delta P_{rad} = (P_{ri} - H_{ri}) - (P_{pi} - H_{pi})$$

P_{pi} = Measured Pres. at Pump inlet.

P_{ri} = Measured Pres. at Radiator inlet

H = Measured static head for each pressure transducer

Application of this formula to a range of flow-rates set by using a series of fixed thermostat valves of different apertures is seen to result in large errors between the \dot{V}_{rad} and flow-rates measured from a turbine flow-meter (TFM).

A2.8.3. HYPOTHESIS.

Source of errors in the calculations is not obvious but the most likely source is thought to be measurement errors in P_{pi} . This pressure measurement is made close to the inlet to the pump and is seen to include sinusoidal noise of relatively high amplitude (compared to other pressure measurements in system) with component frequencies corresponding to the combustion frequency of the engine and its harmonics.

It is thought that inaccuracies in the measurement of P_{pi} may occur due to disturbances in the coolant flow caused by proximity to the pump impeller.

Theoretically for a given flow rate, the pressure drops across each component in the cooling system should remain the same irrespective of temperature and pressure rise within the system thereby allowing the flow rates to be calculated based on the differential pressures. This is seen to be the case across the engine block where the pressure drop between pump outlet and thermostat is seen to remain relatively constant under the full range of temperature and pressure conditions.

Therefore in order to identify the source of error we may consider the pressure drops across the coolant pump and also across the radiator as follows;

$$\Delta P_{rad} = (P_{ri} - H_{ri}) - (P_{pi} - H_{pi})$$

$$\Delta P_{pump} = (P_{po} - H_{po}) - (P_{pi} - H_{pi})$$

P_{po} = Measured Pres. at Pump outlet.

P_{pi} = Measured Pres. at Pump inlet.

P_{ri} = Measured Pres. at Radiator inlet

H = Measured static head for each pressure transducer

We know that;

- i) ΔP_{pump} should remain constant in all flow conditions
- ii) Both ΔP_{rad} and ΔP_{pump} are functions of P_{pi}

Therefore given that there is variation in ΔP_{pump} and errors observed in \dot{V}_{rad} , then if the cause of these two effects are measurement errors in P_{pi} then ΔP_{pump} and errors in \dot{V}_{rad} will be seen to correlate in some way.

A2.8.4. TEST PROCEDURE

Measure pressures at coolant pump inlet, pump outlet and radiator inlet. Record coolant flow rate to radiator with a TFM on inlet hose. The coolant system employs a double thermostat valve arrangement designed to open and close at a given temperature in order to regulate flow to the radiator.

Prescribe a range of flows to the radiator using a set of thermostat valves with preset apertures as follows;

Test Number	Thermostat 1 Nominal Aperture (mm)	Thermostat 2 Nominal Aperture (mm)
1	0	1
2	1	1
3	2	2
4	4	4
5	Fully open	Fully open

Table A2.6 Thermostat valve settings

Run engine at a series of different loads with step changes for each test in order to give a suitable range of pressures and temperatures in the coolant system. Loads for each test were chosen as a 'staircase' of 0, 20, 40, 60, 40, 20, 0 kW. The generator set was allowed to 'heat soak' for approx. 20 minutes at each load before a set of data was taken for each load.

Approximately 20,000 data points were taken at 1kHz in each set to allow simple averaging of pressure signals and hence minimise effect of sinusoidal and random noise sources known to be incident on the system.

A2.8.5 RESULTS.

Figure A2.13 shows the relationship between ΔP_{pump} and errors in \dot{V}_{rad} .

A best-fit line obtained by least squares regression has been obtained and is indicated on the graph in figure A2.13. This line represents a possible correction factor based on the ΔP_{pump} which should improve results of flow estimation from ΔP_{rad} .

The application of this correction factor to results obtained is shown in Figure A2.14.

Where measured flows from TFM are compared with calculated flows using;

$$\dot{V}_{rad} = 0.087\sqrt{\Delta P_{rad}} + CF \quad (l/min)$$

CF is correction factor from Figure A2.13

$$CF = -947.3\Delta P_{pump} + 477.6$$

Figure A2.15 shows a comparison of errors between the uncorrected flow calculation and the corrected version. The histograms show that the spread of errors in the corrected version is significantly smaller and more closely centred around zero.

	Uncorrected Data	Corrected Data
Mean of Errors	-8.36	-1.38
Standard Deviation of Errors	21.3	10.1

Table A2.7 Error Comparison.

A2.8.6. CONCLUSION.

Results indicate that the hypothesis is proven correct and that the errors lie in the measurement of P_{pi}

John Twiddle

18-8-99

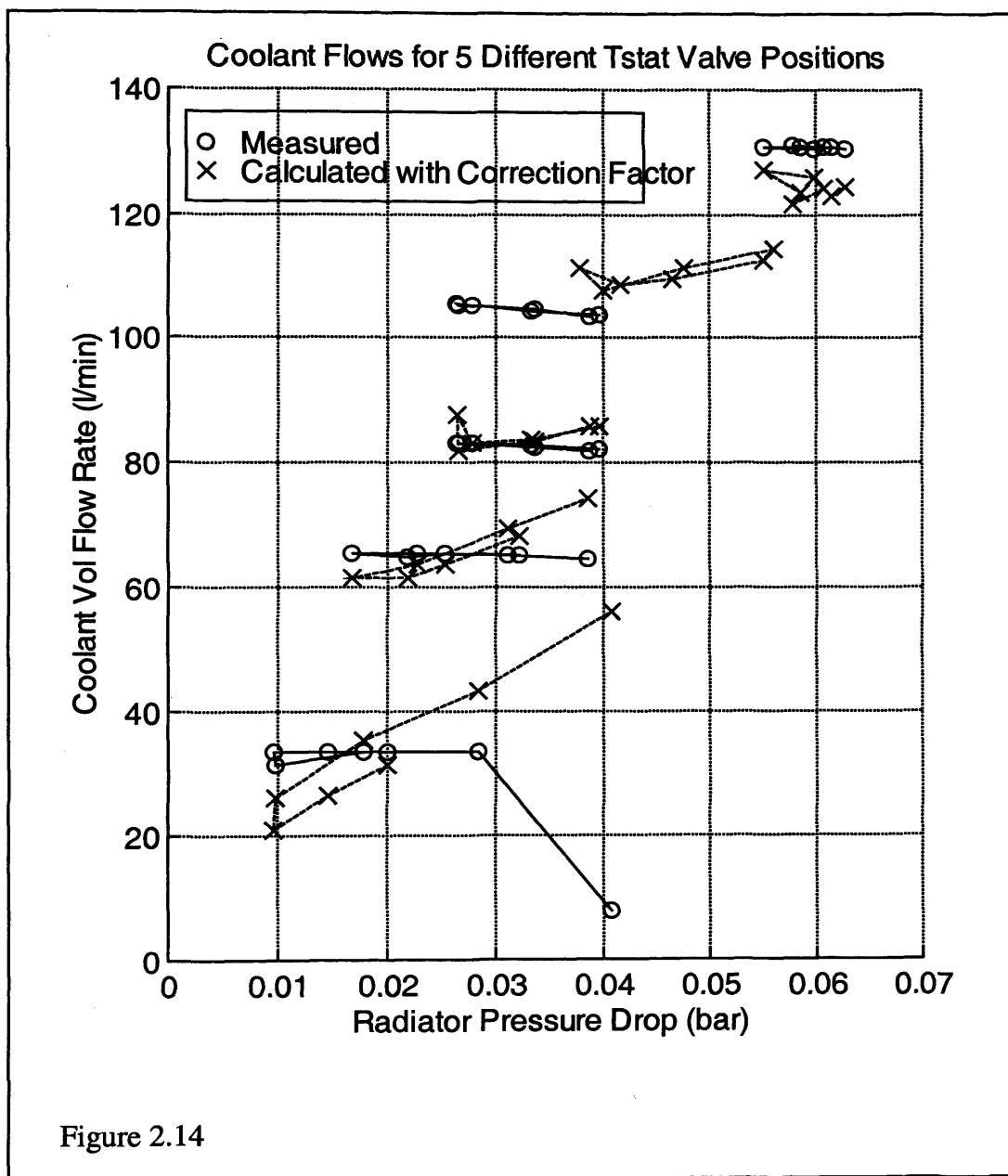


Figure 2.14

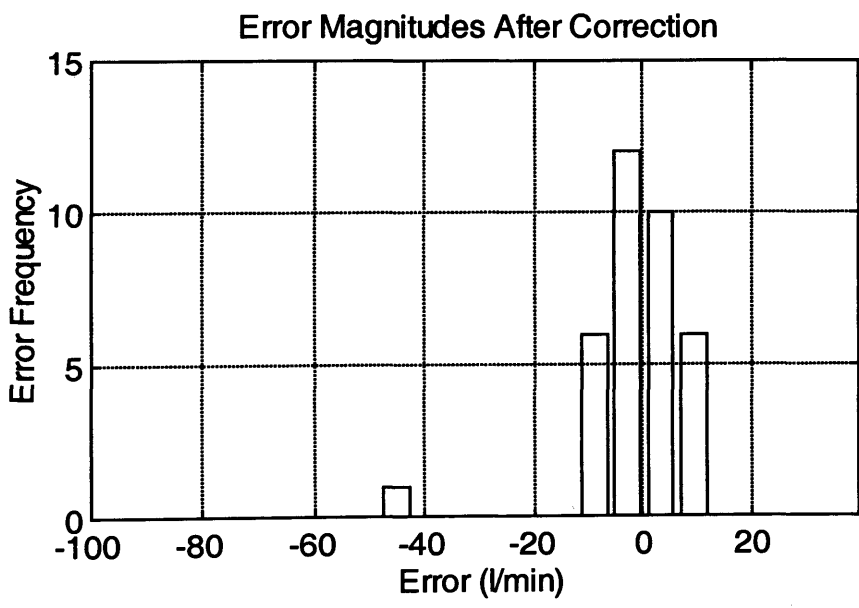
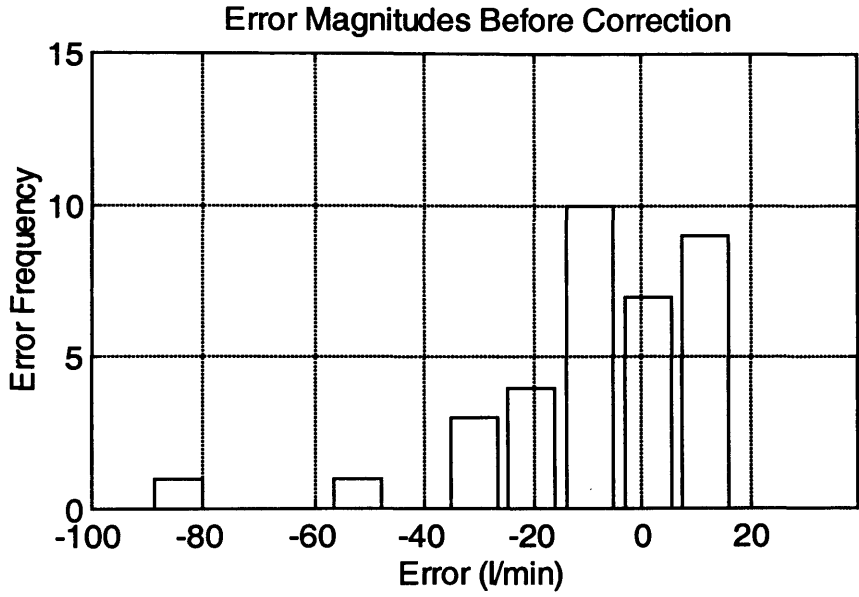


Figure A2.15

SPECIAL NOTE

THE FOLLOWING
IMAGE IS OF POOR
QUALITY DUE TO THE
ORIGINAL DOCUMENT.

THE BEST AVAILABLE
IMAGE HAS BEEN
ACHIEVED.

A2.8.7 ENGINE COOLANT FLOW RATES. CALIBRATION SHEETS

Flow characteristic of 1004-4T cylinder block
 Calibration between transducer tapping points 5 (timing case cover cab heater tapping)
 and 6 (thermostat housing below t/stat)

Plate B2 Differ. mm Hg	Flow ² (litres/sec) ²	Flow (litres/sec)	Flow (litres/min)	Engine			Calculated Flow (litres/sec)	ERROR Flow %
				Differential pressure mm Hg				
				Test 1	Test 2	Average		
0	0	0.0000	0.0000	0	0	0	0	0.000%
30	0.6269	0.7918	47.5065	27	27	27	0.788134	0.460%
60	1.2538	1.1197	67.1843	54	55	54.5	1.119738	0.000%
90	1.8807	1.3714	82.2836	83	83	83	1.381839	-0.762%
120	2.5076	1.5835	95.0129	110	113	111.5	1.601606	-1.140%
150	3.1345	1.7705	106.2277	140	138	139	1.788239	-1.004%
180	3.7614	1.9394	116.3666	167	165	166	1.954215	-0.762%
210	4.3883	2.0948	125.6903	190	190	190	2.090716	0.197%
240	5.0153	2.2395	134.3686	220	216	218	2.239476	0.000%
270	5.6422	2.3753	142.5194	248	243	245.5	2.376534	-0.051%
300	6.2691	2.5038	150.2286	275	270	272.5	2.503811	0.000%

K factor base on flow² = 0.023005756

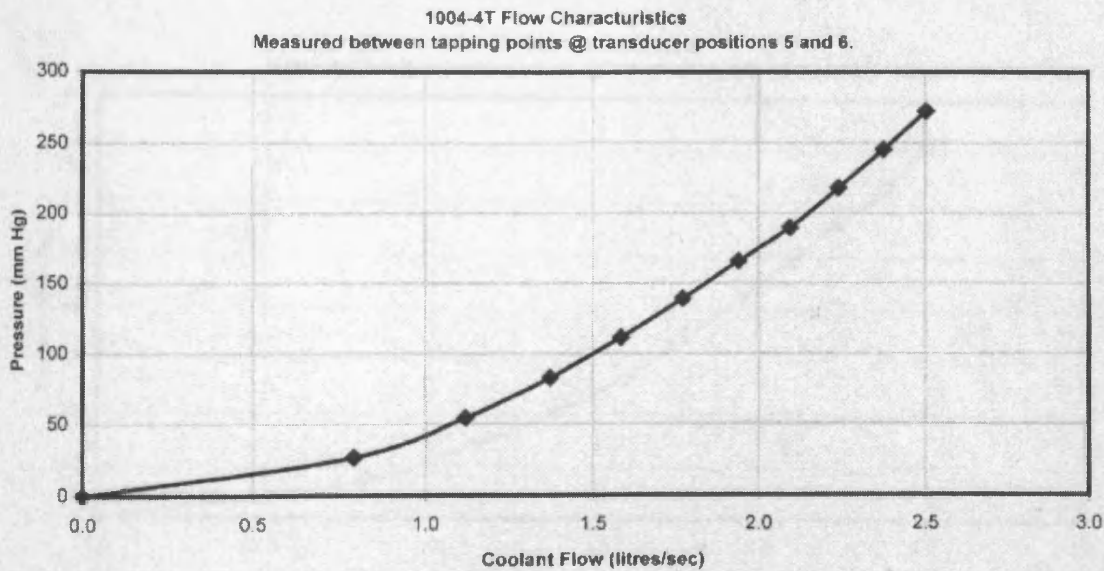


Figure A2.16 Engine block coolant flow rate calibration sheet

Figure A2.17 Raw data coolant flow rate calibration sheet

Flow characteristic of 1004-4T Electropac radiator
 Calibration between transducer tapping points 7 and 8

Plate B2 Differl. mm Hg	Flow ² litres/sec ²	Flow (litres/sec)	Flow (litres/min)	Engine Differential pressure mm Hg			Calculated Flow (litres/sec)	ERROR Flow %
				Test 1	Test 2	Average		
0	0	0.0000	0.0000	0	0	0	0	0.000%
30	0.626907	0.7918	47.5065	7	7	7	0.783425	1.055%
60	1.253814	1.1197	67.1843	14	14	14	1.10793	1.055%
90	1.880721	1.3714	82.2836	21	20	20.5	1.340681	2.240%
120	2.507627	1.5835	95.0129	27	27	27	1.538616	2.837%
150	3.134534	1.7705	106.2277	35	35	35	1.751792	1.055%
180	3.761441	1.9394	116.3666	43	42	42.5	1.930381	0.467%
210	4.388348	2.0948	125.6903	50	49	49.5	2.083296	0.551%
240	5.015255	2.2395	134.3686	57	57	57	2.235558	0.175%
270	5.642162	2.3753	142.5194	63	63	63	2.350275	1.055%
300	6.269068	2.5038	150.2286	72	71	71.5	2.503811	0.000%

K factor base on flow² = **0.087679279**

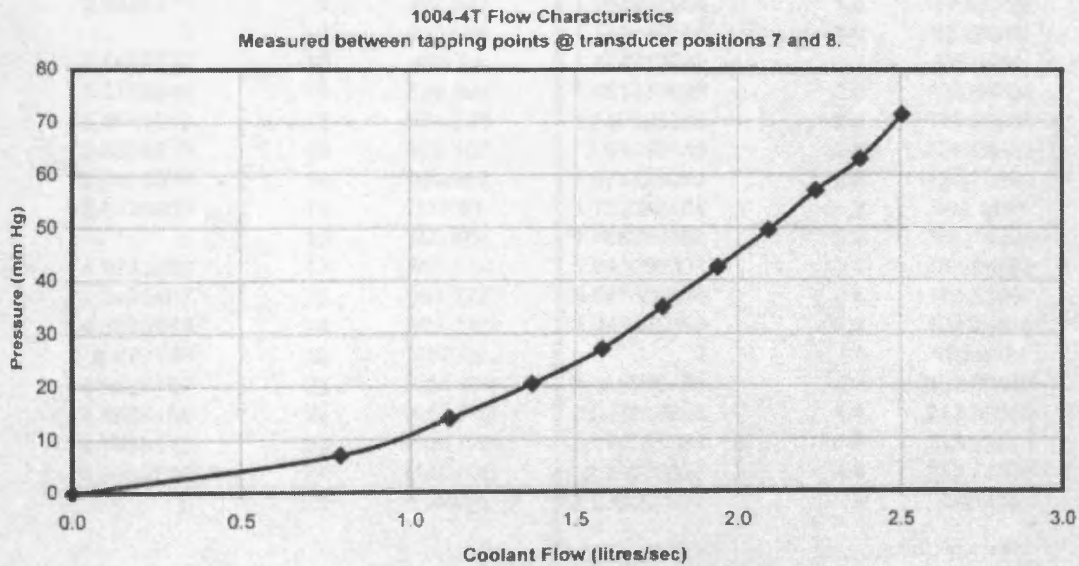


Figure A2.17 Radiator coolant flow rate calibration sheet

Flow characteristics of orifice plate 'B2'

Ref. calibration certificate 255F2/876

Flow litres/sec	Flow ² (litres/sec) ²	Differential pressure mm Hg	Calculated Flow (litres/sec) ²	y = 0.020896x (litres/sec)	ERROR %
0	0	0	0	0	0.000%
1.67	2.7889	133.51	133.4600206	1.67031267	-0.019%
2.5	6.25	303.02	299.0875	2.516381735	-0.651%
3.33	11.0889	528.79	530.6482206	3.3241644	0.176%
4.17	17.3889	830.32	832.1284206	4.165466315	0.109%
5	25	1196.35	1196.35	5	0.000%

Flow 0 - 5 litres / sec			Flow 0 - 2.23 litres / sec		
Flow litres/sec	Flow ² (litres/sec) ²	Differential pressure mm Hg	Flow litres/sec	Flow ² (litres/sec) ²	Differential pressure mm Hg
0	0	0	0	0	0
1	1	47.854	0.447213595	0.2	9.69664
1.4142136	2	95.708	0.632455532	0.4	19.39328
1.7320508	3	143.562	0.774596669	0.6	29.08992
2	4	191.416	0.894427191	0.8	38.78656
2.236068	5	239.27	1	1	48.4832
2.4494897	6	287.124	1.095445115	1.2	58.17984
2.6457513	7	334.978	1.183215957	1.4	67.87648
2.8284271	8	382.832	1.264911064	1.6	77.57312
3	9	430.686	1.341640786	1.8	87.26976
3.1622777	10	478.54	1.414213562	2	96.9664
3.3166248	11	526.394	1.483239697	2.2	106.66304
3.4641016	12	574.248	1.549193338	2.4	116.35968
3.6055513	13	622.102	1.61245155	2.6	126.05632
3.7416574	14	669.956	1.673320053	2.8	135.75296
3.8729833	15	717.81	1.732050808	3	145.4496
4	16	765.664	1.788854382	3.2	155.14624
4.1231056	17	813.518	1.843908891	3.4	164.84288
4.2426407	18	861.372	1.897366596	3.6	174.53952
4.3588989	19	909.226	1.949358869	3.8	184.23616
4.472136	20	957.08	2	4	193.9328
4.5825757	21	1004.934	2.049390153	4.2	203.62944
4.6904158	22	1052.788	2.097617696	4.4	213.32608
4.7958315	23	1100.642	2.144761059	4.6	223.02272
4.8989795	24	1148.496	2.19089023	4.8	232.71936
5	25	1196.35	2.236067977	5	242.416

Table A2.8 Flow characteristics of standard orifice plate B2 used for flow rate calibration.

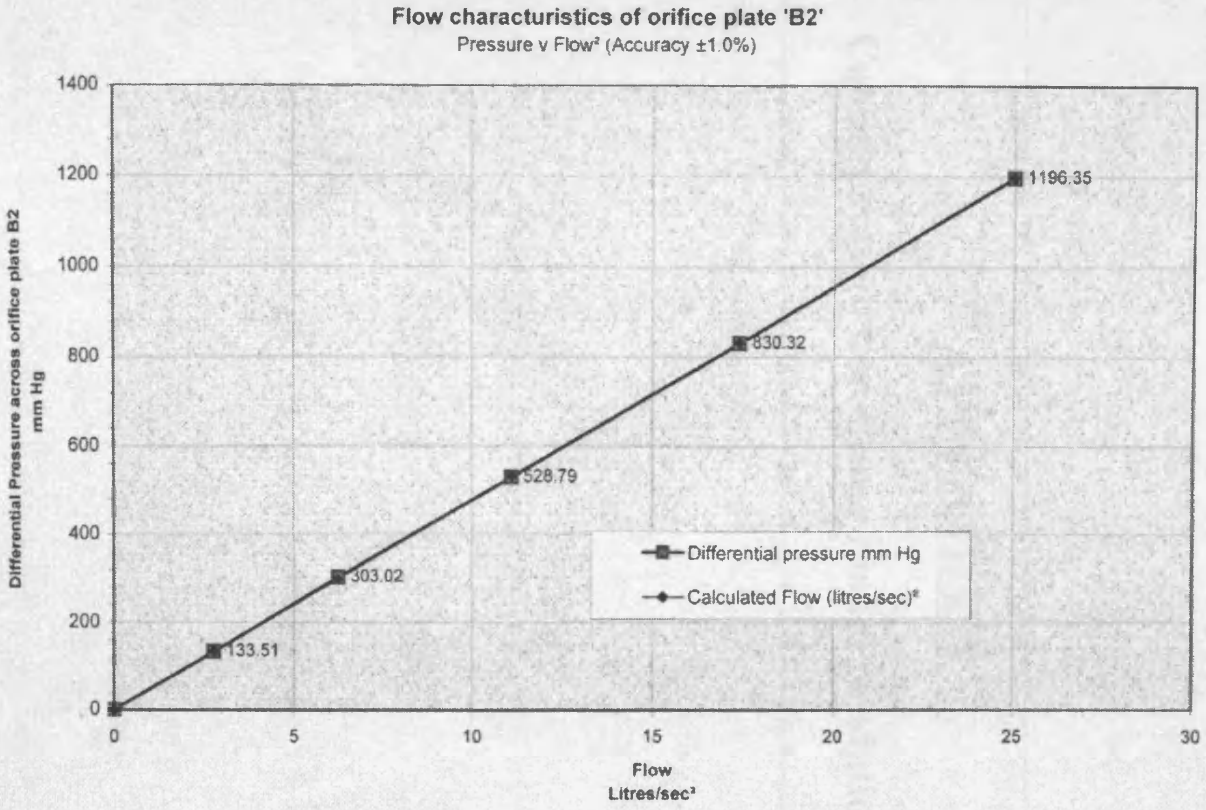


Figure A2.18 Plot of square of flow rate against pressure difference for standard orifice plate 'B2'

APPENDIX 3.

Cooling system non-linear model validation results

SUMMARY

This document describes the processes undertaken in the development of two non-linear models representing heat transfer in the diesel engine cooling system. The test procedures and methods for data acquisition are outlined along with the techniques for estimating the parameters of the model.

The non-linear parameters of the model are estimated using the series-parallel model approach, and the resulting parameters are compared to those obtained by theoretical analysis. This exercise showed that the theoretical approach and the series-parallel model results were complementary, in that the theoretical approach established the functional relationship between the parameters, but estimations from the series-parallel model allowed appropriate scaling. Parameters associated with heat transfer coefficients have been noted to vary little within the temperature range investigated here, and could be regarded as constants within this range at the cost of little additional model error.

Resulting parameters have been implemented in two non-linear models and simulated in Simulink. The model results are presented and discussed and the models have been documented in some detail as an appendix to the main report. A fuzzy model for thermostat valve operation with respect to temperature has been successfully implemented as a component of the non-linear model for the outlet temperature from the radiator.

Results from the two non-linear models are shown to be generally good with low errors. However, the model errors for the radiator outlet temperature, T_3 , are noted to be high when the thermostat valve is closed, probably due to the change in mode of heat transfer to the sensor used to measure T_3 when there is low or no flow through the radiator.

The low errors in the model demonstrate that the parameters have been successfully estimated, indicating that they may be usefully employed in a sliding mode observer system for fault diagnosis of the cooling system.

CONTENTS

Nomenclature

1. Introduction

2. Background theory and parameter estimation procedures

2.1 Radiator Heat Transfer Model

2.1.1 Objective

2.1.2 Theory

2.1.3 Justification of this approach to radiator modelling

2.1.4 A technique for radiator model validation

2.1.5 Test procedure

2.2 Heat Transfer from Block to Coolant

2.2.1 Objective

2.2.2 Theory

2.2.3 A technique for heat transfer model validation

2.2.4 Test procedure

3. Results

3.1 Introduction

3.2 Engine Block to Coolant Heat Transfer Model ('T₂ Model')

Validation

3.2.1 Data Acquisition.

3.2.2 Data Analysis

3.2.3 Comparison of estimated and theoretically derived parameters

3.2.4 Model Simulation Results.

3.3 Radiator Heat Transfer Model ('T₃ Model') Validation

3.3.1 Data Acquisition.

3.3.2 Comparison of estimated with theoretically derived parameters.

3.3.3 Results from non-linear T₃ model simulation.

4 Discussion

5 Conclusions

References

Appendices

A1 Matlab 'm-files'

A2 T2 Model Documentation

A3 T3 Model Documentation

NOMENCLATURE

VARIABLE	DESCRIPTION	UNITS	CHANNEL NUMBER(S)* (WHERE APPLICABLE)
a_i	Non-linear parameters. (i=1 - 3)	-	
f	Frequency	Hz	
f_s	Sampling frequency	Hz	
h	Heat transfer coefficient	kW/m ² .K	
k	Thermal conductivity	kW/mK	
k_i	Correction factors (i=1, 2)		
m	Mass	kg	
\dot{m}	Mass flow-rate	kg/s	
u	Velocity		
A	Surface area	m ²	
A_{min}	Minimum free flow area through radiator	m ²	
C_p	Specific heat capacity	kJ/kg.K	
D_h	Hydraulic Diameter	m	
F	Shape factor	-	
G	Mass Velocity	kg/sm ²	
L	Flow length of radiator	m	
N	Rotational speed	r.p.m.	Ch#1
P	Pressure	bar	
P_1	Coolant pump outlet pressure.	bar	Ch#11
P_2	Engine block coolant outlet pressure	bar	Ch#12
P_3	Radiator coolant outlet pressure	bar	Ch#10
P_{ri}	Radiator inlet pressure	bar	Ch#13
Pr	Prandtl's number	-	
Re	Reynolds' number	-	
St	Stanton's number	-	
T	Temperature	K	
T_1	Coolant pump outlet temperature.	K	
T_2	Engine block coolant outlet temperature	K	Ch#3

* See Appendix A2.2

T_3	Radiator coolant outlet temperature	K	Ch#2
T_b	Engine block surface temperature	K	Ch#23
T_{amb}	Air temperature at radiator	K	Ch#[31,32,33,34]/4
T_a	Air temperature at inlet to gen-set canopy	K	Ch#30
T_{ri}	Coolant temperature at radiator inlet	K	Ch#4
\dot{Q}_{amb}	Heat transfer to ambient from radiator	kW	
\dot{V}	Volume flow-rate	l/s	
\dot{V}_{rad}	Coolant volume flow-rate at radiator inlet	l/s	
\dot{V}_b	Coolant volume flow-rate through block	l/s	
W	Engine Load	kW	
β_i	Regression coefficients (i=0-3)	-	
Σ	Relative emissivity	-	
μ	Coefficient of molecular Viscosity	Pa.s	
λ	Arbitrary constant for parameter estimation	-	
ν	Dynamic Viscosity	m ² /s	
ϕ_i	Parameterised temperature variable	-	
σ	Boltzmanns Constant	kW/m ² K ⁴	
ρ	Density	kg/m ³	
α	Normalised volume flow rate to radiator;	-	
	$\frac{\dot{V}_{rad}}{\dot{V}_{rad max}}$		

SUFFIXES (SUB-SCRIPT);

SUFFIX	MEANING
a	Air
amb	Ambient
b	Block
c	Coolant
rad	Radiator
ri	Radiator inlet

1 INTRODUCTION

This document describes the development of two non-linear models for heat transfer in the cooling system of a diesel engine. The models are obtained from theory originally developed by Chiang et al [Chiang 82] and are modified as appropriate so as to be suitable for the diesel generator set test-bed. The thermodynamic cooling system models were also developed for use as a source of simulation data in Fuzzy Model Based Fault Diagnosis of a Diesel Engine Cooling System [Twiddle 99]. Parameters for the heat transfer equations are estimated from acquired engine data using the *series parallel* model [Ioannu 96].

This analysis will generally aim to increase knowledge of the cooling system, knowledge which will be later be used as the basis for the development of diagnostic techniques. The parameter estimation procedure will result in a set of parameters, which may then be directly implemented in a sliding-mode observer-based system for fault diagnosis.

The document is divided into a number of sections, firstly the theoretical background for the cooling system model and the approach to parameter estimation is explored in section 2, concluding with the derivation of suitable test procedures. Section 3, presents the results from the model development processes and discussion and conclusions made in sections 4 and 5 respectively. A number of appendices are added to document the models which have been produced.

2 BACKGROUND THEORY AND PARAMETER ESTIMATION PROCEDURES

2.1 RADIATOR HEAT TRANSFER MODEL

2.1.1 OBJECTIVE

Acquire data to validate the non-linear model of heat dissipation from the radiator

2.1.2 THEORY

The radiator provides a means of dissipating heat from the coolant. Heat transfer from a radiator is improved by addition of finning to increase the effective heat transfer area.

The heat transfer from the radiator may be described by the following first order differential equation; [Twiddle 99]

$$\frac{dT_3}{dt} = \frac{\dot{m}_{rad} C_p}{m_{rad} C_p} (T_2 - T_3) - \frac{h_{rad} A_{rad}}{m_{rad} C_p} (T_3 - T_{amb}) - \Sigma \sigma F A_{rad} (T_3^4 - T_{amb}^4) \quad \dots \quad 2.1$$

where;

m_{rad} is the mass of coolant in the radiator

\dot{m}_{rad} is the mass flow rate of coolant through the radiator

2.1.2.1 NTU METHOD FOR RADIATOR MODELLING

There are two possible approaches to modelling the heat transfer from a radiator. Chiang et al [Chiang 82] employ the Number of Transfer Units method (NTU) to express the effectiveness of the radiator. This compares the heat gained by the air blown over the radiator by the fan to the heat rejected from the coolant as it passes through the radiator. This technique requires the ambient air mass flow rate over the radiator to be measured or estimated and the temperature of the ambient air to be measured at inlet and outlet of the radiator.

2.1.2.2 HEAT TRANSFER COEFFICIENT APPROACH TO RADIATOR MODELLING

Ozisik [Ozisik 85 pp571] describes the approach to evaluation of the heat transfer coefficient for a finned surface radiator. This method requires only the temperature of the inlet ambient air along with its velocity over the radiator to be measured or estimated to allow calculation of a value for h_{rad}

Three dimensionless groups are used to describe the heat transfer from the radiator these are;

$$\text{Stanton's Number } St = \frac{h_{rad}}{Gc_p} \quad \dots \quad 2.2$$

$$\text{Reynolds Number, } Re = \frac{GD_h}{\mu} \quad \dots \quad 2.3$$

$$\text{Prandtl's Number, } Pr = \frac{c_p \mu}{k} \quad \dots \quad 2.4$$

where the working fluid is air and;

$$G = \frac{\text{mass flow rate of air}}{\text{minimum cross sectional area of radiator}} = \frac{\dot{m}_{air}}{A_{min}} = \text{mass velocity}$$

$$D_h = \frac{4LA_{min}}{A} = \text{hydraulic diameter}$$

By arranging;

$$(St)(Pr)^{2/3} = f(Re) \quad \dots \quad 2.5$$

h_{rad} may be presented in the form of a chart [Kays 55]. From the above relationship it may be seen that h_{rad} is a function of the fluid properties of the ambient air at ambient temperature, air velocity over the radiator which is some function of fan speed, and hence engine speed and also the geometry of the radiator itself which is fixed. Therefore for the given radiator $h_{rad} = f(N, T_{amb})$. In the diesel generator set application the speed is fixed therefore $h_{rad} = f(T_{amb})$.

2.1.3 JUSTIFICATION OF THIS APPROACH TO RADIATOR MODELLING

The modelling of the radiator using the heat transfer method will require one less measured variable to be monitored in the validation process and more significantly, will also require one fewer measured variable to be monitored to provide inputs to the radiator diagnostic.

The radiator will transfer heat to ambient via both convection and radiation. The validation procedure for the stated model [Twiddle 99] needs to estimate values for both h_{rad} and Σ_{rad} . However, how significant is the heat radiated compared with the heat transferred by convection?

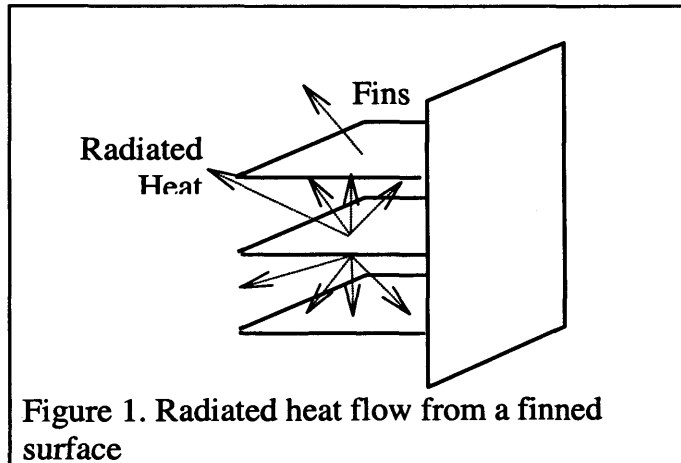
We know that the radiated and convected heat transfer from the finned surface, are given by;

$$\dot{q}_{conv} = h_{rad} A (T_3 - T_{amb}) \quad \dots \quad 2.6$$

$$\dot{q}_{rad} = \Sigma \sigma F A (T_3^4 - T_{amb}^4) \quad \dots \quad 2.7$$

The shape factor, F , is a scalar between 0 and 1 and depends on the geometry of the surface radiating the heat. For the purposes of the model we are considering the heat exchange between the finned surface and the atmosphere surrounding it. It is clear from

figure 3.1 that heat dissipated as infra-red radiation will only have certain paths which will allow transfer of heat to the surrounding atmosphere. Other paths will exchange heat with adjacent fins and surfaces on the radiator. Therefore for the radiator's finned surface, we would expect F to be very much less than unity.



For compact automotive radiators, typical values for h_{rad} are given as 0.08-0.13 (Lilly 84 pp 15/12). We can write;

$$\frac{\dot{q}_{rad}}{\dot{q}_{conv}} = \frac{\Sigma \sigma F A (T_3^4 - T_{amb}^4)}{h A (T_3 - T_{amb})} \quad \dots \quad 2.8$$

However, we know that;

$$\Sigma \leq 1, F \leq 1, \sigma = 56.7 \times 10^{-12} \text{ kW/m}^2 \text{K}^4, \text{ and } \sigma = 56.7 \times 10^{-12} \text{ kW/m}^2 \text{K}^4$$

Therefore;

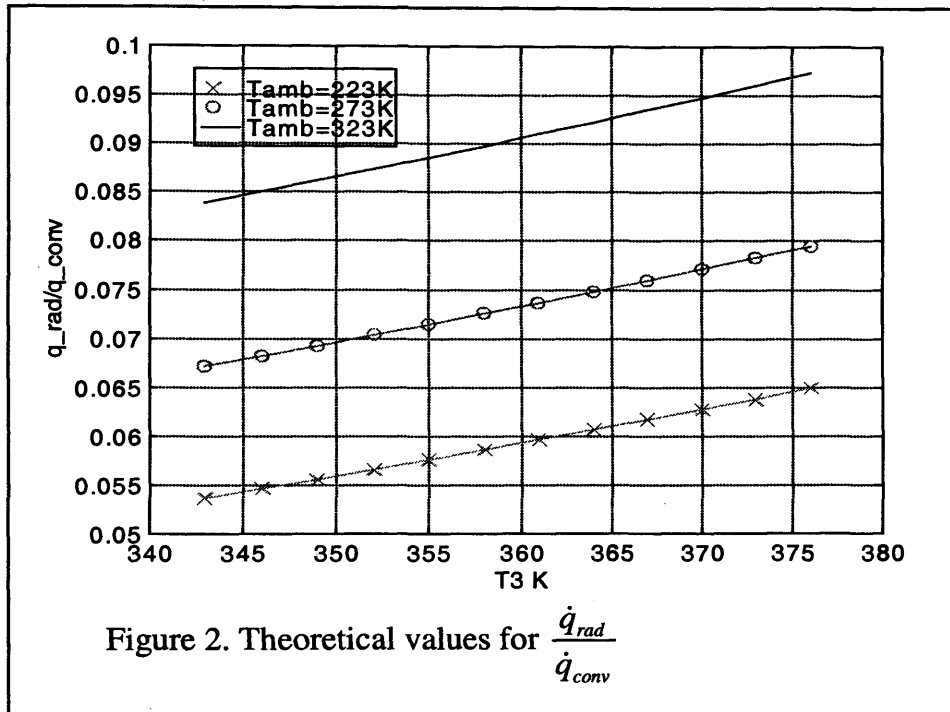
$$\frac{\dot{q}_{rad}}{\dot{q}_{conv}} \Big|_{\max} = \frac{56.7 \times 10^{-12} (T_3^4 - T_{amb}^4)}{0.08 (T_3 - T_{amb})}$$

$$\frac{\dot{q}_{rad}}{\dot{q}_{conv}} \Big|_{\max} = 7.085 \times 10^{-10} \frac{(T_3^4 - T_{amb}^4)}{(T_3 - T_{amb})} \quad \dots \quad 2.9$$

Choosing three possible temperatures for T_{amb} at extremes of 223K (-50°C) and 323K(50°C) and also at 273K show the maximum percentage of heat dissipated by radiation. Substituting a range of possible temperatures for T_3 between maximum inlet temperature to radiator at 103°C and min. outlet temperature of 70°C [See Appendix 1.2, Perkins Electropaks 1004TG Technical Data Sheet]. The range of possible values for $\frac{\dot{q}_{rad}}{\dot{q}_{conv}}$ given by equation 2.9 are shown in figure 2.

Ozisik [Ozisik 85 pp614] charts data which suggests that Σ_{rad} for the copper finning on the radiator will be around 0.4 - 0.5, which would reduce the maximum value for the radiative heat dissipation compared with convective to around 4% before consideration of the shape factor F.

This relatively small proportion of radiated heat leads to the suggestion that only convective heat transfer coefficient need be modelled at potential cost of a percentage error in modelled heat dissipation always less than 10% . I.e. only a value for the convective heat transfer coefficient, h_{rad} need be estimated to account for heat dissipation from the radiator. This result may be confirmed by inclusion of an extra variable for the radiative term in the regression which follows in section 2.1.4.



2.1.4 A TECHNIQUE FOR RADIATOR MODEL VALIDATION

Neglecting the heat transfer via radiation the differential equation for radiator outlet temperature is (from equation 2.1);

$$\frac{dT_3}{dt} = \frac{\dot{m}_{rad} C_p}{m_{rad} C_p} (T_2 - T_3) - \frac{h_{rad} A_{rad}}{m_{rad} C_p} (T_3 - T_{amb}) \quad \dots \quad 2.10$$

Equation 2.10 may be rearranged to give;

$$\frac{dT_3}{dt} = \frac{\dot{m}_{rad} C_p}{m_{rad} C_p} T_2 - \left(\frac{h_{rad} A_{rad}}{m_{rad} C_p} + \frac{\dot{m}_{rad} C_p}{m_{rad} C_p} \right) T_3 + \frac{h_{rad} A_{rad}}{m_{rad} C_p} T_{amb} \quad \dots \quad 2.11$$

Renaming coefficients gives;

$$\frac{dT_3}{dt} = a_1 T_2 - a_2 T_3 + a_3 T_{amb} \quad \dots \quad 2.12$$

The task of this validation exercise is to confirm the values of these coefficients and estimate the only unknown h_{rad} . A least squares algorithm presents one suitable approach to this task. The theoretical analysis for this approach is well known and is described by Montgomery [Montgomery 91 pp479] amongst others.

One approach to the problem of estimating the parameters of a differential equation is that of the *series-parallel-model* [Ioannou 96]. Noise in the data for T_3 means that numerical differentiation of equation 2.12 will cause large errors in the regression analysis. Therefore the series-parallel model will be applied as follows;

$$\frac{dT_3}{dt} = a_1 T_2 - a_2 T_3 + a_3 T_{amb}$$

Inclusion of an arbitrary term in T_3 to each side of the equation gives;

$$\frac{dT_3}{dt} + \lambda T_3 = a_1 T_2 - a_2 T_3 + \lambda T_3 + a_3 T_{amb}$$

Choice of λ will be explained later. Now taking Laplace transforms gives;

$$sT_3(s) + \lambda T_3(s) = a_1 T_2(s) - (a_2 + \lambda)T_3(s) + a_3 T_{amb}(s)$$

$$T_3(s) = a_1 \frac{T_2(s)}{s + \lambda} - (a_2 + \lambda) \frac{T_3(s)}{s + \lambda} + a_3 \frac{T_{amb}(s)}{s + \lambda} \quad \dots \quad 2.14$$

Now let;

$$\phi_1(s) = \frac{T_2(s)}{s+\lambda}, \quad \phi_2(s) = \frac{T_3(s)}{s+\lambda}, \quad \phi_3(s) = \frac{T_{amb}(s)}{s+\lambda}$$

Therefore it may be seen from the substitutions into equation 2.14, that the substituted variables $\phi(s)$ are effectively filtered versions of the original variables. This indicates how the value for λ should be chosen. Clearly λ should be positive to provide a pole in the left half of the s-plane and ensure stability for the filter. The gain and phase characteristics of the filter transfer function are defined by setting the magnitude of λ . In general terms λ should be determined from analysis of the monitored signal and chosen to preserve the dynamics of interest whilst removing high frequency components usually corresponding to measurement noise.

Assuming that parameters a_1 , a_2 and a_3 are constant, taking inverse Laplace transforms of 2.14 gives;

$$T_3(t) = a_1\phi_2(t) - (a_2 + \lambda)\phi_3(t) + a_3\phi_{amb}(t) \quad \dots 2.15$$

Use of a the multi-linear regression algorithm [Montgomery 91] will result in a model of the form;

$$y = \beta_0 + \beta_1 T_2 - \beta_2 T_3 + \beta_3 T_{amb} \quad \dots 2.16$$

where

$\beta_0 = \text{constant}$

$\beta_1, \beta_2, \beta_3 = \text{regression coefficients.}$

By comparison between equation 2.15 and 2.16, where we let y be the vector of values for T_3 , the regression coefficients may be compared to the coefficients of equation 2.15.

Also from 2.15 and 2.16 it may be noted that there is no constant term therefore $\beta_0=0$.

This may be explained by the fact that at $t=0$, the engine all temperatures are at ambient and consequently there is no heat transfer between block and coolant or coolant and ambient.

All the values in the differential equations are known or may be measured except for h_{rad} which may therefore be estimated from;

$$\beta_3 = a_3 = \frac{h_{rad} A_{rad}}{m_{rad} C_p} + \epsilon \quad \dots 2.17.$$

where ϵ is experimental error

Similarly the regression coefficients β_1 and β_2 may be used to validate the coefficients, a_1 and $a_2 + \lambda$. It is important to note that if the value for y becomes zero the simultaneous equations may be 'ill-conditioned.' This problem occurs when the determinant of the coefficients of the matrix set is relatively small causing error in the solutions due to rounding in the computation. Also if the determinant is zero the simultaneous equations may prove to be insoluble.

A number of estimations for h_{rad} will need to be made at different ambient temperatures. This could take advantage of the fact that the ambient temperature will rise steadily over the course of the test run. Each estimation for h_{rad} will require around two minutes worth of data. Over the course of two minutes the ambient temperature will have risen only slightly. Therefore the value for h_{rad} may be estimated for the mean temperature over that two minute period. This will result in a set of data pairs for T_{amb}, h_{rad}

Estimation of h_{rad} in this manner may lead to either a first order linear model of $h_{rad} = f(T_{amb})$ or alternatively if suitable measurement techniques for airflow across the radiator, u_{air} , are available, then h_{rad} may be obtained in the form of the relationship in equation 2.4.

2.1.5 TEST PROCEDURE

2.1.5.1 ENGINE SET-UP

- a) The generator set has fixed speed of 1500 rpm, therefore fan speed and coolant flow rate are fixed.
- b) Thermostat valve should be fixed to be in a known position to allow flow through to radiator.
- c) Ambient temperature is uncontrolled but is assumed to rise gradually over the course of the test run. This temperature rise may limit the permissible length of the test run.

2.1.5.2 OPERATION PROCEDURE

- a) Run the engine up from cold.
- b) Begin data acquisition at start-up
- c) Sampling rate should be a function of dynamics of the system and also the memory available for data storage. An appropriate sampling rate should be established by consideration of a preliminary step response test of the system
- d) Measured variables T_{amb} T_3 T_2 \dot{m}_{rad} (or ΔP_{rad}) Load (P) and N
- e) Initially run engine at no load.
- f) Switch load between pre-selected 'high' and 'low' values.

- g) Time at each load step should be sufficient to allow T_2 to settle i.e. for the inlet temperature to the radiator to stop increasing. (There will however be an upward trend in T_2 to match the upward trend in T_{amb}).
- h) Stop when a sufficient amount of data is obtained or the ambient temperature has reached a sensible limit.
- i) Validate the obtained regression models at a series of different ambient and inlet temperatures to radiator

2.2 HEAT TRANSFER FROM ENGINE BLOCK TO COOLANT

2.2.1 OBJECTIVE

Acquire data to validate the model for heat transfer from engine block to coolant

2.2.2 THEORY

$$m_b C_p \frac{dT_2}{dt} = (\dot{q}_{Block_to_coolant} - \dot{q}_{Coolant_heat_gain}) \quad \dots 2.18$$

$$\frac{dT_2}{dt} = \frac{h_b A_b}{m_b C_p} (T_b - T_2) - \frac{\dot{m}_b C_p}{m_b C_p} (T_2 - T_1) \quad \dots 2.19$$

From the expanded equation, 2.18, it is noted that the variables in the equation are \dot{m}_b, T_1, T_2 and T_b . These are all directly measurable with the exception of \dot{m}_b which is estimable via calculation from the coolant pressure differential across the engine block. The specific heat capacity of coolant, C_p , which will vary with temperature and may be obtained from tables. The total mass of coolant contained in the block, m_b , may be obtained from the manufacturers literature and confirmed by draining the coolant system and directly measuring the volume of fluid obtained.

The two parameters, $h_b A_b$, are the convective heat transfer coefficient between the block and the coolant, h_b , and the internal area of contact between the block and the coolant over which this heat transfer takes place. The empirical determination of these two parameters is the main aim of this procedure. The heat transfer coefficient h is given in the form below [Chiang 82];

$$h_b = \phi_h (Re)^{0.8} (Pr)^{0.4} \frac{k_a}{Bore} \quad \dots 2.20$$

where

$$\text{Re} = \frac{\dot{m}}{\rho v_c (\text{Bore})}$$

ρ = Coolant density, k_a = Conductivity of coolant, v_c = Kinematic viscosity of coolant
 Bore = Engine Bore and ϕ_h = Correlation coefficient

2.2.3 A TECHNIQUE FOR HEAT TRANSFER MODEL VALIDATION

From the above, h_b may be identified as function of temperature, T_2 , mass flow rate of coolant and the engine block geometry. A least squares approach may be undertaken as generally as described in section 2.1.4. Equation 2.18 may be arranged to give;

$$\frac{dT_2}{dt} = a_1 T_b - a_2 T_2 + a_3 T_1 \quad \dots \text{2.21}$$

Applying the series parallel model approach (see section 2.1.4) to equation 2.21 gives;

$$T_2(t) = a_1 \phi_{block}(t) - (a_2 + \lambda) \phi_2(t) + a_3 \phi_1(t) \quad \dots \text{2.22}$$

Equation 2.19 may then be compared to the least squares model in equation 2.16, in order to estimate h_b and validate the measurable parameters;

$$T_2 = \beta_1 \phi_b + (\beta_2 - \lambda) \phi_2 + \beta_3 \phi_1 \quad \dots \text{2.23}$$

where β_1 , β_2 , and β_3 are regression coefficients and $\beta_2 = -(a_2 + \lambda)$

A set of estimated values for h_b may be estimated for various T_2 . This could result in either a first order linear model for $h_b = f(T_2)$ or a model in the form of equation 2.20. For the model as described by equation 2.20, the fluid properties of the coolant may be evaluated at the engine block outlet temperature, T_2 , from data tables. Thus, the problem is reduced to finding a value for the correlation coefficient, ϕ . The parameter, A , may also prove to be difficult to obtain but may perhaps be estimated from design drawings. Alternatively A could be lumped in with the coefficient ϕ and parameter ϕA may be estimated.

2.2.4 TEST PROCEDURE

2.2.4.1 ENGINE SET-UP

- a) The generator set has fixed speed of 1500 rpm, therefore coolant flow rate is fixed.
- b) Thermostat valve should be fixed to be in a known position to allow flow through to coolant.
- c) Ambient temperature is uncontrolled but is assumed to rise gradually over the course of the test run. This temperature rise may limit the sensible length of the test run.

2.2.4.2 OPERATION PROCEDURE

- a) Run the engine up from cold.
- b) Begin data acquisition at start-up
- c) Sampling rate should be a function of dynamics of the system and also the memory available for data storage. An appropriate sampling rate should be established by consideration of a preliminary step response test of the system
- d) Measured variables: T_{amb} , T_1 , T_2 , \dot{m} , (or ΔP_{block}) Load (W) and Engine Speed (N)
- e) Initially run engine at no load.
- f) Switch load between pre-selected 'high' and 'low' values.

- g) Time at each load step should be sufficient to allow T_2 to settle i.e. for the inlet temperature to the radiator to stop increasing. (There will however be an upward trend in T_2 to match the upward trend in T_{amb}).
- h) Stop when a sufficient amount of data is obtained or the ambient temperature has reached a sensible limit.
- i) Validate the obtained regression models at a series of different ambient and inlet temperatures to radiator

3. RESULTS

3.1 INTRODUCTION

This section will present results from data acquisition, processing, system modelling and analysis of the diesel engine cooling system. Theoretical analysis of the cooling system, along with data acquisition, test and data analysis procedures have been outlined in section 2.

The results are presented on a sub-system by sub-system basis. The sub-systems under investigation in this section are;

- i) heat transfer from engine to coolant
- ii) heat transfer from coolant to ambient via the radiator

Data from this set of engine tests were recorded using the Matlab/Simulink/dSpace system. A block diagram representation of the desired data acquisition system is designed as a Simulink model. Code may then be generated directly from this model using the Matlab 'Real Time Workshop' toolbox. The code is then imported into the dSpace system and downloaded onto a dedicated DS1103 PPC Controller Board. Data

recorded via this controller board is then re-sampled and recorded directly to the hard drive of the PC, via dSpace's experiment management software, 'ControlDesk'.

Analysis of the power spectral density of these pressure transducer signals has shown that there are frequency components of significant magnitude at 25Hz, 50 Hz and, to a lesser degree, at 100 Hz. All input channels were filtered using anti-aliasing filters, designed with-cut off frequency at 1Hz, to avoid any aliasing effects due to these frequency components in the pressure data. This data acquisition and filtering system was run at 1kHz on the DS1103 PPC Controller Board and then down-sampled by a factor of 100 to give a final sampling rate of 10Hz, prior to recording data to disk.

Having acquired suitable data, the next step is to parameterise the regressors as outlined in section 2.1.4. The parameterisation filters the data with a transfer function $\frac{1}{s + \lambda}$.

[See appendix A1.3 for parameterisation m-file].

The filtering was performed using the '*filtfilt*' function in 'Matlab™'. The advantage of this function is that the data is filtered in both forward and reverse directions resulting in zero phase distortion in the filtered data. Initial choice of the arbitrary design constant λ was made to be $\lambda = 1$, for the parameter estimation exercises for both equations.

3.2 ENGINE BLOCK TO COOLANT HEAT TRANSFER MODEL (' T_2 MODEL') VALIDATION

3.2.1 DATA ACQUISITION.

Data was acquired for the radiator model validation from the appropriate coolant PRT's, engine block surface temperature transducers and coolant pressure transducers. (See appendix 2.1 and 2.2 for full list of locations and calibrations.)

Direct measurement of coolant flow rate through the engine block is impractical due to the fact that the coolant flow-paths are fully enclosed within the block and there is no suitable position to mount a direct flow transducer (e.g. turbine flow meter type). However measurement of the pressure difference between the coolant pump outlet and the thermostat valve allows the flow-rate to be calculated.

A number of data sets were obtained with the thermostat valve fixed to provide a series of different openings, and therefore coolant volume flow rates to the radiator, \dot{V}_{rad} .

Although the thermostat valve is not designed to control the flow rate to the engine block, the total flow resistance around the circuit changes when the valve is operated, resulting in reduced flow through the block, \dot{V}_b when the thermostat valve is closed.

The variables for the model validation procedure are defined to be;

T_2 , the coolant temperature at inlet to the radiator.

T_3 , the coolant temperature at outlet from the radiator.

T_b , the surface temperature of the engine block.

Local temperature differences between the surface temperature transducers situated at each location on the engine block were seen to be significant. Temperatures from the thermocouples located on the cylinder heads were seen to be higher than those lower down on the block, and the right hand side transducers, also gave higher readings than the

ones situated on the left hand side of the engine. This was thought to be due to the proximity of the exhaust system to the transducers. The temperatures recorded from the engine block are lower than the outlet temperature of the coolant from the engine block recorded at the thermostat valve, T_2 . If T_b is lower than T_2 , the parameter estimation procedure will result in a parameter of opposite sign to that which would be expected from knowledge of the direction of heat transfer from the engine block to the coolant. Therefore T_b is defined to be the temperature recorded from the right-hand side of the cylinder head.

Step	1	2	3	4	5	6	7
Load kW	0	20	40	60	40	20	0

Table 1: Load Profile

The steps in load were performed as per table 1. Ten thousand data points were recorded at each load in each of the five valve positions. The data series for each valve position were parameterised using the series-parallel model as described in Section 2.1.4.

3.2.2 DATA ANALYSIS

The use of regression analysis to estimate the parameters, a_1 , a_2 and a_3 , is essentially a linear process, however the three parameters are known to be non-linear. Some additional theoretical analysis is made here to allow the non-linear parameter estimation to be made. From equation 2.19;

$$a_1 = \frac{h_b A_b}{m_b C_p} \quad \dots \quad 3.1$$

Where m_b is the mass of coolant contained within the block;

$$a_2 = (a_1 + a_3) \quad \dots \quad 3.2$$

$$a_3 = \frac{\dot{m}_b C p_c}{m_b C p_c} = \frac{\rho_c \dot{V}_b C p_c}{\rho_c V_b C p_c} = \frac{\dot{V}_b}{V_b} \quad \dots 3.3$$

It can be seen from this analysis that a_3 may be directly obtained from measurements of \dot{V}_b and the volume of coolant contained in the block, V_b . The second parameter, a_2 , is a function of a_1 and a_3 therefore the problem is reduced to one of finding a_1 .

From equation 4.7 in Appendix 1;

$$T_2 = \beta_1 \phi_b - (\beta_2 - \lambda) \phi_2 + \beta_3 \phi_1 \quad 3.4$$

Where

$\beta_1, \beta_2, \beta_3$ = regression coefficients.

and $\beta_1 = a_1$; $\beta_2 = (a_2 + \lambda)$; $\beta_3 = a_3 = \frac{\dot{V}_b}{V_b}$;

From this definition of a_3 the regression may be reduced to two variables as follows;

$$y = (T_2 - \beta_3 \phi_1) = \beta_1 \phi_b + (\beta_2 - \lambda) \phi_2 \quad \dots 3.5$$

The data matrix made up of the vectors for y , and the parameterised variables, ϕ_b and ϕ_2 , are now separated into a set of smaller matrices each of which has been defined to cover a 20°C interval in T_b . The choice of the interval size is a trade-off between ensuring that the matrix has enough data points to minimise the error in the multi-linear regression analysis, whilst ensuring that the matrix is short enough with respect to temperature, to gain a reasonable approximation to the parameter at that particular temperature point.

The multi-linear regression procedure is then employed and a matrix containing values for a_1 , a_2 and a_3 is obtained. The mean values for T_b , T_2 and \dot{V}_b are recorded for each interval. See appendix A1 for script files containing the multi-linear regression and series-parallel model parameterisation algorithms.

3.2.3 COMPARISON OF ESTIMATED AND THEORETICALLY DERIVED PARAMETERS

Expanding equation 2.20 in appendix 1, a theoretical relationship for a_1 may be obtained as follows;

$$h_b = \phi_h (\text{Re})^{0.8} (\text{Pr})^{0.4} \frac{k_a}{\text{Bore}} \quad \dots 3.6$$

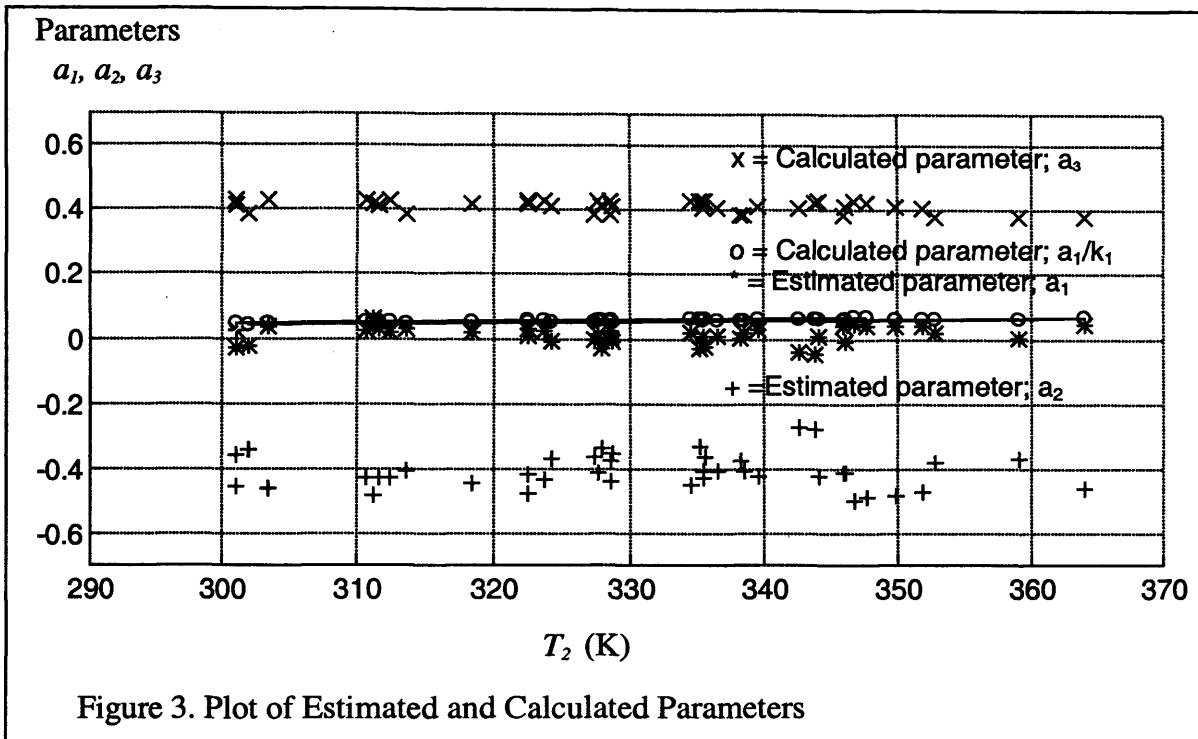
$$a_1 = \left(\frac{hA}{mc} \right)_{\text{block}} = \phi_h \left(\frac{\dot{m}}{\rho v_c (\text{Bore})} \right)^{0.8} (\text{Pr})^{0.4} \left(\frac{k_a}{\text{Bore}} \right) \left(\frac{A}{mc} \right)_{\text{block}}$$

$$a_1 = \underbrace{\left(\frac{\phi_h}{(\text{Bore})^{1.8}} \frac{A_{\text{block}}}{V} \right)}_{\text{Constant}} \underbrace{\left(\frac{\dot{V}}{v_c} \right)^{0.8} \left(\frac{1}{\rho} \right) (\text{Pr})^{0.4} \left(\frac{k_a}{c_{\text{block}}} \right)}_{f(T_2, \dot{V})} \quad \dots 3.7$$

where; k_1 is a constant; Bore the cylinder bore; ϕ_h is a scalar constant

$$a_1 = k_1 \{f(T_2, \dot{V})\}$$

Assuming the properties of the coolant to be those of water, reference to the appropriate data tables [Simonson 88] allows the calculation of $\frac{a_1}{k_1}$. Comparison between this value and estimated values for a_1 is presented in figure 3.



The results shown in figure 3 have been obtained from splitting the data into a set of 20°C intervals, prior to regression. The points on the axis, T_2 in the figure, represent the mean temperature of each individual interval. Values for a_1/k_1 have also been calculated using the mean temperatures and volume flow rates measured over each 20°C interval to allow a direct comparison to be made.

The mean and standard deviation of the estimated parameter values are shown in table 2

Table 2. Mean and standard deviation of the estimated parameter values.

	a_1	a_2	a_3
Mean Value (3dp)	0.024	-0.434	0.413
Standard Deviation (3dp)	0.015	0.035	0.019

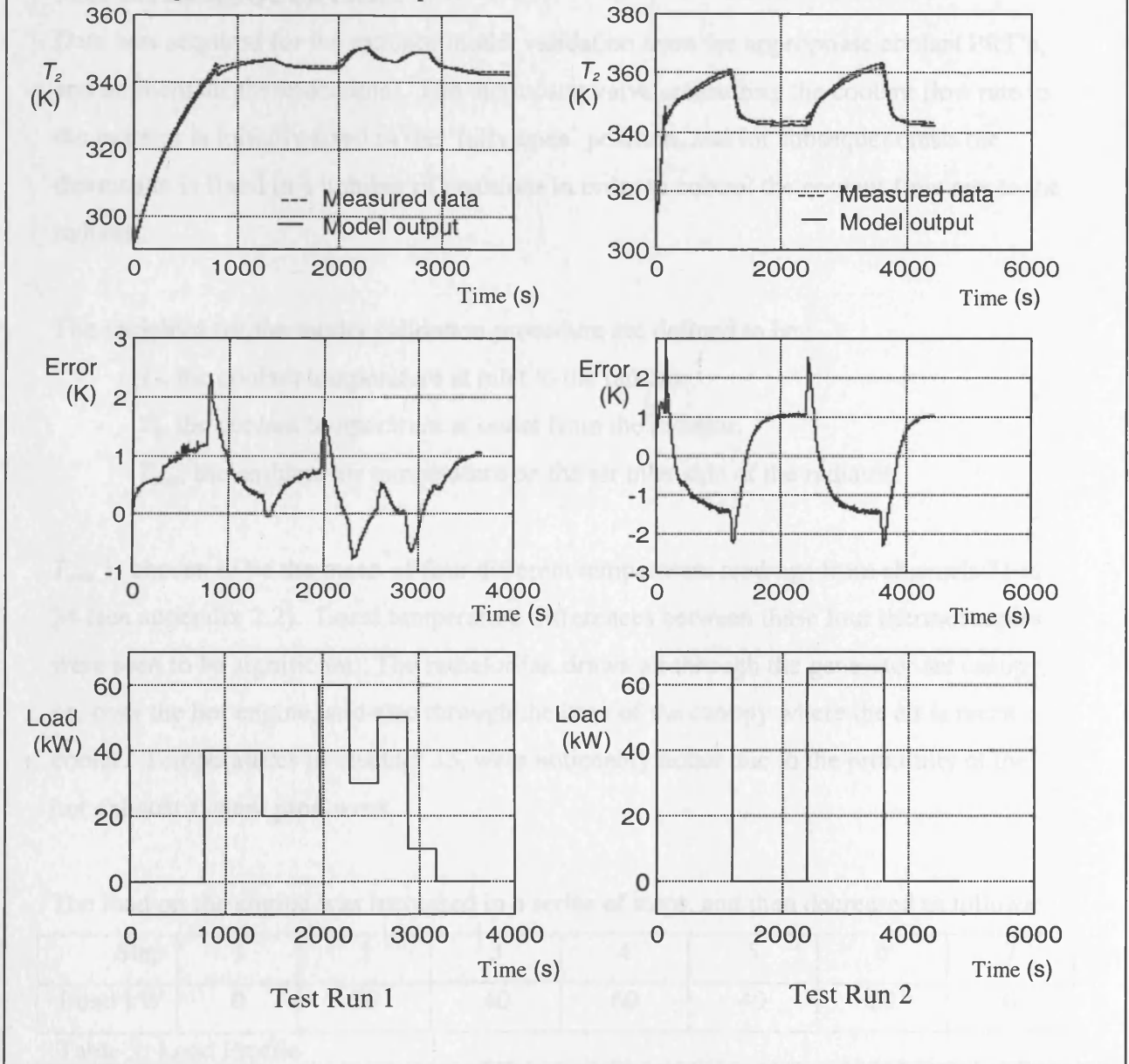
The magnitude of the errors in the estimated value for a_1 are seen to be very high with respect to the magnitude of the parameter itself, reducing the possibility of establishing a valid relationship for $a_1 = f(T_2, \dot{V})$.

A number of estimated values for a_1 were also rejected on the grounds that they were negative numbers. Clearly a_1 must be positive to ensure that the flow of heat in the model is in the correct direction. Comparison of the mean positive values for a_1 , with the mean value for a_1/k_1 , (0.057), show that $k_1 \approx 0.4$.

3.2.4 MODEL SIMULATION RESULTS

The estimated parameters for the model have been incorporated in to a simulation detailed in appendix A2. Fluid property data required for parameter a_1 have been included as look-up tables. Obtaining suitable test data for the model has allowed the values for the constant, k , to be finalised by a process of trial and error. The final value employed in the model is $k=0.55$.

Figure 4. T_2 Model Outputs and Error Values for Test Runs 1 and 2.



Two test runs were carried out to provide test data for the non-linear model. Heat input into the cooling system was varied by controlling the load on the engine. Data was obtained for variables T_b , T_2 , T_1 and \dot{V}_b to provide input and test output data for the model. The results and errors from this exercise along with the electrical load changes applied to the engine are shown in figure 4.

3.3 RADIATOR HEAT TRANSFER MODEL VALIDATION

3.3.1 DATA ACQUISITION.

Data was acquired for the radiator model validation from the appropriate coolant PRT's, and ambient air thermocouples. The thermostat valve controlling the coolant flow rate to the radiator is initially fixed in the 'fully open' position, and for subsequent tests the thermostat is fixed in a number of positions in order to control the coolant flow rate to the radiator.

The variables for the model validation procedure are defined to be ;

T_2 , the coolant temperature at inlet to the radiator.

T_3 , the coolant temperature at outlet from the radiator.

T_{amb} , the ambient air temperature on the air inlet side of the radiator.

T_{amb} is chosen to be the mean of four different temperature readings from channels 31 to 34 (see appendix 2.2). Local temperature differences between these four thermocouples were seen to be significant. The radiator fan draws air through the generator-set canopy, i.e. over the hot engine, and also through the base of the canopy where the air is much cooler. Temperatures in channel 33, were noticeably hotter due to the proximity of the hot exhaust system pipe-work.

The load on the engine was increased in a series of steps, and then decreased as follows;

Step	1	2	3	4	5	6	7
Load kW	0	20	40	60	40	20	0

Table 3: Load Profile

After each step change in load data, a period of approximately 20 minutes was allowed for the temperature variables to rise to a steady state. Data was sampled continuously during this period. After averaging the thermocouple channels the recorded data for the three variables is shown in figure 5.

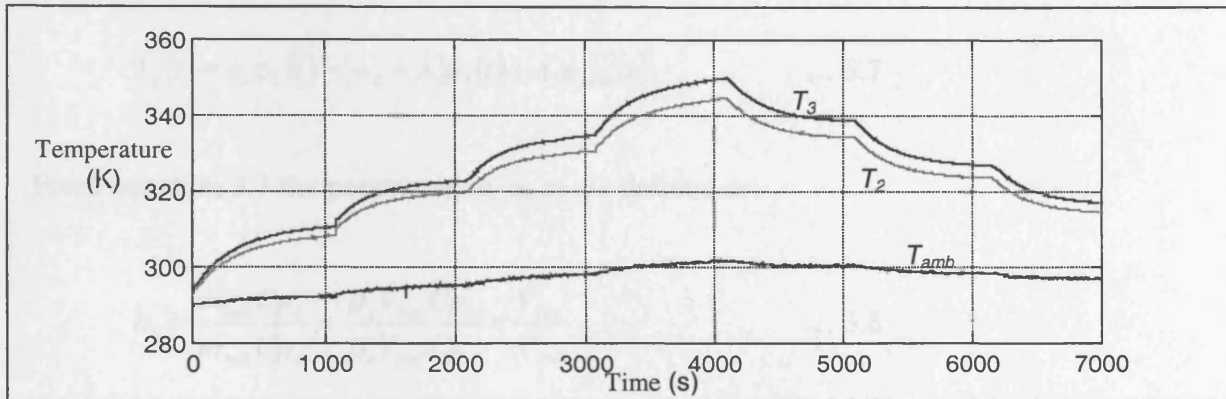


Figure 5. Temperature data for parameter estimation procedure

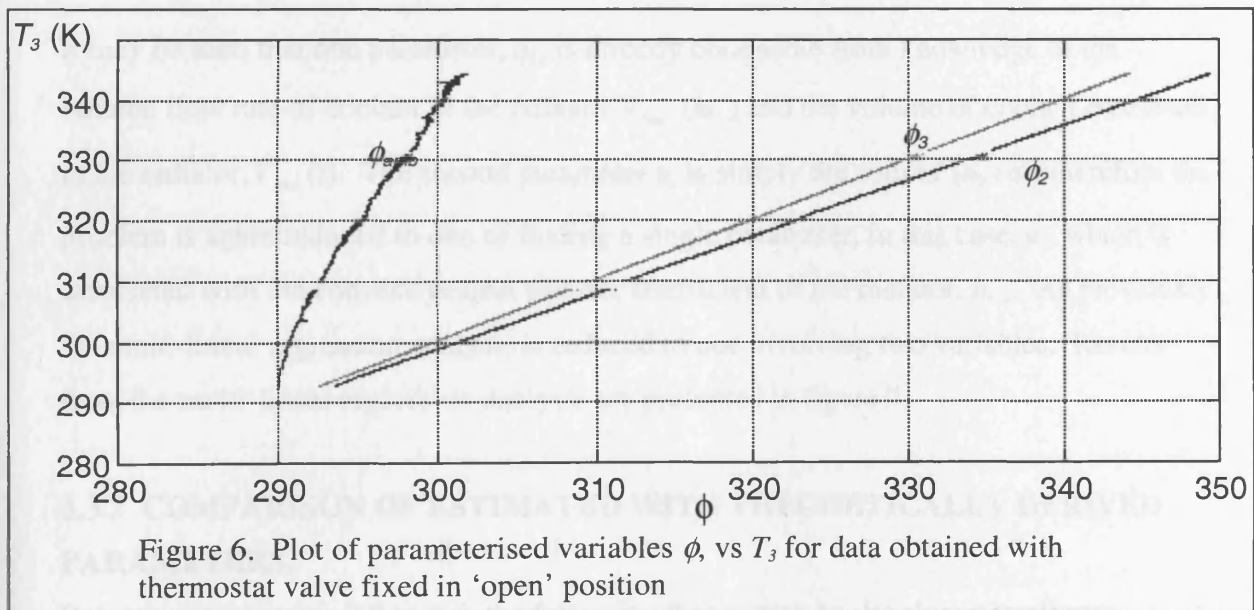


Figure 6. Plot of parameterised variables ϕ , vs T_3 for data obtained with thermostat valve fixed in 'open' position

It may be noted from figure 6 that the parameterised variables ϕ_2 and ϕ_3 have a linear relationship with T_3 , whereas ϕ_{amb} exhibits a slight deviation from the linear with temperature.

Referring to equation 2.15, we see that;

$$T_3(t) = a_1 \phi_2(t) - (a_2 + \lambda) \phi_3(t) + a_3 \phi_{amb}(t) \quad \dots 3.7$$

From equation 3.7 the parameters a_1 a_2 a_3 are defined as;

$$a_1 = \frac{\dot{m}_{rad} C_{p_c}}{m_{rad} C_{p_c}} = \frac{\rho_c \dot{V}_{rad} C_{p_c}}{\rho_c V_{rad} C_{p_c}} = \frac{\dot{V}_{rad}}{V_{rad}} \quad \dots 3.8$$

$$a_2 = (a_1 + a_3) \quad \dots 3.9$$

$$a_3 = \frac{h_{rad} A_{rad}}{m_{rad} C_p} \quad \dots 3.10$$

It may be seen that one parameter, a_1 , is directly obtainable from knowledge of the volume flow rate of coolant in the radiator \dot{V}_{rad} (ls^{-1}) and the volume of coolant contained in the radiator, V_{rad} (l). The second parameter a_2 is simply the sum of $(a_1 + a_3)$ therefore the problem is again reduced to one of finding a single parameter, in this case, a_3 , which is associated with the convective heat transfer coefficient of the radiator, h_{rad} . As previously the multi-linear regression analysis is reduced to one involving two variables. Results from the multi-linear regression analysis are presented in figure 7.

3.3.2 COMPARISON OF ESTIMATED WITH THEORETICALLY DERIVED PARAMETERS.

Referring to equation 2.2 to 2.5, the following theory may be developed to allow a comparison between theoretical and estimated results for the heat transfer coefficient h_{rad} ;

$$(\text{St})(\text{Pr})^{2/3} = f(\text{Re}) \quad 3.11$$

$$\left(\frac{h_{rad}}{GC_{p_a}} \right) \left(\frac{C_{p_a} \mu}{k} \right)^{2/3} = f \left(\frac{GD_h}{\mu} \right)$$

$$\left(\frac{A_{\min}}{\dot{m}_a} \cdot \frac{h_{rad}}{Cp_a} \right) \left(\frac{Cp_a \mu_a}{k_a} \right)^{\frac{2}{3}} = f \left(\frac{\dot{m}_a}{A_{\min}} \cdot \frac{1}{\mu_a} \cdot \frac{4L_{rad} A_{\min}}{A_{rad}} \right)$$

$$\left(\frac{1}{\rho_a u_a} \cdot \frac{h_{rad}}{Cp_a} \right) \left(\frac{Cp_a \mu_a}{k_a} \right)^{\frac{2}{3}} = f \left(\frac{\rho u_a A_{\min}}{\mu_a} \cdot \frac{4L_{rad}}{A_{rad}} \right) \quad 3.12$$

Substituting values for fluid properties for air [Simonson 88] at 300K;

$$Cp_a = 1.006 \left(\frac{\text{kJ}}{\text{kgK}} \right), k_a = 2.62 \times 10^{-5} \left(\frac{\text{kW}}{\text{mK}} \right), \rho_a = 1.177 \left(\frac{\text{kg}}{\text{m}^3} \right), \mu_a = 1.85 \times 10^{-5} \text{ (Pa s)}$$

The physical parameters of the radiator required for the calculation may be obtained directly from measurements. The air velocity over the radiator u_a , was measured using a simple hand-held anemometer at a number of different points across the frontal area of the radiator. A set of readings was taken for u_a ranging between 4ms^{-1} at the centre of the radiator (the hub of the cooling fan) to 12ms^{-1} at the top edge of the radiator. These figures were found to compare well with the data quoted on the manufacturers data sheet which states that the fan should provide 100m^3 of air per minute, implying that with $A_{\min}=0.25\text{m}^2$ the mean value for u_a should be;

$$\bar{u}_a = \frac{100}{60} \cdot \frac{1}{0.25} = 6.7\text{ms}^{-1}$$

Taking the median of the measured values for u_a , physical parameters of radiator are measured to be; Air velocity over radiator $u_a=8\text{ms}^{-1}$, $L_{rad}=0.09\text{m}$, $A_{rad}=47.6\text{m}^2$ $A_{\min}=0.25\text{m}^2$. Reynolds number is calculated to be 918, therefore;

$$(0.11h_{rad})(0.71)^{\frac{2}{3}} = f(918)$$

From the 'typical' chart for heat transfer coefficient across a finned compact heat exchanger [Ozisik 95, pp573], $f(918)=0.0114$ therefore;

$$h_{rad} = \frac{0.0114}{0.11 \cdot (0.71)^{\frac{2}{3}}} = 0.13 \left(\frac{\text{kW}}{\text{m}^2 \cdot \text{K}} \right)$$

Also;

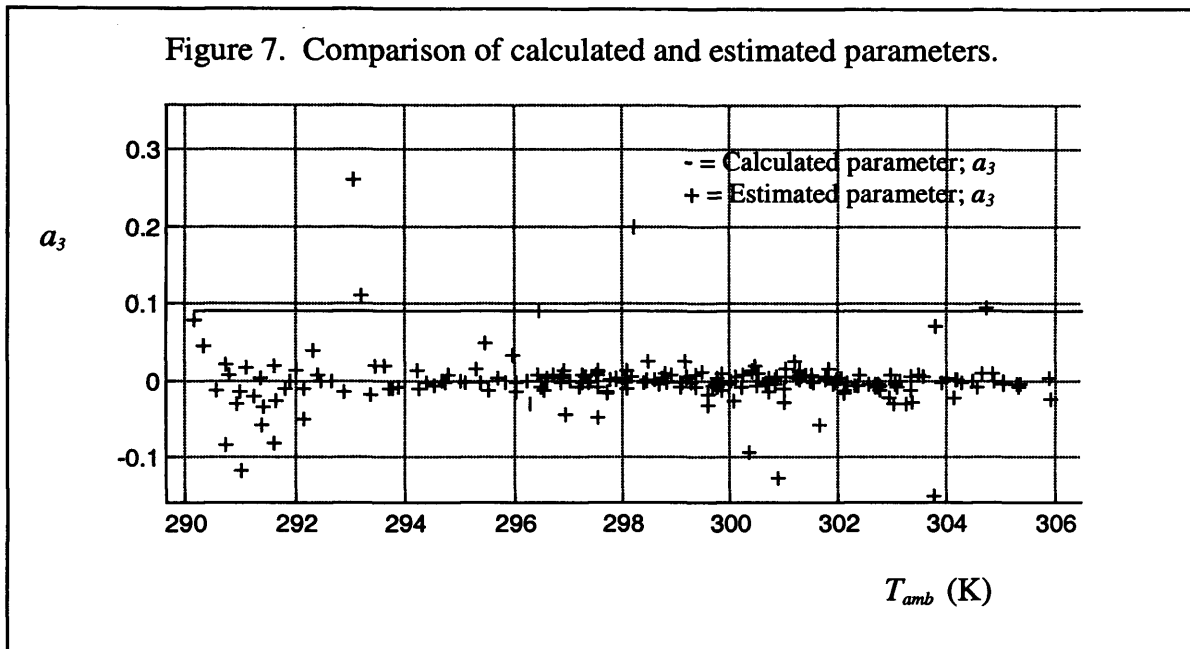
$$a_3 = \frac{h_{rad} A_{rad}}{m_{rad} C p_c} = \frac{0.13 \times 47.6}{16.50 \times 4.2} = 0.089$$

Substituting the extreme values for u_a of 12 and 4ms^{-1} result in calculated values for h_{rad} of 0.15 and 0.09 respectively

Comparison of the calculated and estimated parameters (assuming $u_{air} = 8\text{ms}^{-1}$) for a_3 in figure 7, shows that the estimated parameters have a wide spread of values and that the calculated points show little variation with temperature. Figure 7 also shows that the estimated values have a much lower mean value than the calculated values. A number of the negative values for estimated parameters were disregarded as erroneous, because a_3 must be positive to give the correct direction for heat flow. The mean of the positive values for a_3 is 0.03 suggesting a correction factor will be required to match the calculated parameters to the model.

The non-linear model for T_3 has been simulated in order to test the results of the parameter estimation and the accuracy of the calculated parameters.

Figure 7. Comparison of calculated and estimated parameters.

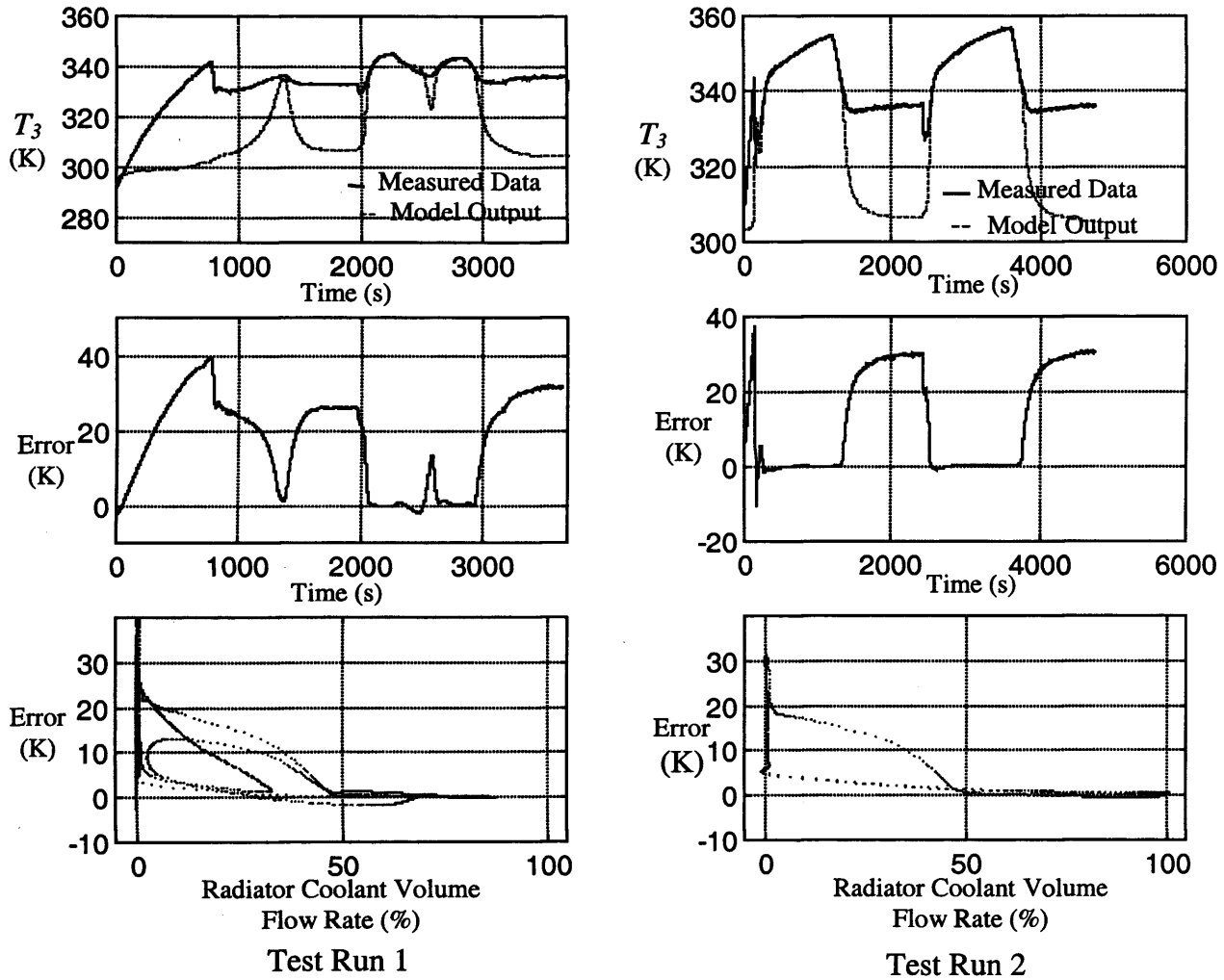


3.3.3 RESULTS FROM NON-LINEAR T_3 MODEL SIMULATION.

The model simulations were tested using data from the same batch as the testing of the model for T_2 . One practical problem encountered in testing the radiator has been the accurate measurement of the coolant flow rate through the radiator, \dot{V}_{rad} . Although a transducer was not available to measure \dot{V}_{rad} directly, a fuzzy model, which had been previously developed for the estimation of \dot{V}_{rad} with respect to T_2 , has been incorporated into the non-linear model. The non-linear model is fully documented in appendix 5.

The first test of the simulation employed the calculated parameter for a_3 . The results from the test showed that the model errors were high indicating that the calculated parameter, a_3 , was too high. The best results have been obtained by imposing a scalar 'correction factor' of 0.165 on the calculated value for a_3 . Results from this arrangement of the model are shown in figure 8.

Figure 8. T_3 Model Outputs and Error Values for Test Runs 1 and 2



4. DISCUSSION

The *series-parallel model* parameter estimation technique has proved to be helpful in producing the two heat-transfer models outlined here. However some quite detailed theoretical analysis was required to obtain reasonable results. Conversely, the parameters for the models would have been difficult to obtain purely analytically, showing that where some theoretical knowledge of the system is available the series-parallel model may be employed as a useful tool to assist in parameter estimation.

The parameters associated with the heat transfer coefficients have been shown to vary little with respect to temperature, within the operating temperature range of the engine which has been investigated here, and could be treated as constant parameters within this range

Suitable inputs to the non-linear model need to be chosen quite carefully. The heat transfer equations are based on the fact that the direction of heat flow is always from a body with higher temperature to a one of lower temperature. Averaging over the whole heat transfer area from engine block and cylinder head to coolant flowing through the galleries within the block the heat transfer will always be from block to coolant. However, the temperature at a single point on the surface of the block may not always be representative of this average temperature, and at some time may be cooler than the outlet temperature of coolant from the block. These facts will be reflected by errors in the model. It is for this reason that the input, T_b in the T_2 model has been chosen to be from the hottest region on the surface of the cylinder head to minimise the time periods in which errors occur due to $T_b < T_2$. These points mean that the model should be seen as a relationship between transducer outputs, rather than a detailed physical model of the system.

The parameter associated with the heat transfer coefficient from the radiator was found to be much less than the calculated version. This is indicated by the need to apply a

correction factor of 0.165 in the simulation. The calculated value for h_{rad} falls within expected range for a radiator of this type, of between 0.08 and 0.13kW/m²K [Lilly 84] and the calculations appear to be in order. Therefore, it seems that the reduction in heat transfer coefficient could be due to the fouling of the radiator with oil and grime from the engine, which is noted to be present.

The model outputs for T_3 are seen to fit the measured data well when the thermostat valve is in the fully open position with errors falling to low values when $\alpha > 50\%$. (figure 8). This effect is thought to be due to change in dominant mode of heat transfer to the transducer which is used to measure T_3 when there is zero or low flow through the radiator. When the valve is open, heat transfer is due to convection from coolant flow. However, when the valve is closed, the proximity of sensor to engine block causes heat transfer by conduction and convection to sensor. This change in mode of heat transfer is not included in the model and therefore large errors are seen to occur. However with reference to the aims of the modelling exercise to generate knowledge of the system for fault diagnosis purposes it should be noted that faults in the radiator may not be diagnosed effectively when the thermostat valve is in the closed position.

Errors in parameter estimation arise mainly from the mainly from regression analysis. Larger blocks of data were generally found to found to give better results than smaller intervals. For the purposes of this exercise, where parameters are fairly linear with respect to temperature, splitting the data up 20°C intervals was found to give adequate results.

Measurement of \dot{V}_b is difficult to achieve practically, and an expression has been employed to calculate \dot{V}_b with respect to the measured pressure drop across the block, ΔP_b . Results previously obtained from running the engine with the thermostat in fixed in the open position and recording the flow rate at the inlet to the radiator with a turbine

flow meter suggest that the results from calculation $\dot{V}_b = f(\Delta P_b)$ need to be scaled with an additional factor of (132/145). This correction factor has been applied to scale the calculated value for \dot{V}_b in the simulation. It is also thought that ΔP_b may change with temperature due to the different rate of heating between the two transducer points, causing further errors in the calculation.

The method for calculation of $\dot{V}_{rad} = f(\Delta P_{rad})$ was found to be particularly unreliable. This calculation is based on energy loss when coolant is forced through an orifice under pressure. Low pressure difference between the inlet and outlet of the radiator suggest that flow through the radiator is due to gravity and therefore the assumptions which are the basis for the pressure loss equation are not applicable. Therefore, as a turbine flow meter has not been available during the course of the data acquisition procedure, the volume flow rate has been estimated for the purposes of non-linear model testing, using a fuzzy model. This fuzzy model has previously been identified to estimate coolant flow rate through the thermostat valve with respect to T_2 . Some errors in the non-linear model simulation are certainly due to the use of the fuzzy model, particularly around the temperatures at which the valve starts to open. This implementation represents an interesting use of a fuzzy model were a more conventional approach may not be as effective.

5 CONCLUSIONS

A combination of theoretical analysis and parameter estimation using the series-parallel model approach, has resulted in the derivation of a set of parameters for two non-linear heat transfer models.

The two approaches were found to be complementary. Neither approach gave conclusive results on its own, but the theoretical analysis helped to establish the relationships between the parameters and the series-parallel model allowed appropriate scaling of the parameters.

The accuracy of the parameters has been demonstrated by implementing the non-linear models as a simulation in Simulink, and testing with real data from the engine.

REFERENCES

- [Chiang 82] Development and evaluation of a diesel powered truck cooling system
Chiang, EC; Ursini, VJ; Johnson, JH.
SAE Paper 821048, 1982
- [Heywood 88] Internal Combustion Engine Fundamentals
Heywood, JB;
McGraw-Hill International Editions 1988
- [Ioannou 96] Robust Adaptive Control
Ioannu, PA; Sun, J
Prentice-Hall 1996
- [Kays 55] Compact Heat Exchangers
Kays WM; London AL
McGraw-Hill 1955
- [Lilly 84] Diesel Engine Reference Book
Lilly, LCR;
Butterworth and Co Ltd 1984
- [Montgomery 91] Design and Analysis of Experiments
Montgomery, DC
Wiley 1991
- [Ozisik 85] Heat transfer A basic approach
Ozisik MN
McGraw-Hill International Editions 1988
- [Simonsen 88] Engineering Heat Transfer,
Simonsen, JR,
MacMillan Education 1988
- [Twiddle 99] Model based fault diagnosis of a diesel engine cooling system
Twiddle, JA
Leicester University Engineering Dept, Internal Paper, 99-1 Jan 99

**APPENDIX A1 SCRIPT FILE TO ESTIMATE HEAT TRANSFER
PARAMETERS USING SERIES PARALLEL MODEL AND MULTI-LINEAR
LEAST SQUARES REGRESSION**

```
%Script file to break data up into segments
% and evaluate parameters a1 a2 a3 with respect to block temperature
%Data = [Tb T2 T1] Data columns;
```

```
%Initialise variables
```

```
%-----
%Data and parameterisation information
fs=10; %sample freq Hz
lambda=1;
```

```
%-----
data_file=dat_mat;
%-----
break_point=[];
sec_info=[];
beta=[];
beta_N=[];
phi=[];
%-----
```

```
%Find size data matrix and
%split data into 'int' degC intervals
int= 20;
min_T=min(data_file(:,1));
break_point(1)=1;
c=2;
L=length(data_file);
%-----
```

```

%define vector of break points
for j=1:L
    if abs(data_file(j,1)-min_T)>=int;
        break_point(c)=j;
        min_T=data_file(j,1);
        c=c+1;
    end
end

%Record vector headings for each section of data:
sec_info_n='index No. Mean_Tb Mean_T2 Mean_Vdot';

%Parameterise variables
phi=param4(data_file,lambda,fs);

%split data into smaller sections w.r.t. Tb and record info regarding each section
num_sections=length(break_point);

for sec_num=1:num_sections-1;
    index=[break_point(sec_num):break_point(sec_num+1)];
    sec_info(sec_num,:)=[break_point(sec_num) mean(data_file(index,1))
mean(data_file(index,2)) mean(data_file(index,5))];

    beta(sec_num,:)=multregZ(data_file(index,2),phi(index,:),(mean(data_file(index,5))/(6*60)
));
end

%-----
%calculate a normalised version of beta 'beta_N' scaled wrt Vdot
%NB Not necessary with multregZ

[a,b]=size(beta);

for i=1:a;
    beta_N(i,[1:4])=beta(i,[1:4])*sec_info(i,4)/(6*beta(i,4));
end

%-----
%split data into smaller sections w.r.t. calculate T2=f(a*phi) for each section
% and calculate model error vector, e, for each section

index=[];
num_sections=length(break_point);

```

```
for sec_num=1:num_sections-1;
    index=[break_point(sec_num):break_point(sec_num+1)];
    T2_hat(index)=[(beta(sec_num,1)+beta(sec_num,2)*phi(index,1))+((beta(sec_num,3)+1)*
phi(index,2))+(beta(sec_num,4)*phi(index,3))];
    e(sec_num,[1:2])=[mean(dat_mat(index,2)-T2_hat(index)'),std(dat_mat(index,2)-
T2_hat(index'))];
end

%-----
%save and tidy

save p_res2 beta beta_N sec_info e;
clear data_file min_T L a b c fs
clear i index int j lambda num_sections sec_num
pack
```

APPENDIX A1.2 MULTI-LINEAR REGRESSION ANALYSIS FUNCTION

```

function [a]=multregZ(y,phi,beta3,lambda,i1,i2,inc);

% format beta=multregR(y,phi,lambda,i1,i2,inc);
% beta are parameters
% T= [phi1 phi2 phi3];
% i1,i2 are start point and end point of data from vectors
% inc = increment to allow reduction of vector size if required

%set defaults
if nargin==3
    lambda=1;
    i1=1;
    i2=length(y);
    inc=1;
end;
i=[i1:inc:i2];

% reduce to two variable problem (beta3 is known: Vdot (l/sec) / V (l) )
y=y(i)-(beta3*phi(i,3));

%define regressor matrix
[a,b]=size(phi);
X_raw=[ones(length(phi),1),phi(i,1:b)];
X=[ones(length(phi),1),phi(:,[1,2])];

%Regression algorithm
beta0=inv(X'*X)*(X'*y);
beta0(4)=beta3; % NB Add known value for beta3 to results

%Calculate model error
%test output

y_hat=zeros(length(X_raw),1);
for column=1:b+1;
    y_hat=y_hat+X_raw(:,column)*beta0(column);
end

%error calcs
error=y-y_hat;
eta=mean(error);
std_error=std(error);

%Output values for a1 a2 a3 = beta([2,3 4])
a=beta0-[0 0 lambda 0]'; %subtract value for lambda

```

APPENDIX A1.3 SERIES-PARALLEL MODEL PARAMETERISATION FUNCTION;

```

function [paras]=param4(datfile,lambda,fs);

%estimates parameters for 1st order ode for a given engine block data
%Input format is      [paras]=param([Tb,T2,T1],lambda,fs);
%Output format;      Paras = [phib phi2 phi1] parameters;
%where fs is sample frequency

%set defaults;
if nargin==1
    lambda=1;
    fs=10;
end
if nargin==2
    fs=10;
end

%Generate discrete transfer function for parameterisation using bilinear
%transformation from Laplace transfer function

num=1;
den=[1 lambda];
[numd,dend]=bilinear(num,den,fs);

%Parameterise Variables
phib=filtfilt(numd,dend,datfile(:,1));
phi2=filtfilt(numd,dend,datfile(:,2));
phi1=filtfilt(numd,dend,datfile(:,3));

%output parameterised variables
paras=[phib phi2 phi1];

```

APPENDIX A2: T₂ MODEL DOCUMENTATION:NON-LINEAR MODEL FOR ENGINE BLOCK OUTLET TEMPERATURE, T₂

The following text describes the non-linear model for T₂ listing parameters and presenting the model block diagrams from Simulink [figure A2.1];

MODEL EQUATION

$$\frac{dT_2}{dt} = a_1 T_b - a_2 T_2 + a_3 T_1$$

Where;

$$a_1 = k_1 \left(\frac{\dot{V}_b}{v_c} \right)^{0.8} \left(\frac{1}{\rho} \right) (\text{Pr})^{0.4} \left(\frac{k_c}{c_p} \right); \quad k_1 = 0.55$$

$$a_2 = (a_1 + a_3)$$

$$a_3 = \frac{\dot{V}_b}{V_b}; \quad V_b = 6 \text{ (l)};$$

Data for Look-up Tables

%coolant data tables – assumed coolant is water [Ref Simonson 88]

```
temp=[0:20:300]+273;          %K
rho=[1002 1001 994.6 985.4 974.1 960.6 945.3 928.3 909.7 889.0 866.7 842.4 815.7 785.9 752.5 714.3];
Cp=1e-3*[4218 4182 4178 4184 4196 4216 4250 4283 4341 4417 4505 4610 4756 4949 5208 5728];
nu=1e-5* [.179 .101 .0658 .0477 .0364 .0294 .0247 .0214 .0189 .0173 .0160 .0149 .0143 .0137 .0135
.0135];
k=1e-3*[0.552 0.597 0.628 .651 .668 .680 .685 .684 .680 .675 .665 .653 .635 .611 .580 .540];
Pr=[13.6 7.02 4.34 3.02 2.22 1.74 1.446 1.241 1.099 1.004 0.937 0.891 .871 .874 .910 1.019];
```

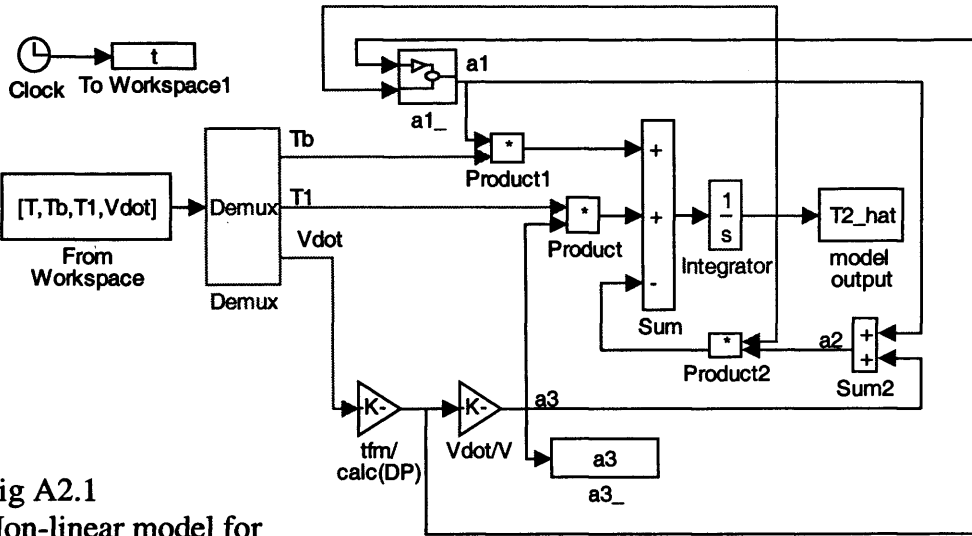


Fig A2.1
Non-linear model for
Engine block outlet
temperature, T_2

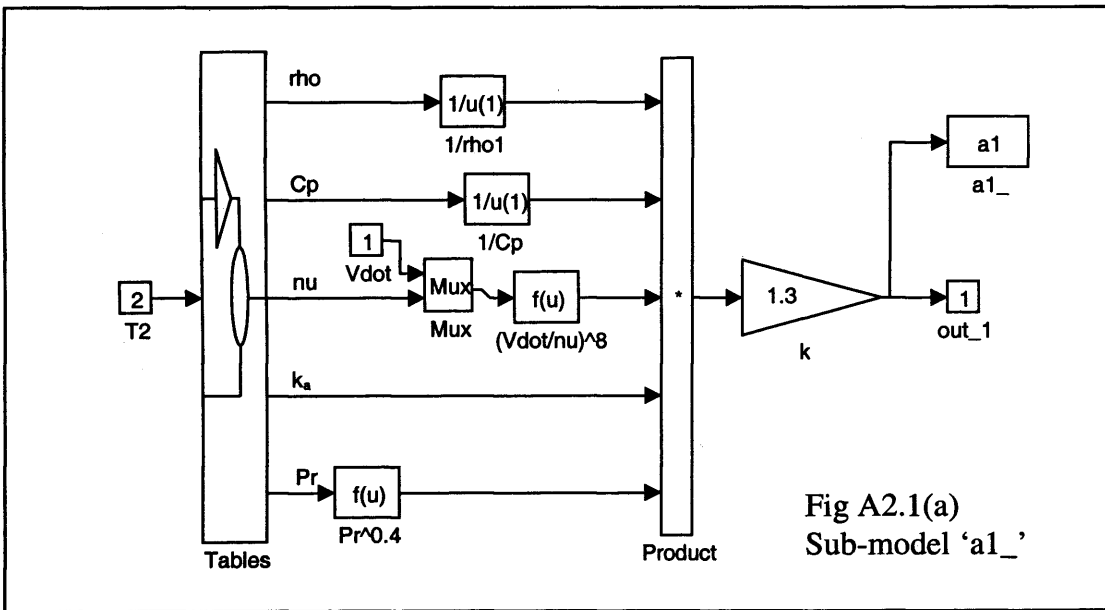


Fig A2.1(a)
Sub-model 'a1_'

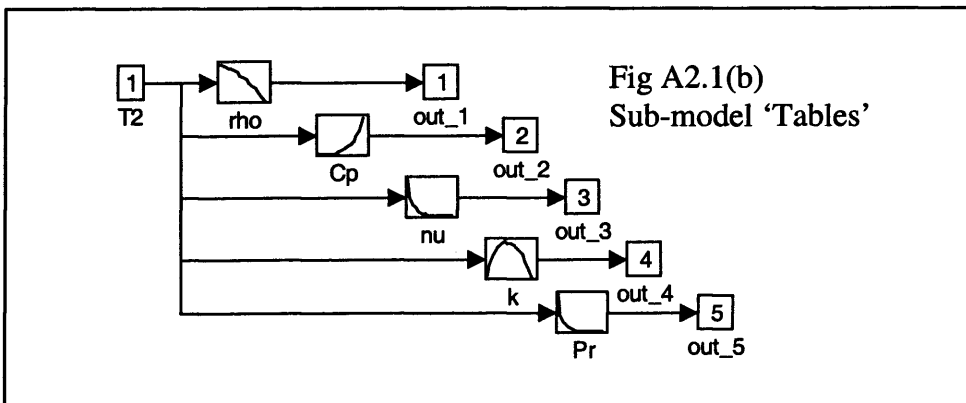


Fig A2.1(b)
Sub-model 'Tables'

APPENDIX A3: T₃ MODEL DOCUMENTATION:NON-LINEAR MODEL FOR ENGINE BLOCK OUTLET TEMPERATURE, T₃

The following text describes the non-linear model for T₃ listing parameters and presenting the model block diagrams from Simulink [figure A3.1];

$$\frac{dT_3}{dt} = a_1 T_2 - a_2 T_3 + a_3 T_{amb}$$

where

$$a_1 = \frac{\dot{V}_{rad}}{V_{rad}}; \quad V_{rad} = 16.5 \text{ (l)}, \quad \dot{V}_{rad} \text{ (ls}^{-1}\text{)}$$

$$a_2 = (a_1 + a_3);$$

$$a_3 = k_2 \frac{h_{rad} A_{rad}}{m_{rad} C_{p_c}}$$

where;

$$k_2 = 0.165; \quad A_{rad} = 47.6 \text{ (m}^2\text{)}; \quad m_{rad} = 16.5 \text{ (kg)}; \quad C_{p_c} = 4.2 \text{ (kJkg}^{-1}\text{K}^{-1}\text{)}; \quad h_{rad} \approx 0.09 \text{ (kW/m}^2\text{K)}$$

Also h_{rad} is calculated from;

$$\left(\frac{1}{\rho_a u_a} \cdot \frac{h_{rad}}{C_{p_a}} \right) \left(\frac{C_{p_a} \mu_a}{k_a} \right)^{\frac{2}{3}} = f \left(\frac{\rho u_a A_{min}}{\mu_a} \cdot \frac{4L}{A_{rad}} \right)$$

Geometrical constants for radiator;

$$A_{min} = 0.24 \text{ (m}^2\text{)}; \quad L = 0.09 \text{ (m)}; \quad A_{rad} = 47.6 \text{ (m}^2\text{)}$$

Fluid property look-up tables for air [Simonson 88];

Air temperature (K);

[250, 300, 350, 400, 450, 500, 550, 600, 650, 700, 750, 800, 850, 900, 950, 1000]

Prandtl's number, Pr;

[0.7220, 0.7080, 0.6970, 0.6890, 0.6830, 0.6800, 0.6800, 0.6800, 0.6820, 0.6840, 0.6860, 0.6890, 0.6920, 0.6960, 0.6990, 0.7020]

Viscosity μ (Pa.s);

[0.1600, 0.1850, 0.2080, 0.2290, 0.2480, 0.2670, 0.2850, 0.3020, 0.3180, 0.3330, 0.3480, 0.3630, 0.3770, 0.3900, 0.4020, 0.4150]

Density ρ , (kgm^{-3})

[1.4130, 1.1770, 0.9980, 0.8830, 0.7830, 0.7050, 0.6420, 0.5880, 0.5430, 0.5030, 0.4710, 0.4410, 0.4150, 0.3920, 0.3720, 0.3520]

$C_{p_a} = 1.006 \text{ (kJkg}^{-1}\text{K}^{-1}\text{)}$. (Assumed constant over ambient temperature range)

Look up table for $(St)(Pr)^{2/3} = f(Re)$ [Ozisik 95]

$Re \times 10^{-3}$;

[0.0001, 0.4000, 0.6000, 0.8000, 1.5000, 2.0000, 4.0000, 6.000, 10.0000]

$(St)(Pr)^{2/3}$

[0.0300, 0.0160, 0.0130, 0.0120, 0.0080, 0.0075, 0.0060, 0.0053, 0.0045]

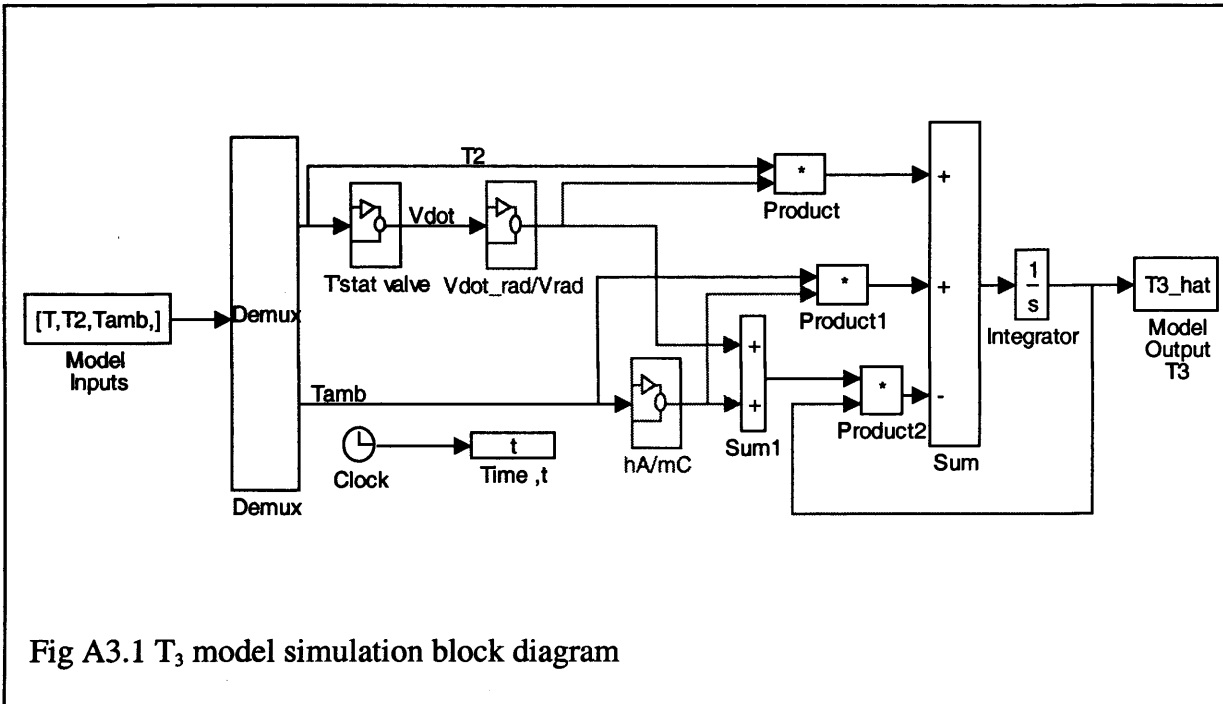


Fig A3.1 T₃ model simulation block diagram

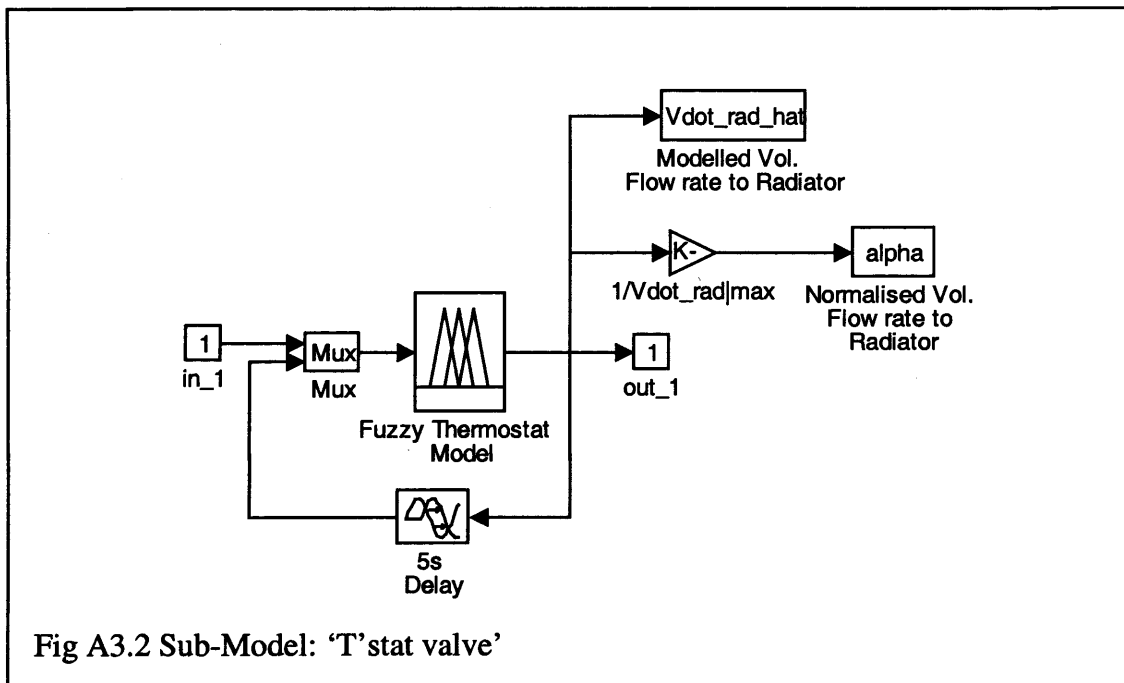
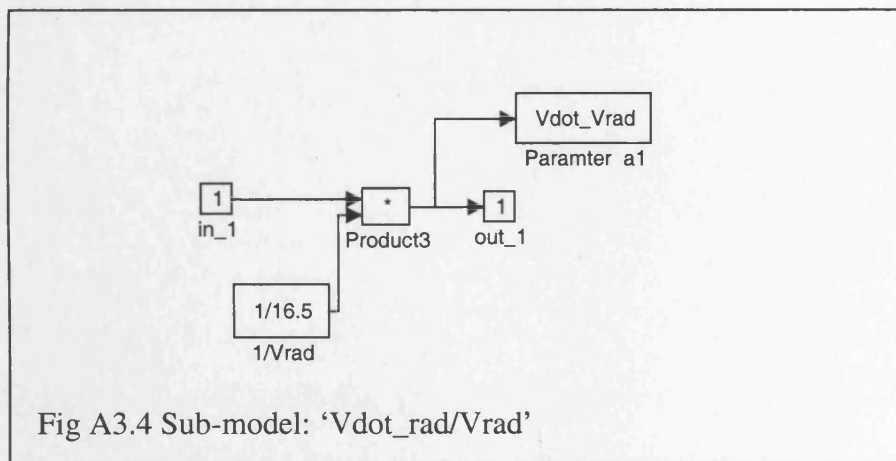
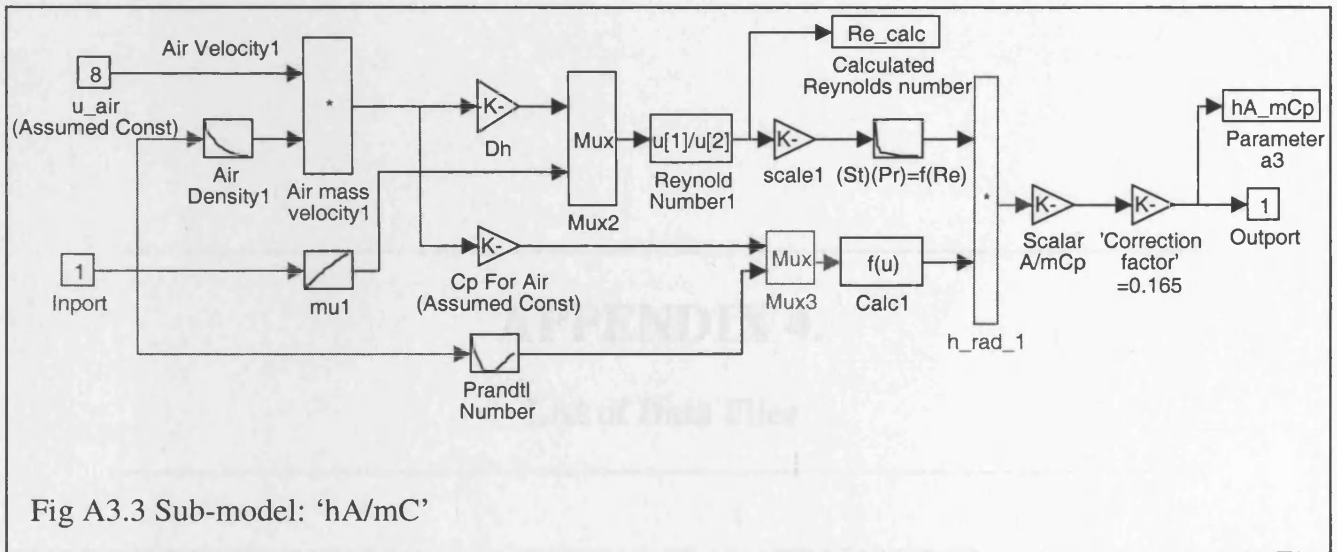


Fig A3.2 Sub-Model: 'T' stat valve'



APPENDIX 4.

List of Data Files

TABLE A4.1 COOLING SYSTEM TEST DATA FILES

File name (.mat files)	Description	Load (kW)	Date
bp01_1	Thermostat valve No.1 fixed to 1mm open TSV 2 closed. Data Channel numbers [# 1,5,3,2, 6, 21, 22, 23, 24, 30 11 12] (see appendix A2.2)	0	06-01-2000
bp01_2	as per bp01_1	20	06-01-2000
bp01_3	as per bp01_1	40	06-01-2000
bp01_4	as per bp01_1	60	06-01-2000
bp01_5	as per bp01_1	40	06-01-2000
bp01_6	as per bp01_1	20	06-01-2000
bp01_7	as per bp01_1	0	06-01-2000
cold01	Reference data – ambient prior to engine start up	-	06-01-2000
bp_1_1	TSV No.1 fixed to 1mm open TSV 2 1mm. Data Channel numbers [# 1,5,3,2, 6, 21, 22, 23, 24, 30 11 12] (see appendix A2.2)	0	07-01-2000
bp_1_2	as per bp_1_1	20	07-01-2000
bp_1_3	as per bp_1_1	40	07-01-2000
bp_1_4	as per bp_1_1	60	07-01-2000
bp_1_5	as per bp_1_1	40	07-01-2000
bp_1_6	as per bp_1_1	20	07-01-2000
bp_1_7	as per bp_1_1	0	07-01-2000
cold_1	Reference data – ambient prior to engine start up		07-01-2000
bp_2_1	TSV No.1 fixed to 2mm open TSV 2 2mm. Data Channel numbers [# 1,5,3,2, 6, 21, 22, 23, 24, 30 11 12] (see appendix A2.2)	0	10-01-2000
bp_2_2	as per bp_2_1	20	10-01-2000
bp_2_3	as per bp_2_1	40	10-01-2000
bp_2_4	as per bp_2_1	60	10-01-2000
bp_2_5	as per bp_2_1	40	10-01-2000
bp_2_6	as per bp_2_1	20	10-01-2000
bp_2_7	as per bp_2_1	0	10-01-2000
cold_2	Reference data – ambient prior to engine start up		10-01-2000
bp_4_1	TSV No.1 fixed to 4mm open TSV 2 4mm. Data Channel numbers [# 1,5,3,2, 6, 21, 22, 23, 24, 30 11 12] (see appendix A2.2)	0	11-01-2000
bp_4_2	as per bp_4_1	20	11-01-2000
bp_4_3	as per bp_4_1	40	11-01-2000
bp_4_4	as per bp_4_1	60	11-01-2000
bp_4_5	as per bp_4_1	40	11-01-2000
bp_4_6	as per bp_4_1	20	11-01-2000
bp_4_7	as per bp_4_1	0	11-01-2000
cold_4	Reference data – ambient prior to engine start up		11-01-2000
bp_op_1	TSV No.1 fixed open .TSV fixed open Data Channel numbers [# 1,5,3,2, 6, 21, 22, 23, 24, 30 11 12] (see appendix A2.2)	0	11-01-2000
bp_op_2	as per bp_op_1	20	11-01-2000
bp_op_3	as per bp_op_1	40	11-01-2000
bp_op_4	as per bp_op_1	60	11-01-2000
bp_op_5	as per bp_op_1	40	11-01-2000
bp_op_6	as per bp_op_1	20	11-01-2000
bp_op_7	as per bp_op_1	0	11-01-2000

cold_op	Reference data – ambient prior to engine start up		11-01-2000
bp01_1	TSV No.1 fixed to 1mm .TSV fixed closed Data Channel numbers [# 5,3,2,6,21,22,23,24,10,11,12,13,31,32,33,34] (see appendix A2.2)	0	13-01-2000
bp01_2	as per bp01_1	20	13-01-2000
bp01_3	as per bp01_1	40	13-01-2000
bp01_4	as per bp01_1	60	13-01-2000
bp01_5	as per bp01_1	40	13-01-2000
bp01_6	as per bp01_1	20	13-01-2000
bp01_7	as per bp01_1	0	13-01-2000
cold01	Reference data – ambient prior to engine start up		13-01-2000
jan14			
bp_1_1	TSV No.1 fixed to 1mm .TSV fixed to 1mm Data Channel numbers [# 5,3,2,6,21,22,23,24,10,11,12,13,31,32,33,34] (see appendix A2.2)	0	14-01-2000
bp_1_2	as per bp_1_1	20	14-01-2000
bp_1_3	as per bp_1_1	40	14-01-2000
bp_1_4	as per bp_1_1	60	14-01-2000
bp_1_5	as per bp_1_1	40	14-01-2000
bp_1_6	as per bp_1_1	20	14-01-2000
bp_1_7	as per bp_1_1	0	14-01-2000
cold_1	Reference data – ambient prior to engine start up		14-01-2000
coldtest	Reference data – ambient prior to engine start up		18-01-2000
modtest1	Model test data [# 5,3,2,6,21,22,23,24,10,11,12,13,31,32,33,34]	[0-40-20-60- 30-50-10-0]	18-01-2000
coldtest2	Reference data – ambient prior to engine start up		18-01-2000
modtest2	Model test data [# 5,3,2,6,21,22,23,24,10,11,12,13,31,32,33,34]	[0-65-0-65-0]	18-01-2000
cold1	Reference data – ambient prior to engine start up		31-01-2000
tsf_cl1	Step loads with alternative TSV, set-point at 82C to simulate thermostat valve fault Data channels [# 1,10,11,12,13,5,3,2,6,21,31,32,33,34,30,23]	[0-65]	31-01-2000
tsf_cl2	as per tsf_cl1	[0-65]	31-01-2000
cold2	Reference data – ambient prior to engine start up		01-02-2001
tsf_cl3	as per tsf_cl1	[0-65]	01-02-2001
cold3	Reference data – ambient prior to engine start up		01-02-2001
tsf_cl4	as per tsf_cl1	[0-65]	01-02-2001
tsf_cl5	as per tsf_cl1	[0-65]	01-02-2001
feb02			
cold4	Reference data – ambient prior to engine start up		02-02-2001
tsf_cl6	as per tsf_cl1	[0-65]	02-02-2001
lcfcold1	Reference data – ambient prior to engine start up		02-02-2001
lcf_blk1	Low coolant flow through engine block System bypass valve open Data channels: [# 1,10,11,12,13,5,3,2,6,21,31,32,33,34,30,23]	[0-65]	02-02-2001
lcf_blk2	as per lcf_blk1	[0-65]	02-02-2001
feb03			
lcfcold2	Reference data – ambient prior to engine start up		03-02-2001
lcf_blk3	as per lcf_blk1	[0-65]	03-02-2001
lcf_blk4	as per lcf_blk1	[0 40 10 65 0]	03-02-2001

		65 0]	
lcf_blk5	as per lcf_blk1	[0-65]	03-02-2001
lcf_blk6	as per lcf_blk1	[0-65]	03-02-2001
feb07			
radcold1			07-02-2001
rad25_1	Simulate radiator fault – 25% of radiator frontal area obstructed with card. Data channels: [# 1,10,11,12,13,5,3,2,6,21,31,32,33,34,30,23]	[0-65]	07-02-2001
rad25_2	as per rad25_1	[0-65]	07-02-2001
rad25_3	as per rad25_1	[0-65]	07-02-2001
rad25_4	as per rad25_1	[0-65-40-0-40-0-40-0]	07-02-2001
radcold2	Reference data – ambient prior to engine start up		08-02-2001
rad10_1	Simulate radiator fault – 10% of radiator frontal area obstructed with card. Data channels: [# 1,10,11,12,13,5,3,2,6,21,31,32,33,34,30,23]	[0-65]	08-02-2001
rad10_2	as per rad25_1	[0-65]	08-02-2001
rad10_3	as per rad25_1	[0-65]	08-02-2001
rad10_4	as per rad25_1	[0-40-0-40-0-40-0]	08-02-2001
r_plcid1	Reference data – ambient prior to engine start up		09-02-2001
rplf_1	Multiple-fault test. Radiator obstruction 10% + Low coolant flow through engine block (system bypass valve open) Data channels: [# 1,10,11,12,13,5,3,2,6,21,31,32,33,34,30,23]	[0-65]	09-02-2001
rplf_2	as per rplf_1	[0-40-0-40-0]	09-02-2001
cool10_1	Low anti-freeze/coolant ratio. (Normal anti-freeze= 50%) Test case =10% AF 90% water Data channels: [# 1,10,11,12,13,5,3,2,6,21,31,32,33,34,30,23]	[0-65]	16-02-2001
cool10_2	as per cool10_1	[0-65]	16-02-2001
cool10_3	as per cool10_1	[0-65]	16-02-2001
cool10_5	as per cool10_1	[0-65]	17-02-2001
cool10_6	as per cool10_1	[0-65]	17-02-2001
cool10_7	as per cool10_1	[0-40-0-40-0]	17-02-2001
cool25_1	Low anti-freeze/coolant ratio. (Normal anti-freeze= 50%) Test case =25% AF 75% water Data channels: [# 1,10,11,12,13,5,3,2,6,21,31,32,33,34,30,23]	[0-65]	17-02-2001
cool25_2	as per cool25_1	[0-65]	17-02-2001
cool25_3	as per cool25_1	[0-65]	18-02-2001
cool25_4	as per cool25_1	[0-65]	18-02-2001
cool25_5	as per cool25_1	[0-65]	18-02-2001
cool25_6	as per cool25_1	[0-40-0-40-0]	18-02-2001
cooln_1	normal anti-freeze/coolant ratio. (Normal anti-freeze= 50%) Test case =25% AF 75% water Data channels: [# 1,10,11,12,13,5,3,2,6,21,31,32,33,34,30,23]	[0-65]	18-02-2001
cooln_2	as per cooln_1	[0-65]	18-02-2001

cooln_3	as per cooln_1	[0-40-0-40-0]	18-02-2001
cooln_4	as per cooln_1	[0-65]	21-02-2001
cooln_5	as per cooln_1	[0-40-65]	21-02-2001
cooln_6	as per cooln_1	[0-40-65-0-65-40-0]	21-02-2001
cooln_7	as per cooln_1	[0-65]	21-02-2001
bpv_oc1	Intermittent Low coolant flow fault. Open and close system	[0-65]	21-02-2001

TABLE A4.2 COMBUSTION SYSTEM TEST DATA FILES**Notes on Aspiration and exhaust system data files****File contents**

Each file contains four matrices:

trace_y	This is the data matrix a set of row vectors i.e. the 'trace' from the y axis
trace_y_n	These are the row vector labels for y axis trace i.e. variable names
trace_x	this is the x axis trace ie time
trace_x_n	x axis lable (empty)

Data acquisition

All data were acquired at 200Hz followed by filtering 100th Order Fir with cut off at 1Hz followed by down sampling to 20Hz. i.e. all data in these files has been recorded at 20Hz

File names

eg. d1_t1_0112

d1 is the condition of the engine as per list d1 – d11

t1 (or f1 in the case of fault simulation tests) is the test number for a given date

0112 is the date that the test was performed eg 0112 is 1st December

tcold#_# files are 'cold' tests I ran with the engine switched off to check instrumentation against ambient conditions prior to test runs. I think you'll be able to ignore these files.

Training data

I used data from 20th Oct as training data and 25th Oct as checking data for my fuzzy models

Variable names in 'trace_y_n'

These are self explanatory. Vdot and Vdot_f both refer to fuel volume flow rate in cm³/s

Known Problems

Noise in the fuel metering is a bit of a problem due to the nature of the transducer and the interpretation of the signal. Also our fuel meter transducer failed in late October half way through this test run. We refitted the transducer but it had slightly different noise characteristics. Later files have two recorded fuel signals, if the file contains both, use 'Vdot' rather than 'Vdot_f'.

Also the pressure transducers used sometimes, and for no apparent reason, 'jump' slightly. Relative to most of the signals the size of these 'jumps' are not a problem. But compared to the pressure differences across the air inlet filter they may be.

Useful m-file

M-file 'ityn.m' which simply gives a numbered index of the trace_y file

Filename	Description	P_{amb} mmHg	T_{amb} degC
d4_f1_0111.mat	d4, 35mm exhaust orifice	736.40	18.0
d11_f1_0112.mat	d11, 3mm manifold vent	742.20	21.5
d11_f1_0712.mat	d11, Manifold vent 'slightly open'	743.25	22.0
f1_1411.mat	NB: No fuel meter reading	745.15	19.0
d11_f1_1511.mat	d11, 7mm manifold vent	750.00	18.5
d11_f1_1711.mat	d11, 1mm manifold vent	750.90	20.5
d4_f1_2510.mat	d4, Air inlet restrictor cap set to 21mm	749.00	22.0
d4_f1_2610.mat	d4, Air inlet restrictor cap set to 19mm	753.15	18.0
d4_f1_2710.mat	d4, Air inlet restrictor cap set to 9.5mm. NB Test run aborted - no fuel meter reading	748.85	18.0
d5_f1_3011.mat	d5, Air inlet vent 20mm at inlet to air flow meter.	750.20	19.0
d4_f1_3110.mat	d4, 35mm Exhaust orifice	737.00	21.0
f2_1411.mat	Air filter removed. No decrease in differential pressure (in fact an increase) use inlet vents to simulate d5	745.15	19.0
d11_f2_1511.mat	d11, 7mm manifold vent. Test run aborted after engine trip	749.10	20.0
d4_f2_2610.mat	d4, Air inlet restrictor cap set to 16.6mm	753.35	20.0
d4_f2_2710.mat	d4, Air inlet restrictor cap set to 9.5mm.	748.85	18.0
d5_f2_3011.mat	d5, Air inlet vents 2x20mm at inlet to air flow meter.	751.20	20.0
d11_f3_0112.mat	d11, Intermittent fault. Open and close valve on manifold vent	742.30	22.0
d4_f3_2610.mat	d4, Air inlet restrictor cap set to 14.3mm	753.25	21.0
d4_f3_2710.mat	d4, Air inlet restrictor cap set to 4.25mm.	749.00	20
d5_f3_3011.mat	d5, Air inlet vents 4x20mm at inlet to air flow meter.	750.00	20.5
d4_f4_2710.mat	d4, Intermittent fault, restrictor cap lowered to 4.25mm and raised to 21mm	749.00	21.0
d5_f4_3011.mat	d5, Air inlet vent 10mm at inlet to air flow meter.	749.00	21.5
d5_f5_3011.mat	d5, Intermittent fault, 2x20mm vents open/closed	748.50	21.5
d1_t1_0112.mat	d1, Normal	742.75	20.0
d1_t1_0712.mat	d1, Normal	745.45	20.5
d1_t1_1411.mat	NB: Test fuel signals.	745.15	19.0
d1_t1_1511.mat	d1, Normal	750.00	17.5
d1_t1_2010.mat	d1, Normal	754.75	18.0
d1_t1_2310.mat	d1, Normal. NB there may be a problem with exhaust manifold pressure reading in this file	753.55	19.0
d1_t1_2510.mat	d1, Normal	748.35	21.5
d1_t10_2010.mat	d1, Normal	753.80	23.0
d1_t11_2010.mat	d1, Normal	753.80	23.0
d1_t12_2010.mat	d1, Normal	753.80	23.0
d1_t13_2010.mat	d1, Normal	753.80	23.0
d1_t14_2010.mat	d1, Normal	753.80	23.0
d1_t15_2010.mat	d1, Normal	753.80	23.0
d1_t16_2010.mat	d1, Normal	753.80	23.0
d1_t17_2010.mat	d1, Normal	753.80	23.0
d1_t19_2010.mat	d1, Normal	753.80	23.0
d1_t2_0712.mat	d1, Normal	740.05	21.5
d1_t2_2010.mat	d1, Normal	754.05	22.0
d1_t20_2010.mat	d1, Normal	753.80	23.0
d1_t21_2010.mat	d1, Normal	753.80	23.0
d1_t22_2010.mat	d1, Normal	753.80	23.0
d1_t3_2010.mat	d1, Normal	753.80	23.0
d1_t4_2010.mat	d1, Normal	753.80	23.0
d1_t5_2010.mat	d1, Normal	753.80	23.0

d1_t6_2010.mat	d1, Normal	753.80	23.0
d1_t7_2010.mat	d1, Normal	753.80	23.0
d1_t8_2010.mat	d1, Normal	753.80	23.0
d1_t9_2010.mat	d1, Normal	753.80	23.0
tcold1_0111.mat	-	736.40	18.0
tcold1_0112.mat	-	742.75	20.0
tcold1_0712.mat	-	745.45	20.5
tcold1_1411.mat	-	745.15	19.0
tcold1_1511.mat	-	750.0	17.5
tcold1_1711.mat	-	750.90	20.5
tcold1_2010.mat	-	754.75	18.0
tcold1_2310.mat	-	753.55	19.0
tcold1_2510.mat	-	748.35	21.5
tcold1_2610.mat	-	753.15	18.0
tcold1_2710.mat	-	748.85	18.0
tcold1_3011.mat	-	750.20	19.0
tcold1_3110.mat	-	737.00	21.0
tcold2_0112.mat	-	742.30	22.0
tcold2_0712.mat	-	743.25	22.0
tcold2_1511.mat	-	750.00	18.5
tcold2_2010.mat	-	754.05	22.0
tcold2_2610.mat	-	753.35	20.0
tcold2_2710.mat	-	748.85	18.0
tcold2_3011.mat	-	751.20	20.0
tcold3_0112.mat	-	742.20	21.5
tcold3_2010.mat	-	753.80	23.0
tcold3_2610.mat	-	753.25	21.0
tcold3_2710.mat	-	749.00	20.0
tcold3_3011.mat	-	750.00	20.5
tcold4_2710.mat	-	749.00	21.0
tcold4_3011.mat	-	749.00	21.5
tcold5_3011.mat	-	748.50	21.5

TABLE A4.3 COMBUSTION SYSTEM TEST DATA FILES

Filename (.mat)	Description	P_{amb} (mmHg)	T_{amb} deg C
acc_20khz_f01	Sample at 20kHz Filter and down-sample to 10kHz [phi,acc]. NB not sure about filtering here ... could be wrong! Fixed Load Load 0kw	762.10	21.0
acc_20khz_f02	As per acc_20khz_f01 load 10 kW	762.10	21.0
acc_20khz_f03	As per acc_20khz_f01 load 20 kW	762.10	21.0
acc_20khz_f04	As per acc_20khz_f01 load 30 kW	762.10	21.0
acc_20khz_f05	Probable Aliasing probs with this file	762.10	21.0
acc_20khz_f06	Probable Aliasing probs with this file	762.10	21.0
acc20khz_1502_f01	Sample at 20kHz. [phi,acc]. Cylinder 2 disconnected. Acc Cyl 1. NB not sure about sample rate - check! Fixed Load Load 0kw	767.35	20.0
acc20khz_1502_f02	Sample at 20kHz. [phi,acc]. Cylinder 2 disconnected. Acc Cyl 1. NB not sure about sample rate - check! Fixed Load Load 30kw	767.35	20.0
acc20khz_1502_f03	Sample at 20kHz. [phi,acc]. Cylinder 2 disconnected. Acc Cyl 2. Fixed Load Load 0kw	767.35	20.0
acc20khz_1502_f04	Sample at 20kHz. [phi,acc]. Cylinder 2 disconnected. Acc Cyl 2. Fixed Load Load 30kw	767.35	20.0
acc20khz_1502_f05	Sample at 20kHz. [phi,acc]. Cylinder 1 disconnected. Acc Cyl 2. Fixed Load Load 0kw	767.35	20.0
acc20khz_1502_f06	Sample at 20kHz. [phi,acc]. Cylinder 1 disconnected. Acc Cyl 2. Fixed Load Load 30kw	767.35	20.0
acc20khz_1502_f07	Sample at 20kHz. [phi,acc]. Cylinder 4 disconnected. Acc Cyl 2. Fixed Load Load 0kw	767.35	20.0
acc20khz_1502_f08	Sample at 20kHz. [phi,acc]. Cylinder 4 disconnected. Acc Cyl 2. Fixed Load Load 30kw	767.35	20.0
acc20khz_1502_f09	Sample at 20kHz. [phi,acc]. Normal. Acc Cyl 2. Fixed Load Load 0kw	767.35	20.0
acc20khz_1502_f10	Sample at 20kHz. [phi,acc]. Normal Acc Cyl 2. Fixed Load Load 30kw	767.35	20.0
acc20khz_1502_f11	Sample at 20kHz. [phi,acc]. Normal. Acc Cyl 1. Fixed Load Load 0kw NB Crank angle indication fault	767.35	20.0
acc20khz_1502_f12	Sample at 20kHz. [phi,acc]. Normal Acc Cyl 1. Fixed Load Load 30kw NB Crank angle indication fault	767.35	20.0
acctest_20kw	Accelerometer test data vs Crank angle and load. Date 01/Feb/2001	?	?
acctest_40kw	Accelerometer test data vs Crank angle and load. Date 01/Feb/2001	?	?

acctest_60_0kw	Accelerometer test data vs Crank angle and load. Date 01/Feb/2001	?	?
acctest_60kw	Accelerometer test data vs Crank angle and load. Date 01/Feb/2001	?	?
acctest2_paras	Simulink Parameter file for data acquisition	?	?
acctest3	Accelerometer test data vs Crank angle and load. Date 01/Feb/2001	?	?
acctest3b	Accelerometer test data vs Crank angle and load. Date 01/Feb/2001	?	?
acctest4	Accelerometer test data vs Crank angle and load. Date 01/Feb/2001	?	?
pb_20khz_f01			
pb_20khz_f02			
pd_0702_1	Sample rate 1kHz, acc, Pb, Taim, Vdotf, Vdotf_pulse, rpm, phi. Staircase load test with soak time	739.85	21.5
pd_0702_10	as per pd_0702_1	739.85	21.5
pd_0702_11	as per pd_0702_1	739.85	21.5
pd_0702_12	as per pd_0702_1	739.85	21.5
pd_0702_13	as per pd_0702_1	739.85	21.5
pd_0702_14	as per pd_0702_1	739.85	21.5
pd_0702_15	as per pd_0702_1	739.85	21.5
pd_0702_16	as per pd_0702_1	739.85	21.5
pd_0702_17	as per pd_0702_1	739.85	21.5
pd_0702_18	as per pd_0702_1	739.85	21.5
pd_0702_19	as per pd_0702_1	739.85	21.5
pd_0702_2	as per pd_0702_1	739.85	21.5
pd_0702_20	as per pd_0702_1	739.85	21.5
pd_0702_21	Sample rate 1kHz, acc, Pb, Taim, Vdotf, Vdotf_pulse, rpm, phi. Staircase load test. Up	739.85	21.5
pd_0702_22	Sample rate 1kHz, acc, Pb, Taim, Vdotf, Vdotf_pulse, rpm, phi. Staircase load test. Down	739.85	21.5
pd_0702_3	as per pd_0702_1	739.85	21.5
pd_0702_4	as per pd_0702_1	739.85	21.5
pd_0702_5	as per pd_0702_1	739.85	21.5
pd_0702_6	as per pd_0702_1	739.85	21.5
pd_0702_7	as per pd_0702_1	739.85	21.5
pd_0702_8	as per pd_0702_1	739.85	21.5
pd_0702_9	as per pd_0702_1	739.85	21.5
pd_0802_01	Sample rate 1kHz, [acc, Pb, Pti, Vdotf, Vdotf_pulse, rpm, phi.] Staircase load test. Up	741.55	16
pd_0802_02	Sample rate 1kHz, [acc, Pb, Pti, Vdotf, Vdotf_pulse, rpm, phi.] Staircase load test. Down	741.55	16
pd_0802_03	Sample rate 1kHz, [acc, Pb, Pti, Vdotf, Vdotf_pulse, rpm, phi]. Load Steps 0-60kW	741.55	16
pd_0802_05	Sample rate 1kHz, [acc, Pb, Pti, Vdotf, Vdotf_pulse, rpm, phi.] Fixed load 10kW	741.55	16
pd_0802_06	As per pd_0802_05. Load 20kW	741.55	16
pd_0802_07	As per pd_0802_05. Load 30kW	741.55	16
pd_0802_08	As per pd_0802_05. Load 40kW	741.55	16
pd_0802_09	As per pd_0802_05. Load 50kW	741.55	16
pd_0802_10	As per pd_0802_05. Load 60kW	741.55	16
pd_1202_01	Don't seem to have any notes for this: Test files for on-line models. Cylinder one fuel line may be disconnected. Model OP data included.		

pd_1202_02	As per pd_1202_01		
pd_1202_f03	As per pd_1202_01		
pd_1302_cold_01	cold test file.	772.55	18
pd_1302_f01	Test files for on-line models. Cylinder one fuel line disconnected. Sample rate 1kHz, [acc, Pb, Vdotf, rpm, phi]+ Model OP data Acc Cyl 1 Stair: Up	772.55	18
pd_1302_f02	As per pd_1302_f01. Stair: Down	772.55	18
pd_1302_f03	As per pd_1302_f01. Step changes	772.55	18
pd_1302_f04	As per pd_1302_f01. Fixed Load 0kW	772.55	18
pd_1302_f05	As per pd_1302_f01. Fixed Load 10kW	772.55	18
pd_1302_f06	As per pd_1302_f01. Fixed Load 20kW	772.55	18
pd_1302_f07	As per pd_1302_f01. Fixed Load 30kW	772.55	18
pd_1402_f01	Test files for on-line models. Cylinder 4 fuel line disconnected. Sample rate 1kHz, [acc, Pb, Vdotf, rpm, phi]+ Model OP data Acc Cyl 1 Stair: Up	770.00	18
pd_1402_f02	As per pd_1402_f01. Stair: Down	770.00	18
pd_1402_f03	As per pd_1402_f01. Step changes	770.00	18
pd_1402_f04	As per pd_1402_f01. Fixed Load 0kW	770.00	18
pd_1402_f05	As per pd_1402_f01. Fixed Load 10kW	770.00	18
pd_1402_f06	As per pd_1402_f01. Fixed Load 20kW	770.00	18
pd_1402_f07	As per pd_1402_f01. Fixed Load 30kW	770.00	18
pd_1502_cold01	Cold engine check	767.35	20.0
pd_1502_f01	Test files for on-line models. Cylinder 2 fuel line disconnected. Sample rate 1kHz, [acc, Pb, Vdotf, rpm, phi]+ Model OP data Acc Cyl 1. Stair: Up	767.35	20.0
pd_1502_f02	As per pd_1502_f01. Stair: Down	767.35	20.0
pd_1502_f03	As per pd_1502_f01. Step changes	767.35	20.0
pd_1502_f04	As per pd_1502_f01. Fixed Load 0kW	767.35	20.0
pd_1502_f05	As per pd_1502_f01. Fixed Load 10kW	767.35	20.0
pd_1502_f06	As per pd_1502_f01. Fixed Load 20kW	767.35	20.0
pd_1502_f07	As per pd_1502_f01. Fixed Load 30kW	767.35	20.0
pd_1502_f08	Test files for on-line models. Cylinder 2 fuel line disconnected. Sample rate 1kHz, [acc, Pb, Vdotf, rpm, phi]+ Model OP data Acc Cyl 2. Stair: Up	767.35	20.0
pd_1502_f09	As per pd_1502_f08. Stair: Down	767.35	20.0
pd_1502_f10	As per pd_1502_f08. Step changes	767.35	20.0
pd_1502_f11	As per pd_1502_f08. Fixed Load 0kW	767.35	20.0
pd_1502_f12	As per pd_1502_f08. Fixed Load 10kW	767.35	20.0
pd_1502_f13	As per pd_1502_f08. Fixed Load 20kW	767.35	20.0
pd_1502_f14	As per pd_1502_f08. Fixed Load 30kW	767.35	20.0
pd_1502_f15	Test files for on-line models. Cylinder 1 fuel line disconnected. Sample rate 1kHz, [acc, Pb, Vdotf, rpm, phi]+ Model OP data Acc Cyl 2. Stair: Up	767.35	20.0
pd_1502_f16	As per pd_1502_f15. Stair: Down	767.35	20.0
pd_1502_f17	As per pd_1502_f15. Step changes	767.35	20.0
pd_1502_f18	As per pd_1502_f15. Fixed Load 0kW	767.35	20.0
pd_1502_f19	As per pd_1502_f15. Fixed Load 10kW	767.35	20.0
pd_1502_f20	As per pd_1502_f15. Fixed Load 20kW	767.35	20.0
pd_1502_f21	As per pd_1502_f08. Fixed Load 30kW	767.35	20.0
pd_1502_f22	Test files for on-line models. Cylinder 4 fuel line disconnected. Sample rate 1kHz, [acc, Pb, Vdotf, rpm, phi]+ Model OP data Acc Cyl 2. Stair: Up	767.35	20.0

pd_1502_f23	As per pd_1502_f22. Stair: Down	767.35	20.0
pd_1502_f24	As per pd_1502_f22. Step changes	767.35	20.0
pd_1502_f25	As per pd_1502_f22. Fixed Load 0kW	767.35	20.0
pd_1502_f26	As per pd_1502_f22. Fixed Load 10kW	767.35	20.0
pd_1502_f27	As per pd_1502_f22. Fixed Load 20kW	767.35	20.0
pd_1502_f28	As per pd_1502_f22. Fixed Load 30kW	767.35	20.0
pd_1502_f29	Test files for on-line models. Normal Condition. Sample rate 1kHz, [acc, Pb, Vdotf, rpm, phi]+ Model OP data Acc Cyl 1. Stair: Up. NB crank angle indication fault	767.35	20.0
pd_1502_f30	As per pd_1502_f22. Stair: Down. . NB crank angle indication fault	767.35	20.0
pd_1502_f31	As per pd_1502_f22. Step changes. NB crank angle indication fault	767.35	20.0
pd_1502_f32	As per pd_1502_f22. Fixed Load 0kW. NB crank angle indication fault	767.35	20.0
pd_1502_f33	As per pd_1502_f22. Fixed Load 10kW. NB crank angle indication fault	767.35	20.0
pd_1502_f34	As per pd_1502_f22. Fixed Load 20kW. NB crank angle indication fault	767.35	20.0
pd_1502_f35	As per pd_1502_f22. Fixed Load 30kW. NB crank angle indication fault	767.35	20.0
pd_cold_0702_1	cold check data		
pd_cold_0802_01	cold check data		
pti_test1	Turbine Inlet Pressure test data		
pti_test2	Turbine Inlet Pressure test data		
pti_test3	Turbine Inlet Pressure test data		
asp_1402_f01	Aspiration system data for comparison with other faults. Cylinder 4 disconnected		
asp_1402_cold_01	Cold check data		
asp_1302_01	Aspiration system data for comparison with other faults. Cylinder 1 disconnected		
asp_1302_02	Aspiration system data for comparison with other faults. Cylinder 1 disconnected		
asp_1302_cold_01	Cold check data		
datum_chk1	check alignment of crank angle datum after refit	740.1	18.0
datum_chk2	check alignment of crank angle datum after refit	740.1	18.0
datum_chk3	check alignment of crank angle datum after refit	740.1	18.0
pd_2602_01	Test files for on-line models. Normal Condition. Sample rate 1kHz, [acc, Pb, Vdotf, rpm, phi]+ Model OP data. Acc Cyl 1. Stair: Up.	740.1	18.0
pd_2602_02	Test files for on-line models. Normal Condition. Sample rate 1kHz, [acc, Pb, Vdotf, rpm, phi]+ Model OP data Acc Cyl 1. Stair: Down.	740.1	18.0
pd_2602_03	As per pd_2602_01. Step changes 0-20-0-20-0 kW	740.1	18.0
pd_2602_04	As per pd_2602_01. 0 kW	740.1	18.0
pd_2602_05	As per pd_2602_01. 10 kW	740.1	18.0
pd_2602_06	As per pd_2602_01. 20 kW	740.1	18.0
pd_2602_07	As per pd_2602_01. 30 kW	740.1	18.0
pd_2602_08	As per pd_2602_01. 40 kW	740.1	18.0
pd_2602_09	As per pd_2602_01. 50 kW	740.1	18.0
pd_2602_10	As per pd_2602_01. 60 kW	740.1	18.0

pd_2702_01	Test files for on-line models. Normal Condition. Sample rate 1kHz, [acc, Pb, Vdotf, rpm, phi]+ Model OP data Acc Cyl 1. Stair: Up.	740.1	18.0
pd_2702_02	Test files for on-line models. Normal Condition. Sample rate 1kHz, [acc, Pb, Vdotf, rpm, phi]+ Model OP data Acc Cyl 1. Stair: Down.	740.1	18.0
pd_2702_03	As per pd_2602_01. Step changes 0-20-0-20-0 kW	736.0	18.0
pd_2702_04	As per pd_2702_01. 0 kW	736.0	18.0
pd_2702_05	As per pd_2702_01. 10 kW	736.0	18.0
pd_2702_06	As per pd_2702_01. 20 kW	736.0	18.0
pd_2702_07	As per pd_2702_01. 30 kW	736.0	18.0
pd_2702_08	As per pd_2702_01. 40 kW	736.0	18.0
pd_2702_09	As per pd_2702_01. 50 kW	736.0	18.0
pd_2702_10	As per pd_2702_01. 60 kW	736.0	18.0
pd_2802_01	Test files for on-line models. Normal Condition. Sample rate 1kHz, [acc, Pb, Vdotf, rpm, phi]+ Model OP data Acc Cyl 1. Stair: Up.	741.2	15.0
pd_2802_02	Test files for on-line models. Normal Condition. Sample rate 1kHz, [acc, Pb, Vdotf, rpm, phi]+ Model OP data Acc Cyl 1. Stair: Down.	741.2	15.0
pd_2802_03	As per pd_2802_01. Step changes 0-20-0-20-0 kW	741.2	15.0
pd_2802_04	As per pd_2802_01. 0 kW	741.2	15.0
pd_2802_05	As per pd_2802_01. 10 kW	741.2	15.0
pd_2802_06	As per pd_2802_01. 20 kW	741.2	15.0
pd_2802_07	As per pd_2802_01. 30 kW	741.2	15.0
pd_2802_08	As per pd_2802_01. 40 kW	741.2	15.0
pd_2802_09	As per pd_2802_01. 50 kW	741.2	15.0
pd_2802_10	As per pd_2802_01. 60 kW	741.2	15.0
pd_2802_03	As per pd_2802_01. Step changes 0-60-0-60-0 kW	741.2	15.0
pd_2802_f01	Test files for on-line models. Alternate Injector fitted on Cylinder 4. Spec 2645 L009 Condition. Sample rate 1kHz, [acc, Pb, Vdotf, rpm, phi]+ Model OP data Acc Cyl 1. Stair: Up.	741.2	15.0
pd_2802_f02	As per pd_2802_f01. Stair: Down	741.2	15.0
pd_2802_f03	As per pd_2802_f01. Step changes 0-20-0-20-0 kW	741.2	15.0
pd_2802_f04	As per pd_2802_f01. 0 kW	741.2	15.0
pd_2802_f05	As per pd_2802_f01. 10 kW	741.2	15.0
pd_2802_f06	As per pd_2802_f01. 20 kW	741.2	15.0
pd_2802_f07	As per pd_2802_f01. 30 kW	741.2	15.0
pd_2802_f08	As per pd_2802_f01. 40 kW	741.2	15.0
pd_2802_f09	As per pd_2802_f01. 50 kW	741.2	15.0
pd_2802_f10	As per pd_2802_f01. 60 kW	741.2	15.0

pd_2802_f03	As per pd_2802_f01. Step changes 0-60-0-60-0 kW	741.2	15.0
asp_cold_0103_01	Aspiration system data. Cold reference	743.5	14.0
asp_0103_01	Aspiration system data. Alternate Injector fitted on Cylinder 4. Spec 2645 L009 Condition.		
pd_0103_f01	Test files for on-line models. Alternate Injector fitted on Cylinder 3. Spec 2645 L009 Condition. Sample rate 1kHz, [acc, Pb, Vdotf, rpm, phi] Acc Cyl 1. Stair: Up.	743.5	15.0
pd_0103_f02	As per pd_0103_f01. Stair: Down	743.5	15.0
pd_0103_f03	As per pd_0103_f01. Step changes 0-20-0-20-0 kW	743.5	15.0
pd_0103_f04	As per pd_0103_f01. 0 kW	743.5	15.0
pd_0103_f05	As per pd_0103_f01. 10 kW	743.5	15.0
pd_0103_f06	As per pd_0103_f01. 20 kW	743.5	15.0
pd_0103_f07	As per pd_0103_f01. 30 kW	743.5	15.0
pd_0103_f08	As per pd_0103_f01. 40 kW	743.5	15.0
pd_0103_f09	As per pd_0103_f01. 50 kW	743.5	15.0
pd_0103_f10	As per pd_0103_f01. 60 kW	743.5	15.0
pd_0103_f11	As per pd_0103_f01. Step changes 0-60-0-60-0 kW	743.5	15.0
pd_0503_f01	Test files for on-line models. 0.9mm valve stem shim 0.9mm fitted to Cylinder 4. Sample rate 1kHz, [acc, Pb, Vdotf, rpm, phi] Acc Cyl 1. Stair: Up.	757.25	20
pd_0503_f02	As per pd_0503_f01. Stair: Down	757.25	20
pd_0503_f03	As per pd_0503_f01. Step changes 0-20-0-20-0 kW	757.25	20
pd_0503_f04	As per pd_0503_f01. 0 kW	757.25	20
pd_0503_f05	As per pd_0503_f01. 10 kW	757.25	20
pd_0503_f06	As per pd_0503_f01. 20 kW	757.25	20
asp_cold_0503_01	Aspiration system data. Cold reference	757.25	20
asp_0503_01	Aspiration system data. Inlet valve shimmed on Cylinder 4	757.25	20
asp_cold_0603_01	Aspiration system data. Cold reference	757.95	21.5
asp_0603_f01	Aspiration system data. Inlet valve shimmed on Cylinder, 3	757.95	21.5
asp_0603_f02	Aspiration system data. Inlet valve shimmed on Cylinder, 3	757.95	21.5
asp_0603_f03	Aspiration system data. Inlet valve shimmed on Cylinder, 3	757.95	21.5
asp_0603_f04	Aspiration system data. Inlet valve shimmed on Cylinder, 3	757.95	21.5
pd_0603_f01	Inlet valve shimmed on Cylinder, 3 0kW	757.95	21.5
pd_0603_f02	Inlet valve shimmed on Cylinder, 3 0kW	757.95	21.5
pd_0703_f01	0.9mm valve stem shim 0.9mm fitted to Cylinder 3. Sample rate 1kHz, [acc, Pb, Vdotf, rpm, phi] Acc Cyl 1. Steady 0kW	746.9	22.5
pd_0703_f02	As per pd_0703_f01. 10 kW	746.9	22.5
pd_0703_f03	As per pd_0703_f01. 20 kW	746.9	22.5
pd_0703_f04	As per pd_0703_f01. 30 kW	746.9	22.5
pd_0703_f05	As per pd_0703_f01. 30-20-10-0 kW	746.9	22.5
pd_0703_f06	As per pd_0703_f01. 0-10-20-30-40-0 kW	746.9	22.5

pd_0703_f07	As per pd_0703_f01. 0-20-0-20-0kW	746.9	22.5
pd_0803_f01	0.9mm valve stem shim 0.9mm fitted to Cylinder 2. Sample rate 1kHz, [acc, Pb, Vdotf, rpm, phi] Acc Cyl 1. Steady 0kW	744.3	21.5
pd_0803_f02	As per pd_0803_f01. 10 kW	744.3	21.5
pd_0803_f03	As per pd_0803_f01. 20 kW	744.3	21.5
pd_0803_f04	As per pd_0803_f01. 30 kW	744.3	21.5
pd_0803_f05	As per pd_0803_f01. 30-20-10-0 kW	744.3	21.5
pd_0803_f06	As per pd_0803_f01. 0-10-20-30 kW	744.3	21.5
pd_0803_f07	As per pd_0803_f01. 0-20-0-20-0 kW	744.3	21.5
pd_0803_f08	0.9mm valve stem shim 0.9mm fitted to Cylinder 1. Sample rate 1kHz, [acc, Pb, Vdotf, rpm, phi] Acc Cyl 1. Steady 0kW	744.3	21.5
pd_0803_f09	As per pd_0803_f08. 10 kW	744.3	21.5
pd_0803_f10	As per pd_0803_f08. 20 kW	744.3	21.5
pd_0803_f11	As per pd_0803_f08. 30 kW	744.3	21.5
pd_0803_f12	As per pd_0803_f08. 30-20-10-0 kW	744.3	21.5
pd_0803_f13	As per pd_0803_f08. 0-10-20-30-40-0 kW	744.3	21.5
pd_0803_f14	As per pd_0803_f08. 0-20-0-20-0 kW	744.3	21.5
asp_0803_cold-01	Aspiration system data. Cold reference	742	24.0
asp_0803_f01	Aspiration system data. Inlet valve shimmed on Cylinder, 1	742	24.0
asp_0903_cold-01	Aspiration system data. Cold reference	740.9	21.5
asp_0903_f01	Aspiration system data. Normal Condition	740.9	21.5
pd_0903_01	Test files for on-line models. Normal Condition. Sample rate 1kHz, [acc, Pb, Vdotf, rpm, phi]+ Model OP data Acc Cyl 1. Stair: Up.	740.9	21.5
pd_0903_02	Test files for on-line models. Normal Condition. Sample rate 1kHz, [acc, Pb, Vdotf, rpm, phi]+ Model OP data Acc Cyl 1. Stair: Down.	740.9	21.5
pd_0903_03	As per pd_0903_01. Step changes 0-20-0-20-0 kW	740.9	21.5
pd_0903_04	As per pd_0903_01. 0 kW	740.9	21.5
pd_0903_05	As per pd_0903_01. 10 kW	740.9	21.5
pd_0903_06	As per pd_0903_01. 20 kW	740.9	21.5
pd_0903_07	As per pd_0903_01. 30 kW	740.9	21.5
pd_0903_08	As per pd_0903_01. 40 kW	740.9	21.5
pd_0903_09	As per pd_0903_01. 50 kW	740.9	21.5
pd_0903_10	As per pd_0903_01. 60 kW	740.9	21.5
pd_0903_11	As per pd_0903_01. Step changes 0-60-0-60-0 kW	740.9	21.5
pd_1303_01	Test files for on-line models. Fuel injector fault – packing washer removed. Cylinder 4 Sample rate 1kHz, [acc, Pb, Vdotf, rpm, phi]. Acc Cyl 1. 0kW steady	741.1	19.5
pd_1303_02	As per pd_1303_01. 10 kW	741.1	19.5
pd_1303_03	As per pd_1303_01. 20 kW	741.1	19.5
pd_1303_04	As per pd_1303_01. 30 kW	741.1	19.5
pd_1303_05	As per pd_1303_01. 40 kW	741.1	19.5
pd_1303_06	As per pd_1303_01. 50 kW	741.1	19.5

pd_1303_07	As per pd_1303_01. 55 kW	741.1	19.5
pd_1303_08	As per pd_1303_01. 55 50 40 30 20 10 0 kW	741.1	19.5
pd_1303_09	As per pd_1303_01. 0 20 0 20 0 kW	741.1	19.5
pd_1303_10	As per pd_1303_01. 0 10 20 30 40 50 55 kW	741.1	19.5
pd_1303_11	As per pd_1303_01. 0 40 0 40 0 kW	741.1	19.5
asp_1303_cold_01	Aspiration system data. Cold reference	741.1	19.5
asp_1303_f01	Aspiration system data. Fuel injector fault – packing washer removed. Cylinder 4	741.1	19.5
pd_1303_f12	Test files for on-line models. Fuel injector fault – packing washer removed. Cylinder 3 Sample rate 1kHz, [acc, Pb, Vdotf, rpm, phi]. Acc Cyl 1. 0kW steady	743.31	22.0
pd_1303_f13	As per pd_1303_f12. 10 kW	743.31	22.0
pd_1503_01	Test files for on-line models. Fuel injector fault – packing washer removed. Cylinder 3 Sample rate 1kHz, [acc, Pb, Vdotf, rpm, phi]. Acc Cyl 1. 0kW steady	750.1	23.5
pd_1503_02	As per pd_1503_f01. 10 kW	750.1	23.5
pd_1503_03	As per pd_1503_f01. 20 kW	750.1	23.5
pd_1503_04	As per pd_1503_f01. 30 kW	750.1	23.5
pd_1503_05	As per pd_1503_f01. 0 10 20 30 20 10 0 kW	750.1	23.5
pd_1503_06	As per pd_1503_f01. 0 30 0 30 0 kW	750.1	23.5
pd_1503_07	As per pd_1303_f01. 0 10 20 30 0 kW	750.1	23.5
pd_1603_01	Test files for on-line models. Fuel injector fault – additional packing washer. Cylinder 3 Sample rate 1kHz, [acc, Pb, Vdotf, rpm, phi]. Acc Cyl 1. 0kW steady	751.2	19.5
pd_1603_02	As per pd_1603_f01. 10 kW	751.2	19.5
pd_1603_03	As per pd_1603_f01. 20 kW	751.2	19.5
pd_1603_04	As per pd_1603_f01. 30 kW	751.2	19.5
pd_1603_05	As per pd_1603_f01. 40 kW	751.2	19.5
pd_1603_06	As per pd_1603_f01. 50 kW	751.2	19.5
pd_1603_07	As per pd_1603_f01. 60 kW	751.2	19.5
pd_1603_08	As per pd_1603_f01. 0 10 20 30 40 50 60 kW	751.2	19.5
pd_1603_09	As per pd_1603_f01. 60 50 40 30 20 10 00 kW	751.2	19.5
pd_1603_10	As per pd_1603_f01. 0 20 0 20 0 kW	751.2	19.5
pd_1603_11	As per pd_1603_f01. 0 60 0 60 0 kW NB timing gear failure	751.2	19.5
pd_1703_01	Test files for on-line models. Fuel injector fault – additional packing washer. Cylinder 3 Sample rate 1kHz, [acc, Pb, Vdotf, rpm, phi]. Acc Cyl 1. 0kW steady	751.2	19.5
pd_1703_02	As per pd_1703_f01. 10 kW	751.2	19.5

pd_1703_03	As per pd_1703_f01. 20 kW	751.2	19.5
pd_1703_04	As per pd_1703_f01. 30 kW	751.2	19.5
pd_1703_05	As per pd_1703_f01. 40 kW	751.2	19.5
pd_1703_06	As per pd_1703_f01. 50 kW	751.2	19.5
pd_1703_07	As per pd_1703_f01. 60 kW	751.2	19.5
pd_1703_08	As per pd_1703_f01. 60 50 60 40 30 20 10 0 kW	751.2	19.5
pd_1703_09	As per pd_1703_f01. 0 20 0 20 0 kW	751.2	19.5
pd_1703_10	As per pd_1703_f01. 0 10 20 30 40 50 60 kW	751.2	19.5
pd_1703_11	As per pd_1703_f01. 0 40 0 40 0 kW	751.2	19.5
pd_2003_01	Test files for on-line models. Normal Sample rate 1kHz, [acc, Pb, Vdotf, rpm, phi]. Acc Cyl 1. 0kW steady	751.2	19.5
pd_2003_02	As per pd_2003_f01. 10 kW	752.5	18.5
pd_2003_03	As per pd_2003_f01. 20 kW	752.5	18.5
pd_2003_04	As per pd_2003_f01. 30 kW	752.5	18.5
pd_2003_05	As per pd_2003_f01. 40 kW	752.5	18.5
pd_2003_06	As per pd_2003_f01. 50 kW	752.5	18.5
pd_2003_07	As per pd_2003_f01. 60 kW	752.5	18.5
pd_2003_08	As per pd_2003_f01. 60 50 40 30 20 10 0 kW	752.5	18.5
pd_2003_09	As per pd_2003_f01. 0 20 0 20 0 kW	752.5	18.5
pd_2003_10	As per pd_2003_f01. 0 10 20 30 40 50 60 kW	752.5	18.5
pd_2003_11	As per pd_2003_f01. 0 40 0 40 0 kW	752.5	18.5
pd_2003_12	As per pd_2003_f01. 0 60 0 60 0 kW	752.5	18.5
asp_2003_cold-01	Aspiration system data. Cold reference	755.3	18.5
asp_2003_f01	Aspiration system data. Normal Condition	755.3	18.5
pd_1004_02	misc. Instrument checking data	764.55	19.5
pd_1004_03	misc. Instrument check data	764.55	19.5
pd_1104_01	Test files for on-line models. Normal Condition Sample rate 1kHz, [Pb_LPf, Vdotf, rpm, phi, mdota FW TG]. Acc Cyl 1. 0kW steady	764.55	19.5
pd_1104_02	As per pd_1104_01 10kW	764.55	19.5
pd_1104_03	As per pd_1104_01 20kW	764.55	19.5
pd_1104_04	As per pd_1104_01 30kW	764.55	19.5
pd_1104_05	As per pd_1104_01 40kW	764.55	19.5
pd_1104_06	As per pd_1104_01 50kW	764.55	19.5
pd_1104_07	As per pd_1104_01 60kW	764.55	19.5
pd_1104_08	As per pd_1104_01 60-50-40-30-20-10-0 kW	764.55	19.5
pd_1104_09	As per pd_1104_01 0-10-20-30-40-50-60 kW	764.55	19.5
pd_1104_10	As per pd_1104_01 0-60-0-60-0 kW	764.55	19.5
pd_1104_11	As per pd_1104_01 0-20-0-20-0 kW	764.55	19.5
pd_1104_12	Test files for on-line models. Inlet Air Restriction 4.25mm gap. rate 1kHz, [Pb_LPf, Vdotf, rpm, phi, mdota FW TG]. 0kW steady	764.55	19.5

pd_1104_13	As per pd_1104_12 10kW	764.55	19.5
pd_1104_14	As per pd_1104_12 20kW	764.55	19.5
pd_1104_15	As per pd_1104_12 30kW	764.55	19.5
pd_1104_16	As per pd_1104_12 40kW	764.55	19.5
pd_1104_17	As per pd_1104_12 50kW	764.55	19.5
pd_1104_18	As per pd_1104_12 60kW	764.55	19.5
pd_1104_19	As per pd_1104_12 60-50-40-30-20-10-0 kW	764.55	19.5
pd_1104_20	As per pd_1104_12 0-10-20-30-40-50-60 kW	764.55	19.5
pd_1104_21	As per pd_1104_12 0-60-0-60-0 kW	764.55	19.5
pd_1104_22	As per pd_1104_12 0-20-0-20-0 kW	764.55	19.5
pd_1104_23	Test files for on-line models. Inlet Air Restriction 2.8mm gap. rate 1kHz, [Pb_LPf, Vdotf, rpm, phi, mdota FW TG]. 0kW steady	764.55	19.5
pd_1104_24	As per pd_1104_23 10kW	764.55	19.5
pd_1104_25	As per pd_1104_23 20kW	764.55	19.5
pd_1104_26	As per pd_1104_23 30kW	764.55	19.5
pd_1104_27	As per pd_1104_23 40kW	764.55	19.5
pd_1104_28	As per pd_1104_23 50kW	764.55	19.5
pd_1104_29	As per pd_1104_23 60kW	764.55	19.5
pd_1104_30	As per pd_1104_23 60-50-40-30-20-10-0 kW	764.55	19.5
pd_1104_31	As per pd_1104_23 0-10-20-30-40-50-60 kW	764.55	19.5
pd_1104_32	As per pd_1104_23 0-20-0-20-0 kW	764.55	19.5
pd_1104_33	As per pd_1104_23 0-60-0-60-0 kW	764.55	19.5
pd_1104_34	Test files for on-line models. Inlet Air Manifold Leak 7mm Orifice. Sample Rate 1kHz, [Pb_LPf, Vdotf, rpm, phi, mdota FW TG]. 0kW steady	764.55	19.5
pd_1104_35	As per pd_1104_34 10kW	764.55	19.5
pd_1104_36	As per pd_1104_34 20kW	764.55	19.5
pd_1104_37	As per pd_1104_34 30kW	764.55	19.5
pd_1104_38	As per pd_1104_34 40kW	764.55	19.5
pd_1104_39	As per pd_1104_34 50kW	764.55	19.5
pd_1104_40	As per pd_1104_34 60kW	764.55	19.5
pd_1104_41	As per pd_1104_34 60-50-40-30-20-10-0 kW	764.55	19.5
pd_1104_42	As per pd_1104_34 0-10-20-30-40-50-60 kW	764.55	19.5
pd_1104_43	As per pd_1104_34 0-20-0-20-0 kW	764.55	19.5
pd_1104_44	As per pd_1104_34 0-60-0-60-0 kW	764.55	19.5
pd_1104_45	Test files for on-line models. Exhaust Restriction 35mm Orifice. Sample Rate 1kHz, [Pb_LPf, Vdotf, rpm, phi, mdota FW TG]. 0kW steady	766.53	21.0
pd_1104_46	As per pd_1104_34 10kW	766.53	21.0
pd_1104_47	As per pd_1104_34 20kW	766.53	21.0
pd_1104_48	As per pd_1104_34 30kW	766.53	21.0
pd_1104_49	As per pd_1104_34 40kW	766.53	21.0
pd_1104_50	As per pd_1104_34 50kW	766.53	21.0
pd_1104_51	As per pd_1104_34 60kW	766.53	21.0

pd_1104_52	As per pd_1104_34 60-50-40-30-20-10-0 kW	766.53	21.0
pd_1104_53	As per pd_1104_34 0-10-20-30-40-50-60 kW	766.53	21.0
pd_1104_54	As per pd_1104_34 0-20-0-20-0 kW	766.53	21.0
pd_1104_55	As per pd_1104_34 0-60-0-60-0 kW	766.53	21.0
pd_2305_01	Test files for on-line models. Normal Condition. Sample Rate 1kHz, [Pb_LPf, Vdotf, rpm, phi, mdota]. 0kW steady	763.5	29
pd_2305_02	As per pd_2305_01 10kW	763.5	29
pd_2305_03	As per pd_2305_01 20kW	763.5	29
pd_2305_04	As per pd_2305_01 30kW	763.5	29
pd_2305_05	As per pd_2305_01 40kW	763.5	29
pd_2305_06	As per pd_2305_01 50kW	763.5	29
pd_2305_07	As per pd_2305_01 60kW	763.5	29
pd_2305_08	As per pd_2305_01 60-50-40-30-20-10-0 kW	763.5	29
pd_2305_09	As per pd_2305_01 0-10-20-30-40-50-60 kW	763.5	29
pd_2305_10	As per pd_2305_01 0-20-0-20-0 kW	763.5	29
pd_2305_11	As per pd_2305_01 0-60-0-60-0 kW	763.5	29
pd_2405_01	Test files for on-line models. Fuel injector fault Cylinder 4 – packing washer removed. Sample Rate 1kHz, [Pb_LPf, Vdotf, rpm, phi, mdota]. 0kW steady	764.8	28
pd_2405_02	As per pd_2405_01 10kW	764.8	28
pd_2405_03	As per pd_2405_01 20kW	764.8	28
pd_2405_04	As per pd_2405_01 30kW	764.8	28
pd_2405_05	As per pd_2405_01 40kW	764.8	28
pd_2405_06	As per pd_2405_01 50kW	764.8	28
pd_2405_07	As per pd_2405_01 50-40-30-20-10-0 kW	764.8	28
pd_2405_08	As per pd_2405_01 0-10-20-30-40-50-60 kW	764.8	28
pd_2405_09	As per pd_2405_01 0-20-0-20-0 kW	764.8	28
pd_2405_10	As per pd_2405_01 0-40-0-40-0 kW	764.8	28
pd_2505_f01	Test files for on-line models. Inlet Valve Fault Cylinder 3 0.9mm shim. Sample Rate 1kHz, [Pb_LPf, Vdotf, rpm, phi, mdota]. 0kW steady	762.10	25
pd_2505_f02	As per pd_2505_f01 10kW	762.10	25
pd_2505_f03	As per pd_2505_f01 20kW	762.10	25
pd_2505_f04	As per pd_2505_f01 30kW	762.10	25
pd_2505_f05	As per pd_2505_f01 40kW	762.10	25
pd_2505_f06	As per pd_2505_f01 40-30-20-10-0 kW	762.10	25
pd_2505_f07	As per pd_2505_f01 10-10-20-30-40kW	762.10	25
pd_2505_f08	As per pd_2505_f01 10-20-0-20-0 kW	762.10	25
pd_2505_f09	As per pd_2505_f01 10-30-0-30-0 kW	762.10	25